ESA-SRE(2008)4
12 February 2009

TSSM In Situ Elements

ESA Contribution to the Titan Saturn System Mission

Assessment Study Report

European Space Agency
Agence spatiale européenne

CONTRIBUTIONS

This report is compiled from input by the following contributors:

Titan-Saturn System Joint Science Definition Team (JSDT): Athéna Coustenis (Observatoire de Paris-Meudon, France; European Lead Scientist), Dennis Matson (JPL; NASA Study Scientist), Candice Hansen (JPL; NASA Deputy Study Scientist), Jonathan Lunine (University of Arizona; JSDT Co-Chair), Jean-Pierre Lebreton (ESA; JSDT Co-Chair), Lorenzo Bruzzone (University of Trento), Maria-Teresa Capria (Istituto di Astrofisica Spaziale, Rome), Julie Castillo-Rogez (JPL), Andrew Coates (Mullard Space Science Laboratory, Dorking), Michele K. Dougherty (Imperial College London), Andy Ingersoll (Caltech), Ralf Jaumann (DLR Institute of Planetary Research, Berlin), William Kurth (University of Iowa), Luisa M. Lara (Instituto de Astrofísica de Andalucía, Granada), Rosaly Lopes (JPL), Ralph Lorenz (JHU-APL), Chris McKay (Ames Research Center), Ingo Muller-Wodarg (Imperial College London), Olga Prieto-Ballesteros (Centro de Astrobiologia-INTA-CSIC, Madrid), François Raulin LISA (Université Paris 12 & Paris 7), Amy Simon-Miller (GSFC), Ed Sittler (GSFC), Jason Soderblom (University of Arizona), Frank Sohl (DLR Institute of Planetary Research, Berlin), Christophe Sotin (JPL), Dave Stevenson (Caltech), Ellen Stofan (Proxeny), Gabriel Tobie (Université de Nantes), Tetsuya Tokano (Universität zu Köln), Paolo Tortora (Università di Bologna), Elizabeth Turtle (JHU-APL), Hunter Waite (Southwest Research Institute)

CDF Study Team: Stefano Santandrea & Andrea Santovincenzo (Team Leaders), Mark Baldesarra (Systems), Torsten Bieler (Costs), Arnaud Boutonnet (Mission Analysis), Otto Brunner (Programmatics / AIV), Andrew Caldwell (Systems), Jean-Marc Charbonnier/CNES (Balloon Design), Pierre Coste (Mechanisms), Jos Cremers (Structures), Luca Ferracina (Aerothermodynamics), Domenico Giunta (Communications), Peter Holsters (Communications), Robert Klotz (Configuration), Charles Lahorgue (Risk), Antonio de Luca (Power), Jens Romstedt (Payload), Rainer Timm (Ground Systems and Ops), David Schwaller (Thermal), Keith Stephenson (Power), Aitor Viana Sanchez (Data handling), Thomas Voirin (AOCS / GNC)

JPL Engineering Team: Kim Reh (Study Leader), Pat Beauchamp (Payload), John Elliott (Systems), Michael Paul/APL (Interface), Nathan Strange (Mission analysis), Corby Waste (artist's impressions & front cover)

Geosaucer Study Team: Lutz Richter (DLR; Team Leader), Tra-Mi Ho (DLR), Ozgur Karatekin (OMA), Olaf Krömer (DLR), Caroline Lange (DLR), Frank Sohl (DLR)

ESA Study Leaders: Jean-Pierre Lebreton (Study Scientist), Christian Erd (Study Manager), Jens Romstedt (Study Payload Manager), Peter Falkner

Titan Saturn System Mission Overview

Scientific Objectives	• Perform chemical analysis, of both the atmosphere and the liquid of a lake. • Analyze the composition of the liquid and the ice content of the surrounding areas. • Study the forces that shape Titan's diverse landscape.	
In situ Elements	One areal vehicle (Montgolfière) floating at mid latitudes (10 km altitude)	One Lander targeted at a northern lake (Kraken Mare)
Overall dimensions	Front shield: 2.6 m ∅ Balloon: 10.5 m ∅ Gondola: 1.6m ∅	Front shield: 1.8 m ∅ Lander: 1.0 m ∅
Interface mass (w/o interface)	571 kg	190 kg
Payload mass (w/o margin)	21.5 kg	27.0 kg
Model Payload	Montgolfière: • Visible imaging system (0.4 – 0.7 μm, including stereo vision) • Imaging spectrometer (1 – 5.6 μm) • Chemical analyzer (10 – 600 Da mass spectrometer) • Atmospheric structure instrument/meteorological package • Electric environment package • Magnetometer • Radar sounder (>150 MHz) • Radio science using Montgolfière telecommuncation system	Lander: • Probe imager (0.4 – 1 μm) + lamp • Chemical analyzer (up to 10,000 Da mass spectrometer) • Atmospheric structure instrument/meteorological package + electric environment package • Surface properties package + acoustic sensor package with magnetometer • Radio science using Lander telecommuncation system
Power system	MMRTG (100 W_{el})	Battery (806 Wh)
Operational lifetime	6 months (baseline) +6 months (extended)	9 hours
Communications	X-band HGA 50 cm ∅, 55 W to TWTA	X-Band LGA
Mission Profile	Launched by Atlas V 551; carried to Titan by orbiter (similar to Huygens) Launchdate: 2020; arrival at 2029 (9.5 years); EVEE-GA Orbiter acts as telecom relay	

TABLE OF CONTENTS

1 INTRODUCTION

Following the selection of the TandEM mission proposal (Coustenis et al., 2008), it was decided that this mission would be studied in collaboration with NASA. The contributions would be, similar to the earlier agreement on Cassini/Huygens, that NASA would provide the orbiter spacecraft, which would carry the ESA provided *in situ* elements and deliver them to Titan.

This report describes the updated baseline of the internal assessment study that was performed with the assistance of the ESTEC CDF facility in June and July 2008. The main goals of the CDF study were

- to assess the feasibility of the proposed mission
- to prepare for the future competitive industrial assessment studies by identifying critical issues that need addressing at higher priority.
- to provide the building blocks and feed-back for further interaction with the science team for formulation of feasible mission goals.

To this end, the CDF study established bottom-up designs for three elements: a montgolfière, a long-lived lander (powered by an ASRG), and a minimum sized small lander of limited lifetime (powered by battery). As the main result feasible designs were found that fulfilled the science requirements [RD8] and that could accommodate the desired payload instruments. Mass, power and telemetry budgets were obtained, however at the time of the study only a small lander could be accommodated within the mass budget that was available for the *in situ* elements. To provide the maximum mass available to the *in situ* elements by minimizing the required the ΔV, and to provide end-to-end study results on all three elements, a release of the ISE's by the orbiter prior to its Saturn orbit injection manoeuvre was assumed. This resulted in long ballistic cruise phases of the ISE's from the point of release to the arrival at Titan. Furthermore the distance between the Titan *in situ* elements and the orbiter, which was required for telemetry data relay, was very large and consequently the available telemetry was limited, even with the application of a high-gain antenna on the montgolfière.

During the execution of the CDF study an updated mission profile of the orbiter became available by using an additional solar electric propulsion stage, which significantly increases the mass delivery capability (830 kg instead of 400 kg) and also enables a more favourable delivery scenario. The increased total mass is commensurate with the delivery of a montgolfière and a small lander. Consequently it was decided by the science team that the *in situ* science would be carried out by using a montgolfière and a lander. The montgolfière would be targeted at mid latitudes (where global circulation winds are strongest), and the lander would be targeted to Kraken Mare, a sea at high northern latitudes. The more favourable delivery scenario included providing a later release, where the montgolfière and lander would be released prior to the first and second Titan fly-by, respectively. As a result the time of transfer by a ballistic trajectory was much reduced mainly for the lander from 4 months to 3 – 4 weeks, while that of the montgolfière changed from 4 – 6 months to ~3 months (for the montgolfière the transfer time is not of concern, as it is powered by an MMRTG and therefore lifetime considerations are not an issue). Also the telemetry budget became much more favourable, since the distance from the montgolfière to the orbiter was reduced

from a maximum of 13×10^6 km to 3×10^6 km with the orbiter being closer and having more frequent fly-bys. The delivery of the lander is such that the orbiter passes over it at a distance ranging from 60,000 to 3,000 km.

The definition of this new baseline however came too late for inclusion in the CDF study, and is therefore described in this report. This report relies on the results from the CDF study and uses much of the design that was derived as building blocks. Differences to the CDF report will be highlighted. With the respect to the science objectives and science return, divergences from the original proposal are explained, including an updated description of the science case.

2 PURPOSE AND SCOPE

This report describes the design of the chosen baseline after the first technical iteration and incuding an updated mission profile providing enhanced mass capability of the delivery of the *in situ* elements, after the addition of a solar electric propulsion stage of the NASA orbiter.

This document is intended as input in support of down-selection for further study between the two proposed outer planet missions (Laplace/EJSM and TandEM/TSSM). The purpose is to describe the feasibility of the technical implementation of the proposed mission baseline as derived by an initial detailed assessment.

This report is the result of an independent ESA internal assessment study. Assuming successful selection more technical details will be addressed in the following industrial studies, where two industrial teams will analyse in competition possible designs to a greater level of detail, than was feasible during the limited time frame of the internal assessment.

3 SCIENCE INVESTIGATION

3.1 Science Overview

Titan, a complex, Earth-like moon with organics, shares features with both other large icy satellites and the terrestrial planets. Indeed, Cassini revealed that Titan has the largest known abundance of organic material in the solar system aside from Earth, and Titan's active hydrological cycle is analogous to that of Earth, but with methane replacing water. Titan's clouds, rain, flash floods, and greenhouse and anti-greenhouse effects may provide important analogs for Earth's long-term climate evolution. Albeit with dramatically different components, Titan's landscape appears remarkably Earth-like, featuring dunes, liquid-carved channels, and mountain ridges, as well as polar lakes filled with liquid hydrocarbons. Also like Earth, Titan's dearth of impact craters demonstrates that its surface is young and geologically active. In addition to pervasive aeolian and fluvial erosion, it is likely that cryovolcanism exists where liquid water, perhaps in concert with ammonia and carbon dioxide, makes its way to the surface from the interior. Titan is also subject to tidal stresses which may have helped to shape its mountains, although, as on Earth, erosion complicates the interpretation of tectonic structures. Titan's dense atmosphere is mostly nitrogen—like Earth's— but with methane as its second major constituent, and other hydrocarbons and nitriles. Titan complex atmosphere varies seasonally in temperature, dynamical behavior, and composition, including a winter polar structure analogous to Earth's ozone hole. Finally, although Titan is similar to Earth in many ways, its atmosphere is unique in the solar system; experiencing strong dynamical forcing by gravitational tides generated by Saturn (a trait Titan may share with many extrasolar planets). A mission launched in the 2018–2022 timeframe provides a unique opportunity to measure a seasonal phase complementary to that observed by Voyager and Cassini, including the latter's extended missions.

Recent discoveries of the complex interactions of Titan's atmosphere with the surface, interior, and space environment demand focused and enduring observation on a range of temporal and spatial scales. A ~20-month mission in orbit around Titan, complemented by *in situ* exploration would be able to monitor dynamic conditions in the ionosphere where complex organic chemistry begins, observe seasonal changes in the atmosphere, and make global near-infrared and radar altimetric maps of the surface. This study of Titan from orbit and *in situ* with conceptually new and technologically enhanced instruments would provide the potential for an increase in Titan science return 2–3 orders-of-magnitude over that of the Cassini mission.

Chemical processes operating in Titan's upper atmosphere can be extensively sampled by a spacecraft in Titan orbit down to about 600 km. However, there is a substantial additional benefit to extending the measurements into Titan's lower atmosphere and down to the surface. Key steps toward the synthesis of prebiotic molecules that may have been present on the early Earth as precursors to life may be produced high in the atmosphere, the products then descending towards the surface where they may replicate. *In situ* chemical analysis, both in the atmosphere and on the surface, would enable assessment of the kinds of chemical species that are present in the lower atmosphere and on the surface, and how far such putative reactions have advanced. Titan's thick atmosphere and low gravity make the deployment of *in situ* elements using parachutes vastly easier

than for other large solar system bodies, as we proved with the Huygens probe. The rich inventory of complex organic molecules that are known or suspected to be present in the low atmosphere and at the surface (Lorenz et al., 2008c) gives Titan a strong astrobiological potential. *In situ* elements would also enable powerful techniques such as subsurface sounding and potentially seismic techniques, to be applied to exploring Titan's crustal structure. Our understanding of the forces that shape Titan's diverse landscape will benefit greatly from detailed investigations at a variety of locations, a demanding requirement anywhere else, but one that is uniquely possible at Titan. A montgolfière hot-air balloon can circumnavigate Titan carried by winds, exploring with high-resolution cameras and subsurface-probing radar. Such a combination of orbiting and *in situ* elements would provide a powerful and, for Titan (and indeed, for the outer solar system!), unprecedented opportunity for synergistic investigations. A synthesis of data from these carefully selected instrumentation suites is the pathway to understanding this profoundly complex body.

On the way to Titan and while in orbit around Saturn, at the early stages of the mission, opportunities exist to significantly extend our understanding of Saturn's magnetosphere and its influence on Titan. Furthermore, the tour through the Saturn system will take the proposed orbiter through the plumes of Enceladus, allowing taking samples and analyzing them using instrumentation not available on the Cassini spacecraft. These investigations would not only inform us about these fascinating components of the Saturn system, but help us address important questions about Titan as well.

The TSSM Science Goals as given hereafter respond directly to NASA's science objectives, ESA's Cosmic Vision 2015-2025 themes, the NASA science objectives, and the science questions raised by the extraordinary Cassini-Huygens discoveries. In particular, this mission concept addresses directly several of the scientific questions highlighted in the ESA Cosmic Vision 2015-2025 call: not only *1.3 "Life and habitability in the Solar System" and 2.2 "The giant planets and their environments",* but also *2.1 "From the Sun to the edge of the Solar System".*

TSSM science would embrace geology, meteorology, chemistry, astrobiology, comparative planetology, dynamics, geophysics, space physics, hydrology, and a host of other disciplines, engaging a wider community than for virtually any other target in the outer Solar System. Clearly, Titan, a rich and diverse body offering the potential for extraordinary scientific return, is emerging as the compelling choice for the next Joint ESA-NASA Outer Planet Flagship mission, in the steps of Cassini-Huygens.

3.1.1 THE IMPORTANCE AND TIMELINESS OF TITAN'S EXPLORATION

Saturn's largest moon, Titan, has been a fascinating world at every stage of its exploration. For three decades after the hazy atmosphere was discovered from ground-based observations in the 1940s (Kuiper 1944; Khare and Sagan 1973), debate followed over whether it was a thin layer of methane or a dense shield of methane and nitrogen. Voyager 1 settled the matter in favor of the latter in 1980 (Broadfoot et al., 1981), but the details it discovered about the atmosphere raised even more intriguing questions about the nature of its hidden surface and the sources of methane to resupply the atmosphere. The simplest possibility, that an ocean of methane and its photochemical product ethane might cover the globe (Lunine et al., 1983), was cast in doubt by Earth-based radar studies (Muhleman et al. 1990), then eliminated by HST observations and from adaptive optics

imaging in the near infrared from large Earth-based telescopes in the 1990s (Smith et al., 1996; Combes et al., 1997; Coustenis et al., 2001; 2005; Gendron et al., 2004; Roe et al., 2004; Hirtzig et al., 2007; West et al. 2005). These data, however, did not reveal the complexity of the surface that Cassini-Huygens would uncover beginning in 2004 (e.g., Porco et al., 2005; Elachi et al., 2005; Tomasko et al., 2005). Channels likely carved by liquid methane and/or ethane, lakes and seas of these materials—some rivaling or exceeding the North-American Great Lakes in size—vast equatorial dune fields of complex organics made high in the atmosphere and shaped by wind, intriguing hints of volcanic flows of aqueous materials across an icy crust, and a dearth of impact craters suggest a world with a balance of geologic and atmospheric processes that is the solar system's best analog to Earth. In addition, deep underneath Titan's dense atmosphere and active, diverse surface Cassini instruments data strongly suggest the presence of an interior ocean thought to be largely composed of liquid water.

Cassini-Huygens will leave us with many questions that will require a future mission to answer. These include the methane cycle and whether methane is outgassing from the deep interior or the icy crust today, whether the lakes are fed primarily by rain or underground methane-ethane aquifers (more properly, "alkanofers"), how often heavy methane rains come to the equatorial region, whether Titan's surface supported vaster seas of methane in the past, and whether complex self-organizing chemical systems have come and gone in the water volcanism, or even exist in exotic form today in the high latitude lakes. The composition of the surface and the geographic distribution of various organic constituents remain poorly understood. Key questions remain about the surface-atmosphere interactions, the organic chemistry, the ages of the surface features specifically whether cryovolcanism and tectonism are actively ongoing or are relics of a more active past. Ammonia, circumstantially suggested to be present by models as well as a variety of Cassini-Huygens data, has not been detected. The presence of a magnetic field has yet to be established. Much remains to be understood about seasonal changes of the atmosphere at all levels and the long-term escape of constituents to space.

3.1.1.1 Titan as a Model for Chemistry in the Prebiotic Earth Environment

A key characteristic of Titan is its massive inventory of organic chemicals. The first step in the path toward understanding the role of organics in Titan's atmosphere was the discovery of methane (CH_4) by Kuiper in 1944. Subsequent polarization measurements by Veverka and separately Zellner, both in 1973, indicated the presence of a solid phase component in the atmosphere. These observations were the impetus for the laboratory experiments of Khare et al. (1984), which first suggested that methane photolysis could result in solid organic aerosols that Sagan referred to as "tholins" (Sagan and Khare 1979). When Voyager 1 flew past Titan in the early 1980s, it verified the presence of methane in a thick background atmosphere of nitrogen. Even more interesting was the detection of a host of more complex hydrocarbons and nitriles that resulted from the photolysis and energetic particle bombardment of the atmosphere and the thick organic haze that both scattered and absorbed visible and infrared photons, thereby playing an important role in determining the satellite's thermal structure. The laboratory studies carried out on the basis of the Voyager observations provided a tholin that was a good analogue for the Titan haze (Hodyss et al., 2004). Based on this analog, it was possible to conclude that the haze is composed of refractory organics that, once condensed, do not evaporate and are ultimately deposited on the surface with a

net production rate of ~10^{-14} g cm^{-2} s^{-1} (see reviews in McKay et al. 2001 and Bernard et al., 2006).

Titan is an organic paradise that is certain to tell us much about the chemical evolution that may lead to life. Water ice (Griffith et al., 1991; Coustenis et al., 1995; Lellouch et al. 2003) and carbon dioxide ice (Coustenis et al., 2006; McCord et al. 2008) has been reported to exist currently on the surface. Transient episodes of melting of the water ice by either geologic activity or impacts would expose organics to aqueous alteration, as well as contact with carbon dioxide, leading potentially to reaction pathways that mimic those that occurred on the pre-biotic Earth. No other place in the solar system has this type of ongoing chemistry.

An important question is whether the synthesis pathways from atmospheric photochemistry via photolysis lead to a different assemblage of prebiotic material than those that occur on comets and meteorites, e.g., low-carbon ('Triton') tholin hydrolysis yields appreciable amounts of amino acids including some which are not found in living systems (Hodyss et al., 2004). An important additional consideration is whether the stereochemical preference for life to use homochiral molecules, such as left-handed amino acids, is a mere result of chance, or whether prebiotic synthesis yields non-racemic abundances of these stereoisomers. The answer to both of these questions raised by Cassini-Huygens requires a new mission to be tackled. TSSM is designed to address them.

3.1.1.2 Titan as a Model for Climate Change during Rapid Volatile Loss (Future Earth)

It is at first surprising that the most Earthlike body in the solar system is Titan. Indeed, if Titan orbited the Sun rather than Saturn, we would have no hesitation in calling it a planet in its own right. This strange world is larger than the planet Mercury and has a nitrogen atmosphere like that of Earth, yet denser and laden with an organic smog that hid its surface from view until Cassini-Huygens approached it in early 2004, and later in 2005 when Huygens revealed to us an extraordinary Earth-like landscape. Far from the Sun, methane plays the active role on Titan that water plays on Earth, acting as a condensable greenhouse gas, forming clouds and rain, and pooling on the surface as lakes. Titan's icy surface is shaped not only by impact craters and tectonics, but also by volcanism in which the lava is liquid water ("cryovolcanism"), by rivers of liquid methane, and by tidally driven winds that sculpt drifts of aromatic organics into long linear dunes.

This varied landscape, seascape, and weather make Titan uniquely like Earth, but in some aspects not the Earth of the present. Our planet has a massive reservoir of water in the oceans/seas, which regulates the availability of water for mid-latitude storms and serves as a huge heat sink for climate. Our ocean exists stably on the surface because, at the Earth's distance from the Sun and present solar luminosity, the atmosphere has a profound cold trap at the 15-km altitude level. Over the next one to several billion years, increasing solar brightness will warm the atmosphere, raise the temperature of the cold trap and allow water to flow into the stratosphere and be broken apart by ultraviolet light. This breakup is irreversible, as the hydrogen will escape, leaving the Earth essentially dry. Residual crustal water will outgas and be resident mostly at the poles, while

occasional mid-latitude storms will carve channels amidst a vast equatorial belt of dunes formed by carbonate and silica sediments left behind on the ocean floor.

Venus and Mars both approach end states of volatile loss processes – in Venus' case the water was lost because greenhouse temperatures near the sun failed to keep it below an adequate cold trap, while on Mars the weak gravity and magnetic field may have allowed substantial losses to occur. The few known isotopic ratios in Titan's atmosphere attest to resupply and loss processes, with different results for the nitrogen and carbon reservoirs. The latter, in the form of methane greenhouse gas and surface liquid deposits, makes an appropriate analogue for the Earth's water.

3.2 TSSM Titan Science Goals and Objectives

In conjunction with the orbiter, *in situ* investigation will enable analyses of Titan science features that simply are not feasible remotely. Titan's thick lower atmosphere and low gravity make the deployment of *in situ* elements vastly easier than at any other solar system body. *In situ* elements will allow direct access for atmospheric and surface sampling and analysis. They will also enable powerful techniques such as interior and subsurface sounding to be applied to exploring Titan's interior structure.

A Montgolfière hot-air balloon that can circumnavigate Titan carried by winds, exploring with state-of-the-art new instrumentation, in combination with a probe landing in a northern-hemisphere sea or lake and with observations from an orbiter provides the most powerful and, for Titan, unprecedented opportunity for synergistic investigations—synthesis of data from these extensively-studied selected instrumentation suites is the best approach to understanding this complex body.

In order to respond both to the ESA Cosmic Vision Themes and the NASA 2003 Decadal Survey as defined in the 2007 calls and studies, TSSM would have to return new science insights — among other — on chemical composition and structure, meteorology, dynamics, geology, geophysics, hydrology, solar system physics, among others. To do so, the *in situ* exploration is a key player in this mission, as was demonstrated by the Huygens probe on the Cassini-Huygens mission and as is also clearly shown in the current study.

3.2.1 TITAN'S ATMOSPHERE

Titan has a very complex atmospheric machine within which several different processes combine (Figure 3.2.1-1) to reproduce phenomena observed elsewhere in the Solar System, but rarely with such intensity (except perhaps on our own planet).

Meteorologically, Titan is an outstanding body for comparative planetology. In some sense, it resembles Venus in being a slowly rotating body with a massive, optically thick atmosphere—conditions that lead to super-rotating zonal winds. In other respects, it may resemble Mars, in having a seasonal cycle forced by an appreciable obliquity (Titan 26°, Mars 25°) and having asymmetric seasons, since both have eccentric orbits around the Sun. Titan's southern summer (like that of Mars) is shorter but more intense than the corresponding season in the North (Figure 3.2.1-2).

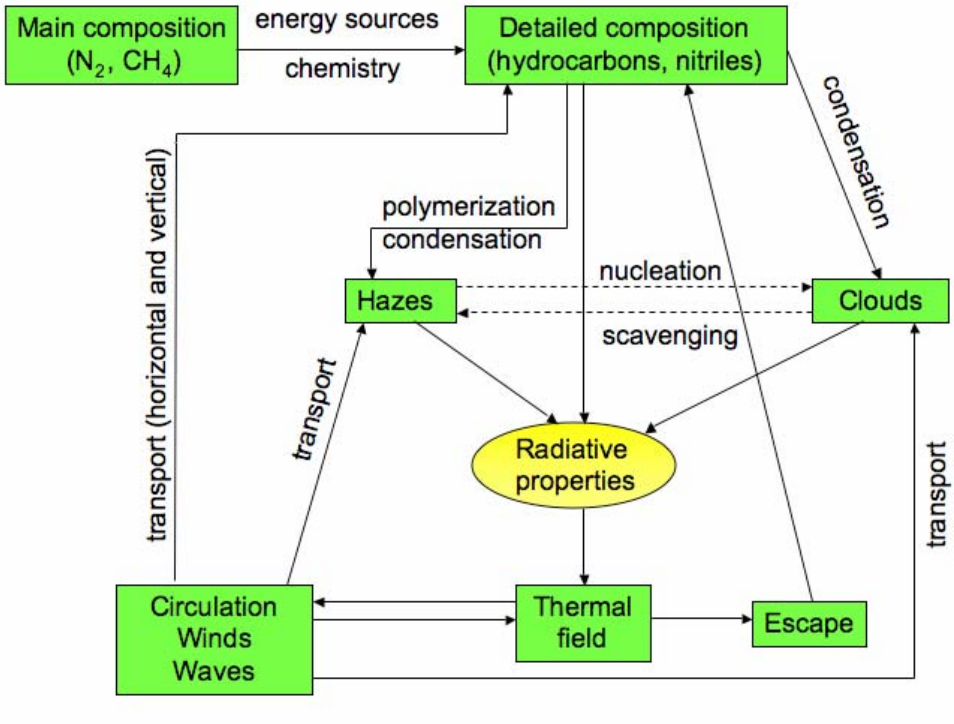

Figure 3.2.1-1 Main couplings between Titan's atmospheric processes.

The seasonally changing solar forcing leads to an asymmetric hemisphere-to-hemisphere meridional ('Hadley') circulation, with only a transient epoch of Venus-like symmetric equator-to-pole Hadley circulation around equinox. Titan's thermally-direct stratospheric meridional circulation transports organic gases and haze, leading to the seasonal north-south albedo asymmetry in the haze observed by Voyager. (The northern hemisphere, observed by Voyager at northern spring equinox in 1980 had more haze and was thus darker at blue wavelengths. This situation had reversed half a Titan year later when the Hubble Space Telescope observed Titan. Substantial changes in the haze structure are apparent even after only one or two years.) Recent ground-based work by Lockwood (2008, preprint) show that this seasonal haze cycle does not perfectly repeat year-to-year; the disk-integrated albedo of Titan in 2002-2006 is a couple of per cent lower than in the same season, 1972-1976. This suggests either an influence of the 11-year solar cycle and/or some internal dynamics (i.e. 'memory' or 'hidden variables' in the climate system, analogous to El Nino which produces inter-annual variability on Earth).

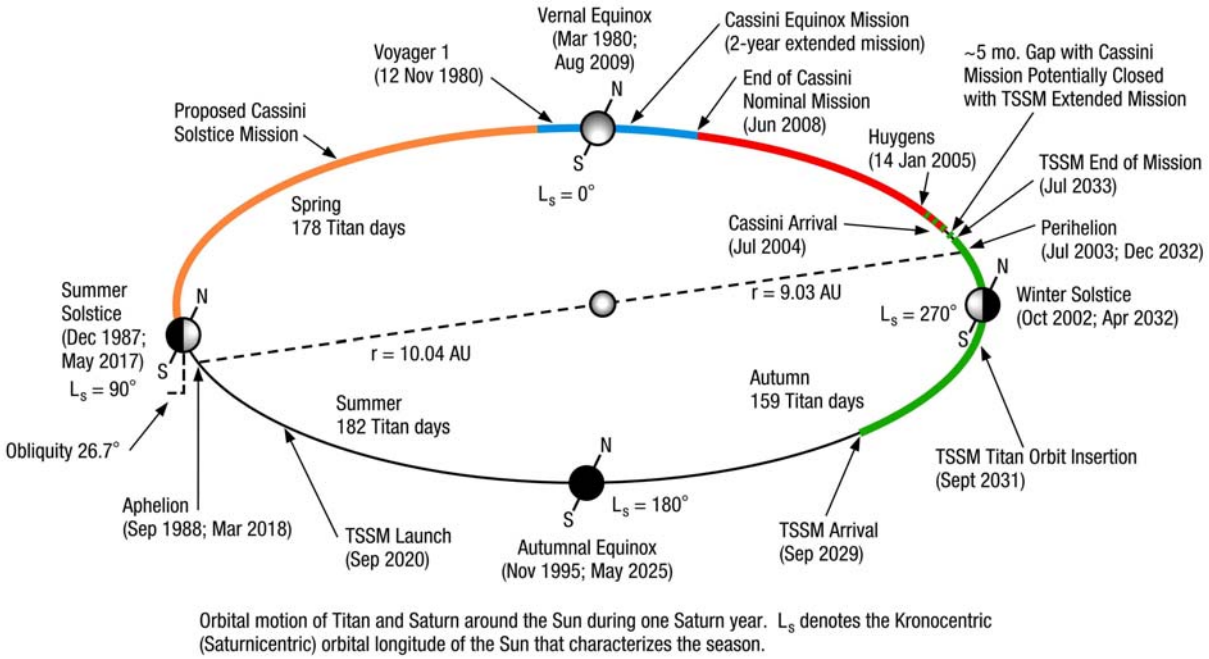

Figure 3.2.1-2 The seasonal cycle on Titan. The TSSM mission will complement the Cassini nominal, extended and possibly 2nd extension missions and help cover a large part of its 30-year rotational period. This will allow us to better address issues such as temporal phenomena.

3.2.1.1 Titan's neutral atmosphere

However, the best atmospheric analogies are between Titan and Earth (Coustenis and Taylor, 2008). Most obvious, is the existence of a hydrological cycle involving methane clouds, rain and at least transient rivers. The possibility of such a cycle had been noted as soon as the proximity of Titan's surface conditions to the methane triple point had been noted in Voyager data, and the first evidence of clouds emerged in spectroscopic data (Griffith et al. 1998) and in Hubble Space Telescope (HST) images (Lorenz and Mitton 2002), both acquired in 1995. Subsequent observations showed clouds to be evolving on timescales of only hours, suggesting that precipitation may be occurring, and several years before Cassini arrived, large ground-based telescopes with adaptive optics systems showed massive variable cloud systems around the south pole (where it was approaching mid-summer) (Brown et al. 2002). Observations by Cassini soon after its arrival in 2004 showed much detail on these clouds, and showed that the cloud tops ascended at velocities comparable with those predicted in models (a few m/s, Porco et al. 2005). These clouds, then, seem fully consistent with cumulus convection like those seen on Earth in desert summer.

From a thermodynamic viewpoint, the relative scarcity of clouds on Titan compared to the Earth can be understood as a consequence of the efficient utilization of a much smaller thermal flux (Lorenz et al. 2005). The geographical distribution, however, is rather different—on Earth rainclouds occur dominantly in the inter-tropical convergence zone, while on Titan models predict that they will, broadly speaking, track the subsolar latitude (e.g., Mitchell et al. 2006), although the details among models differ (e.g., Rannou et al. 2006).

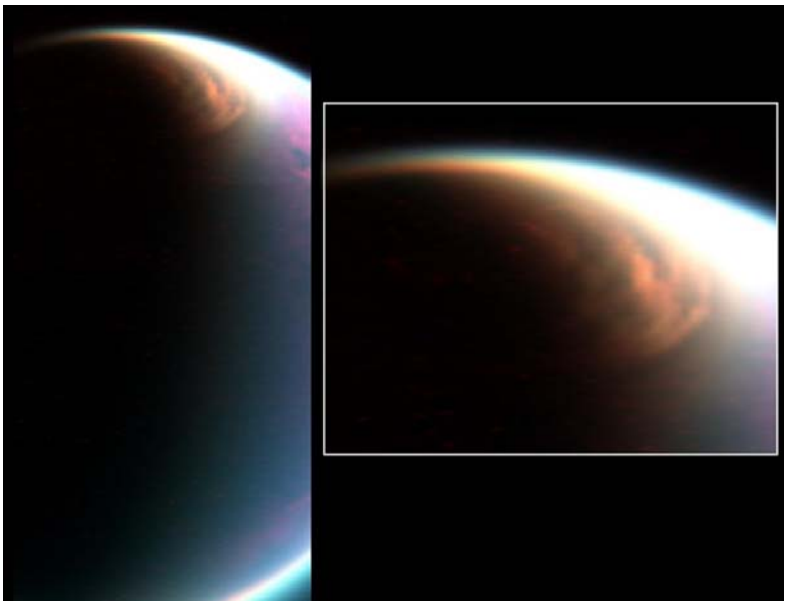

Figure 3.2.1-3 Large north polar cloud imaged by Cassini VIMS. (Credit: NASA/JPL/Univ. of Arizona; *http://saturn.jpl.nasa.gov/multimedia/images/image-details.cfm?imageID=2470*)

Titan presents an interesting extrapolation of the Earth's hydrological cycle. While the overall intensity of the cycle is weak, the solar heating available to evaporate surface moisture and drive the cycle is tiny, and not substantially compensated by the lower latent heat of methane compared with water. Thus instead of the ~100 cm of annual rainfall observed on Earth, Titan must see on average only about 1 cm per (earth) year (Lorenz 2000). However, Titan's thick atmosphere can hold a prodigious amount of moisture, equivalent to several meters of liquid. Thus, were Titan to dump the moisture out of its atmosphere (which to a crude approximation, is what happens in violent rainstorms, as indicated in models of Titan rainclouds, e.g., Hueso and Sanchez-Lavega 2006; Barth and Rafkin 2007), it would require ~1000 years to recharge the atmosphere. (The corresponding numbers are ~10 cm and a month for the present-day Earth.) A warmer atmosphere can hold more moisture, and may thus see more intense storms separated by longer droughts, a pattern being discerned in the present epoch of global warming. Titan thus has a greenhouse hydrology taken to extremes.

Titan's clouds are not limited to convective cumulus. A pervasive, lingering cloud of ethane particles has been observed over the northern polar regions (Figure 3.2.1-3) in the present season (late northern winter, Griffith et al., 2006), probably related to the downwelling of organic-rich air over the winter pole (Rannou et al. 2006). Additionally, sporadic small cloud streaks have been noted at mid-latitudes with a possibly non-uniform longitude distribution. There is presently debate as to whether these might be associated with the Hadley circulation and/or tides, or whether they are tied to surface features, either as orographic clouds or clouds triggered by surface venting of methane. Some support for a low-latitude methane supply has been noted in models (much as the Martian climate causes water to migrate to high latitudes) that point out that the low latitudes on Titan should progressively become methane-dessicated (e.g., Rannou et al. 2006), unless replenished by a surface source.

Another analogy with the Earth relates to the polar stratosphere. Titan was observed by Voyager to have a UV-dark 'polar hood,' a dark haze cap over the winter pole. This cap was seen in high-phase-angle images to stand above the main haze deck, and connect with the detached haze layer. Circulation models (e.g., Rannou et al. 2006) are able to reproduce this behavior. The same latitudes are also known to have both the warmest and coldest parts of the stratosphere, as well as enhancements by factors of ~100 in the abundance of certain nitrile gases. Evidently the upper atmospheric meridional flow converges at the pole and downwelling brings organic-rich air to lower levels. At low altitudes in this feature, low temperatures are found, because the region is in winter shadow and the rich supply of gas and haze provides efficient radiative cooling. In contrast, higher altitudes are illuminated and also heated adiabatically by the descending air. While connected to the detached haze at high altitude, the region is dynamically isolated by the circumpolar vortex. On Earth, the corresponding circumpolar winds isolate the winter stratosphere from the rest of the atmosphere: the catalytic surfaces of polar stratospheric clouds that form in the winter night cause the destruction of ozone whose concentration becomes locally depleted — the ozone hole.

3.2.1.2 Titan's upper atmosphere

The structure of the upper atmosphere of Titan was defined by the Cassini Ultraviolet Imaging Spectrometer (UVIS), which observed the extinction of photons from two stars by the atmosphere of Titan during the second Titan flyby (Shemansky et al., 2005). A mesopause was inferred at 615 km with a temperature minimum of 114 kelvin. Six species were identified and measured: methane, acetylene, ethylene, ethane, diacetylene, and hydrogen cyanide at altitude ranges from 450 to 1600 kilometers. The higher order hydrocarbons and hydrogen cyanide peak sharply in abundance and are undetectable below altitudes ranging from 750 to 600 km, leaving methane as the only identifiable carbonaceous molecule in this experiment below 600 km.

The *in situ* analysis of the thermosphere and ionosphere by the Ion Neutral Mass Spectrometer (INMS) during the closest Cassini flybys of Titan shows the presence of many complex organic species, in spite of the very high altitudes (1100-1300 km) (Waite et al., 2007). Extrapolation of the INMS measurements (limited to mass up to 100 Daltons) and of CAPS data, strongly suggests that high-molecular-weight species (up to several 1000 Daltons) may be present in the thermosphere and the ionosphere. (Figure 3.2.1-4)**.**

This new data – if confirmed – revolutionize the understanding of the organic processes occurring in Titan's atmosphere, with a strong implication that ionospheric chemistry plays a role in the formation of complex organic compounds in Titan's environment, which was not envisaged before (Waite et al., 2007). Thus, it appears that Titan is a chemical factory in which the formation of complex positive and negative ions is initiated in the high thermosphere as a consequence of magnetospheric-ionospheric-atmospheric interaction involving solar EUV, UV radiation, energetic ions and electrons (Figure 3.2.1-5).

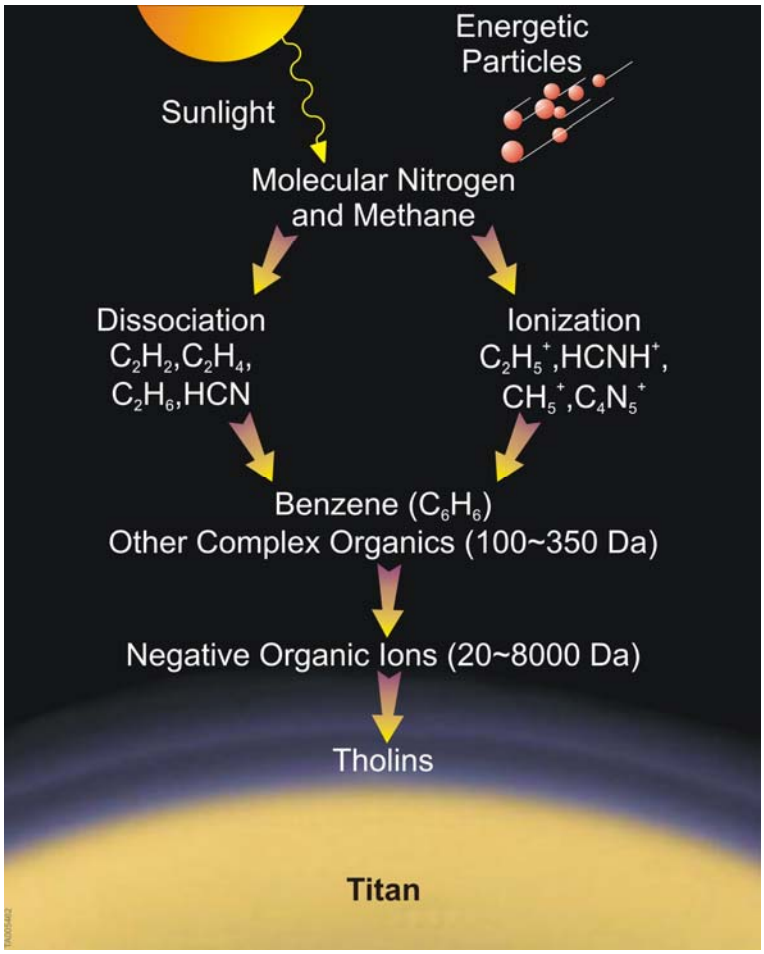

Figure 3.2.1-4 Organic processes in Titan's upper atmosphere resulting in the formation of complex positive and negative ions (Waite et al., 2007).

The figure shows the three main layers of Titan's atmosphere, and its illumination by solar UV (blue rays), solar visible light (yellow rays) and solar infrared light (red rays). The energy input from Saturn's magnetospheric interaction shows a strong interaction with Titan's upper atmosphere and the corresponding induced magnetosphere with draped magnetic field lines. The keV to 10's of keV O^+ ions and energetic H^+ ions E > 50 keV can penetrate across field lines and deposit their energy directly into Titan's atmosphere and lower ionosphere to altitudes < 800 km (Cravens et al., 2008) resulting in heating and escape of suprathermal nitrogen and methane atoms and molecules from Titan's upper atmosphere (Michael and Johnson, 2005). Energetic neutral atoms (ENAs) are also emitted via charge transfer collisions between magnetospheric energetic ions and Titan's atmosphere (Garnier et al., 2008a,b). The magnetospheric electrons are magnetically tied to the field lines but can drift to lower altitudes via gradient and curvature drift mechanisms (Hartle et al., 1982). The magnetospheric electrons plus photoelectrons from the ionizing solar UV striking Titan's upper atmosphere produce a non-thermal electron gas within Titan's ionosphere which can then heat thermal electrons to $T_e \sim 1000°K$ (Wahlund et al., 2005) and correspondingly reduce positive ion recombination rates. The hot electrons can also produce a polarization electric field ($T_e >> T_{ION} \sim 180°K$) which will pull ions out of the ionosphere and produce an ionospheric wind as shown in the form of CH_5^+ and $C_2H_5^+$ ions.

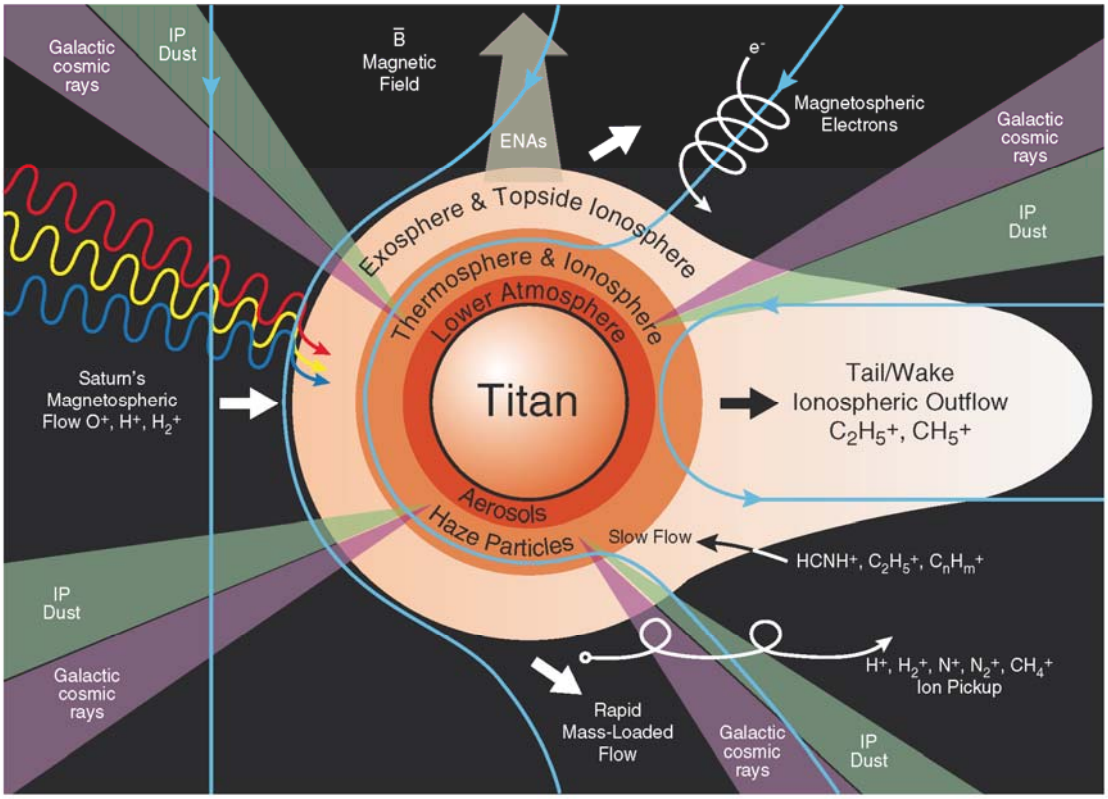

Figure 3.2.1-5 Energy deposition to Titan's upper atmosphere (modified by E. Sittler from figure in Waite et al., 2004)

Also shown on Figure 3.2.1-5 are pickup ions (PUI) from the interaction with Titan's exosphere which slows the external flow at high altitudes > 1400 km and leads to atmospheric escape of keV methane and di-nitrogen PUIs (Hartle et al., 2006a,b) and H^+ and H_2^+ PUIs at even higher altitudes where the H and H_2 corona can extend to Hill sphere distances ~ 55,000 km. The escape of methane from Titan's exosphere will translate to a methane torus in Saturn's outer magnetosphere with dimensions ~ 20 Saturn radii. The figure shows a more isotropic energy input to deeper altitudes from Galactic Cosmic Rays (GCR) with penetration below 100 km altitude (Fulchignoni et al., 2005) and Interplanetary Dust (IP) which can penetrate down to < 740 km altitudes (Molina-Cuberos, 2001). The IP dust flux will tend to peak on the side facing Titan's orbital motion around Saturn. In both cases ionization layers are produced deep into Titan's atmosphere where further chemistry can be driven. Additional growth of haze particles could occur in such layers and the free electrons can attach themselves to the aerosols producing negative heavy ions (Borucki and Whitten, 2008). The negative heavy ions formed in Titan's upper atmosphere (Coates et al., 2007) will fall to lower altitudes and result in a loss of ionospheric ions which must continuously replaced by the ionosphere (Sittler et al., 2008a). These heavy ions are now believed to be the primary source for the aerosols in Titan's lower atmosphere which then fall to the surface, where unknown organic and nitrile chemistry can occur. If the negative ions observed by Coates et al.

(2007) are fullerenes (C_{60}) then magnetospheric keV oxygen ions from Enceladus can become trapped inside the fullerene cages and be a source of free oxygen in the aerosols and thus the surface chemistry (Sittler et al., 2008a).

It is thus essential to determine the ion and neutral composition of the ionosphere with a mass range and resolution allowing the detection and characterization of a very wide range of compounds.

The Cassini observations have also revealed that Saturn's magnetosphere is deformed into a magnetodisk configuration at Titan orbital distances for Saturn local times (SLT) dusk to midnight to dawn LT while more dipolar on the dayside near noon LT. This deformation is ultimately driven by the large amounts of water vapor dumped into Saturn's magnetosphere by Enceladus (originating in a hot interior (Matson et al., 2007)) and possibly other icy moons. As shown in Sittler et al. (2008b), the heavy ions will be confined within a few degrees of the magnetodisk current sheet and light ions will dominate at higher magnetic latitudes, while for dipolar field lines heavy ions are more likely to be encountered by Titan. When heavy ions dominate the external flow the energy input of the magnetosphere can be orders of magnitude greater than that when the field is more disk-like and light ions such as H^+ and H_2^+ dominate the ion composition. In some cases, when Titan encounters the magnetodisk current sheet plasma the heavy ions will be highly abundant and a very high energy encounter can occur such as the T5 Cassini encounter (Sittler et al., 2008b). The TSSM observations will allow us to quantify this phenomenon in order to estimate the long-term energy input to Titan's atmosphere and corresponding atmospheric loss and formation of the complex organic and nitrile chemistry within Titan's ionosphere.

With the current picture of Titan’s organic chemistry, the chemical evolution of the main atmospheric constituents – di-nitrogen and methane – produces complex refractory organics which accumulate on the surface together with condensed volatile organic compounds such as HCN and benzene. The second most abundant constituent, methane, is dissociated irreversibly to produce hydrocarbons (e.g. C_2H_2, C_2H_4, C_2H_6 and C_3H_8) and nitriles, (e.g. HCN, HC_3N), from the coupled nitrogen chemistry (Figure 3.2.1-1). CIRS, on board Cassini has detected these organics in Titan’s stratosphere and determined their spatial and vertical distributions (Coustenis et al., 2007). Comparisons with previous Voyager and ISO results (Coustenis et al., 1998; 2003) have not yet pointed to any significant temporal variations of these species, but the seasons of these measurements were very similar (Figure 3.2.1-2). On the other hand, many of the neutral constituents predicted by models and laboratory measurements and listed on CIRS “shopping list” have failed to turn up (Flasar et al., 2004). The reason could be the geometry or the rarity of the observations, or the detection limit of the instrument.

A mission like TSSM, carrying both a thermal and a sub-millimeter high-sensitivity spectrometer, will be able to significantly improve on our understanding of the degree of complexity attained by Titan’s organic chemistry.

A rich set of chemical, radiative, and dynamical feedbacks is associated with the evolution of the polar hood, with many analogies to the ozone hole on Earth. Cassini may observe the early decay of that in the north, and TSSM should be able to observe the formation of a corresponding feature in the south. Moreover, HST observations of the decay of the south polar hood (Lorenz et al. 2005) at the same season (late southern summer, 2002–2003) show that there are substantial year-to-year changes to observe. An important aspect of studies of these features with a follow-on mission is

not only to observe the optical albedo (possible only in illuminated areas) but to observe the coupled temperature, composition, haze and wind fields, at both poles, in order to disentangle the chain of cause and effect and its seasonal dependence (Figure 3.2.1-2).

A final, and perhaps unexpected, analogy could be made between Titan and many extrasolar planets, if moons like Titan orbit the "hot Jupiters" that have been discovered. These moons would be close enough to the star to have the warmth necessary to develop a "habitability zone" or at least enough to be able to host advanced organic chemistry. Indeed, many of the known planets are close enough to their primary star to be tidally locked and thus rotate synchronously. However, nonzero eccentricity (as for Titan) may mean that there nonetheless are significant tidal effects. Walterscheid and Schubert (2006) have suggested that tidal forcing may be responsible both for the wind shear layer measured by Huygens Doppler tracking (Bird et al., 2005) and for the distinct haze layers observed in Cassini images of Titan's atmosphere. Thus, Titan may provide insight into models of circulation and opacity structure of extrasolar planets.

3.2.2 TITAN'S ORGANIC CHEMISTRY AND ASTROBIOLOGICAL POTENTIAL

The Cassini-Huygens era of investigation has furthered our understanding of Titan as the largest abiotic organic factory in the solar system. The abundance of methane and its organic products in the atmosphere, seas and dunes exceeds by more than an order of magnitude the carbon inventory in the Earth's ocean, biosphere and fossil fuel reservoirs (Lorenz et al. 2008a). Mass spectrometry in the upper atmosphere has shown that the process of aerosol formation appears to start more than 1000 km above the surface through a complex interplay of ion and neutral chemistry initiated by energetic photon and particle bombardment of the atmosphere (Waite et al. 2007), and that it includes polymers of high molecular weight—up to and certainly beyond the C_7 hydrocarbons that the Cassini mass spectrometer was able to measure. Measurements throughout the atmosphere, both remotely and *in situ*, have indicated the presence of numerous hydrocarbon and nitrile gases, as well as a complex layering of organic aerosols that persists all the way down to the surface of the moon (Coustenis et al. 2007; Tomasko et al. 2005; Israel et al., 2005), although their molecular composition remains to be determined. Radar observations suggest that the ultimate fate of this aerosol precipitation is the generation of expansive organic dunes that lie in an equatorial belt. These sand dunes are remarkable in being exactly the same size and shape as linear (longitudinal) dunes on Earth (Lorenz et al. 2006) such as those found in the Namib and Saharan deserts. This type of dune forms in a fluctuating wind regime, which on Titan may be provided by the tides in the atmosphere due to Saturn's gravitation acting over Titan's eccentric orbit.

While the chemical reactions that drive living things take place in liquid water, the reactions themselves are almost entirely between organic (i.e., carbon-bearing) compounds. The study of organic chemistry is an important, and arguably richer, adjunct to the pursuit of liquid water in the solar system. Titan's organic inventory is, as noted above, nothing short of massive, and organic compounds are widespread across the surface in the form of lakes, seas, dunes and probably sedimentary deltas at the mouths of channels.

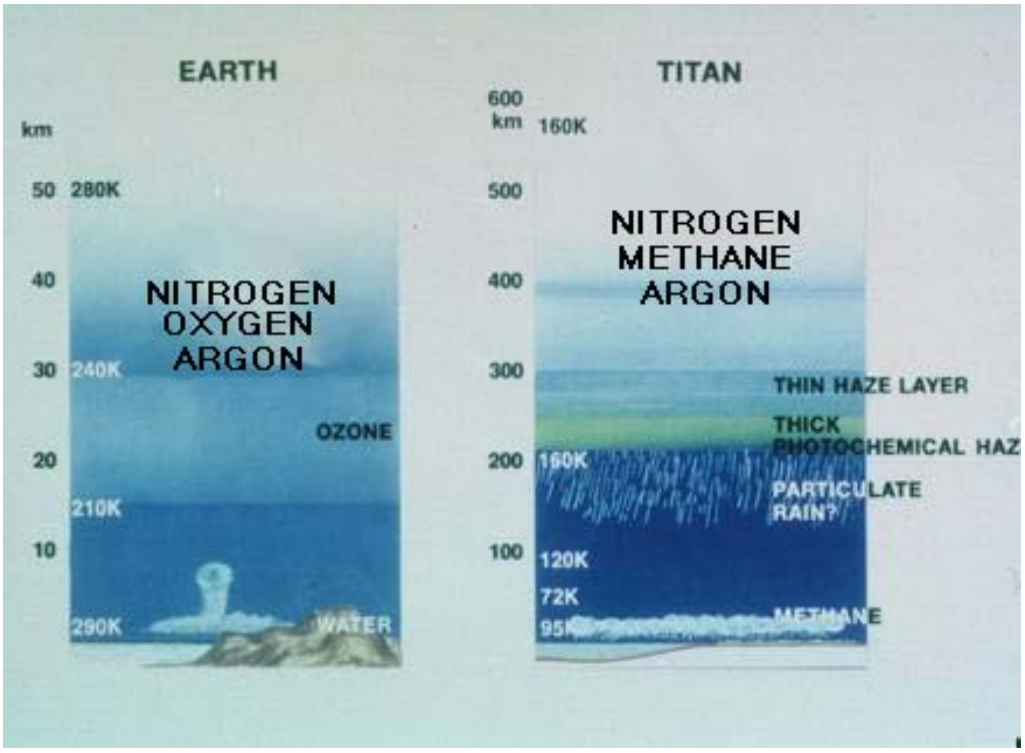

Figure 3.2.1-6 Atmospheric structure of Titan and the Earth. In the case of Titan, argon is a minor constituent (much less than CO for instance), found in the form of ^{40}Ar, degassing from the interior by ^{40}K disintegration. *http://saturn.jpl.nasa.gov/multimedia/images/image-details.cfm?imageID=1105*

In Titan's present, highly reducing atmosphere (Figure 3.2.1-6), photochemistry alone is something of an evolutionary dead end, in that only hydrocarbons and nitriles (i.e., H, C, and N-bearing molecules) are formed in any abundance. Oxygen-bearing compounds are generally too refractory to have a significant presence in Titan's atmosphere—water vapor and carbon dioxide have been detected in IR spectroscopy at part-per-billion levels (Coustenis et al., 1998; Samuelson et al., 1983), but probably (like the traces of sodium and iron in the Earth's upper atmosphere) derive from outside, from the ablation products of meteoroids and possibly Enceladus.

However, as noted by Thompson and Sagan (1992), tholins deposited on Titan's surface might be able to take the next evolutionary step by reacting with transient exposures of liquid water, namely impact melt and cryovolcanic magmas. Subsequent work has confirmed that such geological structures would indeed permit aqueous chemistry to occur for centuries or longer (e.g., O'Brien et al. 2005; Neish et al. 2006). Laboratory experiments have shown that the interaction of water with tholins can yield amino acids in substantial amounts— roughly 1% by mass (e.g., Khare et al. 1986; McDonald et al. 1994). Simpler nitriles have been detected in the gas phase on Titan (and indeed in the solid phase [Khanna 2005a,b; 2007]). These nitriles will be deposited as condensate on the surface and also can react to form astrobiologically interesting material in water. For example, Ferris et al. (1978) show that moderately concentrated HCN solutions can hydrolyze to form oligomers that in turn yield amino acids and pyrimidines. (Purines and pyrimidines—organic rings with some substitution of carbon atoms by nitrogen—form the bases that encode information in DNA in terrestrial living things; this information is used to determine the sequence of amino acids used to assemble into proteins).

Laboratory work is needed to explore the temperature- and pH-dependence of the rates and yields of these reactions, although Titan reactions on a geological timescale cannot be reproduced on Earth, at least not on conventional research timescales. Other factors (e.g., inorganic catalysts, or the pressure and concentration enhancements that can occur at a freezing front) may accelerate these reaction rates; for example, Takenaka et al. (1996) explored how freezing can accelerate by a factor of 100,000 the oxidation of nitrite by dissolved oxygen to form nitrate.

Specific geological sites such as the lakes, the floors of impact features and the margins of cryovolcanic flows would of course be of particular interest for these investigations, but data at the scale of Cassini (or even a Titan orbiter) do not permit confident determination of the feasibility of landing or acquiring desired samples (aerosols or liquid, collected by the instruments on the *in situ* elements). However, the ample evidence of fluvial and aeolian transport on Titan suggests that sediments everywhere likely contain a component of eroded material from such structures, which would be all the more concentrated in lakes. Therefore, *in situ* sampling sites that are large in scale and are likely repositories of such sediments is of high priority. Two such units are the equatorial dunes, which are likely a vast repository of organic sediments (Radebaugh et al. 2007) and the large northern hemisphere seas and lakes, which, if composed of ethane and methane (Brown et al. 2008), could contain within them analyzable amounts (Raulin 1987; Dubouloz et al. 1989) of dissolved organics from elsewhere on Titan. The current TSSM scenario envisions the probe landing in a lake in the North Polar region of Titan.

Titan is an exotic organic place, which is certain to tell us much about the processes of chemical evolution that may lead to life. It is also highly complementary to Mars in terms of questions of origins of life, in that Mars is an oxygen- and water-rich body, with little if any organic carbon, while Titan is an organic-rich body with little available oxygen.

Evidence of an internal water ocean on Titan, which would be confirmed by this mission, opens the possibility of looking for potential habitats. A significant geophysical difference with Europa is that on Titan the liquid water is not currently in contact with a silicate core. However, it has been noted that Titan's internal ocean might support terrestrial-type life forms that would have been introduced there previously, or would have formed when liquid water was in contact with silicates early in Titan's history. During the warmer stage some nutrients would have been available for supporting life. The surface of Titan appears (like those of Mars and Europa) an unlikely location for extant life, at least terrestrial-type life. Nevertheless, cryomagmatism can conduct internal liquids to the surface and expose the composition of water reservoirs for their remote analysis. McKay and Smith (2005) have noted that there are photochemically-derived sources of free energy on Titan's surface which could support life, although it would have to be an exotic type of life using liquid hydrocarbons as solvents (Committee on the Origin and Evolution of Life 2007). In a similar vein, Stoker et al. (1990) observed that terrestrial bacteria can in fact derive their energy and carbon needs by 'eating' tholin. In this sense, a methane-rich atmosphere may act as a 'poor-planet's photosynthesis', providing a means to capture the free energy from ultraviolet light and make it available for metabolic reactions.

The extent to which present-day Titan resembles the prebiotic Earth is not clear, since the oxidation state of the early Earth is not well determined. Certainly Titan is currently more reduced than was Earth, but formation of organic haze on the latter may nonetheless have taken place. Trainer et al. (2004) show that organic haze formation under UV illumination takes place as long

as the carbon-to-oxygen ratio is above about 0.6, and methane photolysis would have provided a richer organic feedstock than the delivery of organics from meteorites. In addition to the prebiotic synthesis role, haze on the early Earth may have been significant in the radiative balance (acting as an antigreenhouse agent) and in particular in providing UV opacity which may have protected nascent biota in the absence of an ozone shield. Thus, while the analogy of Titan to the early Earth is not perfect, it is clear that there are insights to be gained from studying Titan, and furthermore that there may be more Titan- and Earth-like planets in the universe, about whose habitability Titan may usefully inform us.

3.2.3 TITAN'S SURFACE

That the surface of Titan was largely hidden from Voyager's view precluded much understanding of its landscape before the development of Cassini. The detection of rotational variability in Titan's radar and near-IR albedo in the early 1990s suggested that the surface was not homogenous, as might have been expected from a uniform deposition of photochemical debris— something had to be making or keeping bright areas bright and dark areas dark. The variegated surface was revealed with near-IR images by HST in 1994, yielding the first maps (e.g., Smith et al. 1996). However, the poorly resolved patterns of bright and dark gave few clues to these areas' origin, and efforts to interpret the near-IR albedo in the few methane window regions in which the atmosphere is transparent did little more than suggest "dirty ice," with various compositions and amounts of contaminants suggested.

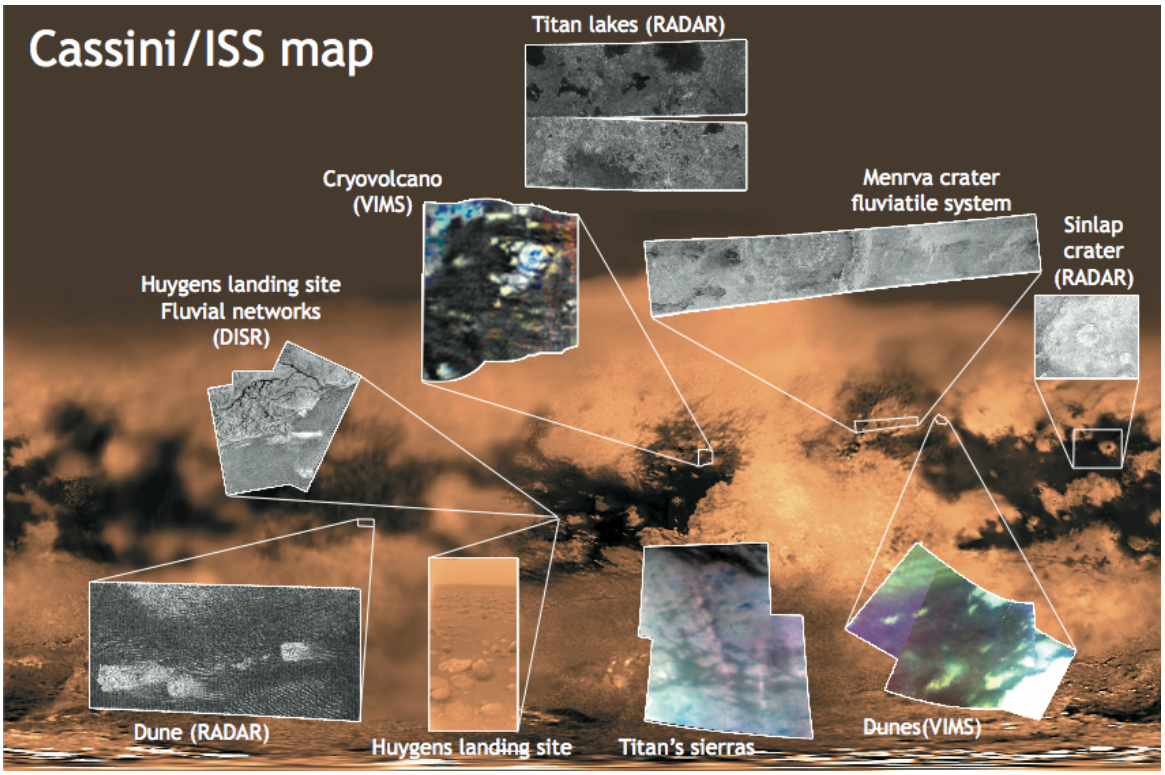

Figure 3.2.1-7 The diversity of Titan's surface: geological features discovered by Cassini/Huygens, many of which remain to be explained. Future landing locations will be selected among such sites. (Credit: Univ. Nantes & CIGAL/LESIA)

The first Cassini data (e.g., Porco et al. 2005; Elachi et al. 2005; Sotin et al. 2005) showed that Titan has striking surface features on all scales, the result of a variety of geological processes (Figure 3.2.1-7). The pattern of bright-dark boundaries is reminiscent in places of terrestrial shorelines; a striking and as yet unexplained observation is that bright–dark contrasts are muted at mid-latitudes.

One remarkable surprise is the relative paucity of impact craters, indicating a relatively young and active surface. Only a handful of impact structures have been named on Titan, ranging from 27 to 440 km in diameter, although some dozens of other likely candidates are identified. Most striking of these are the bright rings such as Guabanito, whose floors are covered in dark sediment (in some places visibly sculpted into dunes). It seems likely that a substantial population of impact structures is buried on Titan, and could be revealed (as in the Martian low-lands [e.g. Buczkowski et al., 2005]) by ground-penetrating radar measurements on TSSM. The present inventory of impact structures, or even that expected by extrapolation into Cassini's extended mission, is too sparse to draw strong conclusions on issues such as leading-trailing asymmetry. Titan's craters appear in some ways to differ morphologically from those on other icy satellites, perhaps due to effects of the atmosphere or subsurface volatiles.

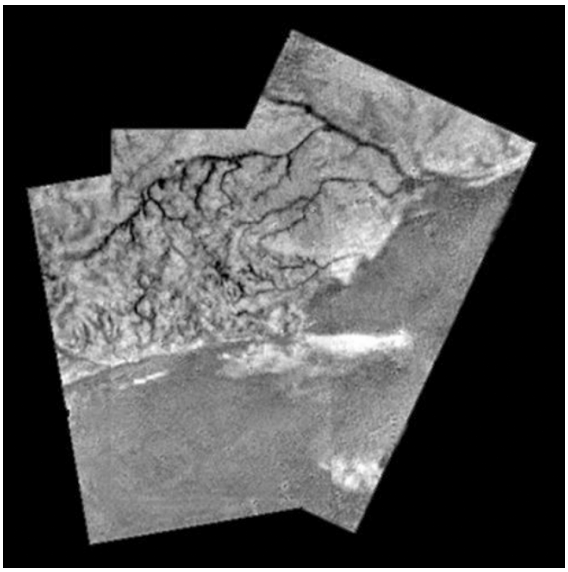

Figure 3.2.1-8 Fluvial features at the Huygens landing site.

Fluvial modification of the surface was very evident at the Huygens landing site (**Figure** 3.2.1-8; Tomasko et al., 2005; Soderblom et al., 2007a]). Not only were steeply incised channels a few kilometers long and ~30 m across observed in the bright highland (which models of sediment transport suggest can be formed in methane rainstorms (Perron et al. 2006)), but the knee-height vista from the probe after landing showed rounded cobbles characteristic of tumbling in a low-viscosity fluid (Tomasko et al., 2005; Soderblom et al., 2007a). Radar and near-infrared imagery has revealed channels on much larger scales than those seen by Huygens.

Radar-bright channels (probably cobbled streambeds like that at the Huygens landing site) have been observed at low and mid-latitudes (Lorenz et al. 2008a), while channels incised to depths of several hundred meters are seen elsewhere, and at high latitudes radar-dark, meandering channels are seen that suggest a lower-energy environment where deposition of fine-grained sediment occurs. Whether these larger channels—some of which exceed a kilometre in breadth—and the large-scale flow features near the landing site (Soderblom et al. 2007a,b) would require a different climate regime to be formed remains to be determined. The flow of methane rivers in an unsaturated atmosphere on Titan is very analogous to the problem of ephemeral water flow on Mars—determining whether the rivers dry out, freeze solid, or drain into an ephemeral sea will require presently unknown topographic and meteorological factors.

Beginning in July 2006, there were a series of flybys of the high northern latitudes of Titan during which the RADAR instrument imaged a variety of very dark features that have been interpreted to be liquid-filled basins—"lakes" (Stofan et al. 2007). The features range in size from less than 10 km2 to at least 100,000 km2. They are confined to the region poleward of 55°N. To date some 655 such features have been identified and mapped over 7 Titan flybys (Hayes et al. 2008) (Figure 3.2.1-9).

Mapping by Hayes et al. (2008) indicates that above 65°N the dark lakes occupy 15% of the imaged surface (which to date is about half of the total surface area of that part of Titan). Bright lakes—features that appear similar to the radar-dark lakes but have little or no brightness contrast with their surroundings— occur equatorward of 70°N. An intermediate class of lakes has a latitudinal distribution similar to that of the bright lakes. Neither is seen above 77°N, where the dark lakes predominate. Size selection does not appear to be present in the dark lakes; both very large and very small examples exist.

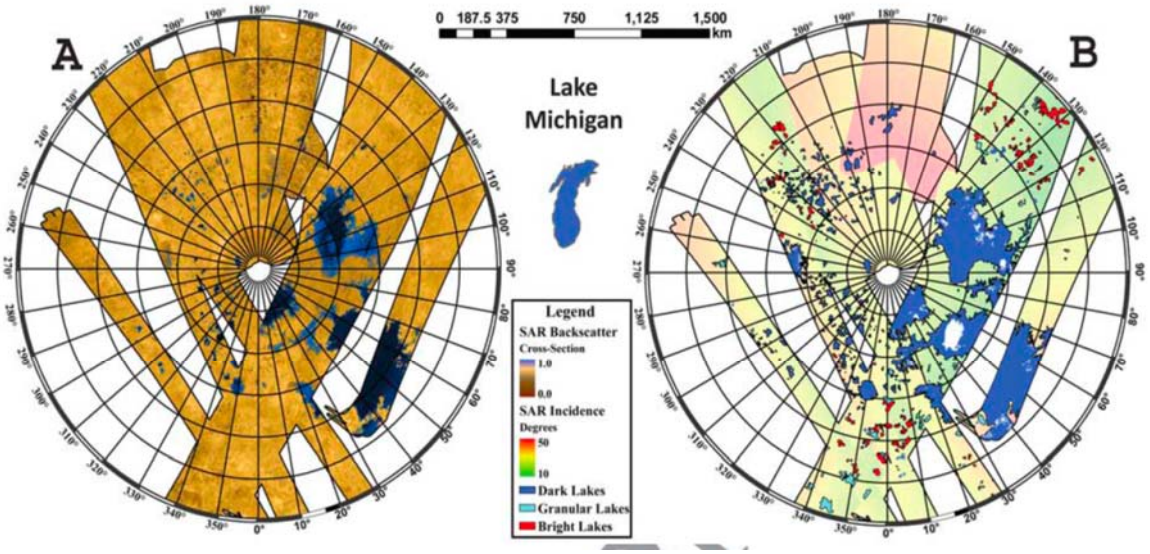

Figure 3.2.1-9 RADAR mosaic (left) and map (right) of the northern hemisphere lakes and seas.

The hypothesis that the dark lakes are filled with liquid is (Stofan et al. 2007) based on several arguments. First, the dark lakes are in many, but not all, places extremely dark, with reflectivity values below the noise level of the RADAR system. Since synthetic aperture radar (SAR) imagery does not operate at 0° — nadir incidence — the lack of return indicates reflection off a surface smooth on the scales of the 2.16 cm wavelength of the radar system. A calm liquid surface or very smooth solid surface would produce this result. The Huygens landing site was littered with 1–10 cm scale pebbles (Tomakso et al., 2005) and appeared bright to Cassini's RADAR (Lunine et al. 2008); features as radar-dark as the lakes do not appear at equatorial or mid-latitudes. Evidently, then, the physical surface causing the coherent reflection away from the antenna is typical only of the high latitudes and not simply of plains areas devoid of pebbles. Thus, either liquid or a recently frozen, smooth, surface is required.

Second, radiometry measuring the natural thermal emission at the 2.16 cm wavelength of the Cassini RADAR indicates that the dark lakes emit more thermal energy than the surroundings—

consistent with hydrocarbons and inconsistent with a smooth surface of water ice or ammonia-ice (Paganelli et al. 2007), assuming the exposed surrounding crustal material is water ice. Third, the morphology of the boundaries between the largest of the dark lakes and the surroundings often resembles a terrain flooded by liquid, with the dark material appearing to fill valleys between hilly terrain and in some cases occupying networks of channels that feed into or out of the lakes Finally, the latitudinal restriction on the occurrence of the dark lakes is consistent with global circulation models that predict precipitation of methane onto both or at least the winter pole (Rannou et al. 2006) together with the decrease in surface temperature poleward (Flasar et al. 2005). Currently the northern pole is approaching spring equinox in an annual cycle that is 29.5 years in length (Figure 3.2.1-2).

All of the above provide circumstantial support for the hypothesis that the dark lakes are filled with liquid, but a definitive demonstration must await identification of liquid methane or ethane, or both, in the lakes, from the Cassini VIMS instrument. Liquid methane is difficult to detect given the large abundance of gaseous methane that dominates much of the near-infrared spectrum from 1–5 microns; liquid ethane features are potentially more detectable. Because the northern reaches are just now experiencing the onset of spring, the Sun is low on the horizon above 64°N given Titan's axial tilt of 26° (Stiles et al. 2008). As the season advances, spectra with progressively higher signal-to-noise on the larger lakes (which are large enough that the IAU has designated them "mare," or seas) may test whether either of the two primary liquids in Titan's hydrological cycle are present in the lakes. Liquid ethane is easier to detect as liquid and VIMS has done so in Ontario Lacus in the southern hemisphere (Brown et al., 2008; Raulin 2008). The northern hemisphere is still too dark to seek ethane in the lakes and must await more sunlight as spring progresses.

Assuming, as is suspected from circumstantial evidence and the indication of liquid ethane in the southern hemisphere's Ontario Lacus (Brown et al., 2008), that the darkest of the northern hemisphere lakes are filled with liquid, knowing their depths is of great interest both to constrain the total amount of liquid they contain and to understand the underlying geological processes that formed them. Both methane and ethane are relatively transparent at 2-cm wavelength, with recent laboratory measurements suggesting absorption lengths (1/e diminution of the signal) of order meters (Paillou et al. 2008). The darkest lakes may therefore have depths that exceed of order 10 m, while the intermediate lakes may be sufficiently shallow that RADAR can see to the bottom. Features seen in the intermediate lakes, such as channels, are consistent with shallow lakes that periodically empty and are then subjected to channel formation through flow of methane from the surroundings.

With 22% of Titan's surface now imaged by RADAR, and the lakes covering 2.4% of this area, roughly 0.6% of Titan's surface is potentially covered by liquid methane and ethane if the remaining unimaged parts contain no lakes. Near-global coverage at 938 nm by Cassini's Imaging Science Subsystem (ISS) suggests that features consistent with lakes and seas cover 1% of Titan's total surface (Turtle et al., 2008). Mitri et al. (2007) constructed a simple model of evaporation off of high-latitude lake surfaces to show that this amount of surface liquid, coupled with advective rates consistent with plausible wind speeds of 0.1–1 m/s (Tomasko et al. 2005), is sufficient to maintain the relative humidity of methane globally on Titan at its present value. However, for an average lake depth of 20 m the reservoir of methane in the lakes is between 1/30 and 1/3 the methane atmospheric inventory (Lorenz et al. 2008b), insufficient to account for the additional

methane required to humidify the equatorial atmosphere and permit the convectively triggered rainstorms that appear to be required to form the dendritic features at the Huygens site. Either the lakes are on average at least an order of magnitude deeper than the minimum inferred from the radar absorption lengths, or additional methane is present in subterranean porous or fractured media (Hayes et al., 2008). Alternatively, the dendritic features might be a relic of a wetter recent past.

Even if the average lake depth is only 20 m, the amount of liquid in the lakes is substantial: two orders of magnitude larger than the known oil and gas reserves on the Earth (Lorenz et al. 2008b). Equally impressive is the range of morphologies of the lake and sea features observed to date, from flooded canyonlands to what appear to be liquid-filled calderas (Hayes et al., 2008).

In contrast to the extensive coverage by RADAR in the northern hemisphere, only one radar pass has been made of the southern hemisphere, revealing only two fairly small lakes. The rest of the terrain appears hilly and there are no obvious dry lake basins as in the northern hemisphere. However, ISS images (at much lower spatial resolution than the 350–1000 m achievable with Cassini RADAR) show the kidney-shaped dark feature about 235 km in length, named Ontario Lacus, which is outside the area of radar coverage, as well as numerous other dark features which could be lakes (McEwen et al. 2005; Turtle et al., 2008). The observation early in the mission of extensive south polar convective clouds (Porco et al. 2005) that subsequently disappeared almost entirely (Schaller et al., 2006) suggests that a source of condensed methane exists or existed very recently in that hemisphere; it is possible that additional radar imagery of the southern hemisphere will reveal lakes or lake basins akin to those in the north. Another possibility is that, in the intervening time (2.5 years), changes in the distribution of south-polar surface liquids have occurred (Turtle et al. 2008). If such rapid changes do occur, then repeated monitoring of the polar regions with Cassini and later on with TSSM will be important for understanding the methane cycle as well as assessing the total methane inventory.

Aeolian activity on Titan has proven to be one of the major forces at work at low latitudes. Almost half the terrain within 30° of the equator is covered in dark (presumably organic-rich) streaks or dunes (Lorenz et al., 2006). In a few of the best-imaged regions, these dunes prove to be many tens of kilometers long and about 150 m high. Almost all appear to be linear (longitudinal) dunes, a type common in the Arabian, Sahara, and Namib deserts on Earth, but very rare on Mars; such dunes form typically in bidirectional wind regimes. A tidal wind origin has been proposed for Titan, but seasonal wind changes may play a role. It is assumed, but has not been shown, that these dunes are presently active. They are certainly young relative to other geologic features.

Titan's tectonism is not well understood. A number of very-large-scale linear features are seen optically (Porco et al. 2005), notably the dark dune-filled basins Fensal and Aztlan (known collectively as the "H"). Smaller-scale "virgae" are also seen but are not understood. Radar imagery of some of these features has not helped in their interpretation and is not yet sufficiently widespread to evaluate tectonic patterns, although some linear mountain ranges (Radebaugh et al. 2007) have been detected, several forming a chevron pattern near the equator. Near-IR imagery by Cassini VIMS has also shown long ridges (**Fig. 3.2.1-7**). An outstanding mystery is the nature of the large bright terrain Xanadu and its adjoining counterpart Tsegihi. These areas are distinct optically, and they have unusual radar properties. SAR imagery shows Xanadu to be extremely

rugged, much like the Himalayas on Earth, although the mountain-forming process(es) on Titan has (have) not been robustly identified and may differ from place to place.

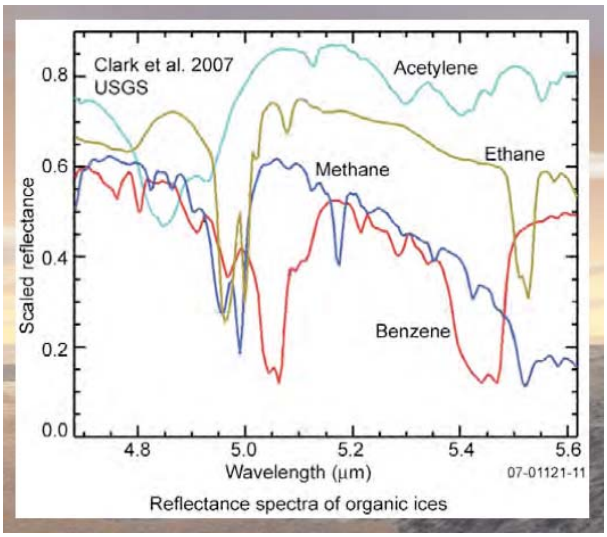

Figure 3.2.1-10. *Spectra of organics that can be observed in the 5-6 micron region.*

Cryovolcanism is a process of particular interest at Titan because of the known astrobiological potential of liquid water erupting onto photochemically produced organics (Fortes et al., 2006). Radionuclides in Titan's interior, possibly augmented by tidal heating, can provide enough heat to drive a substantial resurfacing rate. Kinetically cryovolcanism is much easier in the Saturnian system, where ammonia can facilitate the rise of water through an ice crust. Ammonia not only depresses the freezing point of water by some 97 K, but also lowers the density of the fluid, thus avoiding the negative buoyancy that likely inhibits cryovolcanism on the Galilean satellites (Fortes et al., 2007). Several likely cryovolcanic structures have been identified in Cassini near-infrared (Sotin et al. 2005) and radar (Lopes et al. 2007) images. Although evidence for active volcanism has not yet been widely convincing, there are apparent surface changes in Cassini data that require explanation (e.g., Nelson et al., 2006).

Initial altimeter observations suggested that Titan was rather flat (elevation changes of only a few tens of meters over hundreds of kilometers). Indeed, some sedimentary basins appear to be this flat, but Titan in fact shows substantial relief. Mountain chains with heights in excess of 700 m have been measured (e.g., Radebaugh et al. 2007), and the crater Sinlap is known to be 1300 m deep (Elachi et al., 2006). As more data are acquired, it is clear that Titan in fact has significant topography (>1 km) on a variety of length scales (Lorenz et al., 2008e). Cassini is not well equipped to generate a global topography dataset; therefore generating such data is a key goal for a follow-on mission, not only for geological studies but also as a boundary condition for atmospheric circulation models.

An important Cassini finding needs to be underscored—at all spatial scales, there are structures seen in radar images that correlate with those in the near-IR, however, there are also structures that do not correlate at all. Radar and optical data thus tell us very complementary things about Titan's surface, and consequently a follow-on mission requires high-resolution global coverage by both techniques. In the near-IR, high-resolution coverage is particularly lacking from Cassini because of the short, rapid flybys. While the surface is spectrally diverse the identification of surface materials in the spectral windows Cassini is able to observe has proven challenging, making the extension to slightly longer wavelengths (in the region from 5 to 6 microns; Figure 3.2.1-10) highly desirable.

3.2.4 TITAN'S INTERIOR AND ORIGIN AND EVOLUTION PROCESSES

Titan's overall density (1.88 g/cm^3) requires it to have roughly equal proportions of rock and ice. After It's accretion, Titan was probably warm enough to allow differentiation into a rocky core with a water/ice envelope, but whether an iron or iron–sulfur core formed during the subsequent evolution remains uncertain. Thermal evolution models suggest that Titan may have an icy crust between 50- and 150-km thick, lying atop a liquid water ocean a couple of hundred kilometers deep, with some amount (a few to 30%, most likely ~10%) of ammonia dissolved in it, acting as an antifreeze. Beneath lies a layer of high-pressure ice (Figure 3.2.1-11). The presence of ammonia in the interior is suggested by the existence of the nitrogen atmosphere, presumably derived from the conversion of ammonia during the early stage of Titan's evolution. Cassini's measurement of a small but significant non-synchronous contribution to Titan's rotation is most straightforwardly interpreted as a result of decoupling of the crust from the deeper interior by a liquid layer (Lorenz et al. 2008e).

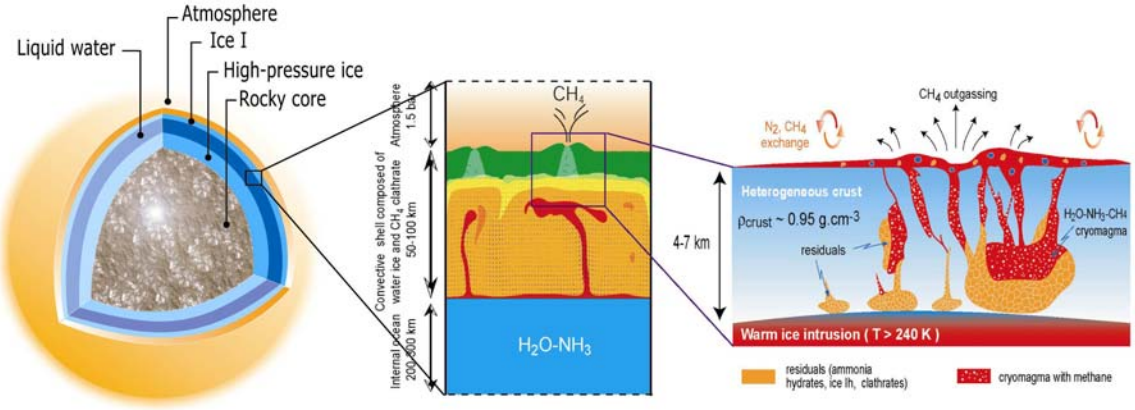

Figure 3.2.1-11 Possible interior structure and cryovolcanic processes on Titan (after Tobie et al. 2005, Choukroun et al. 2008).

The non-zero eccentricity of Titan's orbit also provides key information on its interior. First, the existence of a high eccentricity more than four billion years after the satellite formation, whereas any other satellite in its vicinity is able to significantly force it, indicates that Titan possessed an even larger eccentricity in the past than then progressively decayed owing to tidal dissipation. A thermal evolution model by Tobie et al. (2005) suggests that Titan's icy crust was in fact as thin as Europa's (~15 km) and has experienced tidal stresses similar to Europa's for much of Titan's history, and only thickened to ~50–100 km in the last 500 million years or so (perhaps not coincidentally, the crater retention age determined by Porco et al. 2005 and Lorenz et al. 2007b). Second, the present-day eccentricity of 3% results in a periodical fluctuation of Titan's gravitational coefficients, C_{20} and C_{22}, which should be detectable by the Cassini gravity measurements (Rappaport et al. 2008). These coefficients will change appreciably if the interior is fluid enough to respond to the changing tidal potential. It is expected that the tidal Love number k_2, which is proportional to the gravitational fluctuations, can be determined with modest precision (~0.1), enough to discriminate between the internal ocean and no-ocean cases.

A series of measurements by a Titan orbiter is required to more quantitatively constrain the internal structure, measuring the amplitude of the tidal Love number k_2 and the time lag of the interior response relative to the tidal forcing, and determining higher-order (up to degree 5 or 6) gravity coefficients. (Even after only a few days the tracking dataset for the orbiter would surpass the Cassini data.) The gravity coefficients may shed light on whether continental-scale features on Titan such as Xanadu have associated gravity anomalies. The geodetic combination of orbiter tracking and precision surface ranging by altimeter has been shown at Mars to be very powerful: in addition to k_2 (which reflects the tidally-induced change in mass distribution), surface height changes of several meters detectable by a radar altimeter can also constrain the h_2 Love number and hence reveal the presence of an internal ocean and constrain the thickness of the ice shell.

Titan's rotational dynamics are also a window into its interior. As on Earth, the rotation period of the surface can change over the course of a year as a result of changes in atmospheric angular momentum (Tokano and Neubauer 2005). On Titan, these changes are significant, altering the day length by some hundreds of seconds, leading to many tens of kilometers of displacements if the crust is decoupled from the interior by an ocean, as seems to be the case (Lorenz et al. 2008e). The pole position of Titan also has significance—gravitational torques should cause this to precess (in a Cassini state, the orbit normal and rotational pole precess together, with the obliquity between them dependent on the body's moment of inertia) with a period of around 600 years, perhaps a short enough timescale for differences between a Cassini determination and a follow-on mission to be noticeable. Radar imagery is particularly suited to rotation determination, although with adequate orbital position and attitude knowledge, near-IR sensing may work too.

Accurate determination of Titan's rotation state could be aided by the delivery of a geophysical package onto the surface (currently under consideration for studies during the next phase is a geophysical package to be delivered to the surface carried by the heat shield in the Montgolfière Probe), by using radio tracking techniques similar to those used from Mars with Pathfinder. A single high-frequency seismometer will also answer fundamental questions about Titan: it will reveal if the moon is tectonically active at present time, and the record of seismic signals combined with radar subsurface sounding from the Montgolfière will constrain the subsurface structure of the icy crust.

Magnetometry is a proven tool in the investigation of planetary interiors. In particular, the field generated in an electrically conductive ocean by currents induced by a varying primary field has been used to infer an ocean on Europa. This technique can be applied to Titan, but is more of a challenge because of the much smaller magnetic stimulation by the near-polar Saturnian field and the shielding due to Titan's ionosphere. A magnetometer carried below Titan's ionosphere, by lander or balloon, provides the opportunity to seek the signature of such a field, and in any event will provide a much more sensitive limit on (or actual detection of) a permanent magnetic field for Titan.

Finally, a conductive water–ammonia ocean can act as the lower boundary of a waveguide cavity, with the ionosphere as the upper boundary. This cavity resonates, providing a set of harmonics (the Schumann resonances – on Earth with frequencies of ~8 Hz, 14 Hz, 22 Hz, etc.) in magnetic and electrical field measurements. An electric field sensor on the Huygens probe detected signals that might have been due to Schumann resonance (Simões et al. 2007), but alternative explanations during the probe's dynamic descent, such as parachute oscillations, are possible. A more quiescent

platform such as a lander or balloon will be a far more sensitive means of detecting any Schumann resonance. It is important to obtain a reliable and interpretable detection of this phenomenon because of the significant implications for the presence of a conducting liquid below Titan's crust.

The suite of tools made available by the combination of an orbiter, a Montgolfière and a surface geophysical package[1] (gravity, tidal distortion, rotation, subsurface sounding, and magnetometry) offers a robust capability to probe Titan's present-day interior, exposing not only an icy satellite interior in ways not possible at other satellites, but also allowing an understanding of the particular role interior processes have had in shaping the atmosphere and surface of Titan.

Information on the past evolution of Titan's interior and atmosphere is also available through the accurate measurements of the different volatile compounds present in today's atmosphere and onto the surface. The evolution of Titan's atmosphere operates on two quite different time scales. The longest timescale represented is the billion-year time scale commensurate with the origin and subsequent evolution of the overall system. This time scale is best studied by measuring the noble gas concentrations and their isotopic abundances, as well as the nitrogen and carbon stable isotope ratios. Cassini-Huygens has provided some important information in this regard. The abundance of the radioactively derived ^{40}Ar has indicated that only a few percent of the total volatile inventory has been outgassed from the interior (Waite et al. 2005; Niemann et al. 2005). Whereas, the relatively low abundance of the primordial ^{36}Ar isotope suggests that nitrogen was not delivered during Titan's initial formation as molecular nitrogen, but more likely as ammonia that underwent subsequent chemical conversion into N_2 — the predominant constituent of Titan's present day atmosphere. Furthermore, the enrichment of ^{15}N in N_2 to that of ^{14}N relative to a terrestrial reference suggest that as at Mars Titan has lost most of its nitrogen over the course of its evolution (Waite et al. 2005). This is substantiated by the measurement of isotopic separation in the upper atmosphere measured by the Cassini INMS and the escape of methane and hydrogen inferred from the altitude structure of these species in Titan's upper atmosphere (Yelle et al. 2006; and unpublished data analysis from Cassini INMS) and the modelling of hydrodynamic escape processes by Strobel (2008). Moreover, the non-detection of neon, krypton and xenon by Huygens raises fundamental questions about Titan's origin and evolution: have these compounds never been incorporated in Titan's building blocks, or have they been lost or recycled and hidden at the surface and in the interior since Titan's formation? The accurate measurements of the abundances of these noble gases and of their isotopic ratios will provide important clues about the origin and evolution of Titan, and about the overall role of escape, chemical conversion, outgassing and recycling in the evolution of Titan's atmosphere. In particular, the detection of radiogenically-derived isotopes of neon, xenon and krypton will constrain the evolution of the rocky core and the outgassing history of Titan. All these, must await new surface analysis techniques such as noble gas enrichment cells, which were not present on the Huygens GCMS (Niemann et al. 2005).

Escape processes can also be understood via *in situ* sampling of the plasma and energetic particle environment surrounding Titan and resulting from the interaction of Saturn's magnetospheric particles with Titan's thick upper atmosphere. The study that began during the Cassini-Huygens' mission will benefit greatly from a Titan-orbital mission that samples the atmosphere near the exobase as proposed for the mapping phase of the TSSM. Here a complement of plasma, fields,

[1] Such as a geosaucer, to be studied in the next phase of TSSM. This package would be carried by the Montgolfière Probe's heat shield and dropped somewhere near the equator to conduct, among other, a search for seismic signals.

and energetic particles experiments will be able to determine the three-dimensional structure of the sputtering interactions that lead to the heating and erosion of the upper atmosphere (De La Haye et al. 2007). By understanding the physics of these processes, TSSM measurements will allow scientists to extrapolate the escape processes back in time to appreciate their impact on the evolution of the Titan system.

The second time scale of relevance at Titan is that related to the irreversible conversion of the methane in the atmosphere into higher-order organic/nitrile compounds that eventually end up deposited on the surface of Titan. The irreversibility argument ties back to the escape of hydrogen from the system noted above, so that for each molecule of methane that is photolyzed, a molecular hydrogen molecule escapes. Given the present rate of photolysis and energetic-particle-induced conversion processes and the size of the present atmospheric reservoir of methane the atmospheric methane will be completely converted to higher order organics on a 70 million year timescale if not replenished from the interior. Current escape rates for methane cut this time scale by a factor of 2. Evidence for the replenishment of methane from interior processes is found by observing the ^{12}C to ^{13}C ratio forming the methane of the upper atmosphere. The measured value is near that of our terrestrial reference indicating that methane is resupplied and converted at a rate that prevents the buildup of the heavier isotope over time as is the case of nitrogen. The source of the resupply is a mystery that our future mission must address. Potential candidates include an evolving interior thermal history leading to episodic releases of methane over geological time (Tobie et al., 2006), methane clathrate dissociation, serpentinization processes in the interior, and perhaps reprocessing of higher order organics that have been buried by surface geological processes (see Atreya et al. 2006 for further discussion). In any event the methane/nitrogen conversion process that begins in Titan's upper atmosphere via ion neutral chemistry and leads to the creation of minor higher-order carbon and nitrile gases and their aerosol counterparts throughout the stratosphere is a story whose basic features have been revealed by Cassini-Huygens (Tomasko et al. 2005; Coustenis et al. 2007; Waite et al. 2007), but which begs for a follow-up mission to understand the secrets of the most active abiotic organic factory in the solar system and the ultimate fate of organic residues on its surface.

3.3 Science Goals, Objectives, and Investigations of the in situ *Elements*

The Titan Saturn System Mission *in situ* elements have been designed to respond to the following major two goals (a third one regarding Enceladus and Saturn's magnetosphere can only be addressed from the orbiter and is discussed in the NASA and the Joint ESA-NASA summary reports):

GOAL 1: Explore Titan: an Earthlike System- How does Titan function as a system? How do we explain the similarities and differences between Titan and other solar system bodies in the context of the complex interplay of the geology, hydrology, meteorology, and aeronomy present in the Titan system?

GOAL 2: Examine Titan's Organic Inventory - A Path to Prebiological Molecules. What is the complexity of Titan's organic chemistry in the atmosphere, within its lakes, on its surface, and in

its putative subsurface water ocean and how does this inventory differ *from known abiotic organic material in meteorites and therefore contribute to our understanding of the origin of life in the solar system?*

The *in situ* elements as defined in the current mission architecture comprise a hot-air balloon (Montgolfière) and a short-lived probe which will land in a lake or sea at northern latitude on Titan. An alternative option studied by the JSDT was a long-lived probe to land near the equator on solid ground. The lake lander was preferred over the hard lander on solid surface as it clearly provides easier access to the surface material for chemical analysis.

Additional long-term (2-Titan days, possibly more) investigations relevant to geophysical aspects of Titan's surface could be performed thanks to an Instrumented Heat Shield which would carry a geophysical package (or geosaucer, to be studied in the next phase) allowing for a number of additional investigations to be performed, including: measurements of a) the induced and inducing magnetic fields of Titan and their variation as Titan orbits Saturn with a magnetometer (additional to the balloon one), providing clues on the magnetic environment and possibly on the location and thickness of Titan's internal ocean; b) the tidally-induced solid crustal displacements and forced librations of the outer ice shell through the radio science equipment; c) the level of seismic activity on the surface, the structure of the outer ice shell and hence the internal ocean with a micro-seismometer (Lognonné 2005); d) the environment through an acoustic experiment.

In this subsection we go through the objectives associated with the two goals, and the investigations associated with each objective. To avoid excessive complexity in the narrative, a discussion of the measurements that can satisfy the investigations is deferred to the next subsection.

Thus, the two *in situ* elements currently planned will operate in synergy to achieve the scientific objectives given hereafter. A more detailed description of the science capabilities of the balloon, the lake lander and the optional solid lander will be given in section 3.4.

3.3.1 PRIMARY SCIENTIFIC OBJECTIVES

Primary scientific objectives for the *in situ* elements with the current model payload include

- Perform chemical analysis, both in the atmosphere (§3.2.1) and in the liquid of the lake, the latter to determine the kinds of chemical species that accumulate on the surface, to describe how far such complex reactions have advanced and define the rich inventory of complex organic molecules that are known or suspected to be present at the surface. New astrobiological insights (§3.2.2) will be inevitable from the balloon and the probe investigations.
- Analyze the composition of the surface, in particular the liquid material and in context, the ice content in the surrounding areas (§3.2.3).
- Study the forces that shape Titan's diverse landscape. This objective benefits from detailed investigation at a range of locations, a demanding requirement anywhere else, but that is uniquely straightforward at Titan with the Montgolfière high-resolution cameras and subsurface-probing radar (§3.2.4).

3.3.1.1 Top ten in situ *first-time investigations*

The Huygens probe carried by the Cassini spacecraft is the first human-made machine to ever land so far away from the Sun. In spite of its enormous success, returning to Titan with two additional *in situ* elements such as the equatorial montgolfière and the northern latitudes lake lander, carrying a whole new and more complete set of instrumentation, would allow scientists to achieve the following investigations for the first time:

1. First direct *in situ* exploration of the northern seas of Titan—the only known surface seas in the solar system beyond Earth.
2. Detailed images of thousands of kilometers of Titan terrain, with image quality comparable to that of Huygens during its descent will test the extent of fluvial erosion on Titan at Huygens spatial scales, well matched to the scales mapped globally by the orbiter.
3. First analysis of the detailed sedimentary record of organic deposits and crustal ice geology on Titan, including the search for porous environments ("caverns measureless to man") hinted at by Cassini on Xanadu.
4. Direct test through *in situ* meteorological measurements of whether the large lakes and seas control the global methane humidity—key to the methane cycle.
5. First *in situ* sampling of the winter polar environment on Titan—vastly different from the equatorial atmosphere explored by Huygens.
6. Compositional mapping of the surface at scales sufficient to identify materials deposited by fluvial, aeolian, tectonic, impact, and/or cryo-volcanic processes.
7. First search for a permanent magnetic field unimpeded by Titan's ionosphere.
8. First direct search for a subsurface water ocean suggested by Cassini.
9. First direct, prolonged exploration of Titan's complex lower atmosphere winds.
10. Exploration of the complex organic chemistry in the lower atmosphere and surface liquid reservoirs discovered at high latitudes by Cassini.

3.3.1.2 Detailed synergistic balloon-lake lander measurements

1. Define locally the atmospheric parameters and properties, such as the temperature, the density, the heat balance and the atmospheric electricity from the ground up to 1600 km, during the probe's entry and descent phases and the Montgolfière's cruising phase.
2. Determine the local thermal and chemical structure of the lower atmosphere (from around 130 km in the stratosphere to the ground) during the descent phase of the probe; the same at different longitudes and with some latitudinal coverage with the Montgolfière at around 10 km in altitude.
3. Measure the abundances in noble gases and isotopic ratios in major species in order to constrain the origin and evolution of the atmosphere through photochemistry, escape and outgassing processes.
4. Determine locally with the Montgolfière and the probe the dynamics and heat balance of the atmosphere (circulation, tides, waves, eddies, turbulence, radiation).

5. Determine the meteorology (dynamics, rain, clouds, evaporation, atmospheric electricity, etc)
    a. with the Montgolfière at equatorial and mid-latitudes
    b. locally with the lander
6. Measure climatic (seasonal and long term) variations, stability, and methane and ethane abundances in the lower atmosphere and surface (by comparing with Huygens)
7. Map the surface at equatorial and mid-latitudes, as well as above the probe's landing location, at optical, near-IR, and radar wavelengths with resolution <2.5 m (and in stereo where possible).
8. Determine the surface material from high-resolution *in situ* measurements and compositional mapping of the surface from the montgolfière.
9. Detect recent surface changes including cryovolcanic and alluvial flows, variation in lake levels, and evidence of tectonic and erosion processes.
10. Detect seismic and cryovolcanic events (with the geosaucer; TBC).
11. Determine Titan's spin rate, physical libration and tidally induced distortion with unprecedented accuracy.
12. Measure the subsurface profiles at very high resolution (~few hundred meters spot size and a vertical resolution < 3 m) to
    - detect sedimentary processes and to reconstruct their history;
    - detect structures of tectonic, impact, or cryovolcanic origin, and correlate these structures with the surface morphology for understanding the geologic history;
    - detect subsurface structures of cryovolcanic origin (e.g. channels, chambers, etc.).
13. Detect and measure the depth of shallow subsurface reservoirs of liquid (hydrocarbons) where the probe lands.
14. Determine the nature of surface-atmosphere interactions (volatiles, energy, momentum, planetary boundary layer)
15. Investigate the magnetic fields in order to separate intrinsic or induced internal signals from each other.

3.4 Science Implementation

The scientific objectives and associated measurements described above will be implemented as indicated below, with the payload implemented in the TSSM PDD, but also briefly described in the following subsections.

3.4.1 MONTGOLFIÈRE PROBE

The montgolfière will be targeted at low latitudes (between 20°S and 20°N) and will float at around 10 km altitude (baseline design). The nominal floating altitude and the variations around it will be defined by the design.

The lifetime of the Montgolfière will be at least 6 months (goal 12 months), which corresponds to about one circumnavigation around Titan globe with winds at 1 m/s. Modifications the baseline design to add near surface operation capability (for an additional lifetime of 6 months) will be evaluated.

The nominal payload of the Montgolfière is composed of the following

- a Titan Montgolfière Chemical Analyser **(TMCA**)
- a Balloon Imaging Spectrometer **(BIS**).
- a Visible Imaging System Titan Balloon **(VISTA-B**)
- an Atmospheric Structure Instrument / Meteorological package **(ASI/MET**)
- a Titan Radar Sounder **(TRS**)
- an Atmospheric electricity and waves instrument **(TEEP-B**)
- a Magnetometer **(MAG**)

In addition, Radio science will be performed through the communication system.

The full description of these instruments can be found in the TandEM PDD [RD9].

3.4.2 LANDER PROBE

The short-lived probe should be designed for wet landing in a lake targeted at high northern latitude. However, as with Huygens, the lander will be capable of landing either on the shore or in the sea.

During the descent under parachute, expected to last about 6 hours, the payload will be fully operational. It will also be fully operational for nominally 3 hours after landing.

The lander payload includes the following instruments (described elsewhere in this report and in the TandEM PDD):

- a Titan Lander Chemical Analyser **(TLCA**)
- a Titan Probe Image**r (TIPI**)
- an Atmospheric Structure Instrument / Meteorological package with electrical properties **(ASI/MET-TEEP)**
- a Surface Properties Package (**SPP**)

In addition, Radio science will be performed through the communication system.

How the science objectives and the acquisition of the necessary measurements will be achieved with this payload is described below.

3.4.3 OVERVIEW OF PLANNING PAYLOAD

The notional payload for the Montgolfière and the Lander (which will land in a northern-polar lake) are meant to be complementary and to provide a maximum and optimized scientific return. Their full description and specifications are given in [RD9].

3.4.3.1 The Montgolfière Payload and Science Objectives

The hot-air balloon will include the payload (technically described elsewhere in this report) with the science capabilities as follows:

3.4.3.1.1 Titan Montgolfière Chemical Analyser (TMCA)

The Titan Montgolfière Chemical Analyser instrument consists basically of an ion trap mass spectrometer operating in a mass scanning mode with a mass range from 10 to 600 Da and unit mass resolution. It has an aerosol inlet (ALDI) which ingests aerosol particles by pumping them into the instrument and atmospheric measurements can be made by use of valves admitting gas through small capillary leaks. There is a noble gas concentrator and a pumping system.

Sampling:
Any methane particles will be instantly vaporized and analyzed, while the non-volatile aerosols will be collected on a grid that can be rapidly heated thermally or with a laser. The temperature of the aerosol particles will be ramped until pyrolysis occurs and the subsequently evolved gases analyzed in the ion trap, where electron impact creates ions that can be analyzed in the ion trap. Alternatively samples are collected on a plate and transferred to the vacuum system where they are ionised by laser and/or ion gun to be analysed by a small mass spectrometer. The TMCA will also be capable of the analysis of Titan's atmosphere with minimal overhead, although this would require the development of valves that can seal at low temperatures.

Science:
The primary aim of the TMCA instrument is to analyze the composition of aerosol particles in Titan's atmosphere. At unit mass resolution, interpretation of the mass spectra would involve the difficult de-convolution of the complex mixture of fragmentation patterns of all the ions trapped. However, this will be aided by knowledge of the likely composition obtained from the Lander TCA detailed high resolution mass spectra. The ion trap can also be used in an MSxMS mode, where selected ions of a single mass can be isolated and then subsequently fragmented to identify a unique molecular component. In this way, during the long mission duration of the Montgolfière, a library of molecular components detected can be assembled.

An alternative method is to detect stored ions by current imaging on the endcap electrodes (FFT electronics). This has an increased mass resolution of >5000 Da. TMCA will also be capable of atmospheric measurements. More specifically the TMCA goals include:

- for the atmosphere:
  - Determine the methane and ethane mole fractions
  - Measure the noble gas concentration to 10 s of ppb
  - Detect and characterize molecules at concentrations above ppm levels
- for the aerosols
  - Determine the concentration of aerosol particles
  - Determine the bulk composition of individual particles

- Characterize the chemical composition of aerosol particles

3.4.3.1.2 Balloon Imaging Spectrometer (BIS)

The concept of the instrument is based on a collecting telescope and a diffraction grating spectrometer ideally joined at the telescope focal plane where the spectrometer entrance slit is located. The image of the slit is dispersed by the diffraction grating on a bi-dimensional detector. The instantaneous acquisition on the bi-dimensional detector consists of the slit image diffracted by the grating over the selected spectral range; the complete image is built in time by subsequent acquisitions. The final result is a three-dimensional data set in which a spectrum is associated to each pixel. The detector is working in the range 1–5.6 μm. BIS will also measure the transmittance of the atmosphere at different angles from the nadir, at different altitudes, locations and times.

A pointing mirror is part of the instrument which will have the possibility to make limb observations by moving the mirror.

Science:

- Investigate the composition of the surface of Titan (ices, organics) at regional and local scale with a spectral sampling of 10.5 nm
- Map the temperature of the surface of Titan
- Investigate the troposphere in an altitude range of 3–30 km on the surface, by looking at nadir and at different angles wrt nadir and collecting data at different altitudes
- Investigate the composition and optical properties of the haze
- Investigate variable features in the lower part of the troposphere (clouds, plumes if any).

The BIS instrument onboard the aerial platform is in a unique position to study the lower part of Titan atmosphere, giving the possibility to

- perform more detailed, both downward and limb looking measurements of the troposphere
- obtain data on the optical properties of haze
- perform detailed studies of local, time variable phenomena (clouds, plumes)

The BIS instrument allows studying the surface at a much higher spatial resolution than from the orbiter, giving the possibility to map the composition of the surface, looking for ethane and new/unknown signatures map the surface temperature, and look for hot spots.

3.4.3.1.3 Visible Imaging System Titan Balloon (VISTA-B)

The concept of the Balloon camera is based on (stereo) wide–angle multispectral as well as high-resolution geomorphological imaging of Titan's surface. This will be done by two wide-angle camera heads mounted below the gondola, looking in a forward and backward direction (pointing 20°) for surface context imaging. A third wide-angle head, pointed 60° from Nadir, will provide side-looking images for meteorological observations and atmospheric monitoring. All three will provide resolutions below 10m/pixel.

A filter wheel in front of each camera head provides filter sets for geological and atmospheric science.

For high-resolution imaging a high resolution camera operated in scanning mode (pointing nadir) will complement the instrument. The resolution will be below 1m/pixel. Overall mass will be approximately 2 kg.

Science
The balloon camera will perform stereo panoramic and high-resolution geomorphological studies; side-looking images can provide meteorological observations. The science goals include:

- Stereo, wide angle, multispectral imaging of Titan' surface from 6–10 km height with a resolution (<10 m/px)
- Study the surface characteristics of areas of interest and future landing sites at high resolution (<1 m/px)
- Monitoring of atmospheric phenomena

Performance Requirements
- Derive high-resolution snapshots and imaging swaths at high resolution with a high resolution camera
- Allow for multispectral stereo coverage by imaging areas of interest with two wide-angle camera heads with different tilts (one looking backwards, the other one looking forward, pointing 20° from nadir)
- Allow for monitoring of atmospheric phenomena by means of a third wide angle camera head with sideward pointing (60° from nadir)

3.4.3.1.4 Atmospheric Structure Instrument/Meteorological Package (ASI/MET)

ASI/MET is composed of a suite of sensors that could help in investigating physical properties of Titan's atmosphere. The Atmospheric Structure Instrument (ASI) consists of three core sensor packages: (1) a three axial accelerometer (ASI-ACC), (2) a pressure profile instrument (ASI-PPI), (3) temperature sensors (ASI-TEM).

Science:
The key *in situ* measurements will be the atmospheric vertical pressure and temperature profiles, as well as the evaluation of the density and mean molecular weight profile along the entry module and probe's trajectory. ASI/MET will monitor environmental physical properties of the atmosphere from the aerobot and the landed probe. ASI/MET data will also contribute to the analysis of the atmospheric composition. It will monitor the acceleration experienced by the entry module and probe during the whole descent phase and will provide the unique direct measurements of pressure and temperature through sensors having access to the atmospheric flow.

In situ measurements are essential for the investigation of the atmospheric structure, dynamics and meterorology. The estimation of the temperature lapse rate can be used to identify the presence of condensation and eventually clouds, to distinguish between saturated and unsaturated, stable and conditionally stable regions. The variations in the density, pressure and temperature profiles provide information on the atmospheric stability and stratification, on the presence of winds, thermal tides, waves and turbulence in the atmosphere.

The ASI-ACC will start to operate since the beginning of the entry phase, sensing the atmospheric drag experienced by the entry vehicle.

3.4.3.1.5 Titan Electric Environment Package (TEEP-B)

The TEEP instrument for the Titan Montgolfière includes one vertical and one horizontal dipole antenna. The two dipoles consist of 4 ring electrodes, which measure the conductivity in the active mode, using the mutual impedance technique. Another electrode is used as a relaxation probe and collects electric charges.

The same boom can also carry the acoustic and magnetic sensors. The instrument requires the deployment of a 1–1.5 m boom that, in nominal configuration, allows the measurement of vertical and horizontal electric fields.

Measurements performed by TEEP-B include:

[SM-1] Vertical and horizontal electric field in the frequency range from DC to VLF (~ 10 kHz, TBD)
[SM-2] Electric conductivity and permittivity of the atmosphere and soil
[SM-3] Acoustic turbulence
[SM-4] 1 ELF-VLF magnetic component

Science:
The above measurements will yield information on the:
[SO-1] Coupling between Titan atmosphere/ionosphere and the magnetosphere of Saturn/solar wind;
[SO-2] Global monitoring of atmosphere and ionosphere coupling;
[SO-3] Search for a buried ocean and exploration of Titan internal structure at long wavelengths;
[SO-4] Weather monitoring;
[SO-5] Atmospheric electricity and related chemical processes;
[SO-6] Free electrons and related chemistry;
[SO-7] Global electric circuit and fair weather field;
[SO-8] Acoustic measurements / wind;
[SO-9] Atmospheric cosmic ray effects;
[SO-10] Haze and drizzle induced shot noise;
[SO-11] Aerosol charging and stratification;
[SO-12] Ground truth for global radar mapping;
[SO-13] Constraints on soil composition.

3.4.3.1.6 Titan Radar Sounder (TRS)

The TRS instrument is a nadir-looking radar sounder system at relatively low frequency (between 150 MHz and 300 MHz). The sounder system is based on a robust and mature technology that was already used successfully for two different Mars Missions (Mars Express, with the MARSIS instrument; NASA Reconnaissance Orbiter with SHARAD).

The TRS instrument, thanks to the relatively low frequency of its pulse, has the capability to penetrate the surface and to perform a sub-surface analysis with a penetration depth between few hundred meters and 1 Km (which depends on the specific selected central frequency of the pulse) with a vertical resolution in between some tens meters and few meters (this requirement mainly depends on the bandwidth of the signal). The instrument will transmit radio waves towards the Titan surface, which will be reflected from any surface they encounter. For most, this will be the surface of Titan, but a significant fraction will travel through the crust to be reflected at sub-surface interfaces between layers of different material. This results in the possibility to measure both the surface topography and the subsurface layering.

In order to achieve the above-mentioned goals it is necessary to have high resolution sub-surface profiles with a 3D analysis of the shallow sub-surface units. A penetration depth > 350 m should be obtained with a vertical resolution < 6 m.

Different tradeoffs between penetration depth and vertical resolution can be obtained by tuning the central frequency of the instrument and the bandwidth of the pulse.

Science:
This instrument is very useful for reconstructing the geological history of Titan characterizing and assessing the present day sedimentary environments and geomorphological features and identifying the stratigraphic relationships of ancient sedimentary units. More in general, it would allow one to detect sub-surface profiles and possible interfaces due to the presence of liquid or other structures (e.g. of tectonic or cryovolcanic origin).

The main scientific goals of the Titan Radar Sounder (TRS) on the montgolfière are as follows:

1. Measure the subsurface profiles at high resolution to detect sedimentary processes and to reconstruct the history of them.
2. Measure the subsurface profiles at high resolution for detecting structures of tectonic or cryovolcanic origin, and correlated these structures with the surface morphology for understanding the history of dunes.
3. Detect and measure the depth of any shallow subsurface reservoirs of liquid (hydrocarbons).
4. Detect and measure at very high resolution subsurface structures of cryovolcanic origin (e.g. channels, chambers, atc.).
5. Measurement of the depth and of the bottom topography of methane lakes (only if the latitude of the montgolfière is suitable with the position of the lakes, which is not the working assumption at this time).
6. Altimetry at high/moderate resolution (vertical resolution of few meters).

3.4.3.1.7 Magnetometer (MAG)

The magnetometer consists of two sensors, which would be preferably boom mounted or mounted at an extremity of a lander/probe to minimise magnetic interference, and one or two sensor electronics boards located on the main equipment platform. Two sensors are preferred to facilitate operation as a gradiometer in order to separate the very small target ambient field from anymagnetic disturbance field due to the probe fields.

Science:
The magnetometer will measure the magnetic field in the spacecraft vicinity in the bandwidth DC to 64Hz, depending on science requirements and available telemetry. Also gradiometry measurements will be performed.

3.4.3.1.8 Montgolfière Radio Science

In addition to the above instrumentation, Radio Science will be achieved through the onboard communications system.

The goal of the Radio Science is to provide signals to the Titan orbiter and direct-to-Earth, in order to make possible a precise estimation of the Montgolfière trajectory in Titan atmosphere.

The location of the TSSM *in situ* elements will be known by means of Delta-DOR and Same Beam Interferometry (SBI) The first has a direct link to Earth. The second method (SBI) is an interferometric technique aimed at measuring the differential delay of the signal coming from two spacecrafts received simultaneously at two ground stations. Instead of using a quasar as a calibrator, it uses one of the two spacecraft being tracked, assuming that its orbit is well known. The technique has been experimented by JPL with Pioneer 12 and Magellan at Venus in 1990 and with the Mars missions Currently SBI is not part of ESA facilities.

3.4.3.2 The Lander Payload and Science Objectives

The probe descending through the atmosphere and landing in a northern hemisphere lake will carry the payload with the science capabilities as described hereafter:

3.4.3.2.1 Titan Lander Chemical Analyser (TLCA)

The baseline TLCA instrument consists of a high resolution ToF mass spectrometer (a mass spectrometer with a mass resolution of 10,000 and capable of analyzing molecules of at least 10,000 Daltons) with a GCxGC inlet system. Two additional GC columns are included to give some redundancy and perform 'path finder' experiments. The core of the TLCA instrument uses Gas Chromatography (GC) to separate the complex mixture of Titan's organics into individual components for analysis by the mass spectrometer. The GC system will use several different types of GC column to separate chemical compounds according to different chemical criteria such as polarity and/or functional groups. Greater chemical separation, which will be required for the full characterization of the Titan organics, can be achieved by coupling a different GC column on to the end of the first column i.e. GC x GC. This enables separation of classes of organics and aids in the identification of complex organic mixtures. The baseline instrument uses a single GC x GC channel and two GC columns. A derivatisation/wet chemistry manifold is used to process liquid and solid samples suitable for injection onto the GC columns. Atmospheric gas inlets are used to sample the atmosphere during the lander descent and whilst on the lake surface. The TLCA also includes a stable isotope ratio mass spectrometer and elemental/isotopic converter, as well as a noble gas concentrator and pumping system.

Science:
The great flexibility of a chemical analyser system, science goals and performance requirements are detailed in Appendix A. The science goals and measurement requirements, as well as the data products that are addressed and will be provided by the Lake-lander chemical analyzer are summarized in the Lake-Lander traceability matrix and in the TSSM PDD. Measurement requirements are:

Atmosphere:
- Determine methane and ethane mole fraction
- Measure noble gas concentration to ppb levels
- Measure isotopic ratios of the noble gases
- Measure isotopic ratios of C, N, O and H

Lake:
- Determine the bulk composition of the liquid material
- Measure the chemical composition of organics dissolved in the liquid
- Detect and characterise complex organics in the lake
- Measure the chirality of complex organics
- Detect the presence of any biomarkers

3.4.3.2.2 Titan Probe Imager (TIPI)

TIPI would consist of a descent and surface camera for context imaging and landing site verification during the descent and for characterizing and monitoring the landing site within a camera's FoV after landing, a surface lamp to illuminate the surface after landing and a dedicated electronics assembly to coordinate and control the data collections, data compression and telemetry. Context imaging and landing site verification calls for imaging during final descent (~100 meters), which would require high power for a lamp if using a conventional CCD (dark hydrocarbon lake surface below). However, the instrument concept includes a very sensitive Electron Multiplying CCD Sensor. This device uses a novel output amplifier circuit that is capable

of operating at an equivalent output noise of less than one electron event at high pixel rates. This makes the sensor well suited for imaging under very limited illumination conditions. I.e. descent imaging will be possible at SNR of ~ 30 (at 2 milliseconds exposure time; TBC) while only depending on the available ambient illumination and Saturn shine.

The sensitivity of the detector in the near infrared (up to 1 micron) will enable the camera to image through the haze in the atmosphere during the descent, as infrared wavelengths are being scattered less due to haze (compared to visible wavelengths). Thus, the detection of surface features in the near-infrared will be possible.

Science:
Specificity of descent probe measurements vs. balloon measurements:

- image the local surface at much higher resolution (mm to m) than from the balloon
- probe a different region (high latitude, methane lake) from those covered during the balloon excursion.

Thus, the TiPI science goals aim to

- provide context imaging and landing site verification during the descent (visible and NIR)
- investigate local geology and structure of specific surface features at <meter resolution during the descent
- investigate of lake surface features at landing site (mm resolution)
- characterize the physical and chemical properties of the surface at landing site
- identify and monitor variable features on the surface

3.4.3.2.3 Atmospheric Structure Instrument/Meteorological package (ASI / MET), Titan Electric Environment Package – Lander (TEEP-L)

The ASI/MET instrument is a multi-sensor package that will address the measurements of variousparameters depending on the different mission elements and phases.

During the entry phase, when the aerial platform, the descent probe and surface stations will be included in a unique entry module, atmospheric investigation will rely on the accelerometric data (ASI-ACC) and on measurements of the instrumented heat shield [SHIELD]. The ASI measurements will be performed during the entire descent of the probes, while and ASI/MET package will be operating on the mongolfiere and landed stations.

The TEEP analyzer is designed for the investigation of the electric properties and other related physical characteristics of the atmosphere and surface of Titan, namely conductivity of the atmosphere, permittivity and conductivity of the surface, and ELF-VLF waves. The instrument also includes an acoustic sensor for atmospheric turbulence measurements. The instrument includes significant heritage from the Cassini-Huygens mission (see, for details, Grard et al., 1995; Fulchignoni et al., 2002). The instrument also includes TEEP-B, which is proposed to the balloon payload. The TEEP-L instrument has a few similarities with the Atmospheric Relaxation and Electric field Sensor (ARES) under development for the ExoMars mission (Berthelier et al., 2000). Therefore, TEEP-L has heritage from the Cassini-Huygens and ExoMars missions.

Science:
See description of science goals for ASI/MET and TEEP-B in the montgolfière payload (§3.4.3.1.4-3.4.3.1.5).

The key *in situ* measurements of the ASI/MET will be atmospheric density, pressure and temperature profile by measuring deceleration of the entry vehicle and performing direct temperature and pressure measurements during the descent phase [Fulchignoni *et al.* 2005].

The ASI-ACC will start to operate since the beginning of the entry phase, sensing the atmospheric drag experienced by the entry vehicle.

Direct pressure and temperature measurements will be performed by the sensors with access to the atmospheric flow on board of the descent probe. Also and mean molecular weight profile along the entry module and probes trajectory and to monitor environmental physical properties of the atmosphere from the aerorobot and landed probes. ASI/MET data will also contribute to the analysis of the atmospheric composition.

TEEP-L will achieve:

[SM-1] Vertical and horizontal electric field in the frequency range from DC to VLF (~ 10 kHz, TBD)
[SM-2] Electric conductivity and permittivity of the atmosphere and soil
[SM-3] Acoustic turbulence
[SM-4] 1 ELF-VLF magnetic component

This will yield information on:

[SO-1] Coupling between Titan atmosphere/ionosphere and the magnetosphere of Saturn/solar wind;
[SO-2] Global monitoring of atmosphere and ionosphere coupling;
[SO-3] Search for a buried ocean and exploration of Titan internal structure at long wavelengths;
[SO-4] Weather monitoring;
[SO-5] Atmospheric electricity and related chemical processes;
[SO-6] Free electrons and related chemistry;
[SO-7] Global electric circuit and fair weather field;
[SO-8] Acoustic measurements / wind;
[SO-9] Atmospheric cosmic ray effects;
[SO-10] Haze and drizzle induced shot noise;
[SO-11] Aerosol charging and stratification;
[SO-12] Ground truth for global radar mapping;
[SO-13] Constraints on soil composition.

3.4.3.2.4 Surface Properties Package (SPP)

The package includes an acoustic suite, consisting of one sonar sounder (facing downwards) and a set of two orthogonal pairs of acoustic transducers; a wave motion suite, consisting of a set of orthogonal tilt sensors and a 3-axis accelerometer; a TSM composed of several three axis magnetoresistive sensors positioned at different points on the lander body or co-located with for example TEEP or ASI sensors on any other lander provided boom or mast structure ; the acoustic unit furthere comprises 3 acoustic sensors.

The package could potentially include a Titan Surface Magnetometer (TSM). The TSM can be implemented as either (i) dual vector magnetoresistive sensors (MR) positioned at the tip and inwards from the tip a boom or mast structure. Each sensor provides a measurement of three orthogonal components of the magnetic field in the range 0 to 100Hz. The boom ensures that the magnetometer sensors are offset from any disturbance field due to the lander and a dual magnetometer technique can be used to separate the ambient and lander fields [Georgescu *et al*, 2008]. (ii) A suite of several vector MR sensors fitted along an axis of the lander body. This option would only be recommended if a boom is not possible due to mass and data processing penalties.

Science

- depth of liquid
- physical properties of liquid
  - electrical properties
  - refractive index and optical density
  - thermal properties
- wave motion
  - acoustic properties
  - density
- acceleration
- probe tilt
- magnitude and direction of the *in situ* magnetic field
- Wind speed and direction during the ascent and descent phase of the Montgolfière/Probes and on the surface
- Atmospheric turbulence parameters derived from acoustic properties in the troposphere:
  - acoustic impedance, spectral information up to 10 kHz and sound velocity
  - Methane drizzle and rain

3.4.4 THE SCIENCE RETURN WITH THE *IN SITU* ELEMENTS

All of the above instruments will make measurements to meet the science goals of TSSM with the *in situ* elements. We have established a traceability matrix for each of the *in situ* elements, defining the science objectives and tying them to specific investigations that can be performed with the designed model payload (Tables in Appendix A).

The *in situ* elements, in conjunction with the orbiter investigations, will achieve the following:

Determine the composition and transport of volatiles and condensates in the atmosphere and at the surface, including hydrocarbons and nitriles, on both regional and global scales, in order to understand the hydrocarbon cycle. Determine the climatological and meteorological variations of temperature, clouds and winds.

- Asses surface volatile inventory: $\lambda/\Delta\lambda$ 1000 over 1 – 6 microns (orbiter, montgolfière, lander)
- Determine atmospheric composition from surface to above 1500 km. (orbiter, montgolfière, lander)
- Obtain vertical temperature soundings with $\Delta T = 0.1$ K (orbiter, montgolfière, lander (descent))
- Perform direct measurement of zonal winds (montgolfière, lander (descent))
- Measure profiles of organic gas abundance (orbiter, montgolfière, lander (descent))
- Measure time-series of meteorology (orbiter, montgolfière, lander)
- Determine clouds at all altitudes: distribution, morphology, etc. (orbiter, montgolfière)
- Measure surface temperature distribution (montgolfière, orbiter)
- Measure deposition of sunlight as a function of altitude (montgolfière, orbiter, lander)
- Measure optical properties of aerosol particles (orbiter, montgolfière, lander)
- Measure number density and size of aerosol particles (orbiter, montgolfière, lander)

- Measure the abundance of radiocarbon in surface materials (lander)

Characterize and assess the relative importance today and throughout time of Titan's geologic, marine and geomorphologic processes e.g. cryovolcanic, aeolian, tectonic, fluvial, hydraulic, impact and erosion.

- Detect indicators of exchange (vents etc.): spatial resolution 50 m (orbiter, montgolfière)
- Measure regional topography (1 km spatial,10m vertical resolution) (orbiter, montgolfière)
- Assess regional morphology and texture; spectral reflectance $\lambda/\Delta\lambda$ 1000 (orbiter, montgolfière)
- Observe local-scale morphology (0.1–0.01 m) (montgolfière, lander)
- Observe regional subsurface structure (10 km/100 m) (montgolfière, orbiter)
- Obtain regional very high resolution subsurface profiles (500 m spot size and vertical resolution < 3 m) (montgolfière)
- Map topographic boundaries (100 km/100 m) (orbiter, montgolfière)

Determine internal differentiation, thermal evolution of Titan. Determine if Titan has an internal ammonia-water ocean, a metal core and an intrinsic magnetic field, extent and origin of geodynamic activity.

- Measure rotation parameters to 0.1 degree/yr (orbiter, surface geophysical package[2])
- Measure vector magnetic field around Titan and at the surface (orbiter, surface geophysical package)
- Detect presence of seismic activity (tidal and tectonic) (from the surface geophysical package)

Determine the chemical pathways leading to formation of complex organics at all altitudes in Titan's atmosphere and their modification and deposition on the surface with particular emphasis on ascertaining the extent of organic chemical evolution on Titan.

- Determine CHONPS elemental composition of surface (lander, montgolfière)
- Determine surface composition of complex organics (orbiter, lander, montgolfière)
- Characterize physical state of organics (lander)
- Measure isotope ratios of C, N, O of surface organics (lander)
- Measure chirality of organic compounds (lander)
- Measure chemical abundance of gases in atmosphere (montgolfière, lander)
- Measure chemical composition of particulates (montgolfière, orbiter)
- Measure atmospheric thermal structure as function of latitude (orbiter, montgolfière)

Determine geochemical constraints on bulk composition, the delivery of nitrogen and methane and exchange of surface materials with the interior

- Measure noble gases and isotopes (esp. Kr, Xe) to ppb levels (montgolfière, lander)
- Detect ammonia in surface material: down to 1% in local deposits (montgolfière)

[2] With the instrument on the heat shield (to be studied) as described in the introduction of this section.

- Detect carbon, nitrogen isotopes in surface/atmosphere reservoirs (lander)
- Measure D/H in surface liquids (lander)
- Determine composition of gases released from vents, etc. (montgolfière)

Determine chemical modification of organics on surface e.g. hydrolysis via impact melt.

- Determine CHONPS composition of modified deposits (lander, Montgolfière)
- Determine composition of complex organics in special sites (lander, Montgolfière)

Each of the *in situ* elements will work towards achieving these goals and the measurement requirements with the capabilities described here above.

References

1. Atreya, S. K., Adams, E. Y., Niemann, H. B., Demick-Montelara, J. E., Owen, T. C., Fulchignoni, M., Ferri, F., Wilson, E. H., 2006. Titan's methane cycle. Plan. Space Sci. 54, 1177-1187.
2. Barth, E. L., Rafkin, S. C. R., 2007. TRAMS: A new dynamic cloud model for Titan's methane clouds. Geophys. Res. Let. 34, CiteID L03203.
3. Bernard JM, Quirico E, Brissaud O et al., 2006. Reflectance spectra and chemical structure of Titan's tholins: Application to the analysis of Cassini–Huygens observations. Icarus 185: 301-307.
4. Bird, M. K., Allison, M., Asmar, S. W., Atkinson, D. H., Avruch, I. M., Dutta-Roy, R., Dzierma, Y., Edenhofer, P., Folkner, W. M., Gurvits, L. I., Johnston, D. V., Plettemeier, D., Pogrebenko, S. V., Preston, R. A., Tyler, G. L., 2005. The vertical profile of winds on Titan. Nature, 43, 800-802.
5. Borucki, W. J. and Whitten, R. C., 2008. Influence of high abundances of aerosols on the electrical conductivity of the Titan atmosphere, Planet. Space Sci., 56, 19-26,.
6. Broadfoot, A. L., Belton, M. J. S., Takacs, P. Z., Sandel, B. R., Shemansky, D. E., Holberg, J. B., Ajello, J. M., Atreya, S. K., Donahue, T. M., Moos, H. W., Bertaux, J.L., Blamont, J.E., Strobel, D. F., McConnell, J. C., Dalgarno, A., Goody, R., and McElroy, M. B., 1981. Extreme ultraviolet observations from Voyager 1 encounter with Saturn. Science 212, 206-211.
7. Brown, M. E., Bouchez, A. H., Griffith, C. A., 2002. Direct detection of variable tropospheric clouds near Titan's south pole. Nature 420, 795-797.
8. Brown, R. H., Soderblom, L. A., Soderblom, J. M., Clark, R. N., Jaumann, R., Barnes, J. W., Sotin, C., Buratti, B., Baines, K. H., Nicholson, P. D., 2008. The identification of liquid ethane in Titan's Ontario Lacus. Nature 454, 607-610.
9. Buczkowski, D. L., Frey, H. V., Roark, J. H., McGill, J. E., 2005. Buried impact craters: A topographic analysis of quasi-circular depressions, Utopia Basin, Mars. Journal Geophys. Res., 110, DOI: 10.1029/2004JE002324.
10. Choukroun, M., Grasset, O., Sotin, C., Tobie, G. 2008. Cryovolcanic release of methane on Titan: experimental constraints from the stability of methane clathrates in presence of ammonia. Lunar Planet. Sci. Conf. XXXIX, Abstract #1837, Houston, TX.
11. Coates, A. J., Crary, F. J., Lewis, G. R., Young, D. T., Waite, J. H., Sittler, E. C., 2007. Discovery of heavy negative Ions In Titan's Ionosphere, Geophys. Res. Lett., 34, L22103.
12. Combes, M., Vapillon, L., Gendron, E., Coustenis, A., Lai, O., Wittemberg, R., Sirdey, R., 1997. Spatially resolved images of Titan by means of adaptive optics. Icarus 129, 482-497.
13. Committee on the Origin and Evolution of Life (2007).
14. Coustenis, A., Taylor, F., 2008. « Titan: Exploring an Earth-like World ». World Scientific Publishing, Singapore, Eds.
15. Coustenis, A., Lellouch, E., Maillard, J-P., and McKay, C.P., 1995. Titan's surface: composition and variability from the near-infrared albedo. Icarus 118, 87-104.
16. Coustenis, A., Salama, A., Lellouch, L., Encrenaz, Th., Bjoraker, G., Samuelson, R., de Graauw, Th., Feuchtgruber, H., and Kessler, M. F., 1998. Evidence for water vapor in Titan's atmosphere from ISO/SWS data. Astron. Astrophys. 336, L85-L89.
17. Coustenis, A., Gendron, E., Lai, O., Véran, J.-P. Woillez, J., Combes, M., Vapillon, L., Fusco, Th., Mugnier, L., Rannou, P., 2001. Images of Titan at 1.3 and 1.6 microns with adaptive optics at the CFHT. Icarus 154, 501-515.
18. Coustenis, A., Salama, A., Schulz, B., Ott, S., Lellouch, E., Encrenaz, Th., Gautier, D., Feuchtgruber, H. 2003. Titan's atmosphere from ISO mid-infrared spectroscopy. Icarus 161, 383-403.
19. Coustenis, A., Hirtzig, M., Gendron, E., Drossart, P., Lai, O., Combes, M., Negrao, A., 2005. Maps of Titan's surface from 1 to 2.5 micron. Icarus 177, 89-105.
20. Coustenis, A., Negrao, A., Salama, A., Schulz, B., Lellouch, E., Rannou, P., Drossart, P., Encrenaz, Th., Schmitt, B., Boudon, V., Nikitin, A., 2006. Titan's 3-micron spectral region from ISO high-resolution spectroscopy. Icarus 180, 176-185.
21. Coustenis, A., Achterberg, R., Conrath, B., Jennings, D., Marten, A., Gautier, D., Bjoraker, G., Nixon, C., Romani, P., Carlson, R., Flasar, M., Samuelson, R. E., Teanby, N., Irwin, P., Bézard, B., Orton, G., Kunde, V., Abbas, M., Courtin, R., Fouchet, Th., Hubert, A., Lellouch, E., Mondellini, J., Taylor, F. W., Vinatier, S., 2007. The composition of Titan's stratosphere from Cassini/CIRS mid-infrared spectra. Icarus 189, 35-62.
22. Cravens, T. E., et al., 2008. Energetic Ion precipitation at Titan, Geophys. Res. Lett., in press

23. Coustenis A, Atreya S, Balint T, Brown RH, Dougherty M, Ferri F, Fulchignoni M, Gautier D, Gowen R, Griffith C, Gurvits L, Jaumann R, Langevin Y, Leese M, Lunine J, McKay CP, Moussas X, Müller-Wodarg I, Neubauer F, Owen T, Raulin F, Sittler E, Sohl F, Sotin C, Tobie G. Tokano T, Turtle E, Wahlund J-E, Waite H, Baines K, Blamont J, Dandouras I, Krimigis T, Lellouch E, Lorenz R, Morse A, Porco C, Hirtizig M, Saur J, Coates A, Spilker T, Zarnecki J, and 113 co-authors (2008) TandEM: Titan and Enceladus mission. Experimental Astronomy, DOI: 10.1007/s10686-008-9103-z.
24. De La Haye, V., Waite, J. H., Johnson, R. E., Yelle, R. V., Cravens, T. E., Luhmann, J. G., Kasprzak, W. T., Gell, D. A., Magee, B., Leblanc, F., Michael, M., Jurac, S., Robertson, I. P., 2007. Cassini Ion and Neutral Mass Spectrometer data in Titan's upper atmosphere and exosphere: Observation of a suprathermal corona. J. Geophys. Res. 112, CiteID A07309.
25. Dubouloz, N., Raulin, F., Lellouch, E., and Gautier, D., 1989. Titan's hypothesized ocean properties: The influence of surface temperature and atmospheric composition uncertainties, Icarus 82, 81-94.
26. Elachi, C., Wall, S., Allison, M., Anderson, Y., Boehmer, R., Callahan, P., Encrenaz, P., Flamini, E., Franceschetti, G., Gim, Y., Hamilton, G., Hensley, S., Janssen, M., Johnson, W., Kelleher, K., Kirk, R., Lopes, R., Lorenz, R., Lunine, J., Muhleman, D., Ostro, S., Paganelli, F., Picardi, G., Posa, F., Roth, L., Seu, R., Shaffer, S., Soderblom, L., Stiles, B., Stofan, E., Vetrella, S., West, R., Wood, C., Wye, L., Zebker, H., 2005. Cassini Radar Views the Surface of Titan. Science 308, 970-974.
27. Elachi, C.; Wall, S.; Janssen, M.; Stofan, E.; Lopes, R.; Kirk, R.; Lorenz, R.; Lunine, J.; Paganelli, F.; Soderblom, L.; Wood, C.; Wye, L.; Zebker, H.; Anderson, Y.; Ostro, S.; Allison, M.; Boehmer, R.; Callahan, P.; Encrenaz, P.; Flamini, E.; Francescetti, G.; Gim, Y.; Hamilton, G.; Hensley, S.; Johnson, W.; Kelleher, K.; Muhleman, D.; Picardi, G.; Posa, F.; Roth, L.; Seu, R.; Shaffer, S.; Stiles, B.; Vetrella, S.; West, R., 2006. Titan Radar Mapper observations from Cassini's T3 fly-by. Nature, 441, 709-713.
28. Ferris, J. P. et al. (1978), HCN: a plausible source of purines, pyrimidines and amino acids on the primitive Earth, J. Molecular Evolution, 11, 293–311.
29. Flasar, F. M., Kunde, V. G., Abbas, M. M., Achterberg, R. K., Ade, P., Barucci, A., Bézard, B., G. L. Bjoraker, G. L., Brasunas, J. C., Calcutt, S. Carlson, R., Césarsky, C., Conrath, B. J., Coradini, A., Courtin, R., Coustenis, A., et al., 2004. Exploring the Saturn System in the thermal infared: the Composite Infrared Spectrometer. Space Sci. Rev. 115, 169-297.
30. Flasar, F. M., Achterberg R. K., Conrath B. J., Gierasch, P. J., Kunde V. G., Nixon C. A., Bjoraker G. L., Jennings D. E., Romani P. N., Simon-Miller A. A., Bézard B., Coustenis A., Irwin P. G. J., Teanby, N. A., Brasunas J., Pearl J. C., Segura, M. E., Carlson, R., Matmoukine, A., Schinder, P. J., Barucci A., Courtin R., Fouchet T., Gautier D., Lellouch E., Marten A., Prangé, R., Vinatier, S., Strobel, D. F., Calcutt S. B., Read P. L., Taylor, F. W., Bowles, N., Samuelson R. E., Orton G. S., Spilker L. J., Owen T. C., Spencer, J. A., Showalter, M. R., Ferrari, C., Abbas M. M., Raulin F., Edgington, S., Ade P., Wishnow, E. H., 2005. Titan's atmospheric temperatures, winds, and composition. Science 308, 975-978.
31. Fortes, A. D., 2000. Exobiological Implications of a Possible Ammonia-Water Ocean inside Titan. Icarus 146, 444-452.
32. Fortes, A. Dominic, Grindrod, Peter M., 2006. Modelling of possible mud volcanism on Titan. Icarus 182, 550-558.
33. Fortes, A. D., Grindrod, P. M., Trickett, S. K., Vočadlo, L., 2007. Ammonium sulfate on Titan: Possible origin and role in cryovolcanism. Icarus 188, 139-153.
34. Fulchignoni, M., Ferri, F., Angrilli, F., Bar-Nun, A., Barucci, M. A., Bianchini, G., Borucki, W., Coradini, M., Coustenis, A., Falkner, P., Flamini, E., Grard, R., Hamelin, M., Harri, A. M., Leppelmeier, G. W., Lopez-Moreno, J. J., McDonnell, J. A. M., McKay, C. P., Neubauer, F. H., Pedersen, A., Picardi, G., Pirronello, V., Rodrigo, R., Schwingenschuh, K., Seiff, A., Svedhem, H., Vanzani, V., Zarnecki, J., 2002. The Characterisation of Titan's Atmospheric Physical Properties by the Huygens Atmospheric Structure Instrument (Hasi). Space Sci. Rev. 104, 397-434.
35. Fulchignoni, M., Ferri, F., Angrilli, F., Ball, A.J., Bar-Nun, A., Barucci, M. A., Bettanini, C., Bianchini, G., Borucki, W., Colombatti, G., Coradini, M., Coustenis, A., Debei, S., Falkner, P., Fanti, G., Flamini, E., Gaborit, V., Grard, R., Hamelin, M., Harri, A. M., Hathi, B., Jernej, I., Leese, M. R., Lehto, A., Lion Stoppato, P. F., Lopez-Moreno, J. J., Mäkinen, T., McDonnell, J.A. M., McKay, C. P., Molina-Cuberos, G., Neubauer, F. M., Pirronello, V., Rodrigo, R., Saggin, B., Schwingenschuh, K., Seiff, A., Simões, F., Svedhem, H., Tokano, T., Towner, M. C., Trautner, R., Withers, P., Zarnecki, J. C., 2005. Titan's physical characteristics measured by the Huygens Atmospheric Instrument (HASI). Nature 438, 785-791.

36. Garnier, P., et al., 2008. The lower exosphere of Titan: energetic neutral atoms absorption and imaging, J. Geophys. Res., in press.
37. Garnier, P., Dandouras, I., Toublanc, D., Roelof, E.C., Brandt, P.C., Mitchell, D.G., Krimigis, S.M., Krupp, N., Hamilton, D.C., Waite, H. Wahlund, J.E., 2008b. A non thermal model for the extended Titan exosphere, Icarus (submitted).
38. Gendron, E., Coustenis, A., Drossart, P., Combes, M., Hirtzig, M., Lacombe, F., Rouan, D., Collin, C., Pau, S., Lagrange, A.-M., Mouillet, D., Rabou, P., Fusco, Th., Zins, S., 2004. VLT/NACO adaptive optics imaging of Titan. Astron. Astroph. 417, L21-L24.
39. Georgescu, E., Auster, H. U., Takada, T.; Gloag, J., Eichelberger, H., Fornaçon, K.-H., Brown, P., Carr, C. M., Zhang, T. L., 2008. Modified gradiometer technique applied to Double Star (TC-1). Adv. Space Res. 41, 1579-1584.
40. Grard, R.; Svedhem, H.; Brown, V.; Falkner, P.; Hamelin, M., 1995. An experimental investigation of atmospheric electricity and lightning activity to be performed during the descent of the Huygens Probe onto Titan. J. Atmosph. Terr. Phys. 57, 575-585.
41. Griffith, C.A., Owen, T., Wagener, R., 1991. Titan's surface and troposphere, investigated with ground-based, near-infrared observations. Icarus 93, 362-378.
42. Griffith, C. A., Owen, T., Miller, G.A., and Geballe, T., 1998. Transient clouds in Titan's lower atmosphere. Nature 395, 575-578.
43. Griffith, C. A., Penteado, P., Rannou, P., Brown, R., Boudon, V., Baines, K., Clark, R., Drossart, P., Buratti, B., Nicholson, P., Jaumann, R., McKay, C.P., Coustenis, A., Negrão, A., 2006. Evidence for ethane clouds on Titan from Cassini VIMS observations. Science 313, 1620-1622.
44. Hartle, R. E., et al., 1982. Titan's ion exosphere observed from Voyager 1, J. Geophys. Res., 87, 1383,.
45. Hartle, R. E., et al., 2006a. Preliminary interpretation of Titan plasma interaction as observed by the Cassini Plasma Spectrometer: Comparisons with Voyager 1, Geophys. Res. Lett., 33, L08201,.
46. Hartle, R. E., et al., 2006b. Initial interpretation of Titan plasma interaction as observed by the Cassini Plasma Spectrometer: Comparisons with Voyager 1, Planet. Space Sci., 54, 1211,.
47. Hayes, A., Aharonson, O., Callahan, P., Elachi, C., Gim, Y., Kirk, R., Lewis, K., Lopes, R., Lorenz, R., Lunine, J., Mitchell, K., Mitri, G., Stofan, E., Wall, S., 2008. Hydrocarbon lakes on Titan: Distribution and interaction with a porous regolith. Geophys. Res. Let. 35, CiteID L09204.
48. Hodyss, R., G. McDonald, N. Sarker, M. A. Smith, P. M. Beauchamp, and J. L. Beauchamp (2004), Fluorescence spectra of Titan tholins: in-situ detection of astrobiologically interesting areas on Titan's surface, Icarus, 171, 525–530.
49. Hueso, R., Sánchez-Lavega, A., 2006. Methane storms on Saturn's moon Titan. Nature 442, 428-431.
50. Hirtzig, M., Coustenis, A., Gendron, E., Drossart, P., Hartung, M., Negrao, A., Rannou, Combes, M., 2007. Titan: atmospheric and surface features as observed with NAOS/CONICA at the time of the Huygens' landing. J. Geophys. Res. Planets 112, E02S91.
51. Israël G, Szopa C, Raulin F et al., 2005. Evidence for the presence of complex organic matter in Titan's aerosols by in situ analysis. Nature 438, 796-799.
52. Khanna, R. K., 2005a. Condensed species in Titan's stratosphere: Identification of crystalline propionitrile (C2H5CN, CH3CH2CN) based on laboratory infrared data. Icarus 177, 116-121.
53. Khanna, R. K., 2005b. Condensed species in Titan's stratosphere: Confirmation of crystalline cyanoacetylene (HC3N) and evidence for crystalline acetylene (C2H2) on Titan. Icarus 178, 165-170.
54. Khanna, R.K., 2007. Corrigendum to "Condensed species in Titan's stratosphere: Confirmation of crystalline cyanoacetylene (HC3N) and evidence for crystalline acetylene (C2H2) on Titan" [Icarus 178 (2005) 165 170]. Icarus 186, 589-589.
55. Khare, B.N., Sagan, C., 1973. Red clouds in reducing atmospheres. Icarus 20, 311.
56. Khare B. N., Sagan, C., Arakawa, E. T., et al., 1984. Optical constants of organic tholins produced in a simulated Titanian atmosphere: from soft X-rays to microwave frequencies. Icarus 60, 127-137.
57. Khare. B.N, Sagan. C, Ogino. H, Nagy. B, Er. C, Schram. K.H, Arakawa. E.T., 1986. Amino Acids Derived from Titan Tholins. Icarus 68, 176-184.
58. Kuiper. G.P., 1944. Titan: A Satellite with an Atmosphere. Astrophys J., 100, 378-383.
59. Lellouch, E., Coustenis, A., Sebag, B., Cuby, J. -G., Lopez-Valverde, M., Fouchet, T., Crovisier, J., Schmitt, B., 2003. Titan's 5-micron window: observations with the very large telescope. Icarus 162, 125-142.
60. Lockwood 2008.

61. Lognonne, P. (2005), Planetary Seismology, Ann. Rev. Earth. Planet. Sci., 33, 571–604.
62. Lopes, R. M. C., Mitchell, K. L., Stofan, E. R., Lunine, J. I., Lorenz, R., Paganelli, F., Kirk, R. L., Wood, C. A., Wall, S. D., Robshaw, L. E., Fortes, A. D., Neish, C. D., Radebaugh, J., Reffet, E., Ostro, S. J., Elachi, C., Allison, M. D., Anderson, Y., Boehmer, R., Boubin, G., Callahan, P., Encrenaz, P., Flamini, E., Francescetti, G., Gim, Y., Hamilton, G., Hensley, S., Janssen, M. A., Johnson, W. T. K., Kelleher, K., Muhleman, D. O., Ori, G., Orosei, R., Picardi, G., Posa, F., Roth, L. E., Seu, R., Shaffer, S., Soderblom, L. A., Stiles, B., Vetrella, S., West, R. D., Wye, L., Zebker, H. A., 2007. Cryovolcanic features on Titan's surface as revealed by the Cassini Titan Radar Mapper. Icarus 186, 395-412.
63. Lorenz, R. D., 2000. Post-Cassini Exploration of Titan: Science Rationale and Mission Concepts, Journal of the British Interplanetary Society, 53, 218-234.
64. Lorenz, R. D. and J. Mitton, J., 2002. 'Lifting Titan's Veil', Cambridge University Press.
65. Lorenz, R. D., Griffith, C. A., Lunine, J. I., McKay, C. P., Rennò, N. O., 2005. Convective plumes and the scarcity of Titan's clouds. Geophys. Res. Let. 32, Issue 1, CiteID L01201.
66. Lorenz, R. D., Wall, S., Radebaugh, J., Boubin, G., Reffet, E., Janssen, M., Stofan, E., Lopes, R., Kirk, R., Elachi, C., Lunine, J., Mitchell, K., Paganelli, F., Soderblom, L., Wood, C., Wye, L., Zebker, H., Anderson, Y., Ostro, S., Allison, M., Boehmer, R., Callahan, P., Encrenaz, P., Ori, G. G., Francescetti, G., Gim, Y., Hamilton, G., Hensley, S., Johnson, W., Kelleher, K., Muhleman, D., Picardi, G., Posa, F., Roth, L., Seu, R., Shaffer, S., Stiles, B., Vetrella, S., Flamini, E., West, R., 2006. The Sand Seas of Titan: Cassini RADAR Observations of Longitudinal Dunes. Science 312, 724-727.
67. Lorenz, R. D., Wood, C. A., Lunine, J. I., Wall, S. D., Lopes, R. M., Mitchell, K. L., Paganelli, F., Anderson, Y. Z., Wye, L., Tsai, C., Zebker, H., Stofan, E. R., 2007. Titan's young surface: Initial impact crater survey by Cassini RADAR and model comparison, Geophys. Res. Lett., 34, CiteID L07204..
68. Lorenz, R. D., Lopes, R. M., Paganelli, F., Lunine, J. I., Kirk, R. L., Mitchell, K. L., Soderblom, L. A., Stofan, E. R., Ori, G., Myers, M., Miyamoto, H., Radebaugh, J., Stiles, B., Wall, S. D., Wood, C. A., 2008a. Fluvial channels on Titan: Initial Cassini RADAR observations. Planetary and Space Science 56, 1132-1144.
69. Lorenz, R. D., West, R. D., Johnson, W. T. K., 2008b. Cassini RADAR constraint on Titan's winter polar precipitation. Icarus 195, 812-816.
70. Lorenz, R. D., Mitchell, K. L., Kirk, R. L., Hayes, A. G., Aharonson, O., Zebker, H. A., Paillou, Ph., Radebaugh, J., Lunine, J. I., Janssen, L. A., Wall, S. D., Lopes, R. M., Stiles, B., Ostro, S., Mitri, G., Stofan, E. R., 2008c. Titan's inventory of organic surface materials. Geophys. Res. Lett. 35, CiteID L02206.
71. Lorenz, R.D., B. Stiles, R.L. Kirk, M. Allison, P. Persi del Marmo, L. Iess, J. I. Lunine, S. J. Ostro and S. Hensley, 2008d. Titan's Rotation Reveals an Internal Ocean and Changing Zonal Winds, Science, 319, 1649-1651.
72. Lorenz, R., Stiles, B., Kirk, R., Callahan, P., Hensley, S., Zebker, H., Aharonson, O., 2008e. Hypsometry and Slope Statistics of Titan from Cassini RADAR SARtopo Data. Bull. Am. Astron. Soc., 40, Abstract 34.01.
73. Lunine, J. and Tittemore, W.C., 1983. Origins of outer-planet satellites. In Protostars and Planets III, Levy and Lunine (Eds.) University of Arizona Press, 1177-1252.
74. Lunine, J. I., Stevenson, D. J., Yung, Y. L., 1983. Ethane ocean on Titan. Science, 222, 1229.1230.
75. Lunine, J. I., Elachi, C., Wall, S. D., Janssen, M. A., Allison, M. D., Anderson, Y., Boehmer, R., Callahan, P., Encrenaz, P., Flamini, E., Franceschetti, G., Gim, Y., Hamilton, G., Hensley, S., Johnson, W. T. K., Kelleher, K., Kirk, R. L., Lopes, R. M., Lorenz, R., Muhleman, D. O., Orosei, R., Ostro, S. J., Paganelli, F., Paillou, P., Picardi, G., Posa, F., Radebaugh, J., Roth, L. E., Seu, R., Shaffer, S., Soderblom, L. A., Stiles, B., Stofan, E. R., Vetrella, S., West, R., Wood, C. A., Wye, L., Zebker, H., Alberti, G., Karkoschka, E., Rizk, B., McFarlane, E., See, C., Kazeminejad, B., 2008. Titan's diverse landscapes as evidenced by Cassini RADAR's third and fourth looks at Titan. Icarus 195, 415-433.
76. Matson, D. L., Castillo, J.J.than, Johnson, T. V., 2007. Enceladus' plume: Compositional evidence for a hot interior. Icarus 187, 569-573.
77. McCord, T. B., Hayne, P., Combe, J-P., Hansen, G. B., Barnes, J. W., Rodriguez, S.;,Le Mouélic, S., Baines, E. K. H., Buratti, B. J., Sotin, C., Nicholson, P., Jaumann, R., Nelson, R., The Cassini Vims Team, 2008. Titan's surface: Search for spectral diversity and composition using the Cassini VIMS investigation. Icarus 194, 212-242.
78. McDonald, G. D., W. R. Thompson, M. Heinrich, B. N. Khare, and C. Sagan (1994), Chemical Investigation of Titan and Triton Tholins, Icarus, 108(1), 137–145.
79. McEwen, A., E. Turtle, J. Perry, D. Dawson, S. Fussner, G. Collins, C. Porco, T. Johnson, and Soderblom, L., 2005. Mapping and Monitoring the Surface of Titan, Bull. Am. Astron. Soc., 37, Abstract 53.04.

80. McKay, C. P. and Smith, H. D., 2005. Possibilities for methanogenic life in liquid methane on the surface of Titan, Icarus, 178(1), 274–276.
81. McKay, C. P., Coustenis, A., Samuelson, R. E., Lemmon, M. T., Lorenz, R. D., Cabane, M., Rannou, P., Drossart, P., 2001. Physical properties of the organic aerosols and clouds on Titan. Plan. Space Sci. 49, 79-99.
82. Michael, M. and Johnson, R. E., 2005. Energy deposition of pickup ions and heating of Titan's atmosphere, Planet. Space Sci., 53, 1510-1514,.
83. Mitchell, J. L., Pierrehumbert, R. T., Frierson, D. M. W., Caballero, R., 2006. The dynamics behind Titan's methane clouds. Proc. Natl. Acad. Sci., 103, 18421-18426.
84. Mitri, G., Showman, A. P., Lunine, J. I., Lorenz, R. D., 2007. Hydrocarbon lakes on Titan. Icarus 186, 385-394.
85. Molina-Cuberos, G. J., Lammer, H., Stumptner, W., Schwingenschuh, K., Rucker, H. O., López-Moreno, J. J., Rodrigo, R., Tokano, T., 2001. Ionospheric layer induced by meteoric ionization in Titan's atmosphere. Planet. Space Sci. 49, 143-153.
86. Muhleman, D.O., Grossman, A. W., Butler, B. J., Slade, M. A., 1990. Radar reflectivity of Titan. Science 248, 975-980.
87. Neish, C. D., Lorenz, R. D., O'Brien, D. P., Null, 2006. The potential for prebiotic chemistry in the possible cryovolcanic dome Ganesa Macula on Titan. International J. Astrobiology 5, 57-65.
88. Nelson, R. M., Brown, R. H., Hapke, B. W., Smythe, W. D., Kamp, L., Boryta, M. D., Leader, F., Baines, K. H., Bellucci, G., Bibring, J.-P., Buratti, B. J., Capaccioni, F., Cerroni, P., Clark, R. N., Combes, M., Coradini, A., Cruikshank, D. P., Drossart, P., Formisano, V., Jaumann, R., Langevin, Y., Matson, D. L., McCord, T. B., Mennella, V., Nicholson, P. D., Sicardy, B., Sotin, C., 2006. Photometric properties of Titan's surface from Cassini VIMS: Relevance to Titan's hemispherical albedo dichotomy and surface stability. Plan. Space Sci. 54, 1540-1551.
89. Niemann, H. B., Atreya, S. K., Bauer, S. J., Carignan, G. R., Demick, J. E., Frost, R. L., Gautier, D., Haberman, J. A., Harpold, D. N., Hunten, D. M., Israel, G., Lunine, J. I., Kasprzak, W. T., Owen, T. C., Paulkovich, M., Raulin, F., Raaen, E., Way, S. H., 2005. The abundances of constituents of Titan's atmosphere from the GCMS instrument on the Huygens probe. Nature 438, 779-784.
90. O'Brien, D. P., R. D. Lorenz, and J. I. Lunine, 2005). Numerical calculations of the longevity of impact oases on Titan. Icarus, 173(1), 243–253.
91. Paganelli, F., Janssen, M. A., Stiles, B., West, R., Lorenz, R. D., Lunine, J. I., Wall, S. D., Callahan, P., Lopes, R. M., Stofan, E., Kirk, R. L., Johnson, W. T. K., Roth, L., Elachi, C., The Radar Team, 2007. Titan's surface from Cassini RADAR SAR and high resolution radiometry data of the first five flybys. Icarus 191, 211-222.
92. Paillou, Ph., Mitchell, K., Wall, S., Ruffié, G., Wood, C., Lorenz, R., Stofan, E., Lunine, J., Lopes, R., Encrenaz, P., 2008. Microwave dielectric constant of liquid hydrocarbons: Application to the depth estimation of Titan's lakes. Geophys. Res. Let. 35, CiteID L05202.
93. Perron, J. T., Lamb, M. P., Koven, C. D., Fung, I. Y., Yager, E., Ádámkovics, M., 2006. J. Geophys. Res. 111, CiteID E11001.
94. Porco, C. C., Baker, E., Barbara, J., Beurle, K., Brahic, A., Burns, J. A., Charnoz, S., Cooper, N., Dawson, D. D., Del Genio, A. D., Denk, T., Dones, L., Dyudina, U., Evans, M. W., Fussner, S., Giese, B., Grazier, K., Helfenstein, P., Ingersoll, A. P., Jacobson, R. A., Johnson, T. V., McEwen, A., Murray, C. D., Neukum, G., Owen, W. M., Perry, J., Roatsch, T., Spitale, J., Squyres, S., Thomas, P., Tiscareno, M., Turtle, E. P., Vasavada, A. R., Veverka, J., Wagner, R., West, R., 2005. Imaging of Titan from the Cassini spacecraft. Nature 434, 159-168.
95. Radebaugh, J., Lorenz, R. D., Kirk, R. L., Lunine, J. I., Stofan, E. R., Lopes, R. M. C., Wall, S. D., the Cassini Radar Team, 2007. Mountains on Titan observed by Cassini Radar. Icarus 192, 77-91.
96. Rannou, P., Montmessin, F., Hourdin, F., Lebonnois, S., 2006. The Latitudinal Distribution of Clouds on Titan. Science 311, 201-205.
97. Rappaport, N. J., Iess, L., Wahr, J., Lunine, J. I., Armstrong, J. W., Asmar, S. W., Tortora, P., di Benedetto, M., Racioppa, P. 2008. Can Cassini detect a subsurface ocean in Titan from gravity measurements? Icarus, 194, 711-720.
98. Raulin, F., 1987. Organic chemistry in the oceans of Titan. Adv.Space Res. 7, 571-581.
98. Raulin, F., 2008. Planetary science: organic lakes on Titan. Nature 454, 587-589.
100. Roe, H. G., de Pater, I., Gibbard, S. G., Macintosh, B. A., Max, C. E., Young, E. F., Brown, M. E., Bouchez, A. H., 2004. A new 1.6-micron map of Titan's surface. Geophys. Res. Let. 31, CiteID L17S03.
101. Sagan C and Khare BN (1979) Tholins: Organic chemistry of interstellar grains and gas. Nature 277: 102-107.

102. Samuelson, R. F., Maguire, W.C., Hand, R.A., Kunde, V.G., Jennings, D.F., Yung, Y.L., and Aikin, A.C., 1983. CO2 on Titan, J. Geophys. Res. 88, 8709-8715.
103. Schaller, E. L., Brown, M. E., Roe, H. G., Bouchez, A. H., Trujillo, C. A., 2006. Dissipation of Titan's south polar clouds. Icarus 184, 517-523.
104. Shemansky, D. E., A. I. F. Stewart, R. A. West, L. W. Esposito, J. T. Hallett, and X. Liu (2005). The Cassini UVIS Stellar Probe of the Titan Atmosphere, Science, 308, 978–982.
105. Simões, F., Grard, R., Hamelin, M., López-Moreno, J. J., Schwingenschuh, K., Béghin, C., Berthelier, J.-J., Besser, B., Brown, V. J. G., Chabassière, M., Falkner, P., Ferri, F., Fulchignoni, M., Hofe, R., Jernej, I., Jeronimo, J. M., Molina-Cuberos, G. J., Rodrigo, R., Svedhem, H., Tokano, T., Trautner, R., 2007. A new numerical model for the simulation of ELF wave propagation and the computation of eigenmodes in the atmosphere of Titan: Did Huygens observe any Schumann resonance? Plan. Space Sci. 55, 1978-1989.
106. Sittler, E. C., et al., 2008a. Heavy ion formation in Titan's ionosphere, Magnetospheric introduction of free oxygen and source of Titan's aerosols?, Europlanet Abstract, Muenster, Germany, Sept. 22-26.
107. Sittler, E. C., et al., 2008b. Composition of upstream flow for Titan's Interaction with Saturn's magnetosphere with Saturn LT: Implications for T9, Europlanet Abstract, Muenster, Germany, Sept. 22-26.
108. Smith. P.H, Lemmon. M.T, Lorenz. R.D, Sromovsky. L.A, Caldwell. J.J, Allison. M. D., 1996. Titan's Surface Revealed by HST Imagery. Icarus 119, 336-349.
109. Soderblom, L. A.; Tomasko, M. G.; Archinal, B. A.; Becker, T. L.; Bushroe, M. W.; Cook, D. A.; Doose, L. R.; Galuszka, D. M.; Hare, T. M.; Howington-Kraus, E.; Karkoschka, E.; Kirk, R. L.; Lunine, J. I.; McFarlane, E. A.; Redding, B. L.; Rizk, B.; Rosiek, M. R.; See, C.; Smith, P. H., 2007a. Topography and geomorphology of the Huygens landing site on Titan. Plan. Space Sci., 55, 2015-2024.
110. Soderblom, L. A., Kirk, R. L., Lunine, J. I., Anderson, J. A., Baines, K. H., Barnes, J. W., Barrett, J. M., Brown, R. H., Buratti, B. J., Clark, R. N., Cruikshank, D. P., Elachi, C., Janssen, M. A., Jaumann, R., Karkoschka, E., Mouélic, S. Le, Lopes, R. M., Lorenz, R. D., McCord, T. B., Nicholson, P. D., Radebaugh, J., Rizk, B., Sotin, C., Stofan, E. R., Sucharski, T. L., Tomasko, M. G., Wall, S. D., 2007b. Correlations between Cassini VIMS spectra and RADAR SAR images: Implications for Titan's surface composition and the character of the Huygens Probe Landing Site. Plan. Space Sci. 55, 2025-2036.
111. Sotin, C., Jaumann, R., Buratti, B. J., Brown, R. H., Clark, R. N., Soderblom, L. A., Baines, K. H., Bellucci, G., Bibring, J.-P., Capaccioni, F., Cerroni, P., Combes, M., Coradini, A., Cruikshank, D. P., Drossart, P., Formisano, V., Langevin, Y., Matson, D. L., McCord, T. B., Nelson, R. M., Nicholson, P. D., Sicardy, B., Lemouelic, S., Rodriguez, S., Stephan, K., Scholz, C. K., 2005. Release of volatiles from a possible cryovolcano from near-infrared imaging of Titan. Nature 435, 786-789.
112. Stiles, B. W., Kirk, R. L., Lorenz, R. D., Hensley, S., Lee, E., Ostro, S. J., Allison, M. D., Callahan, P. S., Gim, Y., Iess, L., Perci del Marmo, P., Hamilton, G., Johnson, W. T. K., West, R. D., The Cassini RADAR Team, 2008. Determining Titan's Spin State from Cassini Radar Images. Astron. J. 135, 1669-1680.
113. Stofan, E. R., Elachi, C., Lunine, J. I., Lorenz, R. D., Stiles, B., Mitchell, K. L., Ostro, S., Soderblom, L., Wood, C., Zebker, H., Wall, S., Janssen, M., Kirk, R., Lopes, R., Paganelli, F., Radebaugh, J., Wye, L., Anderson, Y., Allison, M., Boehmer, R., Callahan, P., Encrenaz, P., Flamini, E., Francescetti, G., Gim, Y., Hamilton, G., Hensley, S., Johnson, W. T. K., Kelleher, K., Muhleman, D., Paillou, P., Picardi, G., Posa, F., Roth, L., Seu, R., Shaffer, S., Vetrella, S., West, R., 2007. The lakes of Titan. Nature 445, 61-64.
114. Stoker, C. R., Boston, R. P., Mancinelli, R. L., Segal, W., Khare, B. N., and Sagan, C., 1990). Microbial metabolism of tholin, Icarus, 85(1), 241–256.
115. Strobel, D. F., 2008. Titan's hydrodynamically escaping atmosphere. Icarus 193, 588-594.
116. Takenaka, H.; Kennett, B. L. N.; Fujiwara, H., 1996. Effect of 2-D topography on the 3-D seismic wavefield using a 2.5-D discrete wavenumber-boundary integral equation method. Geophys. J. Intern. 124, 741-755
117. Thompson, W. R., Sagan, C., 1992. Organic chemistry on Titan: Surface interactions. Symposium on Titan, ESA-SP 338, 167-176.
118. Tobie, G., Grasset, O., Lunine, J. I., Mocquet, A., Sotin, C., 2005. Titan's internal structure inferred from a coupled thermal-orbital model. Icarus 175, 496-502.
119. Tobie, G., J. I. Lunine, and C. Sotin 2006. Episodic outgassing as the origin of atmospheric methane on Titan. Nature 440, 61–64.
120. Tokano, T., Neubauer, F.M., 2005. Wind-induced seasonal angular momentum exchange at Titan’s surface and its influence on Titan’s length-of-day. Geophys. Res. Lett. 32, CiteID L24203.

121. Tomasko, M. G., Archinal, B., Becker, T., Bézard, B., Bushroe, M., Combes, M., Cook, D., Coustenis, A., deBergh, C., Dafoe, L.E., Doose, L., Douté, S., Eibl, A., Engel, S., Gliem, F., Grieger, B., Holso, K., Howington-Krause, A., Karkoschka, E., Keller, U., Keuppers, M., Kirk, R., Kramm, R., Lellouch, E., Lemmon, M., Lunine, J., Markiewicz, W., McFarlane, L., Moores, R., Prout, M., Rizk, B., Rosiek, M., Rueffer, P., Schroeder, S., Schmitt, B., Smith, P., Soderblom, L., Thomas, N., West, R., 2005. Results from the Descent Imager/Spectral Radiometer (DISR) Instrument on the Huygens Probe of Titan. Nature 438, 765-778.
122. Trainer, M. G., Pavlov, A. A., Curtis, D. B., McKay, C. P., Worsnop, D. R., Delia, A. E., Toohey, D. W., Toon, O. B., Tolbert, M. A., 2004. Haze Aerosols in the Atmosphere of Early Earth: Manna from Heaven. Astrobiology 4, 409-419.
123. Turtle, E.P., Perry, J.E., McEwen, A.S., DelGenio, A.D., Barbara, J., West, R.A., Dawson, D.D., Porco, C.C. 2008, Cassini Imaging of Titan's High-Latitude Lakes, Clouds, and South-Polar Surface Changes. Geophys. Res. Lett. submitted.
124. Veverka, J., 1973. Titan: polarimetric evidence for an optically thick atmosphere. Icarus 18, 657-660.
125. Wahlund, J.-E., Boström, R., Gustafsson, G., Gurnett, D. A., Kurth, W. S., Pedersen, A., Averkamp, T. F., Hospodarsky, G. B., Persoon, A. M., Canu, P., Neubauer, F. M., Dougherty, M. K., Eriksson, A. I., Morooka, M. W., Gill, R., André, M., Eliasson, L., Müller-Wodarg, I., 2005. Cassini Measurements of Cold Plasma in the Ionosphere of Titan. Science 308, 986-989.
126. Waite, J. H., Niemann, H., Yelle, R. V., Kasprzak, W. T., Cravens, Th. E., Luhmann, J. G., McNutt, R. L., Ip, W.-H., Gell, D., De La Haye, V., Müller-Wordag, I., Magee, B., Borggren, N., Ledvina, S., Fletcher, G., Walter, E., Miller, R., Scherer, S., Thorpe, R., Xu, J., Block, B., Arnett, K., 2005. Ion Neutral Mass Spectrometer Results from the First Flyby of Titan. Science 308, 982-986.
127. Waite, J. H., Young, D. T., Cravens, T. E., Coates, A. J., Crary, F. J., Magee, B., Westlake, J., 2007. The Process of Tholin Formation in Titan's Upper Atmosphere. Science 316, 870-875
128. Walterscheid, R. L., Schubert, G., 2006. A tidal explanation for the Titan haze layers. Icarus 183, 471-478.
129. West, R. A., Brown, M. E., Salinas, S. V., Bouchez, A. H., Roe, H. G., 2005. No oceans on Titan from the absence of a near-infrared specular reflection. Nature 436, 670-672.
130. Yelle, R. V., Borggren, N., de La Haye, V., Kasprzak, W. T., Niemann, H. B., Müller-Wodarg, I., Waite, J. H., 2006. The vertical structure of Titan's upper atmosphere from Cassini Ion Neutral Mass Spectrometer measurements. Icarus 182, 567-576.
131. Zellner, B., 1973. The polarization of Titan. Icarus 18, 661.

4 MISSION ARCHITECTURE OVERVIEW

The baseline mission includes three elements: a NASA provided orbiter and two ESA provided *in situ* vehicles. The *in situ* elements will be carried to Titan by the orbiter spacecraft. They are attached at either side of the orbiter spacecraft and consist of an aerial platform (montgolfière, a hot air balloon) and a lake lander. The composite, shown in Figure 1 will be launched by an Atlas V 551. A solar electric propulsion stage is included. The total launch mass of the composite is 6203 kg, including a total of 830 kg allocated for the *in situ* elements.

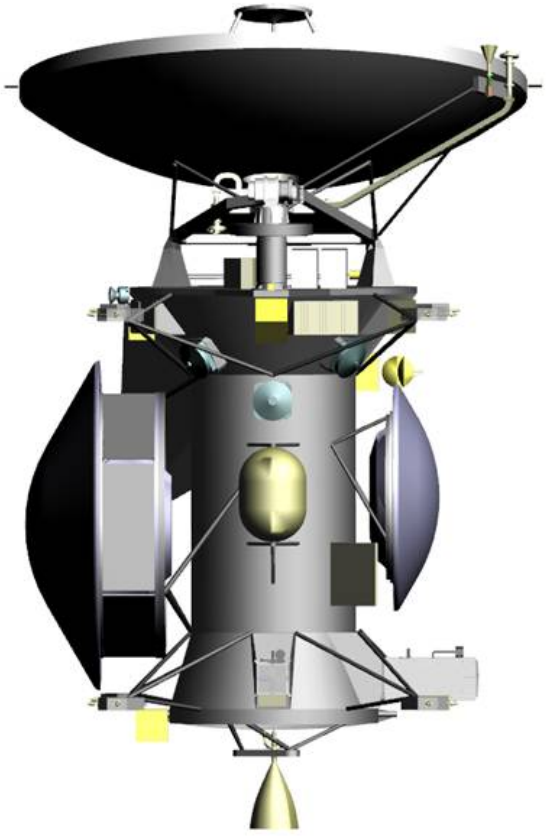

Figure 1 Artist's impression of the NASA orbiter with the *in situ* elements attached (curtousy NASA/JPL). The Montgolfière Probe is attached at the left, and the Lander Probe is attached to the right of the central cylindrical structure of the spacecraft.

4.1 Orbiter Spacecraft

The orbiter is a three-axis stabilized spacecraft that is powered by radio-isotope power generators. It was designed so as to include a 4 m diameter antenna, which can be steered about two axes, and which is using Ka-band transmission for high rate science downlink. This antenna will also be used to collect science telemetry from the *in situ* elements for later transmission to Earth.

A planning payload of seven instruments was accommodated on the orbiter:

- High resolution imager and spectrometer in near IR
- Penetrating radar altimeter
- Polymer mass spectrometer
- Sub-millimetre spectrometer
- Thermal infrared spectrometer
- Magnetometer and plasma package including magnetometer, energetic particle spectrometer, Langmuir probe, and a plasma spectrometer
- Radio science and accelerometer package

4.2 In situ *Elements*

The aerial platform will be realized by using a hot hair balloon. The gas at the inside will be heated by a Multi-Mission Radioisotopic Thermal Power Generator (MMRTG). The MMRTG will also be used as the only power source of the Montgolfière. The gondola, which will be supported by the balloon, contains all necessary subsystems, including instrumentation, and a high gain antenna (50 cm diameter) for communications to the orbiter spacecraft and to Earth.

A high level mass budget of the Montgolfière is shown in Table 1. The mass is broken down per mission phase. There are two separations required: one from the orbiter and one from the Probe to Orbiter Interface System (POIS), which includes radiators and thermal control hardware for cooling of the MMRTG during cruise.

The second *in situ* element is a lander, which will be targeted at a sea, and which therefore is designed for buoyancy during floating, but, as with Huygens, which will be capable of landing either in the sea or on the shore. The lander will be battery powered and therefore only has a lifetime of a few hours on the surface. A mass breakdown of the lander is shown in Table 2.

The *in situ* elements of the baseline mission are described in this report. Additionally a concept was developed for including instrumentation in the heat shield of the Montgolfière Probe (since this is addressing geophysical objectives, it was named “Geosaucer”). This is considered as opportunity instrumentation using spare volume and space mass capacity of the thermal protection system.

Table 1 High level mass breakdown of the Montgolfière Probe. The mass is specified according to mission phase with the launch mass at the top. The remaining mass after each separation is highlighted by a box.

	w/o sys margin	*w/ system margin*
Interface Mass	**428**	**571**
Struts (incl. sep mechs)	48.0	57.6
Radiators	12.1	14.5
Radiator supports	7.2	8.6
Fluid Lines	10.6	12.7
Entry Mass	**398**	**478**
DLS	20.0	24.0
Mechanisms	22.9	27.4
Harness	6.0	7.2
Communications	0.5	0.6
Heat Pumps	8.8	10.6
Front Shield	80.1	96.1
Back Shield	30.0	35.9
Floated Mass	**230**	**276**
Balloon	109.9	131.9
Gondola	120.0	144.1

Table 2 High level mass breakdown of the lander Probe. This table is organized in the same way as Table 1.

	w/o sys margin	*w/ system margin*
Interface Mass	**151**	**190**
Separation Mechanism	7.7	9.2
Entry Mass	**151**	**181**
DLS	14.9	17.8
Mechanisms	14.9	17.8
Harness	6.0	7.2
Communications	0.6	0.7
Front Shield	33.5	40.1
Back Shield	10.6	12.8
Landed Mass	**71**	**85**
Probe	70.5	84.6

4.3 Overview of the In situ *Element Planning Payload*

A model payload was established by the study science team for both ISE's and for an optional element (geosaucer). The suite of scientific instrumentation ensures that the science goals as defined in the Science Requirement Document [RD8] and summarized in Appendix A can be achieved. Dedicated instrument teams provided key information on their respective instrument or instrument package. All payload elements are outlined in the Payload Definition Document [RD9].

Many proposed instruments have a strong heritage from previous missions like Rosetta (cometary mission), Beagle-2 (Mars lander), Venus Express (Venus orbiter), and of course Cassini-Huygens. Others are currently being developed for future missions like ExoMars (foreseen launch 2016) and BepiColombo (planned launch 2014). A third fraction is based on newly accomplished state-of-the-art technical developments.

It is anticipated that already during the early study phases instruments will be further developed such that they match the progress and increasing maturity of mission and spacecraft design.

4.3.1 MONTGOLFIÈRE PLANNING INSTRUMENTATION

The Montgolfière carries 8 different instruments (packages). The mass of the payload accumulates to 21.5 kg. The total power consumption of all instruments is about 45 W, assuming simultaneous operations.

Table 3 Planning instrument complement on the Montgolfière.

Instrument	*Resources*		*Measurement*
	*Mass (kg)**	*Power (W)**	
Visible Imaging System Balloon (VISTA-B)	2.0	5	Camera system of three wide angle and one narrow angle cameras, spectral range 0.4 µm to 0.7 µm, stereo surface characterization and atmospheric phenomena
Balloon Imaging Spectrometer (BIS)	3.0	10	Imaging diffraction grating spectrometer, spectral range 1 µm to 5.6 µm, spectral sampling 10.5 nm. Composition and temperature mapping of surface at regional and local scale. Composition and optical properties of haze and clouds.
Titan Montgolfière Chemical Analyser (TMCA)	6.0	8	Ion trap mass spectrometer with a mass range 10 to 600 Da. Methane/ethane mole fraction, noble gas concentration at 10s of ppb. Characterises molecules in atmosphere above ppm levels. Chemical composition of aerosols.
Atmospheric Structure Instrument / Meteorological Package (ASI/MET)	1.0	5	Accelerometers, temperature sensors, capacitive sensors. Temperature profile, atmospheric density and pressure measurements during entry and throughout the whole mission.
Titan Electric Environment Package Balloon (TEEP-B)	0.95	1	Vertical and horizontal set of antennas. Conductivity of atmosphere and ELF-VLF waves. Coupling atmosphere/ionosphere and magnetosphere of Saturn.

Magnetometer (MAG)	0.5	1.5	Dual fluxgate magnetometer on boom. Field range ±1024 nT @ 23 pT resolution or ±18 nT @ 4 pT resolution.
Titan Radar Sounder (TRS)	8.0	15	Subsurface radar between 150 MHz and 300 MHz. Penetration depth >350 m at vertical resolution < 6 m.
Montgolfière Radio Science Transmitter (MRST)	0.0	-	X-band transmitter generating carrier and ranging signal, carrier frequency received by orbiter and Earth. Position of gondola.
8	**21.45**	**45.5**	

*a system margin of 20% is applicable

In the following key properties are summarized per instrument. A description of the intended science goals is provided in section 3.4.3.1.

The **Visible Imaging System for Titan Balloon** (VISTA-B) consists of a set of 4 cameras, 2 wide angle cameras for stereo imaging (fore-/backward pointing), 1 nadir pointing high resolution camera and 1 sideward looking camera-head for weather observation.

The **Balloon Imaging Spectrometer** (BIS) covers the wavelength range from 1 – 5.6 μm with a spectral sampling of 7 nm. It is a slit spectrometer with imaging capabilities.

The **Titan Montgolfière Chemical Analyzer** (TMCA) is an instrument package using an ion trap mass spectrometer to measure chemical composition of the atmospheres as well as the identification of gaseous species and aerosols. Samples are collected on plates and transferred to the vacuum system where they are pyrolysed, by either laser or a thermal heater. Ionisation is achieved by electron impact using a field effect device, additionally for a laser system, ionisation could be achieved by increasing the power of the laser desorption pulse.

The **Atmospheric Structure Instrument and Meteorological Package** (ASI/MET) combines a set of thermometers, pressure sensors and accelerometers. The individual sensors are distributed all over the gondola for most optimised data acquisition.

The **Titan Electric Environment Package** (TEEP-B) deploys an orthogonal antenna on a 1.5 m boom. It measures the vertical and horizontal field, the electric conductivity and permittivity of the atmosphere.

The **Magnetometer** (MAG) consists of two fluxgate sensors, which would be preferably boom mounted to minimise magnetic interference, and one or two sensor electronics boards located on the main equipment platform.

The **Titan Radar Sounder** (TRS) is planned to work at frequency between 150 and 350 MHz giving a minimum penetration depth of 350 meter and a vertical resolution of in the order of <6 meter. The dipole antenna with a total length of 1 m could be mounted on the skin of the montgolfière's gondola without a deployment mechanism.

The **Montgolfière Radio Science Transmitter** (MRST) will include an X-band transmitter that is received by either, or both, the orbiter and terrestrial deep space antennas. The transmitter is driven by an ultra stable oscillator.

4.3.2 LANDER PLANNING INSTRUMENTATION

The lander will land on a lake. Its nominal operation time on the surface is in the order of a few hours. The payload complement has 4 different elements. However, especially the chemical analyser package and the combined instrument package for meteorological and environmental observations consist of many different sensor units. The total mass of all payload instruments is 27 kg. The power consumption during simultaneous operation is almost 100 W.

Table 4 Planning payload complement on the Lander.

Instrument	***Resources***		***Measurement***
	Mass (kg)*	***Power (W)****	
Titan Probe Imager (TIPI)	1.0	7	Camera for descent and landing site imaging, wavelength range 0.4 µm – 1 µm, includes a lamp; local geology and lake feature at mm resolution
Titan Lander Chemical Analyser (TLCA)	23.0	75	*Atmosphere:* High resolution gas chromatography and mass spectrometry. Methane/ethane mole fraction, noble gas concentration to ppb levels and their isotopic ratios, C, N, O, H isotopic ratios Lake: bulk composition, chemical composition of organics, chirality, presence of biomarkers.
ASI/MET-TEEP-L	1.5	5.5	A multi-sensor package. Density, pressure and temperature during entry and after landing. Electric field and conductivity measurements.
Surface Properties Package (SPP)	1.5	11	A multi sensor package. Depth of liquid, physical properties of liquid, wave motion, magnitude and direction of *in situ* magnetic field. Wind speed and "rain drizzle" detector.
4	**27.0**	**98.5**	

*a system margin of 20% is applicable

In the following key properties are summarized per instrument. A description of the intended science goals is provided in section 3.4.3.2.

The **Titan Probe Imager** (TIPI) is a descent and surface camera that covers the spectral range from 0.4 µm to 1 µm. It uses a lamp to illuminate the adjacent area after landing.

The **Titan Lander Chemical Analyser** (TLCA) instrument consists of a high resolution time-of-flight mass spectrometer with a double column gas-chromatic (GC) inlet system. Two additional GC columns are included providing redundancy and performing 'path finder' experiments. A derivitisation/wet chemistry manifold is used to process liquid and solid samples suitable for injection onto the GC columns. The atmosphere gas inlets are included for atmospheric sampling during the Lander's descent and whilst on the lake surface.

The wet lander carries a mass-optimised combined version of the **Atmospheric Structure Instrument / Meteorological Package (**ASI/MET) and **Titan Electric Environment Package (**TEEP) instrument packages as described within the montgolfière payload compliment.

The **Surface Properties Package** (SPP) contains a variety of sensors. One downward facing sonar sounder and a set of two orthogonal pairs of acoustic transducers to determine sound speed of the liquid. In addition a tilt sensor and a 3-axis accelerometer monitor the Lander's motion while floating on the lake. In this package there is also a magnetometer (TSM) and the Acoustic Sensor Package (ACU) included. The ACU consists of 3 microphones, and an additional one including a membrane for drizzle detection.

4.3.3 OPPORTUNITY INSTRUMENTED HEAT SHIELD (GEOSAUCER)

The Geosaucer has only a very limited volume available for the integration of scientific instruments. A small package with 4 units and a total mass of 2.6 kg was identified. The power consumption is mainly driven by the radio science beacon and amounts to about 21 W.

Table 5 Planning payload complement on the opportunity instrumented heat shield (geosaucer).

Instrument	*Resources*		*Measurement*
	Mass (kg)[*]	*Power (W)*[*]	
Magnetometer (MAG-lite)	0.25	0.2	Magnetoresistive sensors. ±1024 nT at 32 pT resolution. Description of local magnetic field and variations throughout the mission.
Acoustic Sensor Package (ACU)	0.25	0.8	Acoustic sensors. Acoustic noise introduced by environmental sources.
Micro-Seismometer (μ-SEIS)	1.1	0.1	Micromachined silicon suspension unit. Detection of seismic activity, structure of outer shell and clues to the existence of inner ocean.
Geosaucer Radio Science Experiment (RS)	1.0	20	Coherent X band transponder, up/downlink to Earth. Tidally induced surface displacement.
4	**2.6**	**21.1**	

[*] a system margin of 20% is applicable

A **magnetometer** (MAG-lite) will measure the magnetic field in the vicinity of the Geosaucer's landing site. The instrument is a tri-axial magnetometer array based on small magnetoresistive (MR) sensors. The sensor electronics would either be of a digital FPGA-based design, which is currently being developed, or of an ASIC based design, which would require further specific development but offers considerable reduction in instrument power.

The magnetometer will measure both the inducing and induced magnetic field and thus provides clues on the magnetic environment of Titan.

The environmental package **Planetary Acoustics Experiment** (ACU) comprises three acoustic sensors ('microphones'), an acoustic drizzle detector ('microphone plus membrane') and a dedicated data acquisition and processing unit. The 4 sensors would be distributed symmetrically near the outer rim of the front shield's inner surface with 90° angular spacing.

This instrument will detect environmental noise and rain drizzling.

A **Micro-seismometer** (μ-SEIS) will measure body-waves from Titan-quakes at regional and teleseismic distances. The experiment contains a tri-axial seismometer array which enables the identification of the original direction of the respective seismic source and a quantitative analysis

of the signal. The μ-SEIS is a short-period instrument which operates at frequencies above 1 Hz with a noise level of <10 nm s^{-2} $Hz^{-1/2}$ based on a compact set-up. The scientific goals are:

- to determine the level of seismic activity on Titan's surface;
- to determine the structure of the outer ice shell;
- to provide indications on the existence of an internal ocean.

A **radio science** (RS) beacon consists of an X-band transponder that was designed to obtain two-way Doppler measurements from the radio link between the Geosaucer and the Earth. The instrument consists of electronics for the transponder, a patch antenna(s) mounted on the inside of the front shield, and is connected to the Command and Data Management Subsystem and the Power Control and Distribution Unit.

This experiment addresses the tidally-induced surface displacements and forced librations of the outer ice shell. It will provide insights into the atmosphere-ice-ocean system by tracking Titan's rotation.

5 MISSION PROFILE

The composite spacecraft will be launched by an Atlas V 551, and thrusting will continue using the SEP stage. The baseline launch date is in 2020. Multiple inner planet flybys are available, and the optimum for 2020 is an EVEEGA sequence. The SEP stage will be jettisoned after about 5 years from launch, as then its efficiency will be too low, due to the large distance from the Sun. With this anticipated trajectory the total transfer time to Saturn will last for about 9 years. Viable backup launch-dates were also identified with a similar profile.

The TSSM scenario is very similar to the one used by Cassini-Huygens. The *in situ* elements will be carried to the Saturn system by the orbiter spacecraft. After the interplanetary transfer both ISE's will be released after Saturn orbit injection and each prior to two different Titan flybys. This strategy maximizes the mass available to the *in situ* elements, while keeping the distance between the ISE's and the orbiter manageable for communications. The *in situ* elements will be released by spin-and-eject mechanisms, and each element will enter Titan's atmosphere separately. Spin is used for stabilization.

After release, the elements will have a ballistic cruise until entry for about 3 – 4 months and 3 – 4 weeks, for the montgolfière and the lander, respectively. Targeting will be performed by the orbiter prior to release (see section 6 for a discussion of the required accuracies). The montgolfière will be targeted at mid-latitudes, as there, zonal winds will enable it to float around Titan. The Lander will be targeted at Kraken Mare (prime target). During their descents to operational altitude (montgolfière), or to the surface (lander), respectively, both elements will sample the atmosphere.

The entry and deployment will also follow the Huygens experience. The thermal protection system (TPS) consists of a large front shell (aero-shell), which will absorb the main heat-load at entry, and a back shell protection. After entry the back shell will be pulled off by a drogue parachute, and the main parachute will be released. The Lander will continue gliding down on this main parachute. The montgolfière will descend to about 40 km, where the balloon will be released, which will be filled with ambient gas, using the airflow of the continuing descent. At the same time, together

with the balloon deployment, the MMRTG will be pulled into the inside of the balloon and heating the interior gas will start. Due to the warmer gas on the inside, buoyancy will be achieved at an altitude of ~7 km, and subsequently the montgolfière will rise again to its nominal altitude of 10 km.

The operational altitude of the montgolfière will be actively maintained by a vent valve. No further control system for maintenance of attitude and position is required for achieving the required science return. The montgolfière will be pushed by the atmospheric flow (wind; few m/s at 10 km). It is expected that the required duration for floating above one circumference at mid-latitudes will be between 3 and 6 celestial months. The design lifetime for the montgolfière system is 6 celestial months, with a goal of 1 year. There are, however, no consumables, which would limit its lifetime.

It is anticipated the lander would be operational for a total of 8 – 9 hours, with a minimum lifetime of 3 hours on the surface for chemical and mass analysis of the liquid. The lifetime of the lander is limited by battery power, and the batteries will be sized accordingly.

The following mission phases were identified:

- launch
- interplanetary transfer; operations are limited to checkout functions; telemetry interface is through the orbiter's TM/TC system
- ballistic cruise: after release from the orbiter the ISE's have a ballistic trajectory to Titan
- entry and descent
- science operations phase

6 MISSION ANALYSIS

6.1 General Considerations

After their release by the orbiter, the *in situ* elements will fly to Titan on a ballistic trajectory. The orbiter will perform all targeting. The release scenarios are summarized for both elements in Figure 2 and Figure 3.

The Montgolfière Probe will be released at the first Titan fly-by following the SOI manoeuvre, and its ballistic flight will last for about 3 – 4 months. The Montgolfière's entry will occur while the orbiter executes its Titan flyby, delayed by a few hours. The distance between the orbiter and the Montgolfière will therefore be between a few hundred thousand and 1 Mkm during this phase. The orbiter will collect the telemetry emitted during entry and will record it on-board for later transmission to Earth.

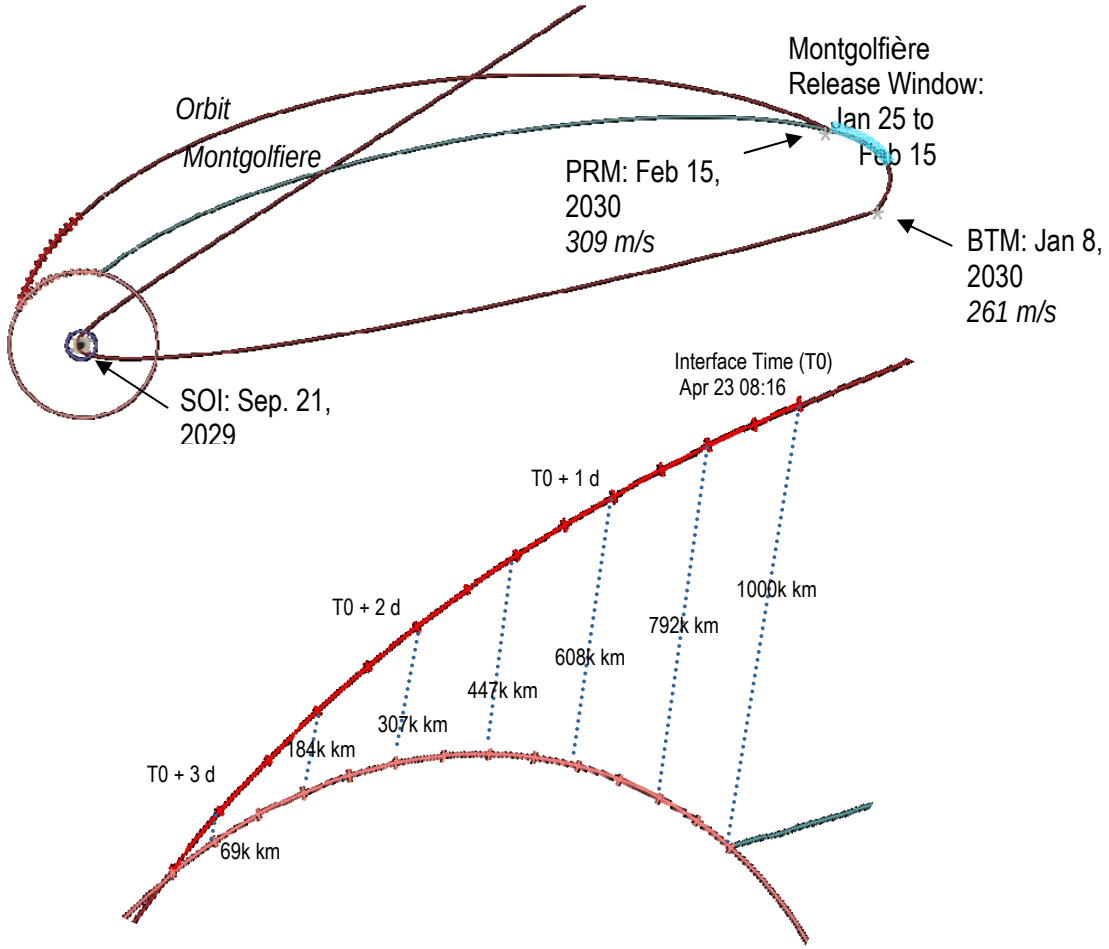

Figure 2 Release of the montgolfière from the orbiter. The upper graph indicates the path of the orbiter around Saturn (ellipse; it is the first orbit following SOI) together with Titan's orbit (circle). The period where the release is possible is indicated by a light blue arc close to apokron. The lower graph shows the evolution of distance between the orbiter and the montgolfière during and after the entry of the montgolfière.

The Lander will be released before the second Titan flyby and will have a ballistic flight duration of 3 – 4 weeks. Its entry will occur nominally 66 days after that of the Montgolfière. During entry, descent and landing, the orbiter fly on a trajectory that will bring it overhead the Lander, after about 9 hours, and thereby providing good communication opportunities for data transmission during all mission phases of the Lander's science mission. This data relay will be similar to what was used for Huygens, but more favourable due to the lower orbiter velocity (3 km/s instead of 6 km/s).

The distance as a function of time since entry is indicated at the right side of Figure 3. The total operational lifetime of the Lander Probe is 9 hours. The relative timing between the orbiter's pass

and the Lander's entry may however be adjusted by changing the release time. The release may occur at any time along the light blue arc in the left drawing of Figure 3.

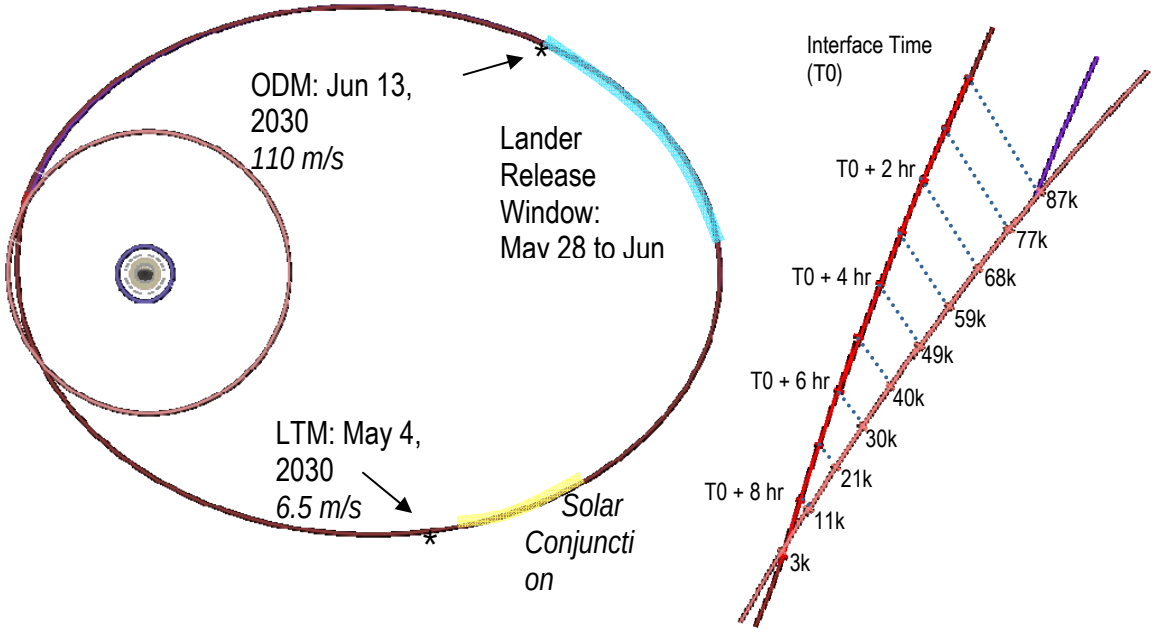

Figure 3 Release of the lander from the orbiter. The left graph indicates the path of the orbiter around Saturn (ellipse) together with Titan's orbit (circle). The period where the release is possible is indicated by a light blue arc close to apokron. Right graph shows the evolution of distance between orbiter and lander. The time refers to the duration since the entry in hours.

The entry velocity of the Montgolfière Probe is 6.3 km/s at the interface altitude of 1270 km, which is similar to what was used for Huygens (6.03 km/s). Due to its later delivery the Lander Probe has a significantly reduced entry velocity of 3.3 km/s.

The entry sequence includes the following steps: First, after entry, and triggered by a measured reduction of the deceleration, a mortar will open a pilot-chute. The pilot-chute is used for release and separation of the back cover. Upon release of the back cover, the main parachute will be deployed. The size of the main parachute is driven by the ballistic coefficient of the heat shield, such that the maximum deceleration between the front shield and descent module can be achieved, which allows for the safest collision-free release of the heat shield. Depending on the margin that is designed for the separation, some adjustment of the size of the main parachute is possible allowing for variations of the descent profile. For both ISE's only one main parachute is proposed. This reduces the complexity but yields longer descent durations, allowing more time for scientific atmospheric sampling. This is a driving requirement for the battery sizing of the Lander. Further trade-off between parachute staging and battery sizing will be required during the next study phase.

For the evaluation of the entry trajectory a reference atmospheric model as was provided by the Atmosphere Model Working Group formed by the JSDT. The model is based on Cassini-Huygens measurements [RD4]. The temperatures and pressures are plotted in Figure 4 as functions of altitude. The uncertainty of the model is represented by a range of three models. Each model was

used independently in the calculations, and the worst case of the results was used as the sizing case.

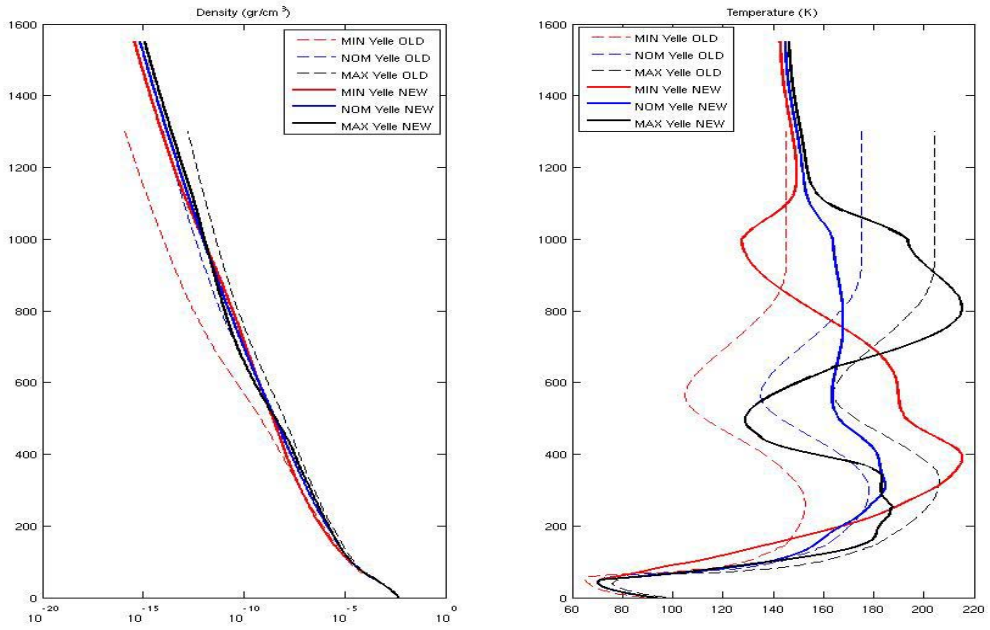

Figure 4 Density (left) and temperature (right) profiles of the three updated Yelle atmosphere models MIN, NOM and MAX (continuous lines) and the pre-Huygens Yelle atmosphere model (used for Huygens' design prior to flight, shown as dashed lines). Data were provided in [RD4].

For the heat protection shield, the same material used for Huygens (AQ-60) was assumed. The study team verified with industry (EADS) that this material could still be procured on a request basis. AQ-60 is qualified to a maximum heat flux of 2.5 MW/m^2, which constrains the ballistic coefficient and the flight path angle (FPA). Keeping the relation to Huygens' heritage the entry velocity was fixed at 6.3 km/s, which constrains the FPA to –59° and –65° for the Montgolfière and the Lander, respectively. Due to navigation uncertainties there is a corridor of ±3° around these FPA's. For steeper FPA's the maximum heat flux becomes too high, while shallower FPA's have the drawback that the total heat load increases, resulting in higher mass of the heat shield, and also increases of the total flying time. However the chosen FPA's have some limited flexibility of a few degrees.

6.2 Trajectory of the Montgolfière

The Montgolfière will be targeted at about 20° N, where the predicted zonal wind has a maximum for the time of arrival 2030 ([RD4]; wind speeds of the order of a few m/s may be expected). Results from a Monte-Carlo dispersion analysis indicate that the dispersion of the FPA is about 3° (at 3 σ). This uncertainty was taken into account for the aerothermal analysis.

The release of the main parachute is triggered by a deceleration event. For the Montgolfière the altitude of this release is at about 130 km ±20 km, depending on the choice of the atmospheric profile, and occurs about 1.5 – 2 hours after entry. The diameter of the main parachute is 9 m, as

required for a safe separation of the 2.6 m diameter heat shield. The terminal velocity of the parachute is 6.5 m/s, which is compatible with the deployment and filling of the balloon.

At an altitude of about 40 km (measured by a pressure gauge, and using an assumed altitude pressure relation) the balloon will be pulled out, and at the same time the MMRTG will be pulled inside the balloon. After having achieved sufficient buoyancy, the float altitude will be actively maintained within a range of ±2 km by a vent valve at the zenith of the balloon. The altitude will be monitored by a pressure sensor.

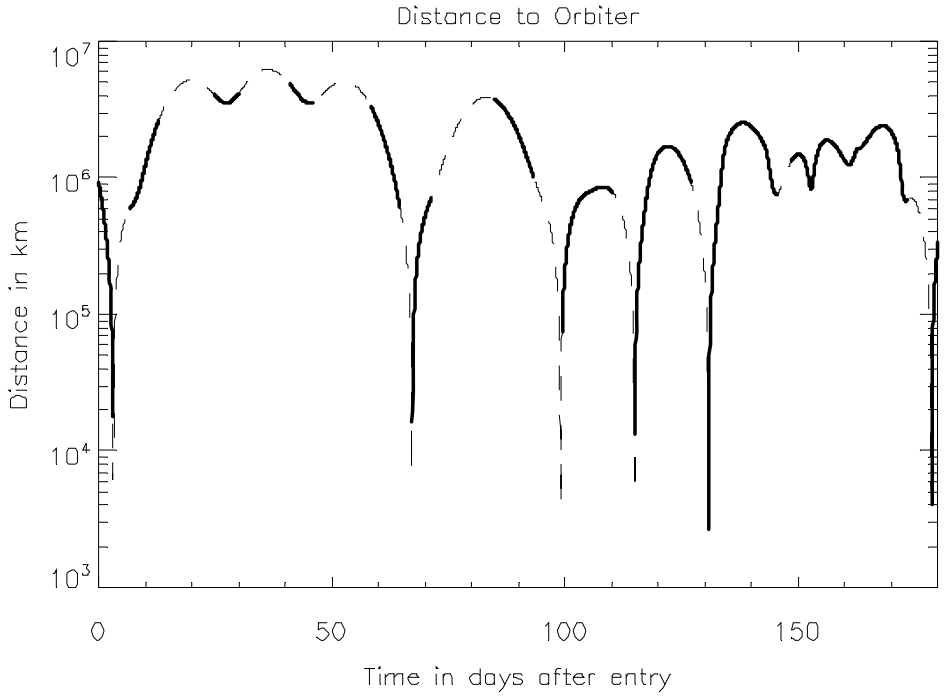

Figure 5 Distance between Montgolfière and orbiter. The evolution of the distance is plotted with a dashed line; periods when the orbiter is above 20° elevation (typical useful limit for telecommunications) are drawn with a full line.

In the following the buoyant Montgolfière will slowly drift around Titan, with an expected velocity of ~2 m/s. During the nominal lifetime of the Montgolfière, the orbiter will still be performing Titan fly-bys. Therefore, the distance to the orbiter varies between 5×10^6 km and a few 1000 km during this phase, and is shown in Figure 5 as a function of time. Figure 5 shows the total evolution of distance. Periods where the orbiter is above an elevation of 20° are plotted with full lines. It can be seen that the orbiter comes significantly closer during short intervals, which provides for the opportunity of higher telemetry capability. These periods may slightly shift on the time axis depending on the actually achieved zonal velocity of Montgolfière, but would not drastically influence the total amount of available telemetry capability.

The elevation of the orbiter as seen from the Montgolfière is shown in Figure 6. For this plot the drift of the Montgolfière has not been taking into account, and the evolution of orbiter elevation is plotted relative to the position (longitude and latitude) of the point of entry.

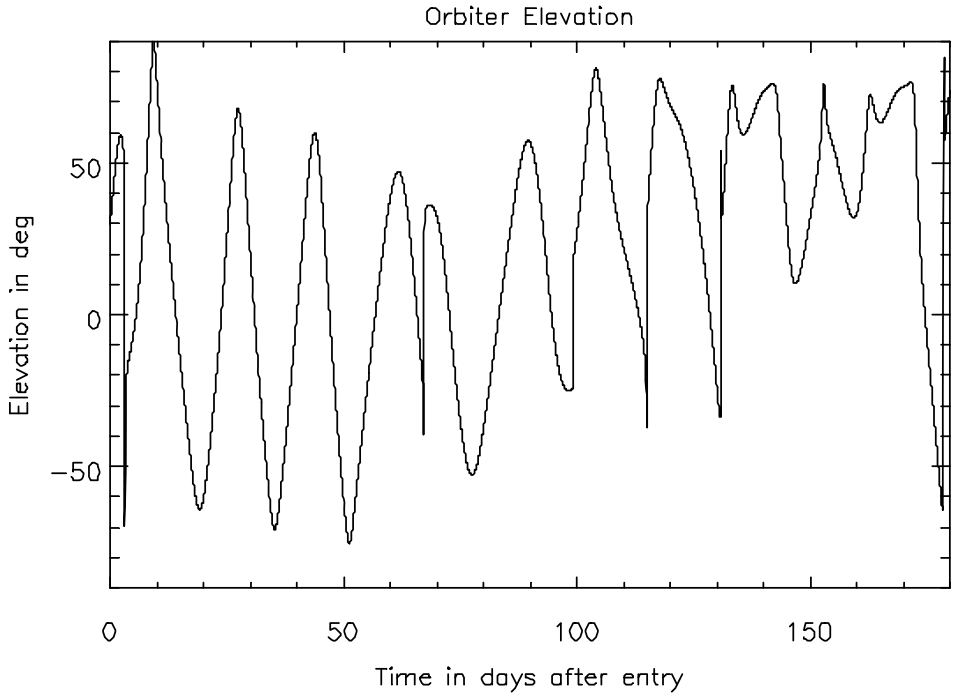

Figure 6 Elevation of the orbiter as seen from the balloon as a function of time.

6.3 Trajectory of the Lander

For the calculation of the trajectory and for the determination of the landing error ellipse the predicted entry velocity of 3.3 km/s was used. The heat-shield of the Lander has a diameter of 1.8 m, and the required size of the main parachute is 7 m, and will be deployed at about150 km altitude. The total time from entry to landing is 5.7 hours, and the terminal velocity with the parachute is 1.9 m/s. The parachute may be discarded at a few 10 m altitude to avoid it falling on the lander (see section 8.2.3.3).

The Lander will be targeted at Kraken Mare, a northern lake between 68° to 72° N and 35° to 70° E (see Figure 8 at the right for an estimated size of Kraken Mare). The entry and descent trajectory is shown in Figure 7. The Lander initially follows the incoming hyperbola of its ballistic trajectory during the entry phase and then drifts eastwards due to the zonal wind.

A full Monte-Carlo dispersion simulation of the EDL was performed to calculate the size of the landing error ellipse. The dominant contributions are from uncertainties of the wind model and of the dispersions at entry. It has been shown that the landing area will be within an ellipse of about 400×160 km (3 σ; the major axis is 16° below the E-W direction), which is compatible with landing in Kraken Mare (requirement <400×400 km; see Figure 8).

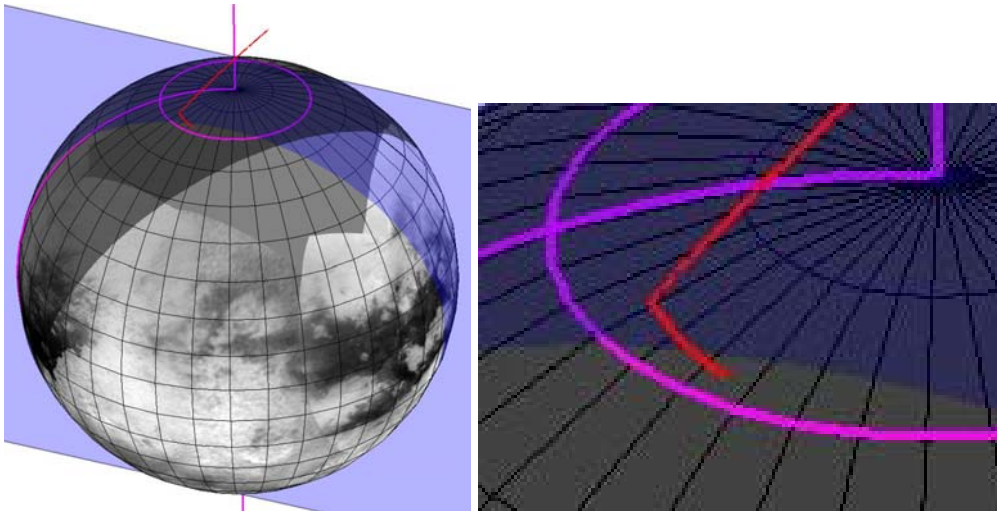

Figure 7 Illustration of the EDL targeting Kraken Mare. Left: View of the Titan globe with the 0° meridian and the 70° N parallel indicated as pink lines. The EDL trajectory is shown as a red line. The plane of the incoming hyperbola is shown in blue. Right: A zoom on the lower part of the trajectory.

The single parachute scenario was considered for simplicity. A possible reduction of the descent duration, and also of the resulting landing error ellipse may be achieved by a moderate reduction of the size of the main parachute, at the cost of reduced margin for separation of the heat shield, or alternatively – as for Huygens – by parachute staging and deployment of a second, smaller parachute. This may be explored further, if needed. It is concluded, however, that with landing in Kraken Mare appears feasible with the current descent strategy.

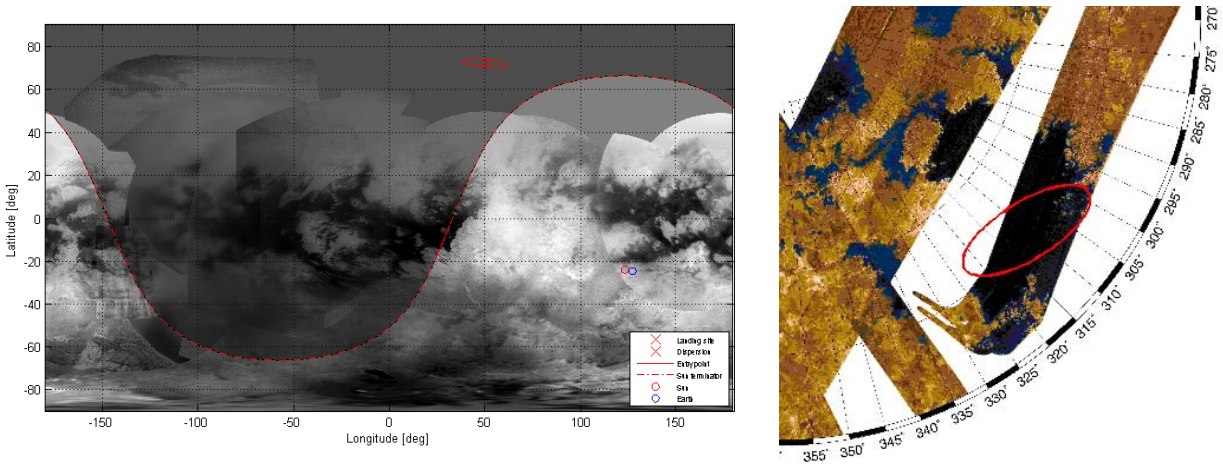

Figure 8 Size of the landing ellipse at Kraken Mare. The error ellipse is indicated on a cylindrical projection (left) and on a polar projection (right). The terminator and the direction to the sun are indicated on the left image (red lines and red circles at –20° latitude). On the right a radar image from Cassini is underlaid, where lakes are indicated in black.

Due to the arrival geometry for the considered interplanetary trajectory, the target area will not be illuminated by the sun (see terminator in Figure 8), but some illumination will provided by Saturn-shine. However, the higher altitude part of the descent will be illuminated by sunlight allowing studying the heat balance and other properties of the atmosphere requiring sun light. The landing strategy and execution of the pre-planned sequence will not be affected by the surface not being

illuminated by the sun. Landing will be controlled mostly by accelerometers and pressure sensors, and possibly by a low-altitude proximity sensor for triggering parachute separation.

Due to the geometry between the orbiter and the Lander (see Figure 3), the distance between the two vehicles steadily decreases during the radio relay phase. The distances are shown in Figure 9, and are decreasing from 80,000 km to less then 10,000 km. This scenario is favourable for data transmission to the orbiter. The Lander operations will be optimized to best take this into account by trading power for earlier data transmission (at lower rate) for critical data, with higher transmission rates towards the end of the Lander mission, using variable data rate.

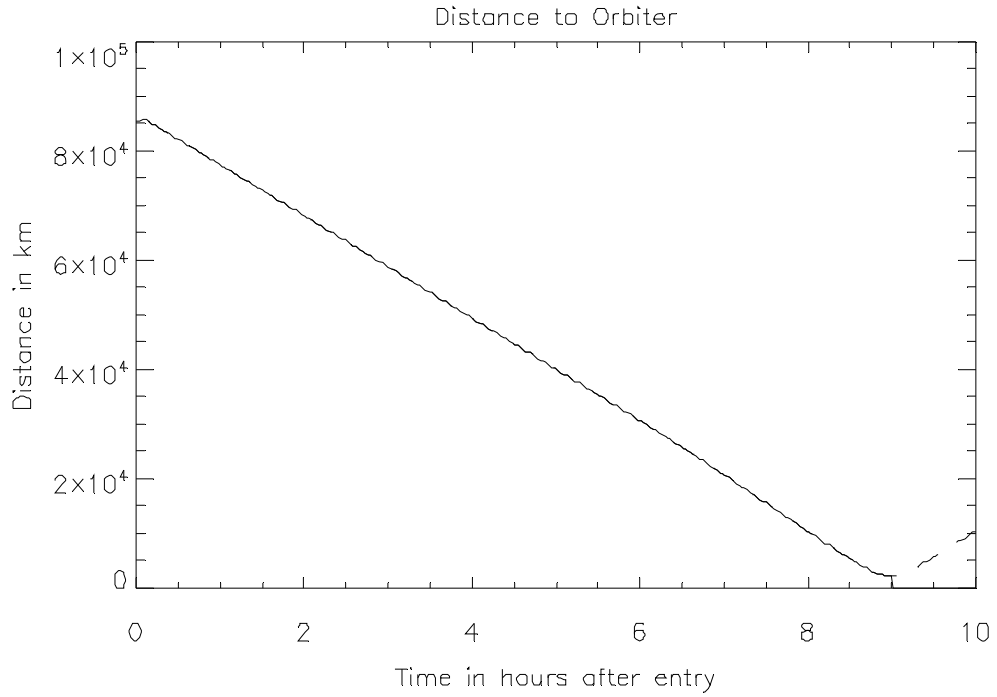

Figure 9 Distance between Lander and orbiter. The evolution of the distance is plotted with a full line for the time when the orbiter is above 20° elevation, and with a dashed line when it is below.

The elevation of the orbiter as seen from the Lander is plotted in Figure 10. It is slightly above 50° for most of the time, and peaks at 80° shortly before the orbiter moves below local horizon.

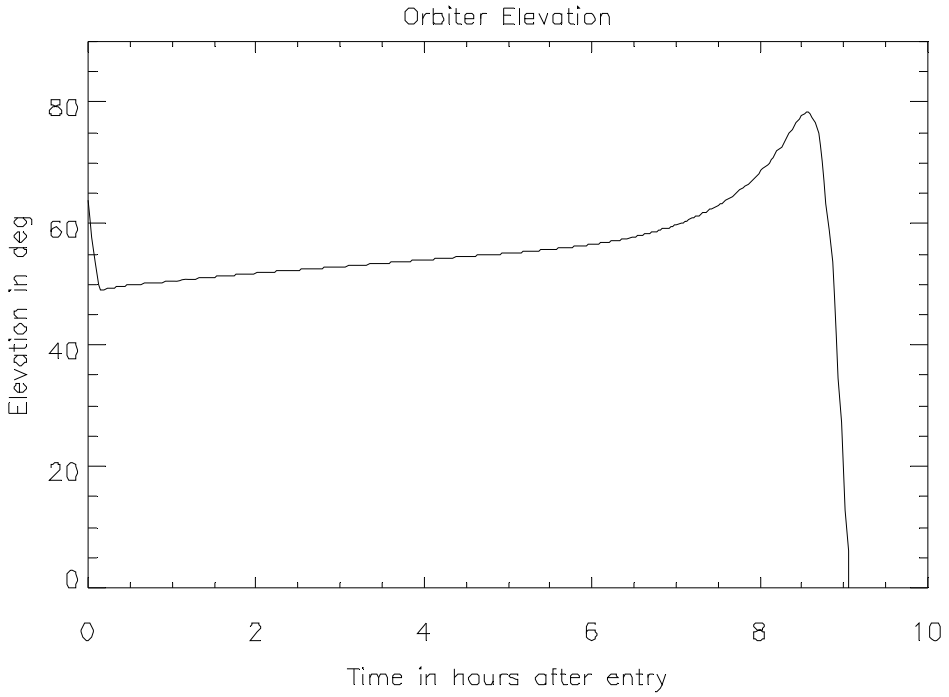

Figure 10 Elevation of the orbiter as seen from the Lander as a function of time from entry.

7 AERO-DYANAMIC AND AERO-THERMODYNAMIC CALCULATIONS

To provide flexibility of the release scenario, and to successfully build on the heritage of Huygens with respect to the design of the thermal protection systems, the entry velocities of both elements were assumed to be the same for the baseline of the CDF study, being 6.3 km/s at the atmospherie interface altitude assumed at 1270 km (compare Huygens 6.03 km/s at 1270 km altitude).[3]

The diameters of the heat shields are 2.6 and 1.8 m and the entry masses are respectively 478 and 181 kg for the Montgolfière and the Lander. This yields respective ballistic mass-to-area ratios of ~95 and ~71 kg/m^2, which are higher than that of Huygens (55 kg/m^2). Simulations were performed with the entry velocity and flight path angles, and it was verified that the heat flux remains in both cases below 2.5 MW/m^2, which is the qualification limit of the AQ-60 ablative material). The dynamic pressure peaks at 9 and at 7.2 kPa for the Montgolfière and the Lander, respectively (4.4 kPa for Huygens).

For the aerothermal and aerodynamical calculations the assumed shapes of the front shells follow the design that was used for Huygens[4]. They have a 60° half angle cone with a rounded nose with a radius of curvature of 1.25 m. The diameters of the wide side of the cone are 2.6 and 1.8 m, respectively. The back cover of the Montgolfière Probe is higher than what was used for Huygens as it has to include the MMRTG and the balloon container. See Figure 11 for a drawing and for indications of dimensions of both probes.

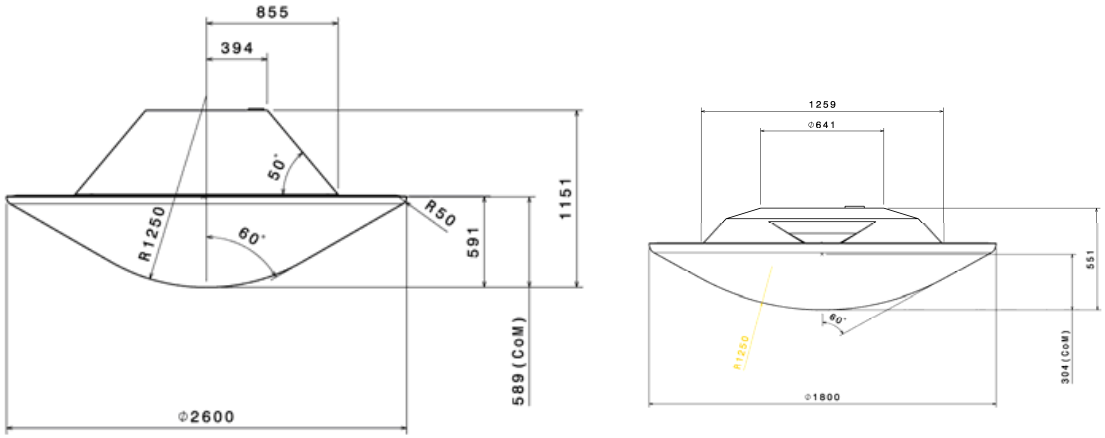

Figure 11 Assumed shape and dimensions of the Montgolfière Probe and the Lander Probe thermal protections.

[3] This is a conservative assumption, which is maintained for added flexibility of the release scenario and for comparison with Huygens; the entry velocity of the lander will likely be lower (see section 6.3).
[4] Alternative designs require building an aerodynamic database including Cd, CI and CM values, which need to be measured through wind tunnel tests and time consuming CFD computations.

7.1 Aerothermodynamic Calculations

7.1.1 PARAMETRIC ANALYSIS

The assumed aerodynamical coefficients that were needed for the trajectory analysis and the modelling were equal to the ones used for Huygens [RD12]. Accordingly, the ballistic coefficients of each probe differ only as a function of mass and base area.

Aerothermal calculations were performed with the following input parameters: the atmospheric profile (temperature and density as function of altitude), characteristic of the probe (mass, diameter, drag coefficient, etc) and the entry conditions (velocity and flight path angle).

Parameterization of heat flux correlations[5] ([RD13] and [RD14]) were used for computing radiative and convective heat fluxes at stagnation point. A margin of 70% and 30% was added respectively for radiative and convective fluxes to account for uncertainties of the models. As a starting point, the heat fluxes at the back shield were considered to be 5 – 10% (depending on the position) of the upstream convective flux at the stagnation point. In order to provide a more detailed analysis of the radiative heat flux and to further check the validity of the used correlations, the emission power of the flow has been computed independently by two steps, first by calculating the chemical reaction flow and secondly by calculating the the emission power and the total radiative heat flux.

For the parameterization of the atmosphere, three different profiles were provided by the atmospheric working group [RD4], reflecting the variability of the atmosphere. These will in the following be referred to as *Yelle MIN*, *Yelle NOM*, *Yelle MAX*, respectively. The temperature and density profiles as functions of altitude are plotted in Figure 4 for each of these models together with the ones used for Huygens pre-launch calculations [RD15]. The atmospheric composition was assumed in all cases to be (in relative mole fractions): 98.49% N_2, 1.4% CH_4, and 0.11% H_2.

Heat flux calculations were performed for

- each of the three atmospheric models;

[5]The functional form of the used correlations were:

- Radiative heat flux correlation:
- $$q_{rad} = 4.85 \cdot 10^5 \cdot \frac{Nose_D}{6.09 \cdot 10^{-1}} \cdot \rho_R^{1.65} \left(\frac{V}{3.048 \cdot 10^3} \right)^{5.6}.$$

  The above correlation was combined with air correlation below CN formation temperature, based on approximate shock temperature.
- Convective heat flux correlation:

$$q_{con} = 374.6 \cdot \sqrt{\frac{6.09 \cdot 10^{-1}}{Nose_D}} \cdot \rho_R^{0.49} \left(\frac{V}{3.048 \cdot 10^3} \right)^{3.81}.$$

Where V indicates the upstream velocity in m/s, $Nose_D$ being the nose diameter in m and $\rho_R = \rho/1.22522$ is the density ratio, with the upstream density ρ in kg/m^3.

- three different entry velocities 5.3 km/s, 6.3 km/s, 7.3 km/s at the interface altitude of 1270 km;
- flight path angles (FPA) ranging from –50° to –70°. Note in this context that the probes are deflected out of the atmosphere for FPA's >–40°. For steeper FPA's the increase in maximum heat flux becomes significantly higher.
- several mass/area coefficients of the entry probes in the range from 50 kg/m^2 to 190 kg/m^2. With this approach the Lander (~71 kg/m^2) and the Montgolfière (~95 kg/m^2) Probes could be covered. For comparison the ratio for Huygens was 55 kg/m^2.

The aerodynamical calculations yielded the heat flux, the total heat load, and the deceleration as functions of time. The peak of the heat flux and of the decelerations occur at the stagnation point and need to be considered together with the total heat load for the design of the TPS system.

It was found that the dependency of the results on the choice of the atmospheric model is rather weak: the maxima of the heat fluxes and the decelerations are both within a factor of 1.1 – 1.2 of each other, and the total heat loads differ by a factor of 1.0 – 1.1. The variation of the entry velocity has a larger impact on the maximum heat flux, it changes by a factor of 2.2 – 2.3 from 5.3 km/s to 6.3 km/s, and by a factor of 2.1 – 2.2 from 6.3 km/s to 7.3 km/s. The total heat load and decelerations vary with similar factors as the maximum heat flux for changes of the entry conditions.

By comparing the results for each atmospheric model, the most demanding case is for the *Yelle MIN* model, which was therefore used as the baseline for further reference of the TPS sizing. The 6.3 km/s entry condition has been selected as reference baseline due to Huygens' heritage. The driving limit for possible design combinations of mass/area ratios and for FPA's is due to the maximum allowed heat flux (<2.5 MW/m^2). Therefore the allowed parameter space can be drawn by using the case for of the 6.3 km/s entry velocity and the *Yelle MIN* atmospheric model. The allowed range of mass over area ratios and FPA's is indicated in Figure 12 as a shaded area. Reference cases for the three elements under consideration in this study and during the CDF study are also indicated: the Montgolfière Probe with its mass over area ratio of 95 kg/m^2 has a minimum possible FPA of –68°, while the Lander Probe with a ratio of 71 kg/m^2 has a minimum possible FPA of –70°.

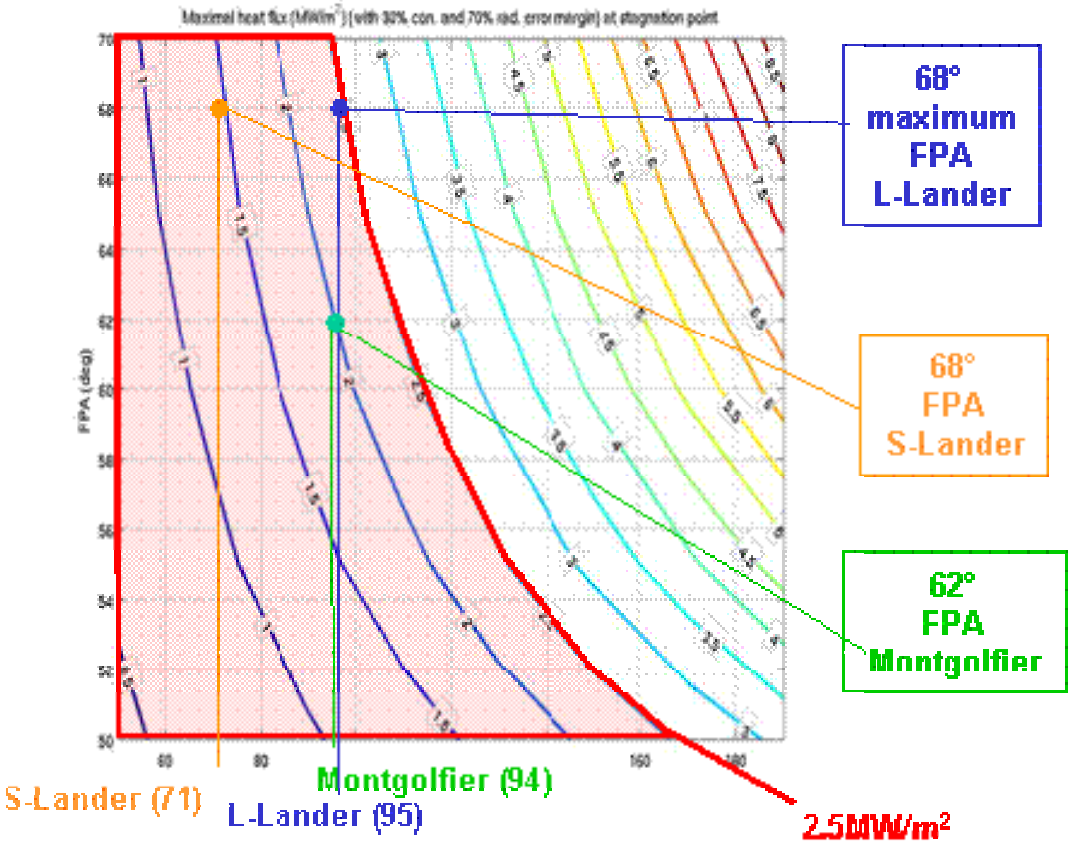

Figure 12 Equipotential lines of the maximum heat flux as calculated with the *Yelle MIN* atmospheric model are drawn as a function of mass over area ratio of the entry elements (abscissa) and of the FPA (ordinate) for the baseline 6.3 km/s entry velocity. The feasible domain is shaded in red. Example reference cases for possible FPA's are indicated per element.

7.1.2 RESULTS

The results of the aerothermodynamics calculations for the selected configurations are:

- Montgolfière Probe: the deceleration profile reaches a peak value of roughly 15 g; the heat flux (at stagnation point) reaches a peak value of approximately of 2 MW/m^2 and the total heat load has a maximal value of almost 60 MJ/m^2 (well below the 200 MJ/m^2 limit).
- Lander Probe: the deceleration profile reaches a peak value just above 16 g; the heat flux (at stagnation point) reaches a peak value of 1.5 MW/m^2 and the total heat load has a maximal value of 42 MJ/m^2 (also below the 200 MJ/m^2 limit).

7.2 Stability Analysis

A preliminary analysis, with a modified Newtonian method[6], indicates stability (in pitching) in the hypersonic regime: the coefficient of moment CM as a function of the angle of attack (AoA) shows a negative slope for positive AoA (w.r.t. possible centre of mass points) – see Figure 13.

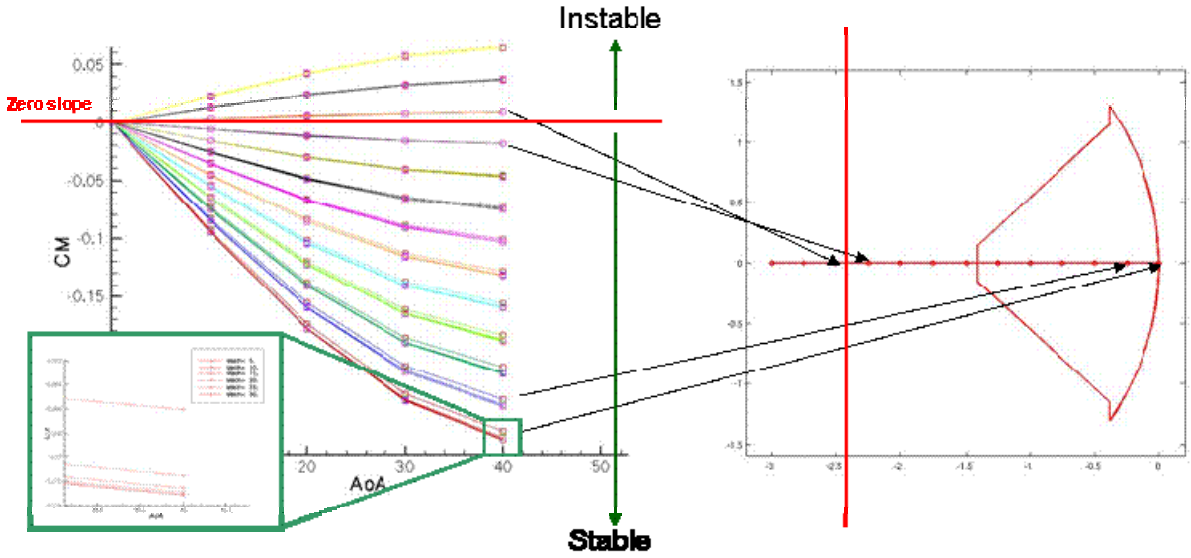

Figure 13 Results of the stability analysis: the coefficient of moment CM (with respect to different points along the axis of the probe) as a function of the angle of attack (AoA) shows a negative slope for positive AoA indicating stability (against pitching).

Within the limited time available for the study aerodynamic stability in the supersonic regime (before parachute opening) was only tested in 0^{th} order. In case the centre of pressure lies below the CoG of the probe, it is assumed that the CoG could further be lowered by increasing the TPS mass of the front shield. A detailed stability analysis will be carried out as part of the following design phases.

[6] The Newtonian method considers the base region, as well as the shadowed region, not facing the flow. Thus it considers the pressure coefficient to be zero there. A better approximation can be obtained introducing one third of the infinite pressure acting on the base. This modification introduces an additional contribution to the axial force coefficient that can be computed by (assuming a uniform distribution) $C_{Base} = \frac{2}{\gamma \cdot M^2} \cdot \left(\frac{p}{p_\infty} - 1 \right)$ where γ is the fractional specific heat, M the Mach number and p the pressure.

8 *IN SITU* ELEMENTS DESIGN OVERVIEW

8.1 Montgolfière Probe

8.1.1 SYSTEM OVERVIEW

The Montgolfière Probe has the following subsystems (see Figure 14): the Montgolfière, an Entry Descent and Inflation Subsystem (EDIS), and the Probe to Orbiter Interface System (POIS). The Montgolfière is the system that is finally floating in Titan's atmosphere. It uses a balloon filled with atmospheric gas, which is internally heated by a MMRTG. This balloon supports a gondola, which includes the scientific instruments and the system equipment. The other main subsystems (EDIS and POIS) are only used during the earlier mission phases.

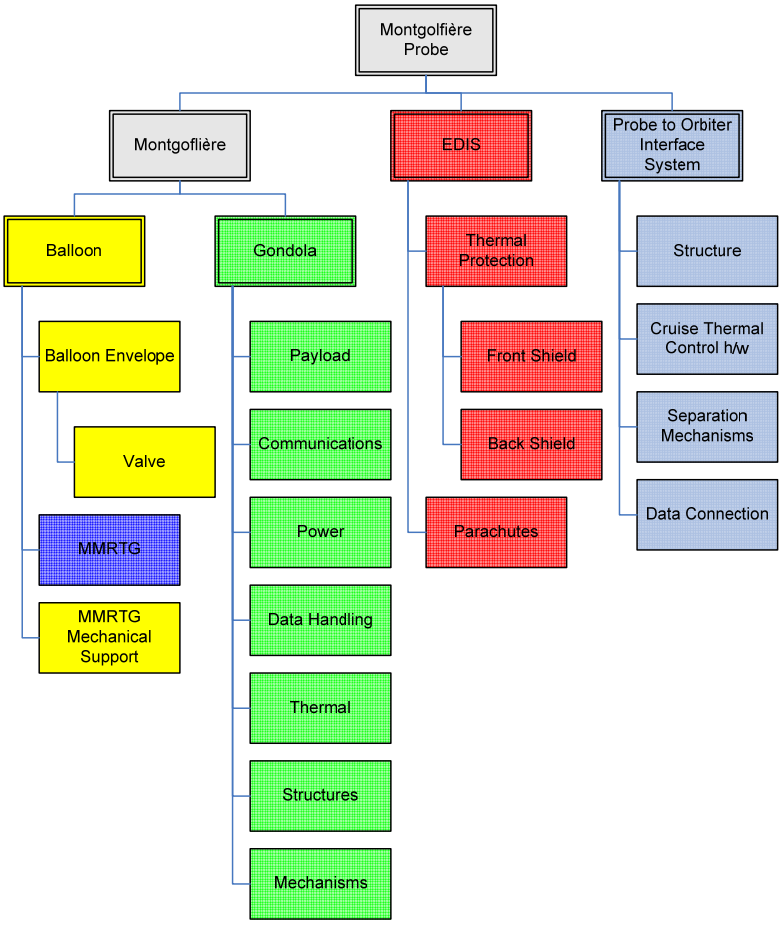

Figure 14 Elements of the Montgolfière Probe.

The main function of the Probe-to-Orbiter Interface Subsystem (POIS) is to provide the interface to the separation mechanism of the orbiter. In addition, this system also provides the structural support of the radiator that is used to radiate heat from the MMRTG when in stowed configuration

during interplanetary transfer and during the ballistic flight prior to the entry. It will remain attached to the Montgolfière Probe after separation from the orbiter, and will be released shortly before entry.

The Entry, Descent and Inflation Subsystem includes all necessary hardware for these phases, thermal protection shields, parachutes and the respective release mechanisms. There are only two parachutes required, a drogue parachute and a main parachute.

The operations phase of the Montgolfière will be split between a science mode and a telemetry mode. As the system is limited by the maximum electric power available from the MMRTG (100 W), it is expected that instrument operations and data transmission will be alternated.

Table 6 describes the high level mass breakdown of the Montgolfière Probe system. The specified masses generally include a design contingency of 20% system margin (ESA standard). The mass of the MMRTG is known (unit as built), and therefore no contingency is included. For the mass of the balloon envelope a contingency margin of 30% was assumed. This will be explained in more detail in section 8.1.2.2.

Table 6 Masses of the main subsystems of the Montgolfière Probe (including margins)

Element	**Mass in kg**
POIS	93
EDIS	202
Balloon 132 Gondola 144 Montgolfière total	276
Total launch mass	**571**
Launch margin	29
Allocated mass	600

8.1.2 MONTGOLFIÈRE SYSTEM

8.1.2.1 Configuration

The goal of the design was to accommodate all required units on a platform that is as small as possible. Additionally, the same geometry for the front shield as was used for Huygens was assumed, which includes a 60° half-angle cone with a nose radius of 1.25 m. The Montgolfière is embedded inside front and back shields for the atmospheric entry (Figure 15).

A cross-section of the Montgolfière in stowed configuration is shown in Figure 16. The front shield is indicated at the bottom of the figure. The POIS including radiators is indicated at the back of the drawing. The dominating feature at the centre is the MMRTG. In this configuration the MMRTG is supported by the main platform, which is the main load carrying structural element. The MMRTG was positioned as low as possible to provide a low CoG.

At the top of the probe, the main items for the descent are accommodated, including the balloon, and the structural interface for the back shell. The back shell supports the back heat shield, and the parachutes. The high gain antenna is also mounted on the top half.

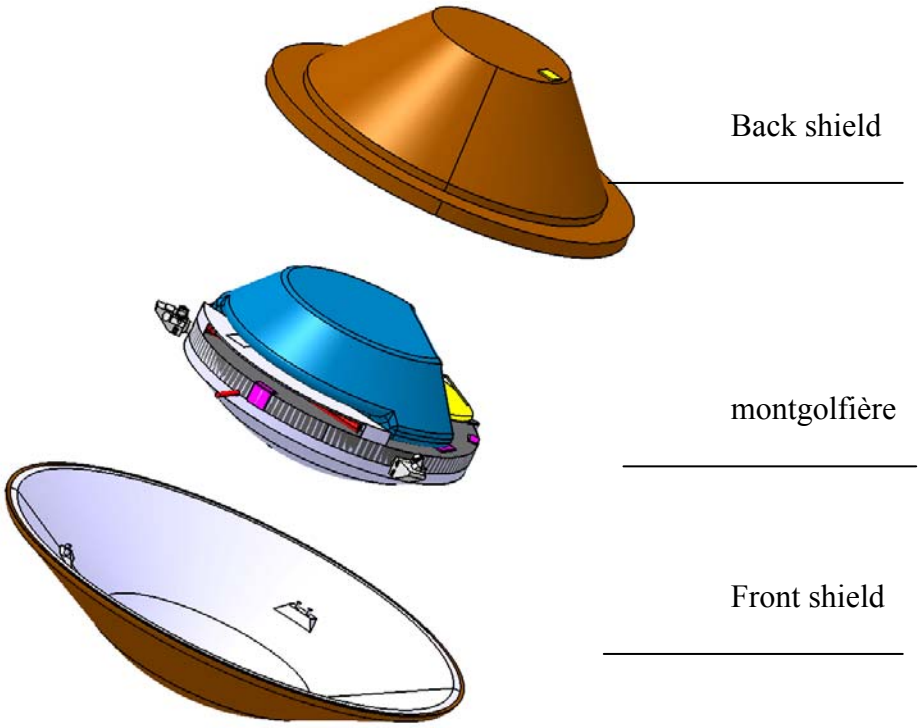

Figure 15 Montgolfière overview

The units for data-handling, power conditioning and telemetry are located at the nadir side of the main platform, together with the payload instrumentation. The nadir side of the gondola is closed by a non-structural skin to provide a thermal barrier.

The front shield, the back shield and spacecraft interface are attached with a three point separation system to the platform. The separation mechanisms considered are a heritage from the Huygens probe separation subsystem SEPS [RD10]. The three connection points are also the main connection points for the balloon and parachute suspension lines.

The DLS components (mortar, drogue and main parachute) will be attached on the back shell. This requires a structurally stronger back shell supporting the mass of the parachute and loads from the mortar ignition, but avoids the necessity for an additional support structure that may hinder the deployment of the balloon. A break-out patch has to be implemented for the mortar ejection.

The back shield encloses the complete gondola. As in Huygens, a labyrinth sealing at the interface with the front shield shall provide a non structural thermal and particulate barrier. A low gain patch antenna on the back shield has been included to assure communication capability during the ballistic cruise and during the atmospheric entry, up to the separation of the back shield.

The MMRTG needs to be integrated at the final stages. The Montgolfière system has therefore been split into three major sub-assemblies, which are all connected at the three mounting points at the side of the main platform: 1. front heat shield, 2. main platform, and 3. back cover including back-shield, parachutes and balloon. In this way the three assemblies can be supported individually, allowing a late integration of the MMRTG, and subsequently facilitating relatively simple final assembly steps. The MMRTG needs to be connected to the main platform for support of launch loads, and needs to be connected to the support cabling of the balloon, such that it can be pulled into the balloon during deployment.

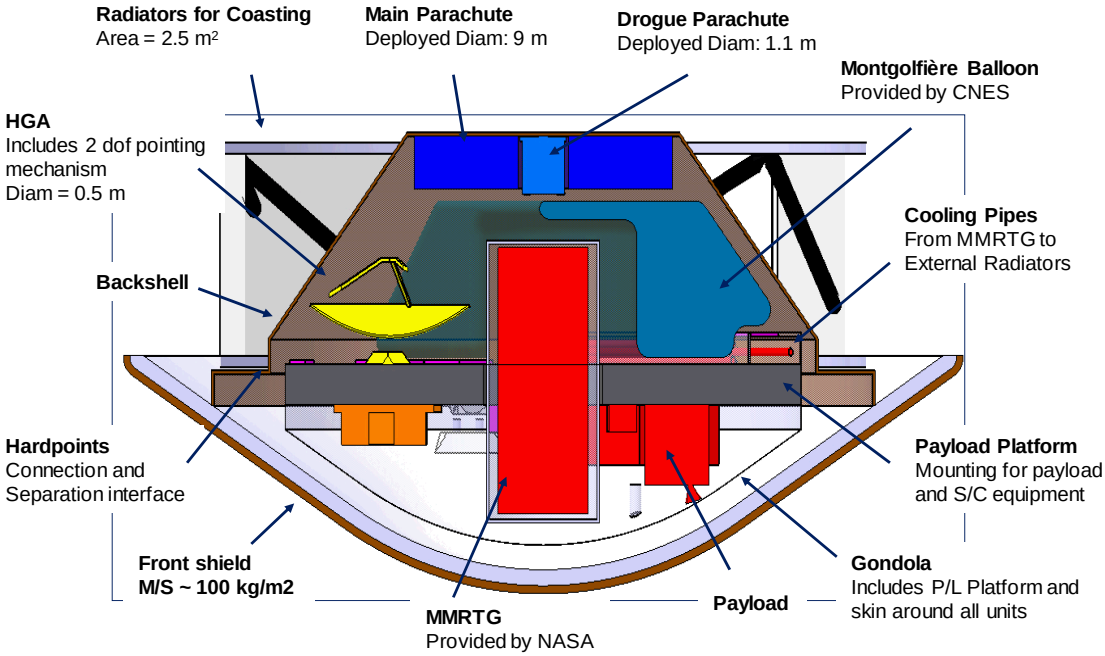

Figure 16 Cross section of the Montgolfière in stowed configuration. The direction of the ballistic flight is downwards in this drawing.

The packed balloon rests on top of the platform covering as much as possible the MMRTG to simplify the transfer of the MMRTG into the balloon. The package of the folded balloon has a cut-out providing the necessary space for the accommodation of the HGA and leaving a side of the MMRTG accessible for integration handling and routing of cooling lines (Moreover this allows some heat to escape from underneath the balloon).

As the balloon envelope must not interfere with mechanisms on the platform (HGA pointing and MMRTG release), it should be extracted through the bottom of its stowage container. This stowage container is attached to the back shield.

The top of the platform (Figure 18) carries the LGA, the RF patch antennas for attitude determination and the HGA that all require a field of view in the zenith hemisphere.

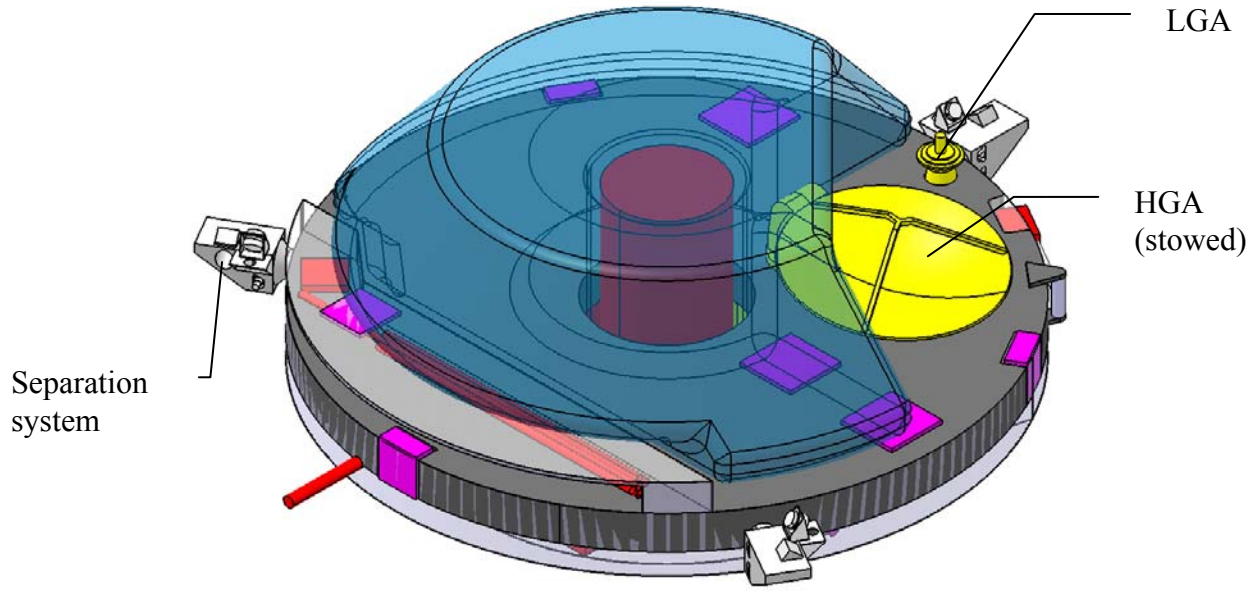

Figure 17 Gondola top view in stowed configuration

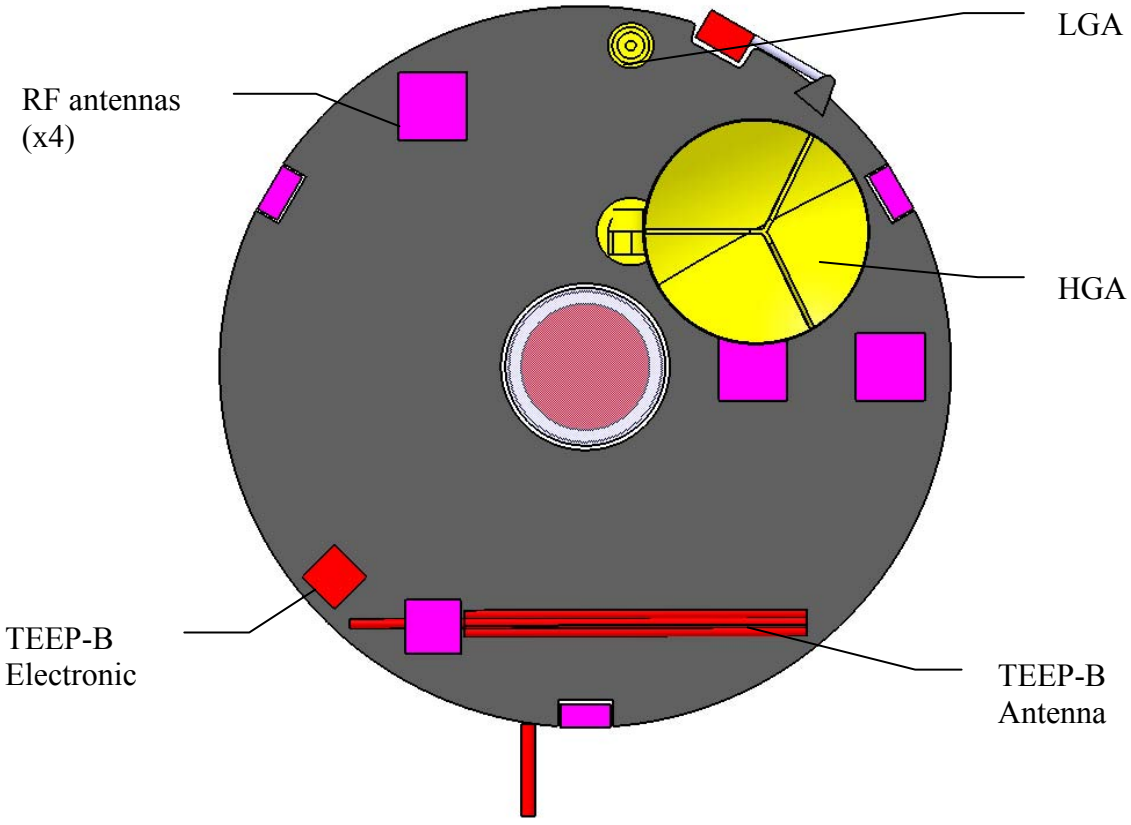

Figure 18 Equipment mounted on the platform zenith side.

Figure 19 and Figure 20 show the nadir side of the gondola with the science payload and spacecraft subsystem equipment mounted on this side of the platform. Payload instruments that have a camera or require access to the atmosphere have been placed accordingly. Equipment of the communication subsystem is accommodated in proximity of the antennas.

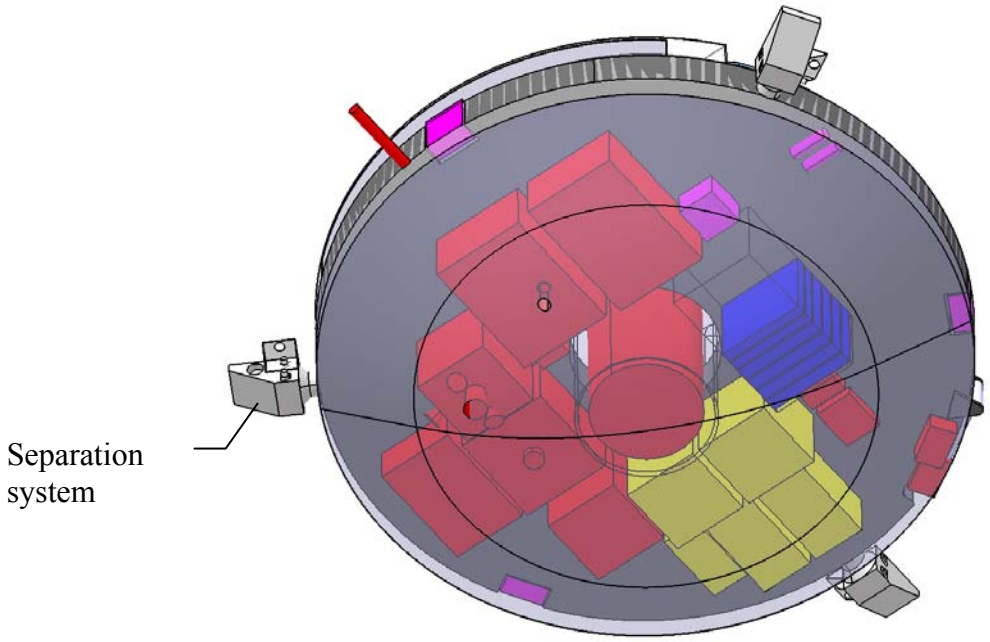

Figure 19 Gondola nadir view

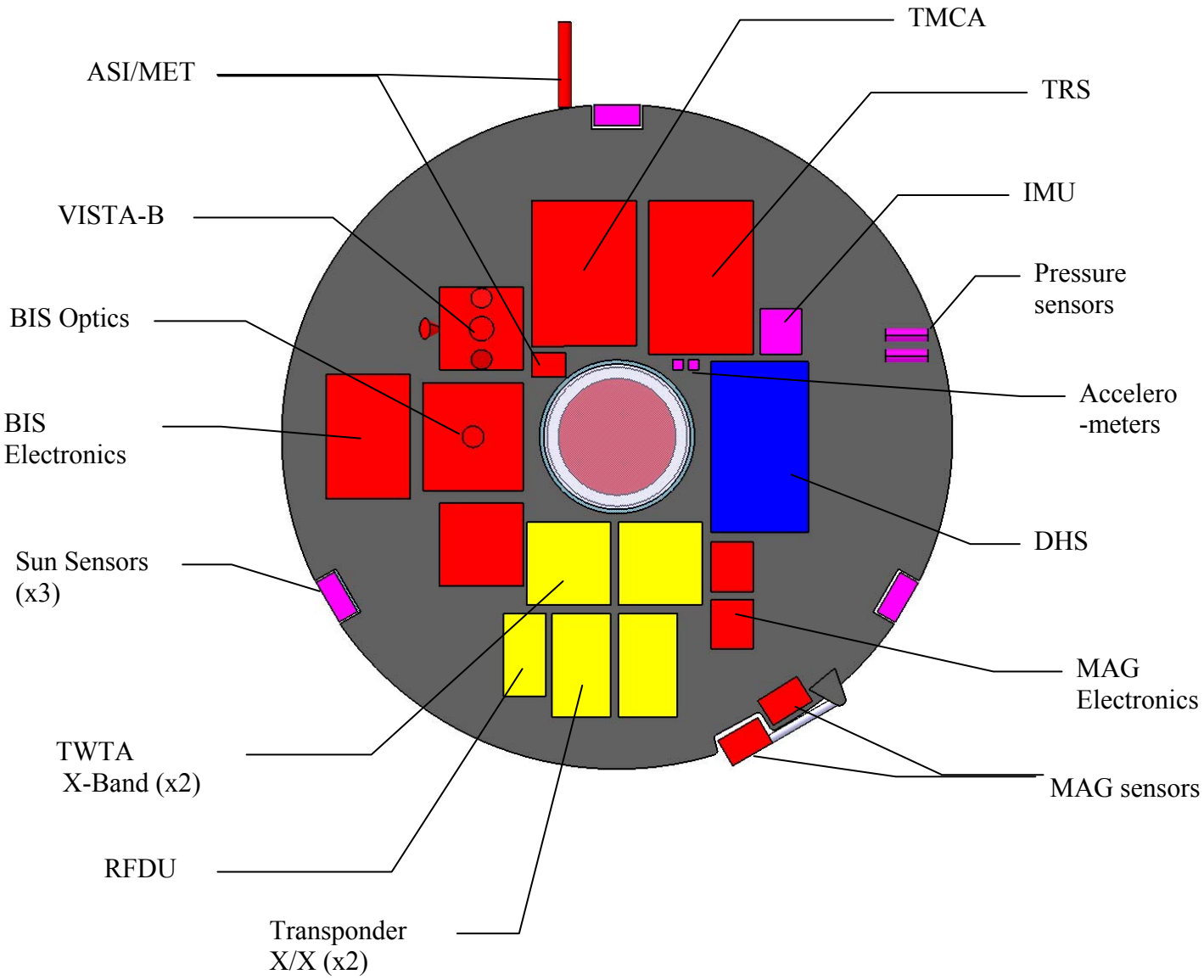

Figure 20 Equipment mounted on the nadir side of the platform.

Figure 21 shows the gondola in deployed configuration. The large deployed structure at its right side is the antenna of the TEEP-B instrument. Also HGA and the short magnetometer boom are indicated. Patch antennas are used for the determination of the direction to the orbiter (through phase measurement of a beacon signal; see section 8.1.2.4.4.2).

The heat generated by the MMRTG during the cruise phase is dissipated through a radiator with 2,5 m^2 surface. The radiator elements have been placed on the support structure for an optimal view factor to space and to make use of an already required structure. The height was sized such that the required area (2.5 m^2) could be accommodated on the circumference, taking into account continuity at the panel edges for the routing of the fluid lines. The option to use the back cover as

radiative surface was discarded, as the available surface is insufficient and furthermore as the back cover has to be an insulated structure so as to withstand the heating during entry.

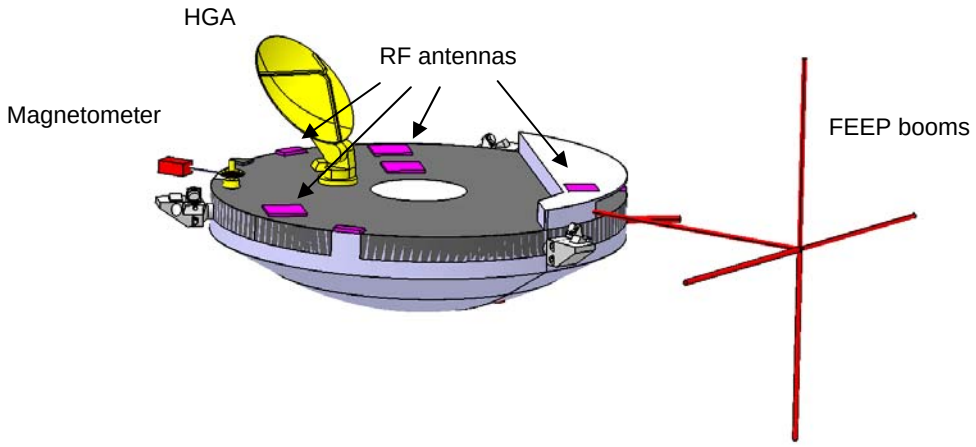

Figure 21 Sketch of the gondola in deployed configuration.

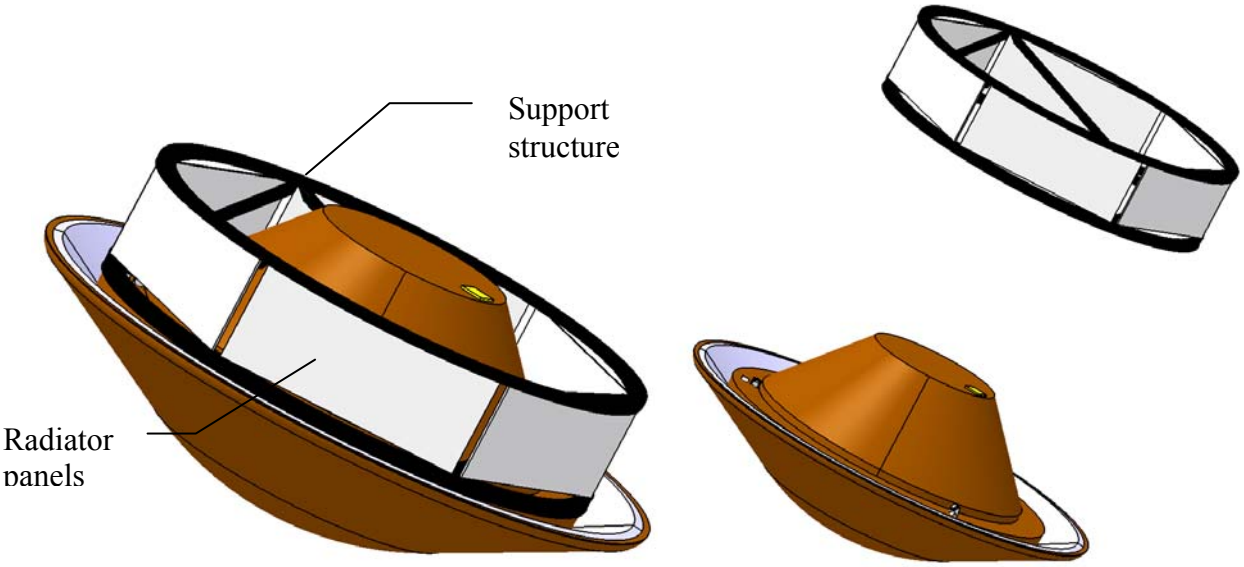

Figure 22 Montgolfière EV with support structure before and after release

The design of the support structure is not part of this study. Nevertheless a possible concept was considered and is shown in the pictures above. The concept is based on the Huygens probe support equipment (PSE). The main components are three bipods and two rings for stabilization and accommodation of asymmetrical loads from the struts.

The overall dimensions and approximate location of the centre of mass of the Montgolfière descent system are given in Figure 23. Figure 24 shows the Montgolfière Gondola dimensions (i.e. platform diameter, and approximate CoM location). The design is compatible with a 2.6 m diameter of the aeroshell.

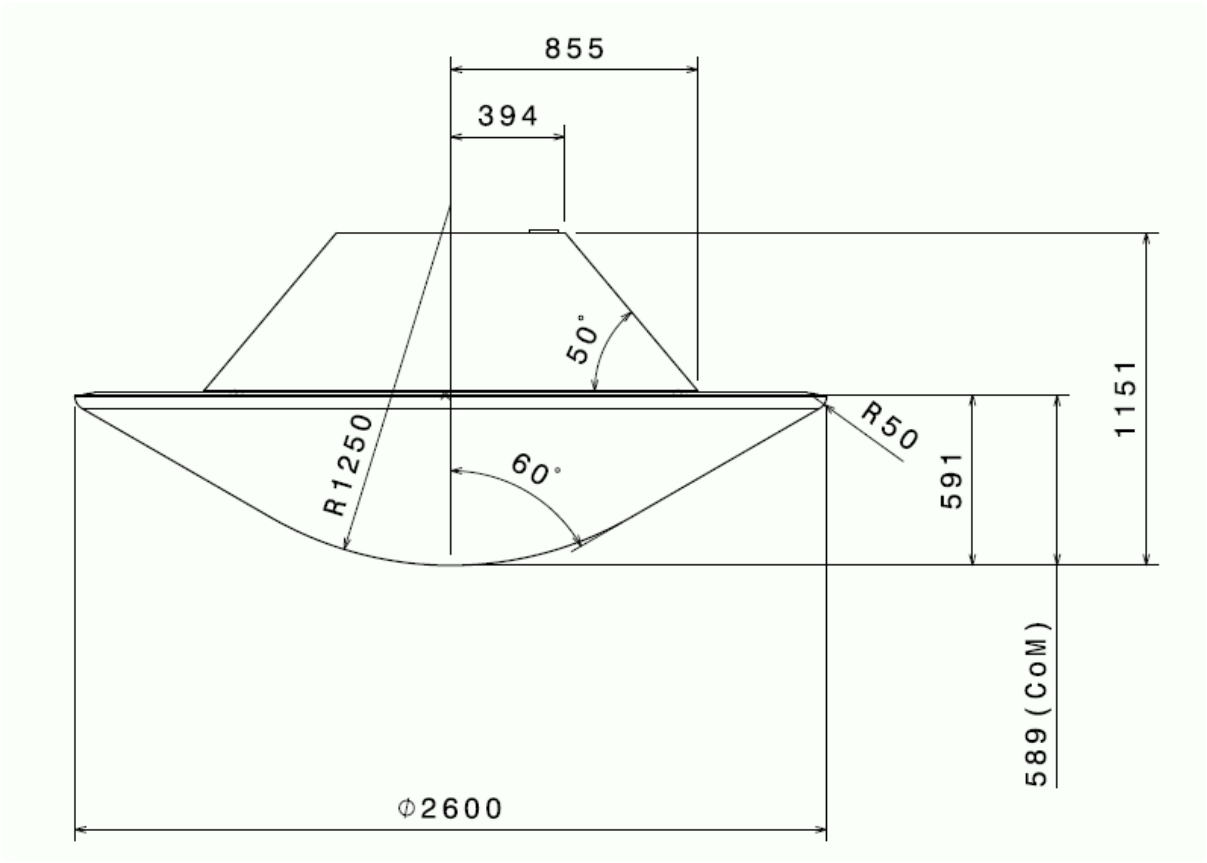

Figure 23 Montgolfière overall dimensions and approximate CoM.

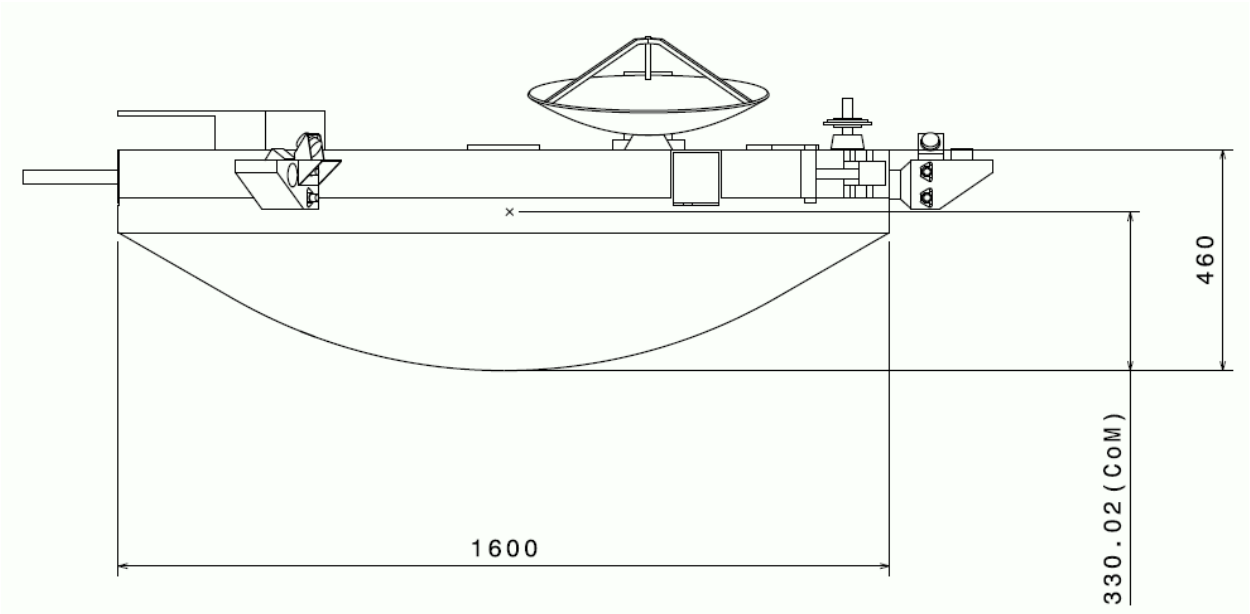

Figure 24: Montgolfière gondola dimensions and approximate CoM.

8.1.2.2 Structures

The mass estimates of the key elements such the load carrying items were verified by a load analysis taking into account the launch loads for Altas V 551 and the mechanical loads from the decelerations during entry (which amount to about 15 g) and during landing. The nominal launch loads were assumed. It was assumed that the loads caused by the mechanisms present in the *in situ* elements are covered by the loads from launch and entry. The analysis included the front and back shields, the payload bench, and support of the outside skin.

It was assumed that the structural parts were made of Carbon Fibre Reinforced Plastic (CFRP) with standard honeycomb cores. The payload items, as well as the stowed Balloon and MMRTG are mounted onto a centrally located, stiff payload bench. The back shield also carries the Descent and Landing System (parachutes). During operation the payload is protected by a hard, non structural, skin. Until separation, the payload bench, front and back shields are held together by three I/F mechanisms that also provide the connection to the S/C during launch.

The front shield, back shield, payload bench and skin have been modelled by means of shell elements (both rectangular and triangular). The mass of items as miscellaneous structural mass, cabling and thermal protection layers was smeared out over the shell elements as Non Structural Mass (NSM).

The dimensions of the front and back shields, payload bench and skin were driven by non structural requirements and constraints. However, the core height of these plates, which is an important characteristic determining strength and stiffness, was optimized during various iterative structural analyses.

The structure has been verified by comparing the lowest Eigenmode with the minimum requirement of 30 Hz. The lowest Eigenmode is found to be 28.4 Hz (back shield oscillation), thus somewhat below the requirement. It is, however, expected that the requirement will be met with detailed designing.

The structure has been verified for 15 g deceleration during entry by imposing a gravity field of 15 g and constraining a number of nodes on the front shield corresponding to an assumed pressure area at the centre of the cone.

The following is concluded from the structural analyses:

- Minimum frequency requirement (> 30 Hz) expected to be fulfilled after more detailed designing (*f* currently 28.4 Hz)
- Maximum stress during maximum entry deceleration 257 MPa well below allowable (±800 MPa); it follows that the design is not strength critical

The table below presents the Montgolfière structural parts and their associated nominal masses.

Table 7 Montgolfière structure mass budget overview.

Mass budget overview	Mass in kg
Front shield support structure	32.1
Back shield support structure	18.5
Payload platform	13.9
Skin	11.1
Gondola support cables	3.6
Miscellaneous (fasteners, inserts)	3.6
Support structure on S/C	48.0
Radiator support structure	7.2
Total	**138**

8.1.2.3 Balloon

Initially several options were considered for the buoyant support of the gondola. These included a Helium filled balloon and a montgolfière-type hot air balloon, among others. Considering the deployment, reliability and most importantly the longer operational lifetime (6 months) in the cold environment, the montgolfière was favoured. Detailed simulations were performed for the comparison of two options for deployment: a) a montgolfière (with single walls) that is assisted during the earlier phases by an additional small Helium filled balloon for additional buoyancy; and b) a montgolfière balloon that has a double wall structure for improved thermal insulation. Finally it was agreed that the latter option shall be used as the baseline.

The baseline altitude was constrained following the recommendation of the Titan Atmospheric Environment Working Group [RD4], which argues that for altitudes <6 km there is increased risk of precipitation, which potentially could cause variations of the mass of the Montgolfière and imposes additional complexity due to contamination and draining. At higher altitudes the atmosphere has reduced density and, therefore to support the same gondola mass, an increased balloon envelope size and mass is required, being less favourable. For the further design a nominal altitude of 10 km was assumed, with a possible range from 6 – 12 km.

The design is based on a single heat source, being the MMRTG with an assumed heat output according to its specification of 1687 W at EOL. It was found that the use of a double walled balloon would provide sufficient thermal insulation for heating the inside gas warm enough for the required buoyancy. The MMRTG will be supported such that it is located inside the balloon, close to the lower half, so as to optimize the transfer of heat to the gas, while at the same time minimizing heat losses through the opening of the balloon at its bottom. The MMRTG will be hanging from cables which are attached to the skin of the balloon. A vent valve at zenith is foreseen for altitude control by venting of inside (warm) gas. The altitude will be determined by a pressure sensor at the gondola, where also the control electronics will be accommodated.

Detailed thermal calculations were performed to simulate the rate of heating and of the inside temperature (for steady state), with the following parameters: The viscosity $\mu(T)$ and thermal

conductivity $k(T)$ of Titan's atmosphere as a function of temperature T, which were obtained from fits to thermodynamic data. The derived parameterizations are:

$$\mu(T) = 10^{-6} \cdot (1.5125 + 0.0558 \cdot T)$$
$$k(T) = 10^{-3} \cdot (1.078 + 0.08365 \cdot T)$$

For the heat transfer correlations the following set of parameters was used –

- for the internal free convection heat transfer (according to JPL's model):

$$N_u = 2.5 \cdot \left(2 + 0.6 \cdot R_a^{1/4}\right) \text{for } R_a \leq 1.5 \cdot 10^8$$
$$N_u = 0.325 \cdot R_a^{1/3} \text{ for } R_a > 1.5 \cdot 10^8$$

- for the external free convection (Campo et al. model):

$$N_u = 0.1 \cdot R_a^{0.34}$$

- for the external forced convection correlation:

$$N_u = \begin{cases} 0.37 \cdot R_e^{0.6} & \text{for} \quad R_e < 2.5 \cdot 10^5 \\ 0.74 \cdot R_e^{0.6} & \text{for} \quad R_e > 2.5 \cdot 10^5 \end{cases}$$

- for the heat transfer coefficient between the two walls (Holmann correlation):

$$N_u = 0.456 \cdot R_a^{0.226} \quad ;$$

where N_u, R_a, R_e are the Nusselt, Rayleigh and Reynolds numbers, respectively, and are using the nominal balloon diameter as reference length. The Prandlt number is taken equal to 0.796.

Based on these calculations, it was decided that a double wall skin would provide the necessary thermal insulation. This solution is also the most mass effective option.

Using these simulations allowed for a parameterization of the size (diameter) and mass of the balloon material as a function of gondola mass. The parameterizations used a 5th order polynomial of the form

$$P(x) = c_0 + c_1 \cdot x + c_2 \cdot x^2 + c_3 \cdot x^3 + c_4 \cdot x^4 + c_5 \cdot x^5 ,$$

were x is the mass of the gondola in kg. The values of the parameters c_i are provided in As can be seen, a balloon with diameter of 10.6 m is required to support the baseline gondola of 144 kg. The total mass of the balloon system is 109.9 kg (131.9 kg including margin).

Table 8, and the resulting functions are plotted in Figure 25. The following items are included in the balloon's mass budget:

- the mass of the double envelope with a preliminary density of 55 g/m^2
- the mass of the MMRTG (45.2 kg; accurate) plus supporting cables
- a protection cage around the MMRTG to protect the balloon envelope against damage during deployment
- the mass of the zenith valve

As can be seen, a balloon with diameter of 10.6 m is required to support the baseline gondola of 144 kg. The total mass of the balloon system is 109.9 kg (131.9 kg including margin).

Table 8 Parameters of the function of the balloon diameter in meters as a function of the mass of the gondola in kg (first row). Parameters of the function of the balloon mass, including balloon container and mechanism, in kg as a function of the mass of the gondola in kg (second row).

	c_0	c_1	c_2	c_3	c_4	c_5
Diameter in m	4.81	4.75×10^{-2}	-8.79×10^{-5}	3.60×10^{-7}	-8.37×10^{-10}	8.00×10^{-13}
Mass in kg	64.0	0.240	5.36×10^{-4}	-8.57×10^{-8}	5.16×10^{-11}	8.0×10^{-14}

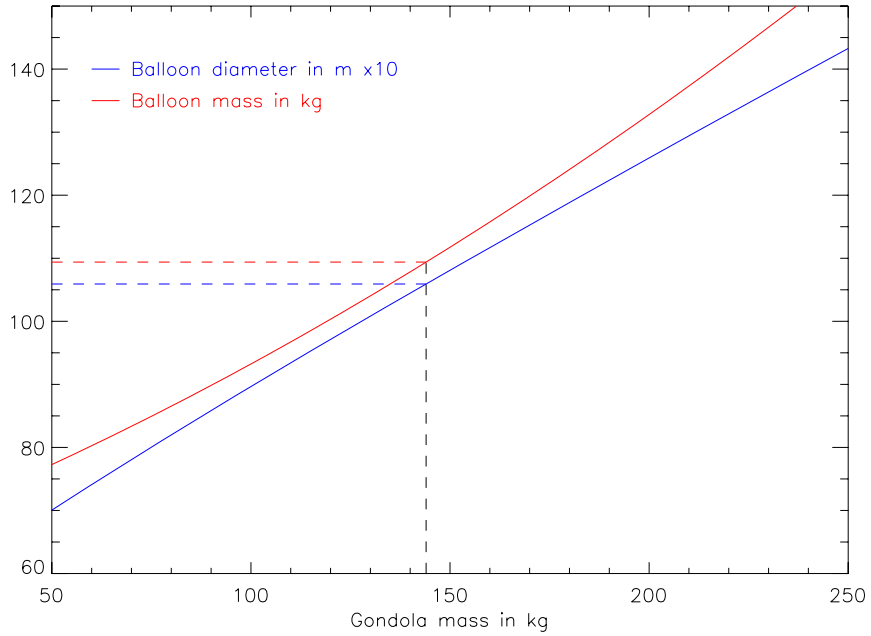

Figure 25 Diameter and mass of the balloon as a function of gondola mass. The diameter of the balloon is multiplied by 10 and plotted in blue; the mass of the balloon is plotted in red. The dashed lines indicate the baseline mass of the gondola (144 kg) and the respective derived values for mass and diameter of the balloon.

Simulations also included the heating of the gas after filling, and the evolution of altitude as a function of time during the filling phase (see Figure 26 for result of the calculation for the final configuration).

A design drawing of the balloon and the gondola in floating configuration is shown in Figure 27, to allow comparing the sizes.

The volume that is required for the folded configuration (blue volume shown at the top in Figure 16 & Figure 17) was estimated from the total surface of the balloon by using CNES' experience with folding efficiency of balloons. The required volume for the back cover was based on this by scaling. As can be seen in Figure 17, the balloon envelope cannot be folded in an axially symmetric way being constrained by the configuration, and specifically by the location of the high gain antenna. This increases the complexity, and will have to be worked out in more detail. The

balloon envelope needs to be folded and placed such that the MMRTG can easily enter into the balloon during deployment.

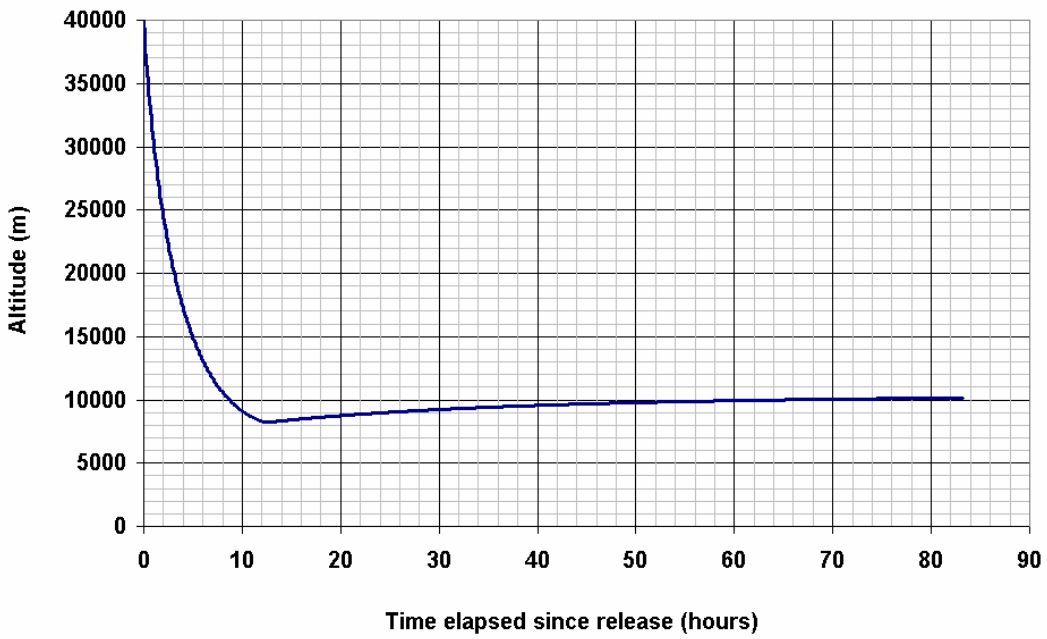

Figure 26 Evolution of the Montgolfière altitude as a function of time during the descent, from the beginning of the balloon deployment (40 km), including the filling and heating phases.

The material of the envelope needs to be assessed for compatibility with about 10 years stowage and deployment and operations in an environment of 80 – 90° K. The assumptions on material density build on existing experience with trials of 25 g/m^2 (having been tested for Mars) and 100 g/m^2 from previous use at CNES. The rigidity of the proposed material for deployment and filling is planned to be demonstrated as part of a development activity at CNES. Further items in need of assessing are the support of the MMRTG and of the vent valve, and the deployment sequence.

The MMRTG will be supported by cables that are attached to the skin of the balloon. To avoid the full dynamic load stresses of the balloon material during deployment and during the initial filling phases, the balloon side of the support lines of the MMRTG will have additional attachment points being connected to the main parachute by additional lines. This design needs further assessment.

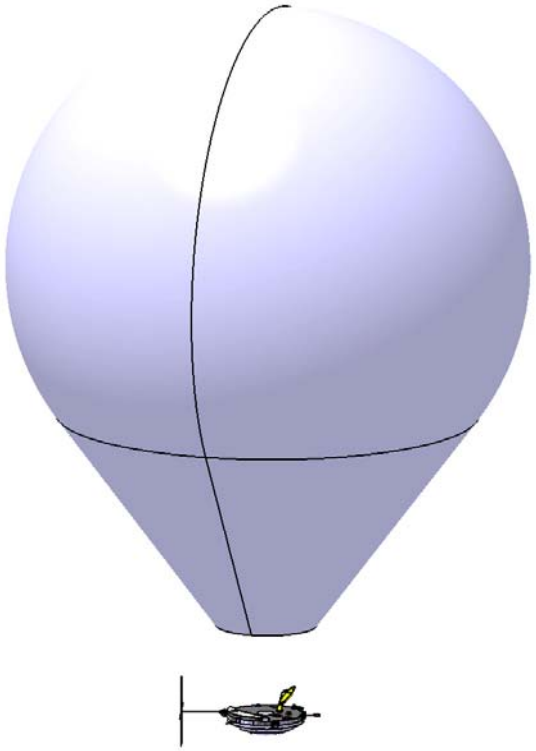

Figure 27 Image of the Montgolfière in floating configuration showing the gondola in deployed configuration below the balloon. The image is to scale.

8.1.2.4 Gondola System

8.1.2.4.1 Power

The MMRTG is the single source of power on the Montgolfière, which effectively limits the available total power. It is foreseen that no electric power will be used for heating; the necessary heating will be realized by spot heating with RHU's. The MMRTG provides a total output of 125 W_{el} BOL, which reduces to 100 W_{el} after 14 years (1.6% per year; the reduction is due to the combined effect of radioactive decay and aging of the thermo-electric element).

It was further assumed that no battery would be included for keeping the total float mass as low as possible. Without battery the electrical system is power-limited rather than energy limited. Therefore challenges to the electrical budget are met by time-sharing the major functions such as instrumentation and telemetry transmission. With the current estimates the largest power consumption occurs during instrument operations in science mode and uplink communications. It was confirmed that the total consumption remains within the limit of 100 W during all modes. The breakdown of allocated power consumption per mode is summarized in Table 9.

The power system also includes a regulated shunt resistor to level the power consumption and to keep the load on the MMRTG at constant level. As a positive side effect this implies constant consumption within the equipment compartment of the Montgolfière, which simplifies the thermal balancing.

Table 9 Montgolfière power budget per mode and mission phase.

	command + LCL+ pyro boards = 5		Thermal	AOCS	Comms	DHS	Mech	Montgolfier Payload	Harness AND PCDU	TOTAL CONSUMPTION
Separated Sleep Mode		Pon	0 W	0.20 W	70 W	3 W	0 W	0.0 W	5.12 W	78 W
		Pstdby	0 W	0.00 W	10 W	0.60 W	0 W	0.0 W	0.74 W	11.34 W
		Duty Cycle	0 %	100 %	10 %	15 %	0 %	0 %		10%
		Paverage	0 W	0 W	16 W	0.95 W	0 W	0.0 W	1.20 W	18.35 W
Tref 203040 min	e Mode NOT Inc	Total Wh	0 Wh	677 Wh	54144 Wh	3215 Wh	0 Wh	0.0 W	2511 Wh	60547 Wh
Entry Mode		Pon	0 W	0 W	70 W	5 W	0 W	0.0 W	10 W	85 W
		Pstdby	0 W	0 W	10 W	2 W	0 W	0.0 W	6 W	18 W
		Duty Cycle	0 %	100 %	50 %	100 %	0 %	0 %		49%
		Paverage	0 W	0 W	40 W	5 W	0 W	0.0 W	8 W	53 W
Tref 6 min	e Mode NOT Inc	Total Wh	0 Wh	0 Wh	4 Wh	0 Wh	0 Wh	0.0 W	1 Wh	5 Wh
Descent Mode		Pon	0 W	0 W	70 W	9 W	0 W	5.0 W	11 W	95 W
		Pstdby	0 W	0 W	10 W	2 W	0 W	5.0 W	6 W	23 W
		Duty Cycle	0 %	100 %	50 %	100 %	0 %	0 %		52%
		Paverage	0 W	0 W	40 W	9 W	0 W	5.0 W	9 W	63 W
Tref 180 min	pse Mode Inclu	Total Wh	0 Wh	1 Wh	120 Wh	28 Wh	0 Wh	15.0 W	19 Wh	182 Wh
Science Mode		Pon	0 W	6 W	15 W	10 W	0 W	43.5 W	10 W	85 W
		Pstdby	0 W	0 W	10 W	2 W	0 W	43.5 W	9 W	64 W
		Duty Cycle	0 %	100 %	0 %	100 %	0 %	0 %		70%
		Paverage	0 W	6 W	10 W	10 W	0 W	43.5 W	10 W	80 W
Tref 262800 min	e Mode NOT Inc	Total Wh	0 Wh	26280 Wh	43800 Wh	45333 Wh	0 Wh	190530.0 W	38832 Wh	344775 Wh
Transmission Mode		Pon	0 W	6 W	70 W	6 W	0 W	0.0 W	11 W	92 W
		Pstdby	0 W	0 W	10 W	2 W	0 W	0.0 W	6 W	18 W
		Duty Cycle	0 %	100 %	100 %	100 %	0 %	0 %		0%
		Paverage	0 W	6 W	70 W	6 W	0 W	0.0 W	11 W	92 W
Tref 0 min	e Mode NOT Inc	Total Wh	0 Wh	0 Wh	0 Wh	0 Wh	0 Wh	0.0 W	0 Wh	0 Wh

In order to regulate and condition the "raw" electrical power from the MMRTG, and to provide a stable power bus to the payload and spacecraft, a linear sequential shunt is provided for the following reasons:

- Heritage: NASA have used this topology on previous spacecraft with RTGs
- Electrical Quietness (EMC): The mass budget challenges of the Montgolfière Probe imply that integration of the EPS and DHS in a common box is preferred. The linear sequential shunt regulator is very low in conducted and radiated emissions, so is particularly suitable for this close integration with the computer systems.
- Thermal Control: Linear shunt means that the total electrical power drawn from the RPS is constant (disregarding the long-term RPS decay). Any electrical power not required by users is dissipated in shunt resistors. So, the thermal dissipation inside the gondola is a maximum at all times, except during transmission when antenna RF power is lost from the environment. In the Montgolfière, the balloon requires the direct heat from the MMRTG casing, so this is unavailable for thermal control of the gondola.

The NASA "New Horizons" spacecraft is a particularly relevant example to use in the frame of this study. It is an outer planet spacecraft, using a single RTG, and was launched very recently, in 2006. Furthermore MSL will use the same MMRTG's as are planned for TSSM. [Carlsson 2005, Uno Carlsson. Proc. Seventh European Space Power Conference, Stresa, Italy, May 2005, ESA SP-589] describes the New Horizons power electronics, and schematics of the power system is reproduced here as Figure 28.

One issue with this system is the use of an extremely large bank of main bus capacitors totalling 33 mF to maintain bus stability against equipment turn-on transients. The same approach would require ~15 mF for the TSSM Montgolfière PCU. Space-qualified metal film capacitors would weigh almost 15 kg. However, the bus stability could be achieved with much less capacitance by

increasing the closed loop gain of the regulator control circuit, thus raising the regulator bandwidth. Scoping calculations show that less than 1 mF would be required, so 1 kg has been assumed in the mass budget for the main bus capacitors, which provides ample margin.

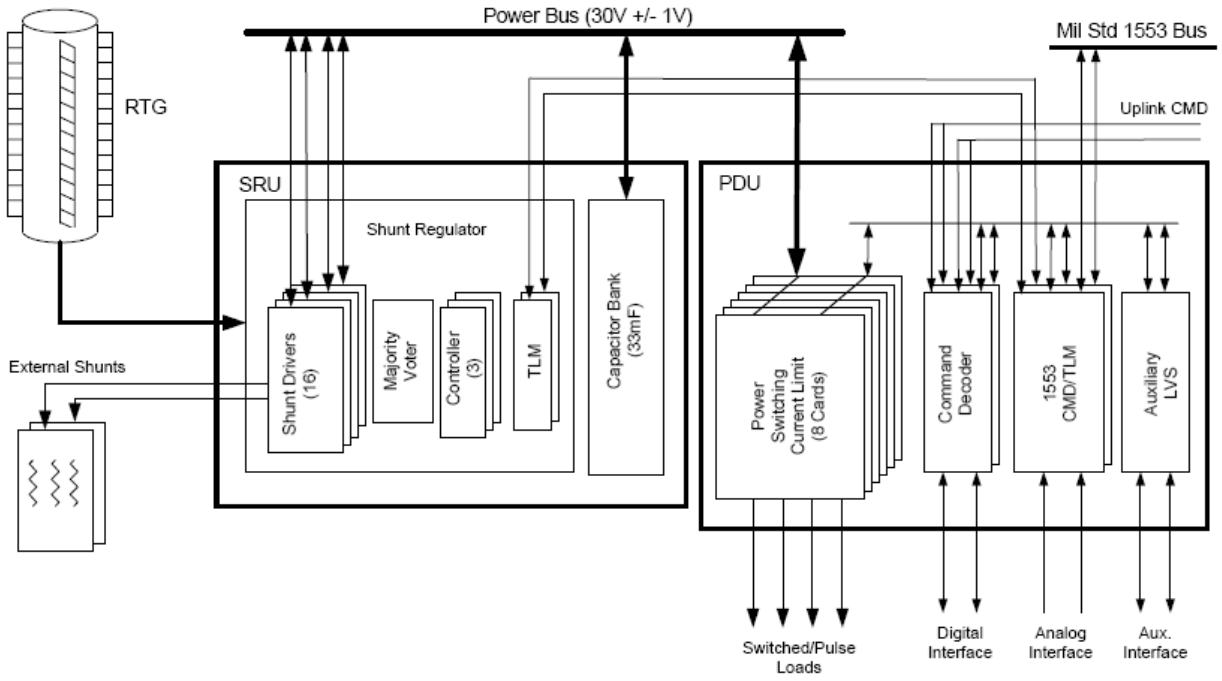

Figure 28 NASA's New Horizons: Simplified Power System Block Diagram [Carlsson 2005]

The design of the power conditioning and distribution unit (PCDU) will driven by be power source being an RPS rather than a more "traditional" solar array and battery combination. Furthermore the PCDU will be integrated with the DHS for mass savings. However, in order to form a realistic mass budget, TERMA 'future power systems' modular conditioning and distribution boards have been used as indicative examples. It should be noted that this implies some approximations (e.g. there is no TERMA Linear Shunt board, so an S^3R board is used for a mass indication).

A count of the various electrical power users within the system and the payload led to an assumption of 30+30 redundant low-current (1.5 A) LCL output lines, and 10+10 redundant pyro outputs. These output lines can be provided by 2 TERMA 1.5 A LCL boards and 2 TERMA pyro control boards. 1+1 redundant command modules are included, but given that the TERMA switching shunt regulator board is capable of handling 500 W (as opposed to the 125 W BOL requirement for the TSSM Montgolfière Probe), only one board was assumed for mass budget and sizing purposes. In reality, some redundancy will be required in the shunt regulator controller.

As discussed above, 1 kg is included as mass budget for the main power bus capacitor bank.

The MMRTG uses the thermoelectric (Seebeck) effect to generate electrical power from the heat arising from the natural radioactive decay process of ^{238}Pu. The ceramic plutonium dioxide is encapsulated in a multi-layer containment module known as a GPHS (general purpose heat source). Eight GPHS modules are stacked together in the centre of the MMRTG, and are

surrounded by the lead-telluride and "TAGS" thermoelectric units. The GPHS heat source, and many design aspects of the MMRTG, have heritage in the "GPHS-RTG", the large 300 W_{el} RTG flown on Galileo, Ulysses, Cassini and New Horizons. The GPHS RTG is unsuitable for use in planetary atmospheres, as it relies on multi-layer insulation. Hence, the MMRTG has been developed, and is planned to be first used on the 2009 NASA Mars Science Laboratory Mission.

The MMRTG has cylindrical shape. There is a cooling pipe included around the outside structure, which will be used to lift the excess heat produced while in stowed configuration during the interplanetary transfer phase.

For the estimate of the mass budget, it was assumed that the PCDU and the DHS will be integrated into one unit. The PCDU components are summarized below (Table 10). No provision is made for the PCDU box structure, as this is to be accommodated in the DHS box sizing.

Table 10 PCDU Equipment

Unit Name	Mass incl. margin kg
Shunt regulator board	0.6
2 PCDU command boards	0.84
2 Distribution board 1.5 A	1.32
2 Pyro control boards	1.2
Power bus Capacitors	1.05
Totals	**5.0**

8.1.2.4.2 Data Handling

The design was led by the low mass and power constraints. A SCOC3 ASIC was selected as the baseline as it may allow designing the probe CDMU highly integrated with low mass and power. But further refinements are necessary to cope with the strict mission mass/power constraints. The same approach as ADPMS where DHS and PCDU were combined in the same unit will be taken for the Montgolfière DHS design, accepting some heritage from the ADPMS implementation but also introducing new elements in both the DHS (e.g. SCOC3) and in the PCDU, achieving an even higher level of integration. The baseline design is depicted in the Figure 29.

Here only the DHS part of the DHS+PCDU unit is described. The DHS baseline design core is a complete internally redundant spacecraft controller incorporating the following functions:

- Processor subsystem containing the LEON3 processor with external user interfaces
- User interfaces for connections with the sensors and actuators anywhere on the spacecraft
- TM/TC subsystem providing packet telemetry encoding and telecommand decoding. Also a housekeeping function allows automatic generation of the housekeeping telemetry.
- Reconfiguration module
- Memory storage
- Two communication buses are needed.

- The command and control bus will be CAN bus, which will also connect low data rate instruments to the DHS (up to 500 kbps); its power consumption is 4 times less than that of MIL-1553.
- High speed point-to-point links for the high data rate instruments are foreseen by means of spacewire links (up to 200 Mbps).

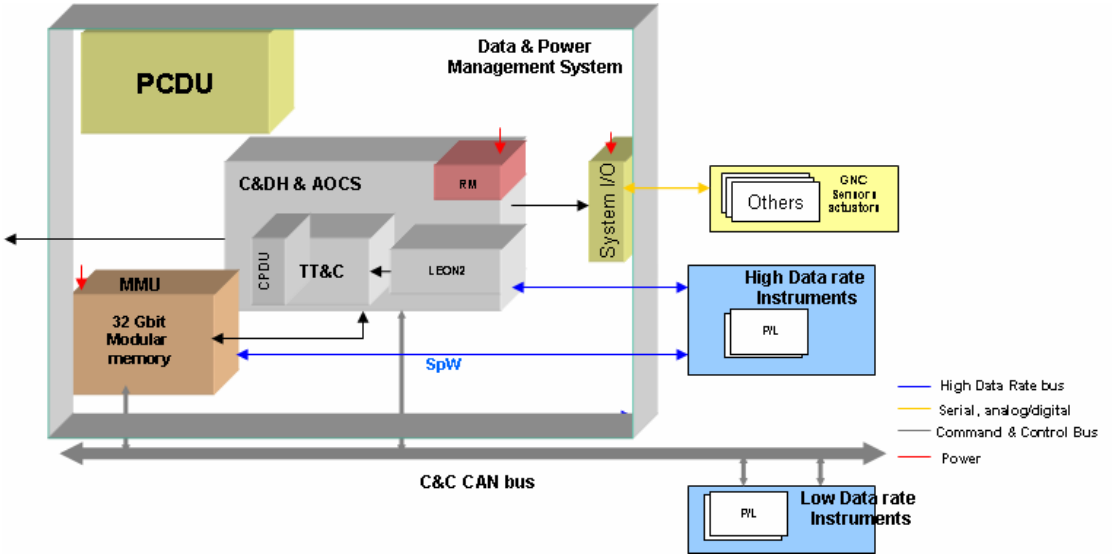

Figure 29 DHS baseline design

The Montgolfière Probe DHS system will foresee 32 Gbits of mass memory, which ensures sufficient space for storage in between periods of uplink to the orbiter (the memory was calculated based on an estimated data rate from the instruments and based on the expected intervals of contact to the orbiter for relay). The memory board will be based on FLASH technology because: –

- The availability of SDRAM memory chips is uncertain five years from now
- The power consumption is much lower in FLASH memory
- The memory density per chip in FLASH technology is much higher

Table 11 shows the assumed mass budget for the DHS system for the Montgolfière Probe.

Table 11 DHS avionics core mass budget. NOTE (*): the power budget is calculated considering cold redundancy in the processor and system I/O units, which means that only one of the two redundant units is considered for the total power budget.

Unit	Mass (kg)	Power (W)
Processor + TM/TC + RM	2×0.8	1×7.0 (*)
System Input/Output	2×0.8	1×3.0 (*)
Mass Memory	1×0.8	1× 1.0
Power Converter	1×0.8	1.7
Box mechanics	3.1	n/a
Avionics core total	**7.9**	**12.7**

In the table above, the Box mechanics includes the mass required to host the PCDU, but the PCDU mass itself was not included, as this is accounted for elsewhere. Including the PCDU mass of 3.9 kg, the complete Power Management System is 11.8 kg. All numbers are without margin.

Equipment-list:

- CDMU: The proposed CDMU comprises the processing, TM/TC and reconfiguration. It will be based on SCOC3 ASIC.
- System Input/Output: This board will provide the I/O to connect the CDMU with the sensors/actuators.
- Decentralized system: CAN bus and spacewire are foreseen to interconnect the different units within the spacecraft. CAN bus will act as the command and control bus, and the data-bus for the low data rate instruments, while point-to-point spacewire links will connect the high data rate instruments.
- Mass Memory: The Mass memory has to be fully developed and FLASH technology will be used. Further studies shall be performed to ensure the availability and readiness FLASH memory technology.

The following options should be further considered:

- Memory: The baseline design considers an external mass memory board based on FLASH technology. It may be possible to provide the same amount of memory on the same CDMU board, eliminating the dedicated mass memory board and further reducing the DHS mass by about 1 kg.
- Instrument interfaces: In the current baseline design, all the instruments have direct interface to the CAN bus. RTU's that are needed for the instruments as interface, and will be accounted on the instrument side.
- Additionally, inclusion of a centralized function for processing of instrument data, e.g. data compression, should be considered (see also [RD9]).

The technology that is required or would be beneficial in this domain is listed in Table 12.

Table 12 DHS Technology requirements

Equipment and Text Reference	Technology	Suppliers and TRL Level	Additional Information
SCOC3	Actual FPGA Final ASIC	Astrium, actual TRL 4 – 5	ASIC implementation ready mid'09
System I/O	NA	Actual TRL 4 – 5	Heritage from many previous projects
Memory	NA	Actual TRL 4 – 5	Some FLASH devices already flown

8.1.2.4.3 Thermal

8.1.2.4.3.1 Function per Mission Phase

The thermal sub-system has to support the following mission phases:

1. Interplanetary transfer phase
2. Ballistic transfer phase
3. Entry and descent
4. Deployed configuration

While the heat of the MMRTG needs to be radiated away during the early phases of the mission (integrated system), after deployment, sufficient heat needs to be available inside the gondola to provide adequate operating temperature for the electronic equipment. During the early phases (interplanetary and ballistic transfer) of the mission the radiation of heat to space will be enabled by a radiator structure. This however also implies adequate ground support equipment, which is capable of cooling the thermal connections during integration and pre-launch.

During the operating phase, when the MMRTG is deployed and when it is exposed to the ambient cold temperatures, its temperature would decrease due to cooling from the outside such that the thermo-electric elements would be below optimum operation point. Additional insulation will therefore be provided to keep the inside of the thermo-electric element at higher temperatures, closer to the optimum operating point. This additional thermal insulation, which was included in the design of the gondola, also provides for increased thermal insulation between the MMRTG and the other sensitive equipment inside the gondola during stowed configuration, thereby delaying the effects of short term transients.

8.1.2.4.3.2 Interplanetary Transfer Phase

During this phase the complete Montgolfière Probe is in stowed configuration and is attached to the orbiter. The heat of the MMRTG (about 2 kW) needs to be radiated to space. In the chosen baseline design, the interface structure to the orbiter s/c will also be used as mechanical support for a radiator. The MMRTG includes a cooling pipe on its outside (at the root of the fins), which will be connected to a pumped cooling pipe leading to the external radiator.

The Montgolfière Probe will be separated from the orbiter together with the interface structure that supports the radiator, as it will also be used for cooling until the beginning of the entry sequence. The structure (including radiators and pumps) will be separated closely before entry. Separation of the interface structure and radiator before entry is most efficient from the point of view of keeping the entry mass as low as possible, as otherwise the total mass would be amplified by higher mass required for the heat shield. Furthermore possible heat leaks through the cooling structure are easier to avoid. The interface structure with radiator is shown in Figure 22 before and after separation.

During the CDF study possible working fluids for the heat transport were investigated and it was concluded that water is the most favourable candidate due to its high heat transport capability being most mass efficient. Its comparably high freezing point was considered, however the heat of

the MMRTG is continuously being produced and hence the risk of freeze-out was considered a secondary priority. A detailed design of the cooling pipes needs to be conducted in a later phase.

It has been confirmed by JPL mission analysis that the radiator could remain in shadow during all phases of the interplanetary trajectory. Actually, the heat shield of the Montgolfière Probe will be used as shield to provide shadow for the orbiter during critical hot illumination (Venus flyby).

8.1.2.4.3.3 Ballistic Coasting Phase

The thermal configuration is very similar to the previous phase. The separation from the orbiter s/c is such that the radiator support structure remains on the side of the probe. The Montgolfière Probe is electrically self supporting, and the cooling pumps will continue to be powered by the MMRTG. Towards the end of this phase, before separation of probe and POIS, possibly the cooling could be somewhat enhanced in order to drive the MMRTG root-fin-temperature to lower values to increase the margin against overheating due to the MMRTG during entry.

At the end of this phase the support structure, including radiator and cooling pumps will be separated.

8.1.2.4.3.4 Entry and Descent

During the short of the entry time there will be no cooling of the MMRTG. This phase lasts about 5 min until removal of the back cover, when the MMRTG will partly be exposed to the cold atmosphere. Deployment of the balloon occurs about 1.4 h after entry, and at this point in time the MMRTG will be removed from the gondola and starts heating the ambient gas.

8.1.2.4.3.5 Deployed Configuration during Science Operations

The gondola system is continuously powered by about 100 W electric power from the MMRTG. The MMRTG itself is heating the gas inside the balloon. Excess power, which is not being used by any equipment, will be dissipated by the shunt resistors inside the bay of the gondola. Therefore the heat dissipation inside the gondola remains constant at all times, except during telemetry transmission when power is radiated by the antenna. This rather constant power dissipation somewhat simplifies the thermal control system of the gondola bay. Obviously, it is foreseen that the gondola is thermally isolated against the cold Titan atmosphere in such a way that the internal temperature is balanced (using insulation material and thermal links on the inside).

Additionally, as the system is power limited, any required heating will be provided by RHU's (including heating of external components such as one pointing mechanism of the HGA and possibly the mechanism of the zenith-valve of the balloon). Heating required internally by instruments is not included in this consideration, and electric power required will be budgeted against the respective instrument(s).

8.1.2.4.3.6 Implementation

The thermal implementation has focused on providing the necessary cooling for the MMRTG during the interplanetary transfer. Isolation and additional heating during the science operations

phase could not be addressed at a great level of detail. Small localized heating may be required. Only MLI and insulation foam with a total mass of little over 6 kg were assumed.

Water was selected as the coolant fluid with an operating range from 0 to 130 °C and a maximum operation pressure of 0.5 MPa such that the fluid remains liquid over the entire temperature range. Centrifugal pumps were selected in cold redundancy (2 in total) with <15 W consumption and 20% efficiency. The total required surface area of the radiator is 2.5 m^2, assuming that no additional illumination take place in the hot case (confirmed by JPL mission analysis). The mass of the radiator is 10 kg. A pyro-cut mechanism is assumed for the separation of the fluid lines when the radiator structure is separated.

8.1.2.4.4 Guidance, Navigation & Control

8.1.2.4.4.1 Entry, Descent and Inflation

During this phase the opening of the two parachutes, the releases of the back shell (including drogue parachute) and of the front shell, and the simultaneous opening of the balloon for inflation and release of the MMRTG need to be controlled. The primary devices are a set of accelerometers, which are supported by timers as backup. Three accelerometers will be used, which include a low pass filter (e.g. 2 Hz) and majority voting. The timers (also in majority voting) will be armed, each after detection of the preceding deceleration event.

The accelerometer detects the rising edge of the non-gravitational acceleration with a threshold of about 40 – 50 m/s^2. During entry the deceleration peaks at about 15 g. Following this detection the timer will be armed. Once the deceleration reduces, the mortar will be fired and the drogue parachute will be released. After about 30 s the back cover will be pulled off and the main parachute will be released. The releases of the front shell and of the balloon will follow in similar fashion. After the descent on the main parachute, pressure gauges will control the release of the balloon cover and the pull-out of the balloon. The required sensors for the entry, descent and inflation phase are listed in Table 13.

Table 13 Required sensors suite for entry, descent and inflation phase.

Sensor	Implementation	Performance	Role
3 Mission Timer Units	Majority Voting 3 independent hot-redundant timer Circuits followed by two hot-redundant command circuits	Stability over the entry duration is required	Backup triggering the sequence of events (parachutes openings & releases, balloon inflation & release)
3 Accelerometers	Majority Voting Two hot redundant input power lines single point failure-tolerant	Shall operate between 0.05 and 20 g to enable entry detection, and buoyancy measurement	Rising Edge detection; setting of initial entry time (T0)

2 G-switch 1	Backup sensor in case of MTU or accelerometer's failure for 1st parachute opening.	Shall be set according to 1st parachute expected acceleration (for Huygens, set to: 5.5 g)	triggering the opening of the drogue parachute deployment
2 G-switch 2	Backup sensor in case of MTU or accelerometer's failure for 2nd parachute opening.	Shall be set according to 1st parachute expected acceleration (for Huygens set to: 1.2 g)	triggering the opening of the main parachute
2 coarse gyros	Enables pointing knowledge during descent	Drift requirement: <1°/hr	Provide data for post flight attitude reconstruction

8.1.2.4.4.2 Science Observation Phase

During the science observation phase, the Montgolfière is passively drifting, being pushed by atmospheric winds at a velocity of a few m/s. Only the altitude will be actively maintained by a vent valve on top of the balloon, which is controlled by electronics of the GNC subsystem inside the gondola. This altitude measurement will be performed via a pressure gauge (baro-altimeter). The correlation of altitude and pressure is considered sufficiently accurate based on the existing atmospheric model. With a baseline floating altitude of 10 km, there is sufficient margin, and the required accuracy on altitude maintenance is not very demanding (in fact, maintaining the altitude of the Montgolfière by pressure difference is a very suitable means of control).

Real time attitude determination is only required for the pointing of the high gain antenna towards the orbiter. Following a brief trade-off with alternative options, such as star tracking, use of a gyro compass, or using sun/Saturn sensing, low gain patch antennas were selected as the most secure option, and using the communication subsystem as the main tool for line of sight estimation. A set of three patch antennas would be mounted on the zenith surface of the gondola, which measure by means of phase differentiation the direction of a beacon signal emitted from the orbiter This chosen baseline is also robust for recovery after long blackout durations, such as when the Montgolfière is in eclipse from the orbiter.

The accuracy of the measurement of elevation $\delta\vartheta$ of a phase-based line of sight estimation is given by

$$\delta\vartheta = \frac{L}{\cos(\vartheta)} \cdot \delta\varphi \ ,$$

where ϑ is the true elevation and $\delta\varphi$ is the accuracy of the phase measurement. For X-band communications, the typical carrier wavelength is about 3 cm, and the phase measurement is

expected to be within about ½ wavelength at worst case. A typical accuracy of the line-of-sight (LOS) estimation as a function of baseline in shown in Figure 30 for X and Ka-bands, respectively.

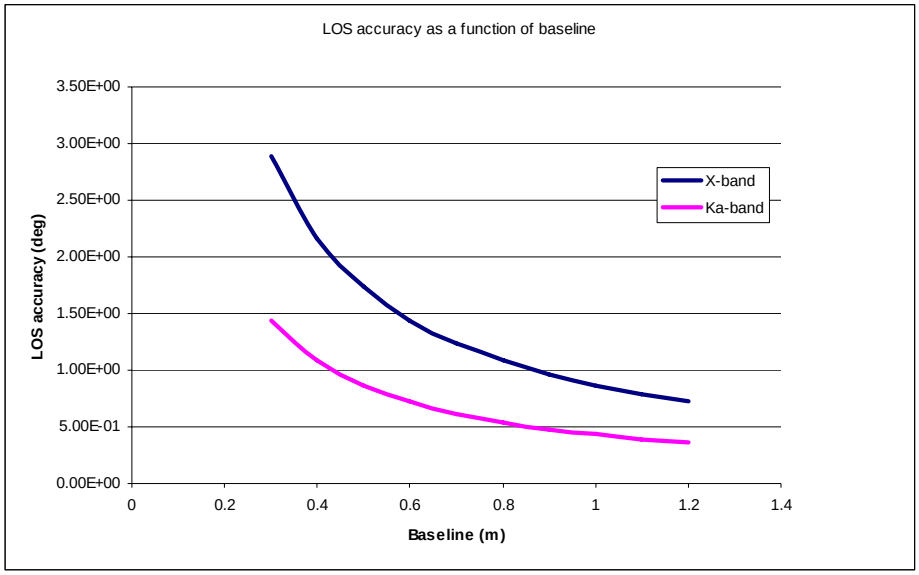

Figure 30 Accuracy of the LOS elevation estimate as a function of baseline distance for X and Ka-band carriers.

The estimated accuracy of the LOS measurement during orbiter visibility is illustrated in Figure 31. The highest accuracy is <1° and is obtained when Orbiter is at zenith (maximal elevation of the orbiter is ~83° during the first 6 months of the mission). It is degraded to 2° and more for orbiter elevations below 20°.

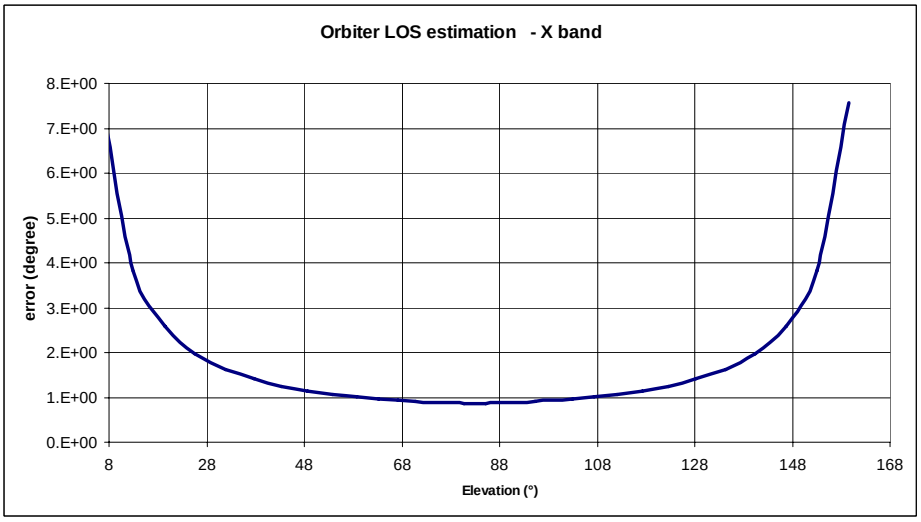

Figure 31 Evolution of the estimated accuracy of the LOS estimate as a function of elevation.

Table 14 summarizes the required sensors for the operations. The altitude will be maintained by a measurement with a pressure gauge. The IMU has only auxiliary purposes. The identified GNC modes are listed in Table 15.

Table 14 Required sensor suite during observation mode.

Sensor	Implementation	Performance	Role
RF antennas	4 Patch antennas 3 with more than 80 cm between them 1 for redundancy	Omni-directional	LOS estimation
Baro altimeter	2 pressure sensors for altitude determination	10 to 100 m accuracy	Maintain altitude control
IMU	3 accelerometers 3 gyros	1 °/hr for the gyro	Inertial pointing knowledge Vertical Sensing through buoyancy measurement; post-flight attitude knowledge
Sun/Saturn sensor	2 – 3 sensors at the limb of the gondola	~1°	these sensors are intended as backup and as assistance for position finding; providing post-flight attitude information

Table 15 Baseline GNC modes.

Entry Mode (EM):	performs ED sequence (parachute opening, heatshield jettisoning) Triggered sequence Sensors: Accelerometers to trigger the events
Balloon Inflation Mode (BIM):	Performs balloon inflation Performs balloon release Sensors: pressure/temperature gauge inside the balloon? Control: passive sequence
Orbiter acquisition Mode (OAM):	Acquires orbiter communication through omni-directional antennas Performs dynamics phase ambiguity resolution (orbiter is moving wrt Montgolfière) When LOS is acquired, points the HGA towards orbiter Sensors: Omni-directional antennas, IMU to aid the acquisition Control: possibly altitude control for minimizing wind impact
Observation Mode (NM):	Normal mode of operation Sensors: RF + IMU for absolute pointing ; possibly: use of science cameras for relative navigation ; pressure altimeter Control: altitude control for maximizing image resolution or field of view
Dark Mode (DM):	Science mode during night No communication with orbiter Sensors: IMU + pressure altimeter for maintaining the pointing knowledge and propagating the relative navigation

Safe Mode (SM)	Triggered by Hazard Avoidance Decision, loss of RF or communication link ; balloon is sent back to a safe altitude (lowest wind to minimize impact on Science return) Sensors: Sun Sensors to re-acquire coarse attitude and restore communication (scanning) + redundant altimeter Control: valve

8.1.2.4.4.3 Equipment List

Mission Timer Unit

The timer is considered as part of the DHS as it will wake up all equipments, and not only GNC equipments.

RF Antennas

X-band omni-directional low gain antennas are required for LOS estimation. Classical patch antennas as used for TT&C can be used for this application. A typical Antenna implementation is given in Figure 32.

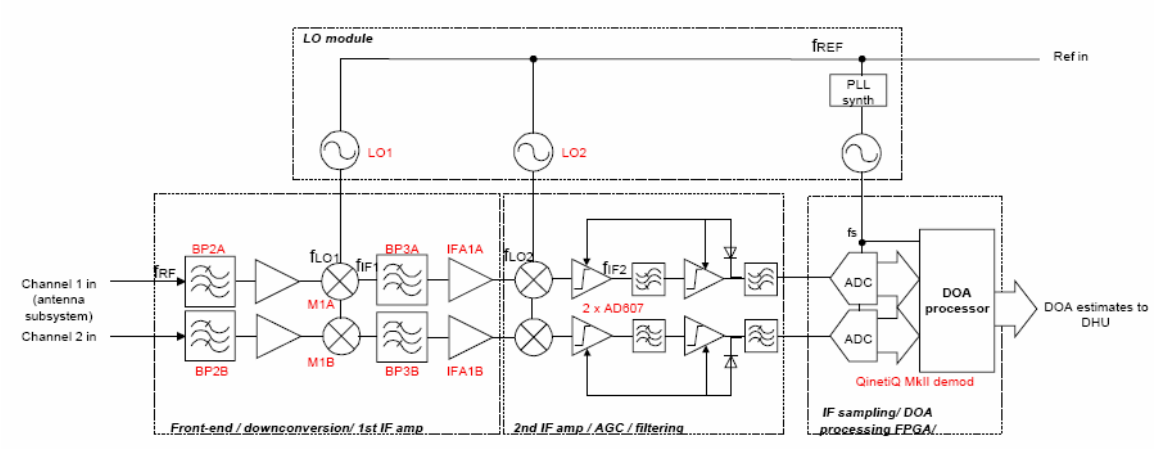

Figure 32 Omni-directional antenna implementation

Accelerometers

Honeywell QA2000 accelerometer is selected for reference. It has a range of operation fully compatible with mission profile and has already flown on interplanetary mission (MEX/VEX/ROSETTA family).

Its range of operation is 60 g with a µg resolution, and a 4 mg bias. Its mass is 71 g.

Figure 33 Honeywell QA2000 accelerometer

Gyroscopes

Triplet of coarse gyros is required to provide attitude information during descent and during non-visibility periods of the orbiter. An accuracy of a few degrees per hour is sufficient for this, and SEA MEMS gyroscope was selected.

This sensor presents a low mass, low power configuration (0.75 kg & 4 W for a 3 gyros inertial unit), and a performance of 0.2°/sqrt(hr) of angular random walk, and 5°/hr of rate bias drift.

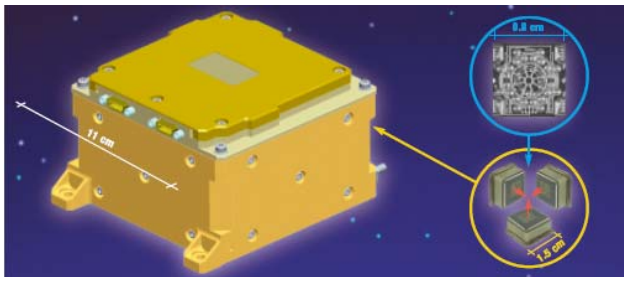

Figure 34 SEA MEMS Rate Sensor

Sun Sensors

The TNO µ-digital sun sensor currently under development is selected. If offers a field of view of 120°×120°, an accuracy better than 0.1°. However, an adaptation to Titan environment (temperature, ~1/000 less sunlight, IR sensitivity) is likely to require a new development.

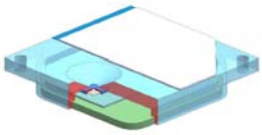

Figure 35 TNO µ-digital sun sensor (under development)

G-switch sensors

Inertia Space Series switch sensors are selected as baseline g-switch. This is a fully space qualified model which provide high reliability switching. It is a purely mechanical device.

Figure 36 Inertial switch g-switch sensor

Baro-altimeter

Typical Pitot-Tube is used for pressure measurement.

The overall mass budget is given in Table 16

Table 16 Mass budget of GNS sensors.

Element 2	Montgolfier		MASS [kg]			
Unit	Unit Name Click on button above to **insert new unit**	Quantity	Mass per quantity excl. margin	Maturity Level	Margin	Total Mass incl. margin
1	Accelerometer	3	0.1	Fully developed	5	0.2
2	g-switch sensors	4	0.1	Fully developed	5	0.0
3	IMU	1	2.5	To be developed	20	3.0
4	RF Antennas	4	0.3	Fully developed	5	1.3
5	Sun Sensor	3	0.3	To be modified	10	1.0
6	Pressure Sensor	2	0.1	To be modified	10	0.2
-	Click on button below to insert new unit		0.0	To be developed	20	0.0
SUBSYSTEM TOTAL		**6**	**5.0**		**13.6**	**5.7**

8.1.2.4.5 Telecommunications

Due to the large distance to Earth (10 AU) the baseline up- and downlink to the Montgolfière is by using the orbiter s/c as a relay.

Patch antennas will be included at the back cover of the back-heat shield and on the gondola such that during the entire entry and descent phases some limited telemetry can be sent for status information, and possibly additionally available bandwidth may be provided for science (mainly from atmospheric measurements).

The power to the telecommunications system will be maximized during data transmission periods in the science operations phase, to avoid using batteries (for low mass), and therefore it was assumed for the power budget that all non-essential equipment would be switched to low power consumption. This results in a total of 55 W being available to the telecommunications system. Assuming 10 W for receivers and 45 W for the TWTA yields typically 25 W for transmit RF power. The maximum size of the HGA that could be accommodated without increasing the gondola envelope is 50 cm diameter.

The orbiter's telecommunication system includes a steerable 4 m diameter HGA with a multiple frequency capability, which will allow using the same telemetry and telecommand system for the Montgolfière and the Lander. The communications link will be in X-band at 8.45 GHz.

The Montgolfière has a 50 cm, 2 degrees-of-freedom steerable HGA with an antenna gain of 31 dB. A pointing accuracy of 1° was assumed. The position to the orbiter will be measured by using a beacon signal from the orbiter. A coarse position determination will be performed by a phase-based line-of-sight measurement (see section 8.1.2.4.4.2), and a fine pointing measurement will be performed by a narrow angle antenna scan.

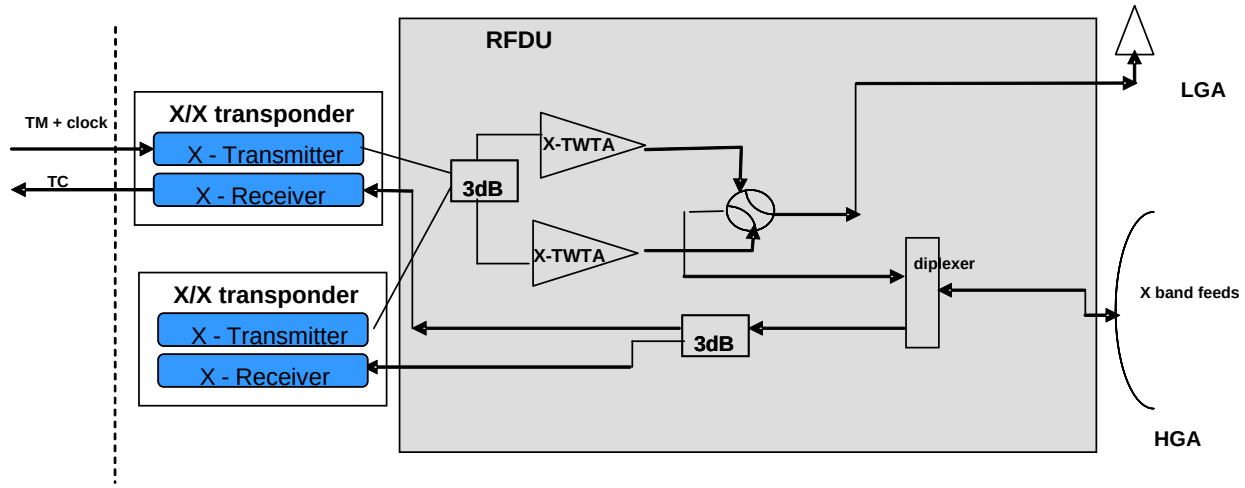

Figure 37 Montgolfière TT&C baseline design.

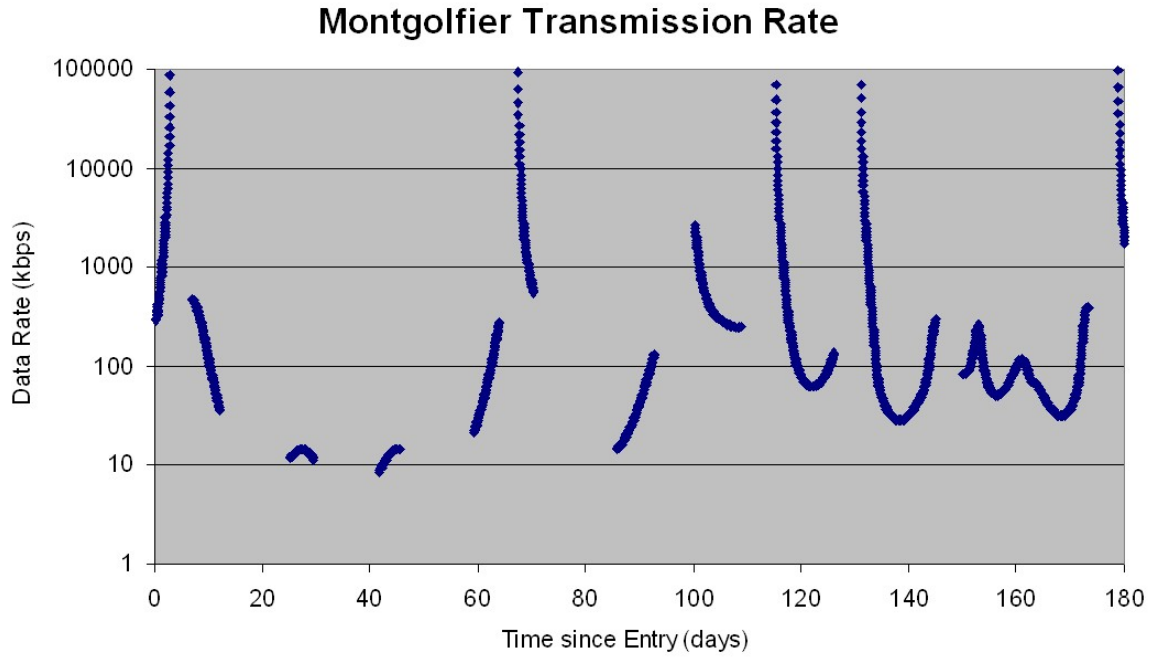

Figure 38 Theoretical data transmission rate from the Montgolfière to the orbiter as a function of mission duration, assuming a link margin of 3 dB, and minimum elevation of 30°.

The theoretical capability of the telemetry link to the orbiter is shown in Figure 38. It ranges from a few 10 kbps to >100 Mbps. At higher levels, the processor and transponder capabilities would likely be saturated, limiting the actual achievable transfer rate. To make the optimum use of this large variation of link capability, a variable transmission data rate will be implemented.

For the fall back of transmission direct to earth, the link has the following characteristics:

Table 17 Link characteristics for Montgolfière DtE data transmission.

Frequency	8.4 GHz
Link distance	11 AU
Ground station	Cerebros
G/T	50.8 dB/K
Turbo coding	¾
Spacecraft EIRP	43 dBW
Data volume for 4 h transmission with 10% overhead	1.6 Mbit

Possibly a USO may be included in the telecommunications system. This may aid the Doppler tracking of the Montgolfière by the orbiter and from ground (DtE and VLBI) for wind measurements and localization determination. DtE transmission using SKA, if available, would provide data rates up to ~70 kbit/s). No requirements on the frequency stability have been established at the time of this study, and therefore this was not further explored.

Table 18 Mass budget of Montgolfière communication equipment.

Element 2	Montgolfier		MASS [kg]			
Unit	Unit Name Click on button above to **insert new unit**	Quantity	Mass per quantity excl. margin	Maturity Level	Margin	Total Mass incl. margin
1	LGA	1	0.50	Fully developed	5	0.5
2	HGA	1	6.00	To be modified	10	6.6
3	X/X transponder	2	2.50	Fully developed	5	5.3
4	TWTA X-band	2	2.70	Fully developed	5	5.7
5	RFDU and harness	1	1.80	To be modified	10	2.0
6				To be developed	20	0.0
7				To be developed	20	0.0
-			0.0	To be developed	20	0.0
SUBSYSTEM TOTAL		**5**	**18.7**		**7.1**	**20.0**

8.1.3 ENTRY DESCENT AND INFLATION SYSTEM

8.1.3.1 Thermal Protection

For the thermal protection system only ablative materials are being considered due to their higher mass efficiency and due to heritage from Huygens.

8.1.3.1.1 Front Shield

The selected material is identical to what was used on Huygens AQ60. The material is available on demand from EADS, and was qualified to a heat flux of up to 2.7 MW/m^2. For the purpose of this study the maximum heat flux was limited at 2.5 MW/m^2. The density of AQ60 is 280 kg/m^3.

Based on a comparison with previous missions the mass fraction of the applied TPS was parameterized as a function of total heat load. A fraction of TPS mass of 20% corresponds to a total heat load of 200 MJ/m^2. Therefore a requirement was derived that the entry conditions (FPA and velocity) should be such that the total heat load remains <200 MJ/m^2. Assuming a constant entry velocity this requirement essentially translates to an upper limit on the total mass of the entry vehicle for a given FPA. The calculated values for heat flux and total heat load are given in section 7.1.2.

A further parametric analysis was performed describing the dependency of ablator thickness as a function of temperature at the inside interface. A suitable limit of the inside interface temperature below 150 °C was chosen. At this value also the gradient of added mass for further temperature reduction becomes less steep, therefore requiring significantly more ablator thickness per degree of temperature reduction.

For the final sizing of the ablator thickness a safety margin of 50% was added to the calculated thickness and an additional 2 mm for over-flux at the half cone.

Based on these considerations and based on the calculated total heat load (cf. section 7.1.2), the required thickness of the front shield is 28.5 mm. With the total surface area of the front shield being 6.03 m^3 the total mass is 48 kg.

8.1.3.1.2 Back Shield

Also for the material of the back shield flight heritage from Huygens is chosen and the material Prosial 2000 was selected. It has a medium density of (500 kg/m^3) and is qualified up to 900 kW/m^2.

A simulation of the heat flux and of the heat load was performed, as for the front shield. A similar parameterization of shield thickness was carried out and a safety margin of 50% on the thickness was included. The required thickness of 6.9 mm the back shield was derived. The surface area of the back shield is 3.33 m^3, which yields a total mass of 11.5 kg.

8.1.3.2 Parachutes

One main parachute is used for the descent. It is opened via use of a drogue parachute that will be released via a mortar. This release sequence is similar to that of Huygens. The drogue parachute pulls off the back cover and pulls out the main parachute with it. The main parachute is opened a few seconds after the opening of the drogue parachute. About 30 s later the front shell is released. The Montgolfière Probe then descends on this main parachute until inflation of its balloon.

The size of the main parachute is driven by the drag of the front shell. The parachute surface was calculated to provide the maximum relative acceleration between the front shield and the descent module, thereby guaranteeing the safest separation and reducing the collision risk. Of course,

depending on the margin that shall be applied on the separation safety, the size of the main parachute could be modified (within limits), and thereby the descent profile changed.

The drogue parachute was sized in order to provide enough force to pull of the back shell and to deploy the main parachute. Its diameter is 1.3 m, and a conical-ribbon design was used as shown in Figure 39.

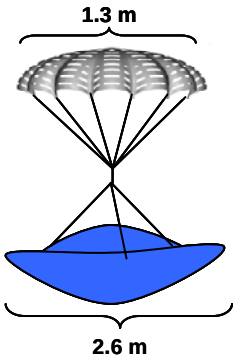

Figure 39 The Drogue Parachute of the Montgolfière

The characteristics of the drogue parachute are:

- Conical Ribbon Design
- Diameter: 1.3 m
- Stowed Volume: 0.008 m^3
- Number of Suspension Lines: 16
- Suspension Lines Length: 1.3 m
- Riser Length: 14.4 m
- Dacron Type 52 Polyester Material
- Braided Nylon Suspension Lines.

For the main parachute a Disc-Gap band design was used. It is shown in Figure 40.

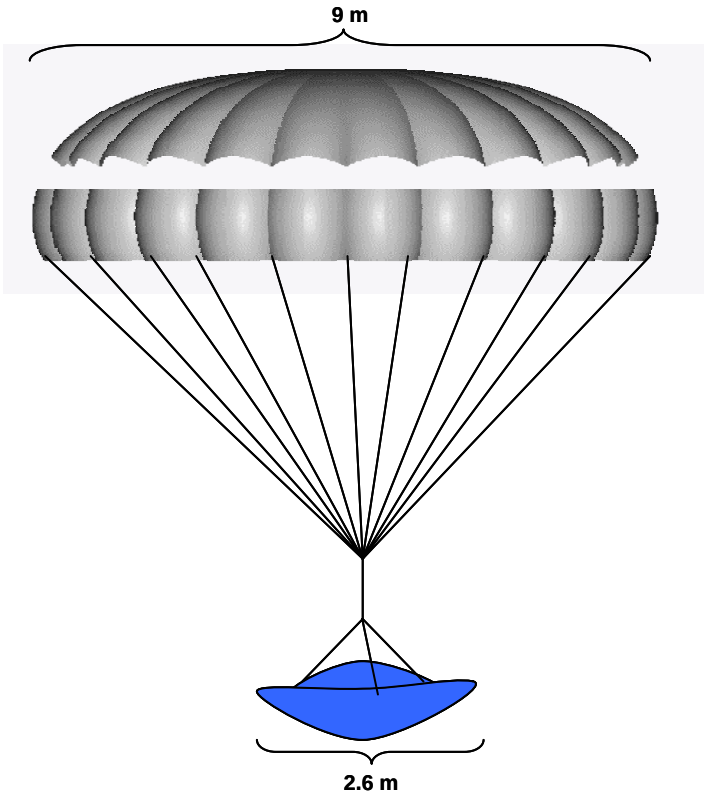

Figure 40 The Main Parachute for the Montgolfière

The characteristics of the parachute are:

- Disc-Gap-Band Design
- Diameter: 9 m
- Stowed Volume: 0.05 m^3
- Number of Suspension Lines: 56
- Suspension Lines Length: 8.6 m
- Riser Length: 7.6 m
- Dacron Type 52 Polyester Material
- Braided Nylon Suspension Lines.

The list of equipment and mass estimates of the parachute equipment is provided in Table 19.

Table 19 Montgolfière parachute equipment list.

Element 2	Montgolfier		MASS [kg]			
Unit	Unit Name Click on button above to **insert new unit**	Quantity	Mass per quantity excl. margin	Maturity Level	Margin	Total Mass incl. margin
1	Drogue Canopy	1	0.0530	To be modified	10	0.1
2	Drogue Suspension Lines and Riser	1	0.3840	To be modified	10	0.4
3	Drogue Bridal	1	0.5000	To be modified	10	0.6
4	Drogue Mortar	1	1.0000	To be modified	10	1.1
5	Drogue Deployment Bag	1	0.2830	To be modified	10	0.3
6	Main Canopy	1	3.1080	To be modified	10	3.4
7	Main Suspension Lines and Riser	1	5.3010	To be modified	10	5.8
8	Main Bridal	2	2.0000	To be modified	10	4.4
9	Main Swivel	1	2.0000	To be modified	10	2.2
10	Main Deployment Bag	1	1.0810	To be modified	10	1.2
11	Main Deployment Bag Bridal	1	0.5000	To be modified	10	0.6
-	Click on button below to insert new unit		0.0	To be developed	20	0.0
	SUBSYSTEM TOTAL	**11**	**18.2**		**10.0**	**20.0**

8.1.4 PROBE TO ORBITER INTERFACE SYSTEM

The probe-to-orbiter interface system (POIS) is shown in Figure 22 and has the following functions:

- Mechanical interface to orbiter; as such it is a load carrying structure
- Support for cruise thermal control h/w (radiators, pumps and cooling pipes)
- Communications interface to orbiter to allow for monitoring and checkout during the interplanetary phase.

The Montgolfière Probe has its own power system which is based on the MMRTG, and which will be used during all phases of the mission.

The radiators for the thermal subsystem will be mounted on this interface structure. The pumps for circulation of the cooling fluid are also mounted on the POIS to keep the mass of the floating vehicle as low as possible. The POIS remains attached to the Montgolfière Probe after separation from the orbiter spacecraft to continue providing cooling power during the ballistic flight. It will be separated shortly before entry.

The mass of the POIS is 100 kg (see Table 6).

8.1.5 MECHANISMS

The following mechanisms are needed:

- spin and eject for separation from orbiter (Huygens heritage)
- separation of the POIS

- mortar for release of drogue parachute (Huygens heritage)
- release of TPS (back shield) and main parachute release (Huygens heritage)
- release of TPS (front shield; Huygens heritage)
- release of balloon cover and balloon deployment
- release of MMRTG
- separation of the main parachute from the balloon after deployment of the MMRTG

The mass of these mechanisms has been taken into account at the various units they are attached to, and is not reported separately.

8.2 Lander Probe

8.2.1 SYSTEM/OVERVIEW

The Lander Probe has the following subsystems (see Figure 41): the Lander, an Entry Descent and Landing Subsystem (EDLS), and the Probe to Orbiter Interface System (POIS). The EDLS consists of similar parts as for the Montgolfière Probe. The POIS is simpler than that for the Montgolfière Probe, as it is only a structural interface system, but for the Lander Probe is includes connections for power and data flow.

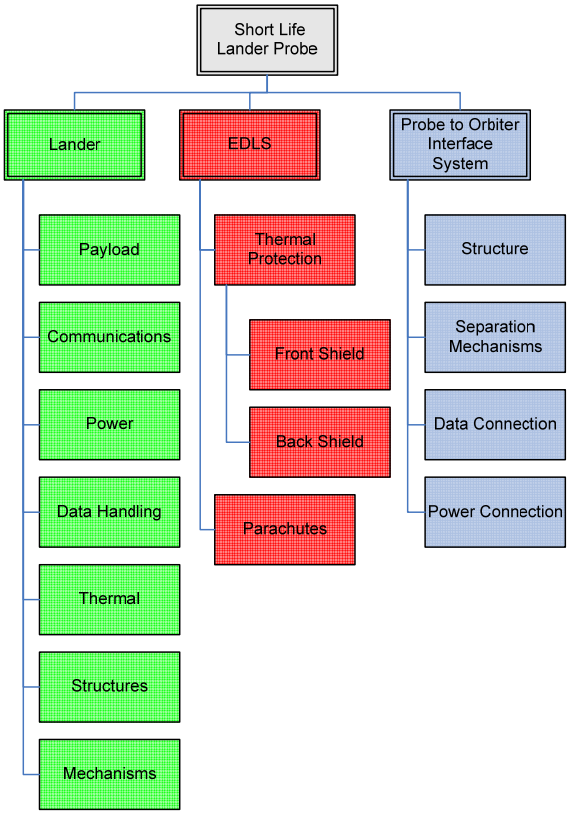

Figure 41 Elements of the Lander Probe.

During the interplanetary cruise the Lander will be powered from the orbiter spacecraft. A limited amount of data for health checks will also be transmitted through the orbiter's data handling system during short periods. Before release the Lander Probe's timing system will be activated and the Lander will fly ballistic to Titan. The Lander Probe does not have an active propulsion and attitude control system.

A high level mass breakdown is shown in Table 20. The specified masses are including a 20% system margin (ESA standard).

Table 20 Masses of the main subsystems of the Lander Probe including 20% system margin.

Element	Mass in kg
POIS	9
EDLS	96
Lander	85
Total launch mass	**190**

8.2.2 LANDER SYSTEM

8.2.2.1 Configuration

The baseline design of the Lander Probe is similar to the design of the Montgolfière Probe (cf. section 8.1.2.1). Its system is subdivided into the front shield, back shield and Lander Figure 42.

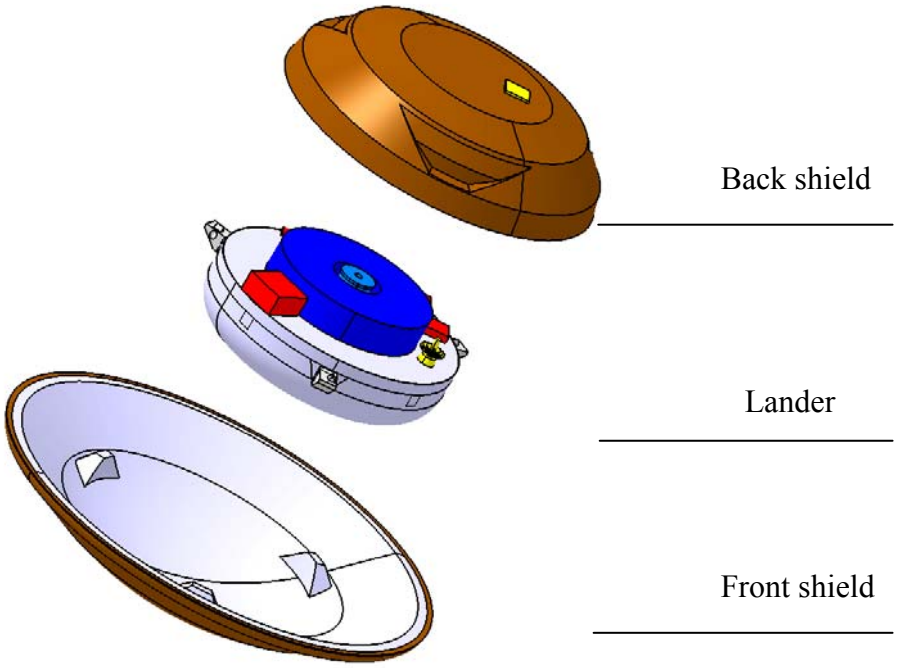

Figure 42 Lander overview

Unlike for the Montgolfière, the DLS can be mounted on the platform of the probe. Moreover the Lander is battery powered and does not require radiators for thermal dissipation. Figure 43 shows a cross section of the probe, Figure 44 and Figure 45 show the view from above, and Figure 46 and

Figure 47 show the Lander seen from the bottom. The equipment mounted on the nadir side of the platform is labelled in Figure 47. Figure 48 shows the Lander in deployed configuration after landing. The TEEP-L antenna is shown unfolded.

The instrument accommodation that is shown in these concepts is preliminary only. Details of the access to atmosphere and sampling of the liquid have not yet been taking into account, partly due to detailed instrument specifications not being available in this phase. Design of this instrument interface aspect should be carried out during the next phase, using Huygens as a starting point. Also no provisions for the illumination device that will be used after landing have been made. It is expected that its accommodation will be relatively straightforward.

The overall dimensions and approximate location of the centre of mass of the complete probe are given in Figure 49, and those of the Lander are given in Figure 50. The volume inside the nadir skin is indicated in Figure 51, which is relevant for the calculation of the buoyancy for the foreseen lake landing.

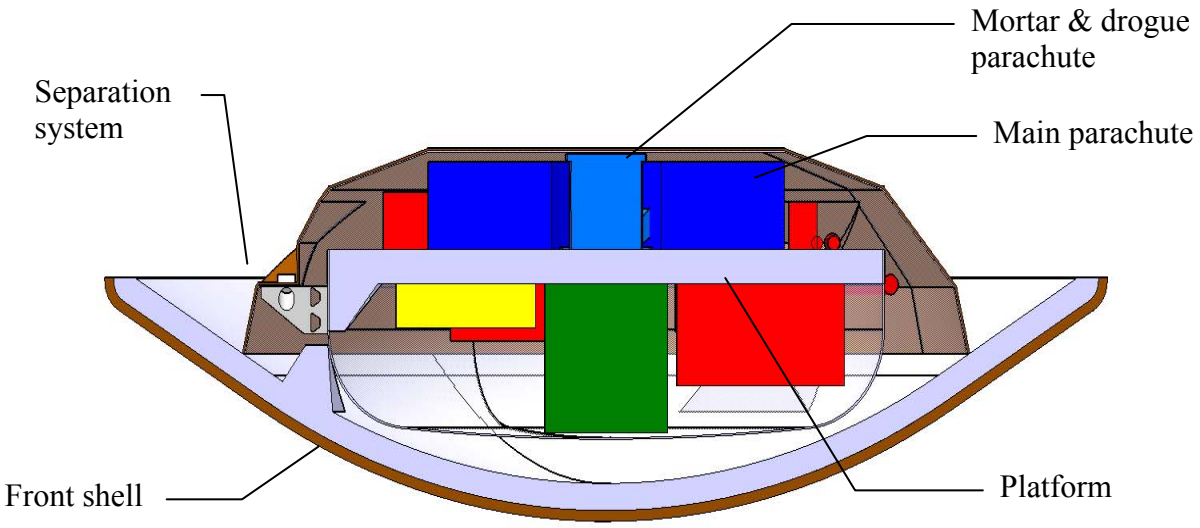

Figure 43 Lander section

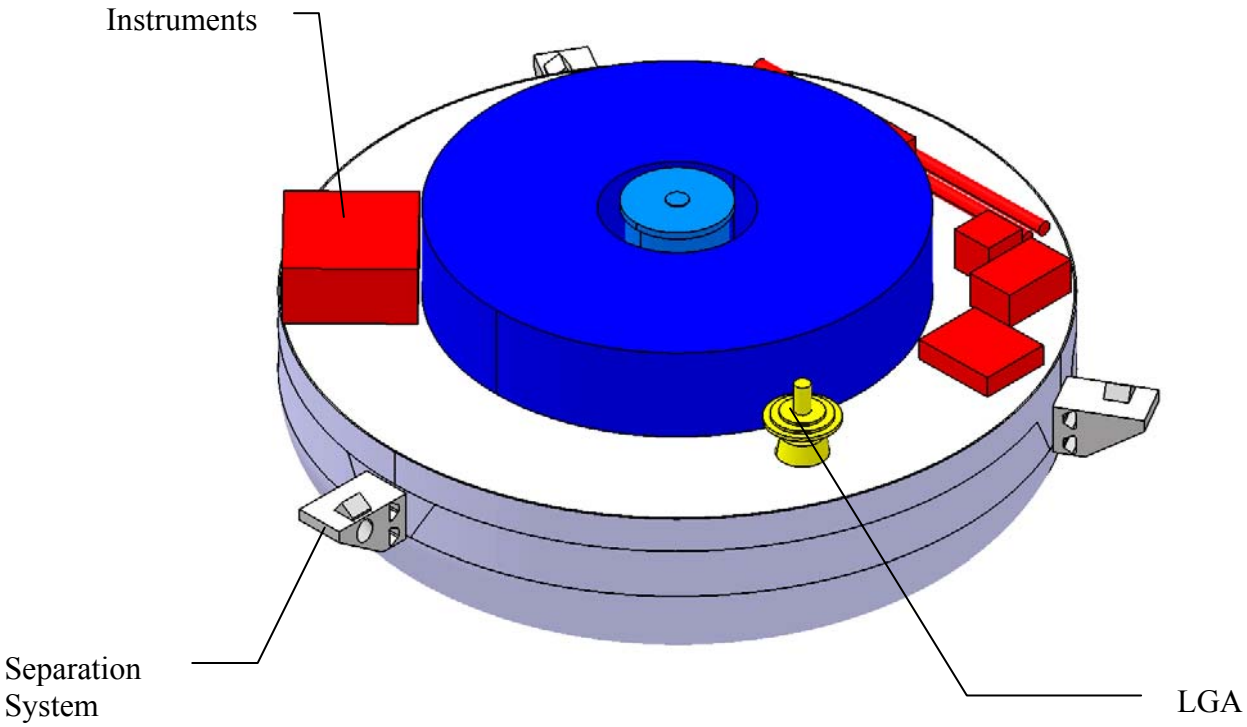

Figure 44 Lander top view

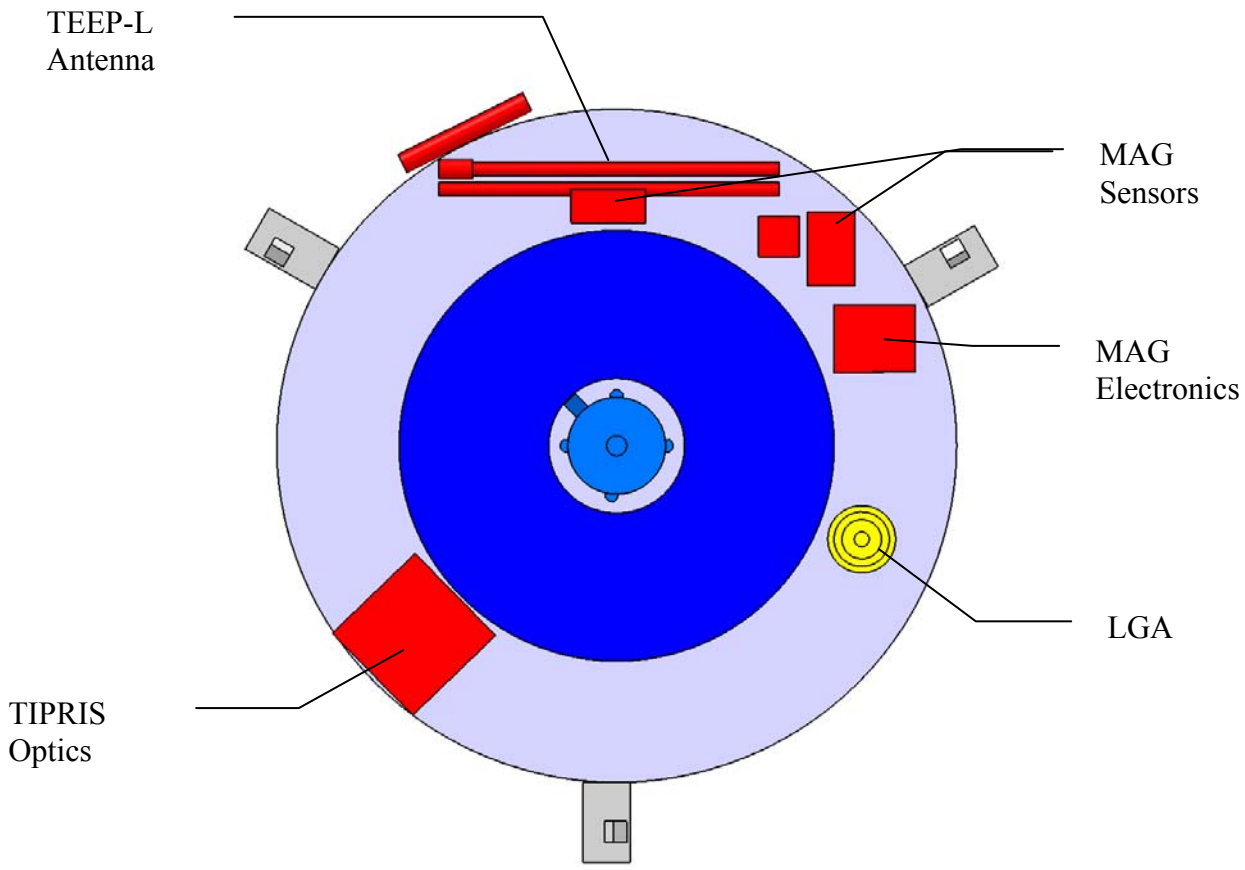

Figure 45 Equipment mounted on the platform top side

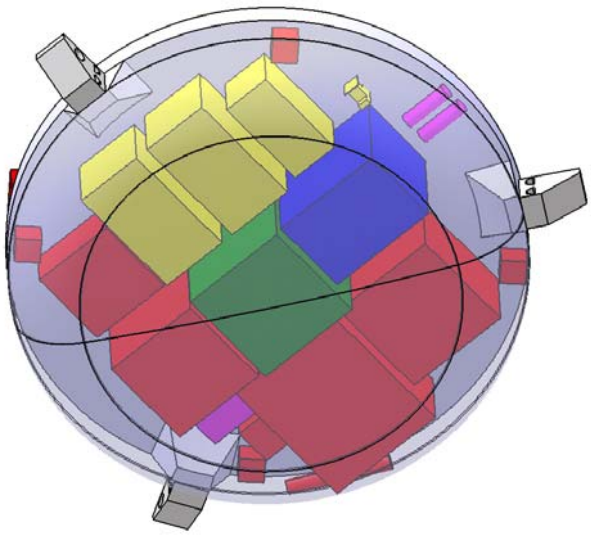

Figure 46 Lander bottom view

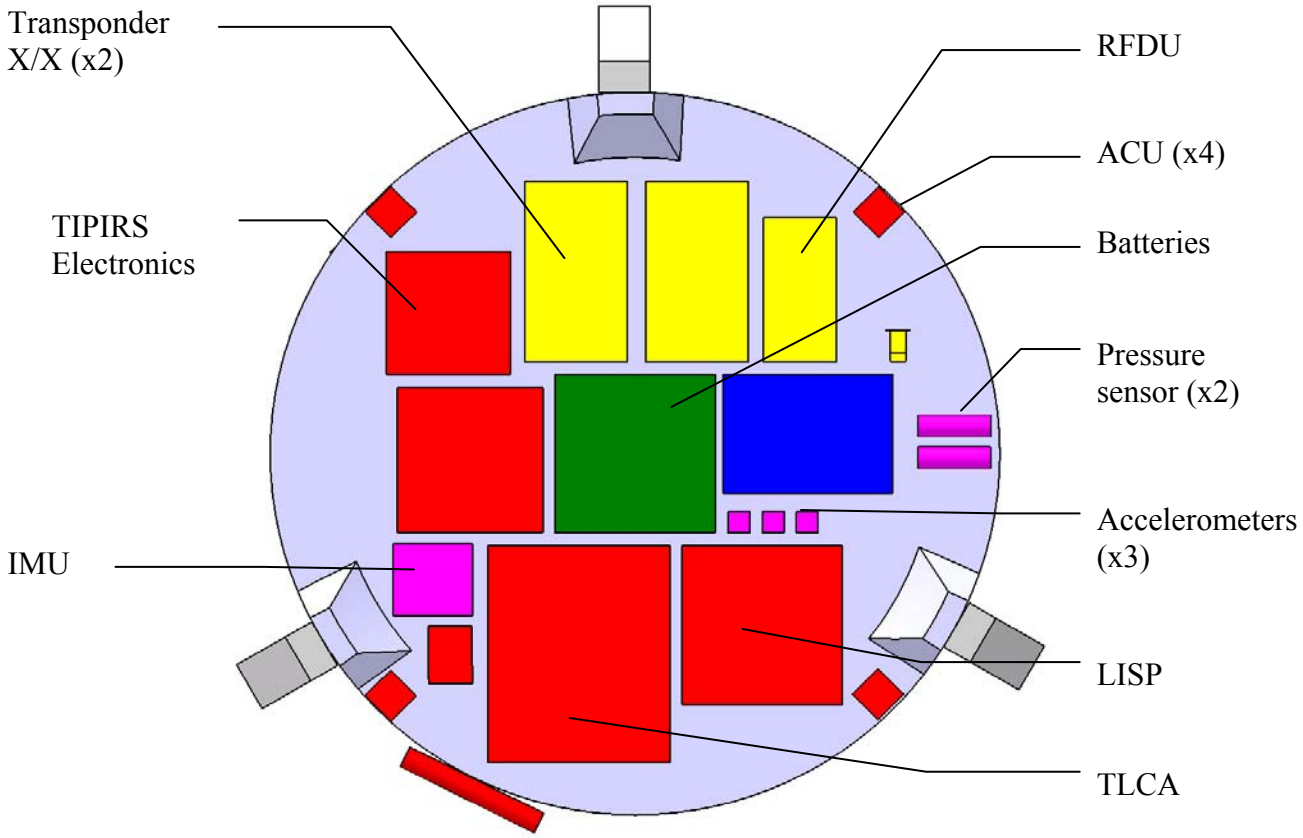

Figure 47 Equipment mounted on the Platform bottom side

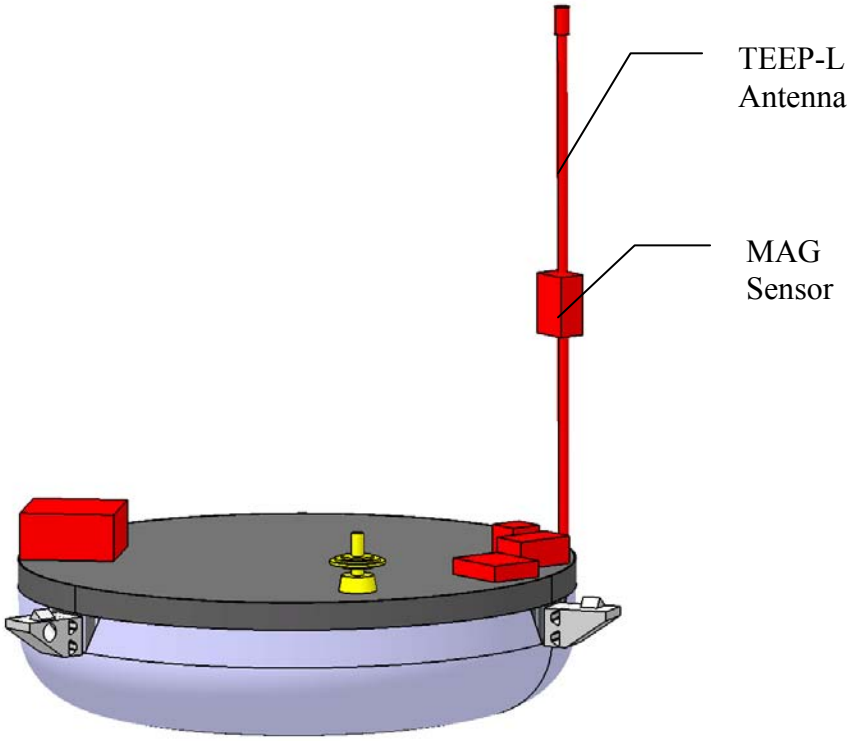

Figure 48 Lander Probe deployed

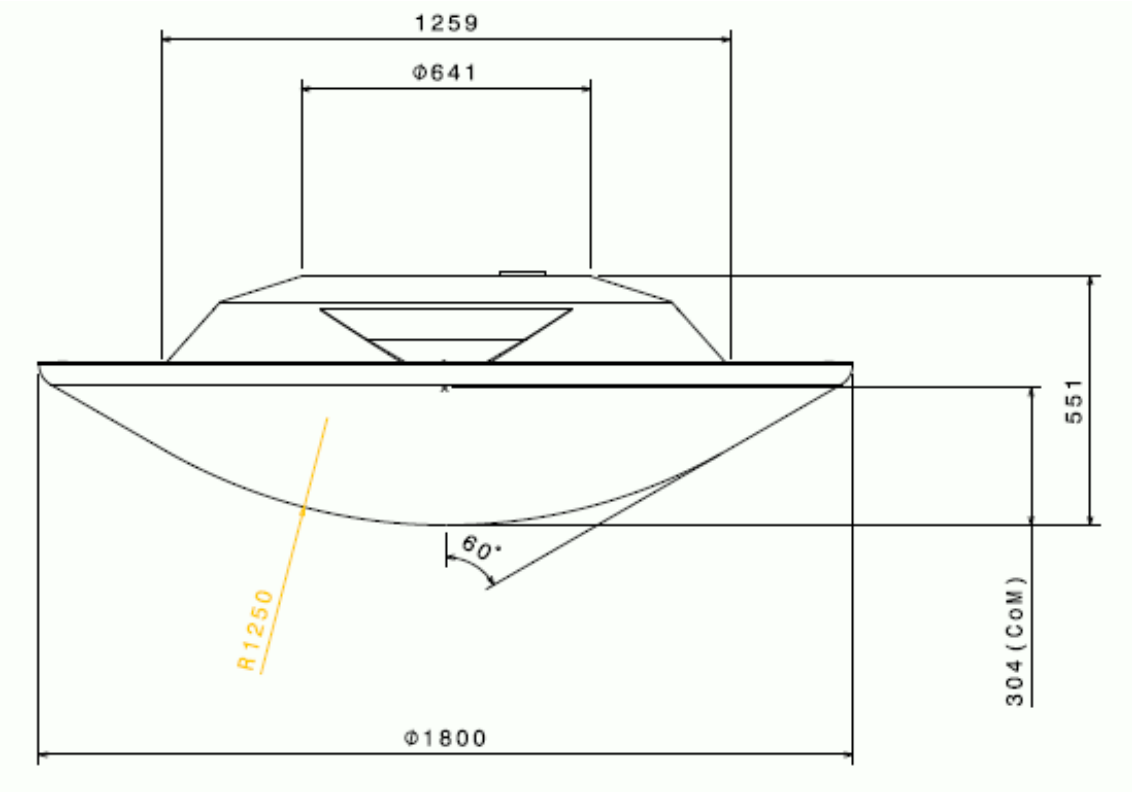

Figure 49 Lander Probe overall dimension

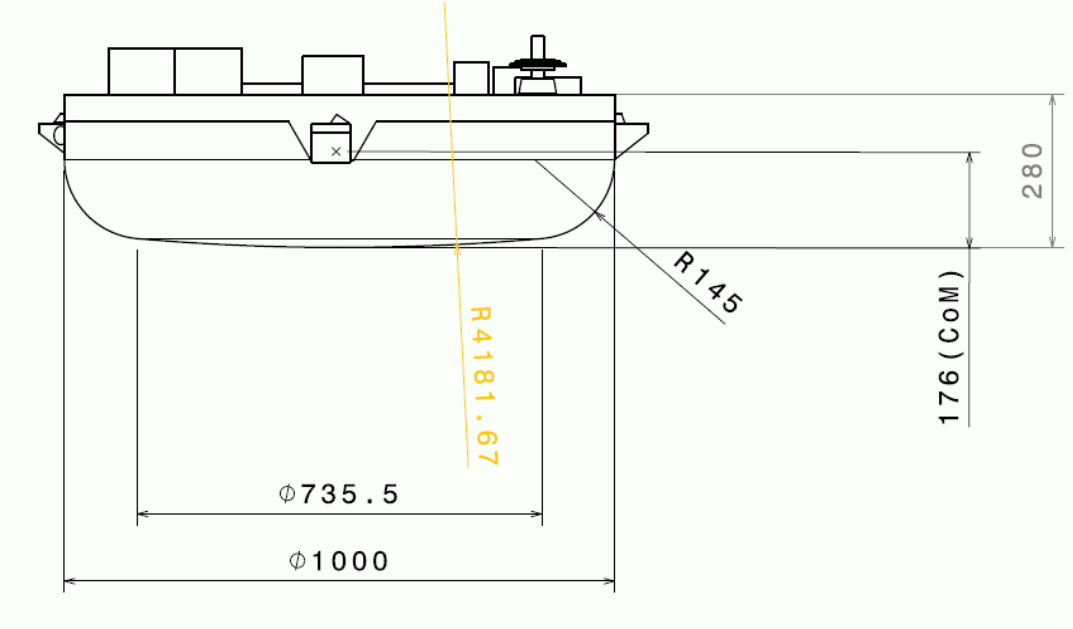

Figure 50 Lander element dimensions

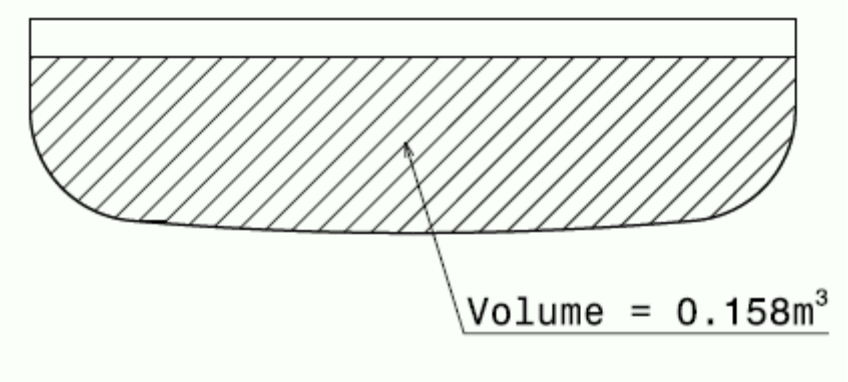

Figure 51 Bottom-skin volume

8.2.2.2 Structures

The same considerations for the structural analysis, which were performed for the Montgolfière (cf. section 8.1.2.2) apply also here and are therefore not repeated. Additionally for the Lander, to limit the deceleration forces to be experienced, a 10 cm thick layer of impact attenuation foam is placed at the bottom of the Lander with an estimated mass of 3.7 kg.

The following mass budget has been calculated for the Lander structure is shown in Table 21.

Table 21 Lander structure mass budget overview

Mass budget overview	Mass in kg
Front shield	12.6
Back shield	6.7
Payload platform	4.3
Skin	6.0
Miscellaneous (fasteners, inserts)	3.6
Impact attenuation foam	3.7

8.2.2.3 Power

During the interplanetary transfer the Lander would be in hibernation for most of the time. Occasional switch-on would occur for testing. These durations would be at regular intervals. During these operations, the Lander will be powered by the orbiter's power system.

The power system has to support operations from before entry, during entry and descent (5.7 hours), and for 3 hours on the surface. The energy budget is summarized in Table 22. Central to this analysis is the assumed power consumption of the timers that are required during the sleep mode. The Huygens consumption 3×0.2 W = 0.6 W has been assumed. Due to same requirements on failure tolerance and radiation hardness, no significant improvement on this consumption could be achieved since. Also the use of G-switches is unlikely to provide reductions of power

consumption during this phase, due to the same requirements to monitor the status of the switches with failure tolerant radiation-hard circuitry.

Table 22 Lander Probe energy budget.

		Thermal	AOCS	Comms	DHS	Short-Lived Lander Payload	Harness AND PCDU	TOTAL CONSUMPTION
		linked	linked	linked	linked	linked	linked	
	Ppeak	0 W	5 W	25 W	12 W	76 W	13 W	131 W
Separated Sleep Mode	Pon	0 W	0.60 W	0 W	0.00 W	0.0 W	0.04 W	0.64 W
	Pstdby	0 W	0.00 W	0 W	0 W	0.0 W	0.00 W	0.00 W
	Duty Cycle	0 %	100 %	0 %	0 %	0 %		93%
	Paverage	0 W	0.60 W	0 W	0.00 W	0.0 W	0.04 W	0.64 W
Tref 31680 min	Total Wh	0 Wh	317 Wh	0 Wh	0 Wh	0.0 W	0 Wh	317 Wh
Entry Mode	Pon	0 W	4 W	25 W	5 W	0.0 W	7 W	41 W
	Pstdby	0 W	0 W	0 W	2 W	0.0 W	5 W	7 W
	Duty Cycle	0 %	100 %	46 %	100 %	0 %		54%
	Paverage	0 W	4 W	12 W	5 W	0.0 W	6 W	27 W
Tref 6 min	Total Wh	0 Wh	0 Wh	1 Wh	0 Wh	0.0 W	1 Wh	3 Wh
Descent Mode	Pon	0 W	4 W	25 W	8 W	5.0 W	8 W	50 W
	Pstdby	0 W	0 W	0 W	2 W	5.0 W	5 W	12 W
	Duty Cycle	0 %	100 %	46 %	100 %	0 %		58%
	Paverage	0 W	4 W	12 W	8 W	5.0 W	7 W	36 W
Tref 360 min	Total Wh	0 Wh	25 Wh	69 Wh	48 Wh	30.0 W	33 Wh	205 Wh
Science Mode	Pon	0 W	0 W	10 W	9 W	75.9 W	12 W	107 W
	Pstdby	0 W	0 W	0 W	2 W	75.9 W	10 W	88 W
	Duty Cycle	0 %	0 %	100 %	100 %	0 %		93%
	Paverage	0 W	0 W	10 W	9 W	75.9 W	12 W	107 W
Tref 150 min	Total Wh	0 Wh	0 Wh	25 Wh	23 Wh	189.8 W	26 Wh	264 Wh
Transmission Mode	Pon	0 W	0 W	25 W	5 W	0.0 W	7 W	37 W
	Pstdby	0 W	0 W	0 W	2 W	0.0 W	5 W	7 W
	Duty Cycle	0 %	0 %	100 %	100 %	0 %		93%
	Paverage	0 W	0 W	25 W	5 W	0.0 W	7 W	37 W
Tref 30 min	Total Wh	0 Wh	0 Wh	13 Wh	2 Wh	0.0 W	3 Wh	17 Wh
Safe Mode	Pon	0 W	0 W	10 W	5 W	0 W	6 W	21 W
	Pstdby	0 W	0 W	0 W	2 W	0 W	5 W	7 W
	Duty Cycle	0 %	0 %	100 %	115 %	0 %		0%
	Paverage	0 W	0 W	10 W	5 W	0 W	6 W	21 W
Tref 0 min	Total Wh	0 Wh	0 Wh	0 Wh	0 Wh	0 Wh	0 Wh	0 Wh
							Battery Capacity	806 Wh

For the batteries SAFT Li-SO_2 cell packages were assumed, which have an energy density of 6 g/Wh and 5 cm^3/Wh. For the sizing 20% redundancy and 3% energy loss per year was assumed. This results in a mass of 4.48 kg and 3.7 litres for the total required 806 Wh.

As for the Montgolfière, an integration of the PCDU and DHS into one units was assumed here too for the estimate of the mass budget. The PCDU components are summarized below (Table 23). No provision is made for the PCDU box structure, as this is accounted for in the DHS table.

Table 23 Lander power subsystem equipment.

Unit Name	Mass incl. margin in kg
Li-SO_2 battery	4.84
BCDR board	0.66
2 PCDU command board	0.84

Distribution board 1.5A	0.66
Pyro control board	0.6
Power bus Capacitors	0.21
Totals	**7.8**

8.2.2.4 Data-handling

The design is similar to what was chosen for the Montgolfière to minimize mass and colume. The DHS is based on SCOC3 ASIC. The CDMU is highly integrated and has a lower mass than HICDS (developed for BepiColombo). Advanced Data and Power Management System (ADPMS) is developed for Proba II and is an example of an integrated power and data handling system. The baseline design concept is similar to that of the Montgolfière (Figure 29).

The baseline memory uses FLASH technology. The memory was sized at 14 Gbit, which was estimated from the data produced by the instruments under the assumption of storage of all instrument data.

The mass budget of the DHS is given in Table 24. The mass of the box includes the mass required for the accommodation of the PCDU, without including the mass of the PCDU board here. The processors are cold redundant, and therefore their power consumption is not added twice in the power budget.

Table 24 Lander DHS mass budget.

Element 1	Long-Lived Lander		MASS [kg]			
Unit	Unit Name Click on button above to **insert new unit**	Quantity	Mass per quantity excl. margin	Maturity Level	Margin	Total Mass incl. margin
1	Processor Module + TT&C	2	0.8	To be modified	10	1.8
2	System I/O	2	0.8	To be modified	10	1.8
3	Power converter	1	0.8	To be modified	10	0.9
4	Box Mechanics	1	2.3	To be modified	10	2.5
-	Click on button below to insert new unit		0.0	To be modified	10	0.0
SUBSYSTEM TOTAL		**4**	**6.3**		**10.0**	**6.9**

8.2.2.5 Thermal

The sizing of the power budget did not include provisions for heating. It is assumed that the thermal design will use heritage from Huygens. Spot heating will be applied by using RHU's. The equipment bay will be protected with thermal insulation foam. Equipment will be located such that it optimally profits from the application of RHU's. The material thermal conductivity will be used for heat distribution. Late access is required for integration of RHU's. This will be addressed at a later phase when more details of the instruments and electronics are available, allowing for a more accurate thermal design.

The permanent dissipation by these RHU's, which occurs during all phases of the mission, will need addressing in a more detailed study. The heat needs to be dissipated in a controlled manner

prior to deployment of the Lander on Titan, i.e. during the interplanetary and the ballistic cruise) phases. At the same time the probe needs to be sufficiently isolated for surface operations in Titan's environment. Heritage from Huygens will be used.

8.2.2.6 Guidance, Navigation & Control

The GNC design is similar to that of the Montgolfière Probe (see section 8.1.2.4.4), but without patch antennas for detection of the direction to the orbiter. Additionally a timer is needed for wake-up of the avionics system prior to entry. The probe will be in hibernation during its ballistic cruise (between separation from the orbiter up to entry).

The parachute will be released a few meters before the landing to avoid it falling on top of the probe after landing. This will be controlled by a short range altimeter. The remainder of the equipment is similar to that of the Montgolfière. The mass budget for the Lander is shown in Table 25.

Table 25 Lander GNC mass budget.

Element 3	Short-Lived Lander		MASS [kg]			
Unit	Unit Name Click on button above to **insert new unit**	Quantity	Mass per quantity excl. margin	Maturity Level	Margin	Total Mass incl. margin
1	Accelerometer	3	0.07	Fully developed	5	0.22
3	Gyro Measurement Unit	1	0.75	To be modified	10	0.83
4	Pressure sensor	2	0.10	To be modified	10	0.22
5	g-switch sensors	4	0.07	To be developed	20	0.34
6	Wake-up Timer	3	0.10	To be developed	20	0.36
-	Click on button below to insert new unit		0.0	To be developed	20	0.00
SUBSYSTEM TOTAL		**5**	**1.74**		**12.7**	**1.96**

8.2.2.7 Telecommunications

As for the Montgolfière the Lander will use the orbiter's telecommunications system as a data relay. The Lander is equipped with a LGA, and will transmit in X-band. Also during the atmospheric descent, a LGA mounted at the back-shell will enable the transmission of mission critical housekeeping data.

For the calculation of the energy budget, it was assumed that 15 W would be available to the TWTA for the entire lifetime of the lander. A link margin of 3 dB was assumed. The theoretically available telemetry rate (Figure 52) is dominated by the geometry of the delivery scenario (see also Figure 2). The distance to the orbiter decreases significantly towards the end of the operational lifetime. This allows for optimization of the power budget, such that less power and telemetry may be used by the telecommunications system in the early phases of the mission, and more power being available to instruments. This may be reversed towards the end of the mission, when the data transmission has a higher efficiency. The transmission scenario also needs to be traded with the criticality/importance of data, such that critical data being transmitted immediately (before landing) to mitigate the risk of data loss due to a possible landing failure. The theoretical total

amount of available telemetry is 3.4 Gbit (assuming transmission would occur at full power for the final 15 minutes). A variable transmission data rate will be implemented to best use this large variation of link capability.

Similarly to Huygens, if permitted by visibility from Earth, the descent of the Lander would Doppler tracked by a large radio-telescope and possibly by VLBI network, allowing for complementary wind measurements and post-mission trajectory reconstruction at least during the descent (see also section 9.1.2.2).

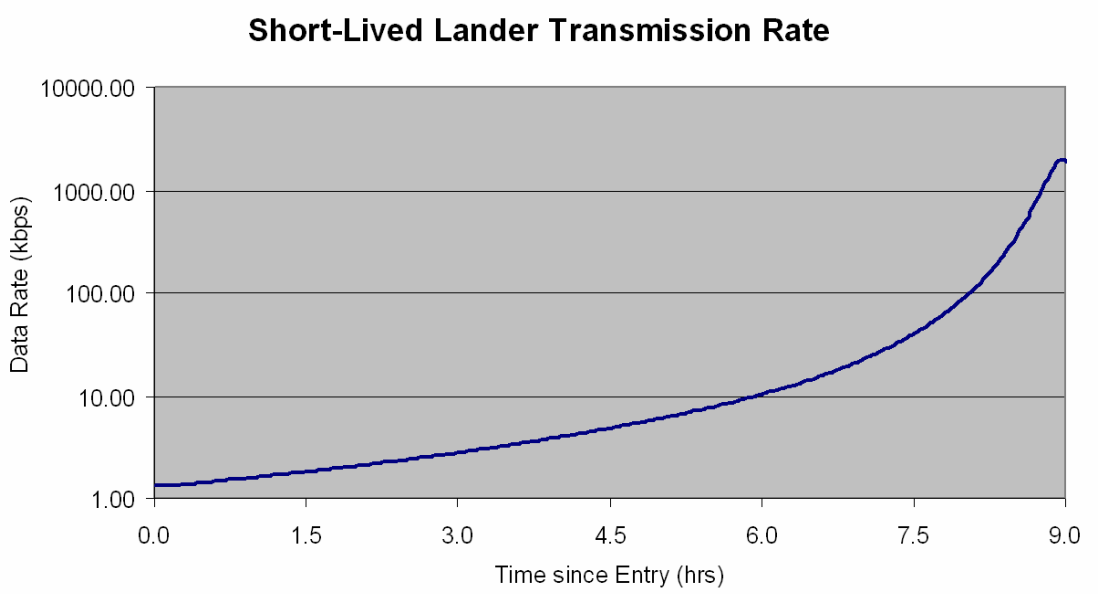

Figure 52 Possible telemetry rate of the Lander Probe as a function of time assuming 3 dB link margin.

8.2.3 ENTRY, DESCENT AND LANDING SYSTEM

8.2.3.1 Thermal Protection

Similar considerations as for the Montgolfière (cf. section 8.1.3.1) were made, and the same conclusions also apply here.

8.2.3.1.1 Front Shield

For the final sizing of the ablator thickness a safety margin of 50% was added and an additional 2 mm for over-flux at the half cone. The required thickness of the front shield is 26.3 mm. Its surface area is 2.84 m^3, which yields a total mass of 21 kg.

8.2.3.1.2 Back Shield

Also for the material of the back shield flight heritage from Huygens is chosen and the material Prosial 2000 was selected. This material has a medium density of (500 kg/m^3) and is qualified up to 900 kW/m^2.

For the back shield a similar parameterization as for the front shield was performed. The required thickness of the back shield was found as 4.8 mm, including a 50% safety margin. The surface area of the back shield is 1.68 m^3, which yields a total mass of 4 kg.

8.2.3.2 Parachutes

The same considerations as for the Montgolfière Probe apply here too. The Lander Probe is more similar to Huygens, which had two parachutes. The purpose of the second parachute on Huygens was to accelerate the descent so as to save battery lifetime. Following a trade-off in this study between the implementation of a second parachute and more mass allocation for batteries, the mass impact was found to be about the same for either option. This is basically due to higher power density of modern batteries, as compared to what was available at the time of Huygens. For arguments of reduced risk (less mechanisms, fewer single point failures, etc) and to provide the possibility of better scientific sampling of the atmosphere during descent, the option of one parachute was chosen.

The drogue parachute was sized in order to allow enough force to pull off the back shell and deploy the main parachute. Its diameter is 1 m, and a conical-ribbon design was used, as shown in Figure 53.

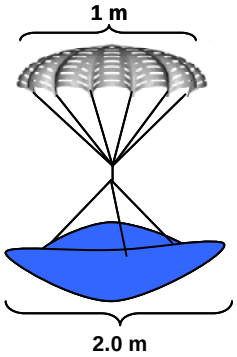

Figure 53 The Drogue Parachute of the Lander

The characteristics of the drogue parachute are given below:

- Conical Ribbon Design
- Diameter: 1 m
- Stowed Volume: 0.0076 m^3
- Number of Suspension Lines = 16
- Suspension Lines Length = 1 m
- Riser Length = 11 m
- Dacron Type 52 Polyester Material

- Braided Nylon Suspension Lines.

Due to the smaller size of the aero-shell of this lander, the front shell has a lower aerodynamic coefficient, and therefore the necessary main parachute diameter is smaller than for the Montgolfière. The parachute has a diameter of 7 m. A Disc-Gap band parachute was used, as is shown in Figure 54.

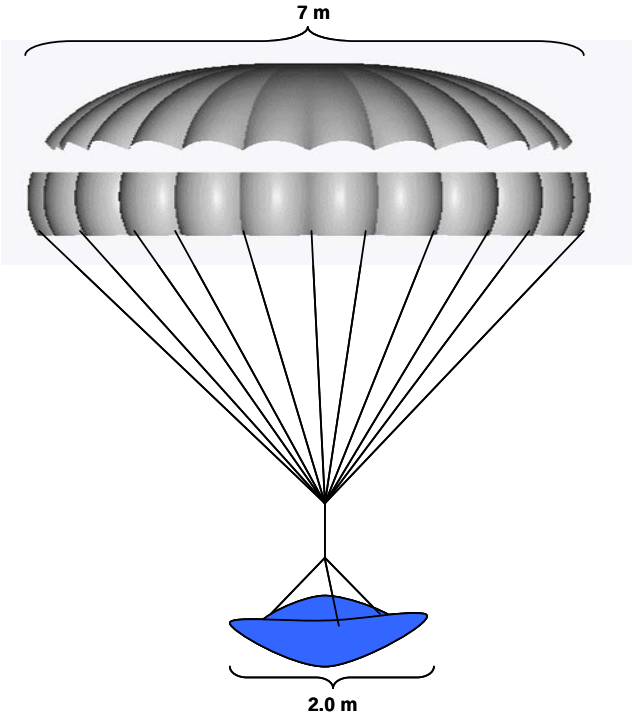

Figure 54 The Main Parachute for the Lander

The characteristics of the parachute are given below:

- Disc-Gap-Band Design
- Diameter 7 m
- Stowed Volume: 0.041 m^3
- Number of Suspension Lines = 56
- Suspension Lines Length = 6.65 m
- Riser Length = 5.75 m
- Dacron Type 52 Polyester Material
- Braided Nylon Suspension Lines.

The diameter of the parachute is driven by the requirement to maximize the difference of drag of the remaining element under the parachute and the aeroshell, after its separation. Over a limited range this merit function is rather flat around the optimum, and therefore the size of the parachute may be somewhat reduced, allowing possibly for faster descent in less time. As the uncertainty of the wind profile is a large contribution to the size of the landing error ellipse, a reduction of the descent time results in a more precise prediction of the landing. A shorter descent time also allows

for longer on surface science measurements, and thereby improving the chemical measurement capability.

Table 26 Lander DLS equipment list.

Element 3	Short-Lived Lander		MASS [kg]			
Unit	Unit Name Click on button above to **insert new unit**	Quantity	Mass per quantity excl. margin	Maturity Level	Margin	Total Mass incl. margin
1	Drogue Canopy	1	0.0320	To be modified	10	0.0
2	Drogue Suspension Lines and Riser	1	0.2969	To be modified	10	0.3
3	Drogue Bridal	1	0.5000	To be modified	10	0.6
4	Drogue Mortar	1	1.0000	To be modified	10	1.1
5	Drogue Deployment Bag	1	0.2755	To be modified	10	0.3
6	Main Canopy	1	1.8803	To be modified	10	2.1
7	Main Suspension Lines and Riser	1	4.1218	To be modified	10	4.5
8	Main Bridal	1	2.0000	To be modified	10	2.2
9	Main Swivel	1	2.0000	To be modified	10	2.2
10	Main Deployment Bag	1	0.9057	To be modified	10	1.0
11	Main Deployment Bag Bridal	1	0.5000	To be modified	10	0.6
-	Click on button below to insert new unit		0.0	To be developed	20	0.0
SUBSYSTEM TOTAL		**11**	**13.5**		**10.0**	**14.9**

8.2.3.3 Dropping Analysis

The main parachute will be cut shortly before touching the surface to avoid it falling on top of the Lander. A preliminary dropping analysis was performed to define the optimum release point. An additional device for altitude measurement of up to 100 m would be required.

Taking into account the gravity on Titan and a vertical descent velocity of 2 m/s before the parachute is cut, the impact velocity and drop times for different drop heights were calculated.

Given that the main parachute diameter for the Lander is 7 m, it would need to be transported by at least 3.5 m so as not to land on the Lander. Presuming that the wind at the surface of Titan is approximately 1 m/s (or less), the time of free-fall would need to be at least 3.5 s, which corresponds to a height of 16 m. These calculations are conservative, as atmospheric drag was not included. The results for a range of free-fall heights are given in Table 27. Under these assumptions the shock acceleration for landing on a hard surface is 70 g, which needs re-evaluation for liquid landing.

The issue of avoiding the parachute landing on the lander module needs to be addressed in more detail during the following study phase.

Table 27 Dropping Analysis. The parameters were calculated equivalent to impact on a hard surface.

Distance	Time to Impace	Impact Velocity	Kineteic Energy	Impact Force	Impact Acceleration	Impact g
(m)	(s)	(m/s)	(J)	(kN)	m/s^2	g
0.00	0.00	2.00	160.00	16.00	200.00	20.39
1.00	0.44	2.59	268.00	26.80	258.84	26.39
2.00	0.79	3.07	376.00	37.60	306.59	31.25
3.00	1.10	3.48	484.00	48.40	347.85	35.46
4.00	1.37	3.85	592.00	59.20	384.71	39.22
5.00	1.62	4.18	700.00	70.00	418.33	42.64
6.00	1.85	4.49	808.00	80.80	449.44	45.81
7.00	2.06	4.79	916.00	91.60	478.54	48.78
8.00	2.27	5.06	1024.00	102.40	505.96	51.58
9.00	2.46	5.32	1132.00	113.20	531.98	54.23
10.00	2.64	5.57	1240.00	124.00	556.78	56.76
11.00	2.82	5.81	1348.00	134.80	580.52	59.18
12.00	2.99	6.03	1456.00	145.60	603.32	61.50
13.00	3.15	6.25	1564.00	156.40	625.30	63.74
14.00	3.31	6.47	1672.00	167.20	646.53	65.91
15.00	3.46	6.67	1780.00	178.00	667.08	68.00
16.00	3.61	6.87	1888.00	188.80	687.02	70.03
17.00	3.75	7.06	1996.00	199.60	706.40	72.01
18.00	3.89	7.25	2104.00	210.40	725.26	73.93
19.00	4.03	7.44	2212.00	221.20	743.64	75.80
20.00	4.16	7.62	2320.00	232.00	761.58	77.63

8.2.3.4 Floating Analysis

A preliminary calculation of the floating capability was performed for landing in the northern methane lakes. The calculations were performed with the baseline design of the Lander, as shown in Figure 50, and with the following assumptions:

- Liquid Methane Density at 90 °K: 450 kg/m^3
- Internal Volume (including upper plate): 0.1783 m^3
- Lander Mass: 79.85 kg
- Lander CoG position from Bottom: 0.176 m.

The minimum volume required for buoyancy in a Titan lake can be found with the following equation:

$$V_{immersed} = \frac{M_{lander}}{\rho_{methane}}$$

Which yields $V_{immersed}$ = 0.18 m^3. Therefore the Lander, as currently designed, would just marginally float. In the following phase design modifications will be required to increase the internal volume.

The static stability of the Lander was also checked. As shown in Figure 55 the Lander is stable (to e.g. surface winds) when the metacentre height (*M*) is positive.

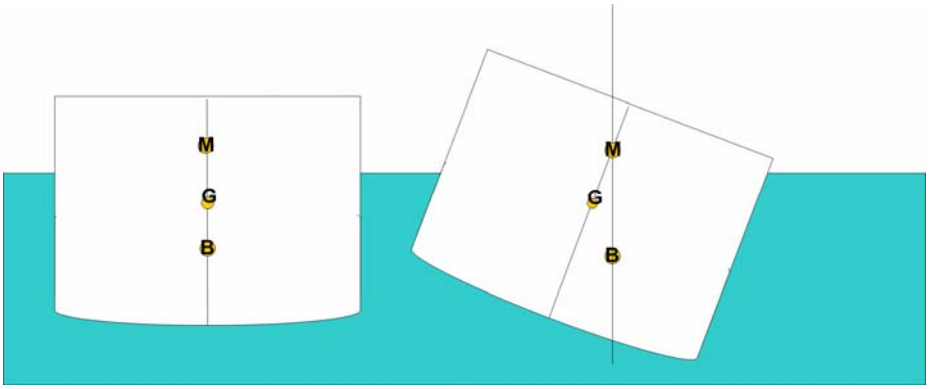

Figure 55 Lander Static Stability Criterion

In this chart *G* represent the centre of gravity (CoG), *B* represents the centre of buoyancy (CoM), and *M* represents the metacentre. The metacentre can be calculated by $M = G - B$.

The distance of the centre of buoyancy from the bottom was determined as 0.14 m. Therefore, the metacentre height is 0.036 m, and positive, although with a small margin.

8.2.4 PROBE TO ORBITER INTERFACE

The interface between the Lander Probe and the orbiter will be a simple spin and eject device, such as was used for Huygens. Additionally the interface will provide for power and data transmission to allow regular checkout of the Lander equipment during the interplanetary cruise, and activation before release. These operations will, however, be infrequent and the probe is expected to be in a hibernation type state for most of the interplanetary transfer phase.

8.2.5 MECHANISMS

The following mechanisms are needed:

- spin and eject for separation from the orbiter
- mortar for release of drogue parachute
- release of TPS (back shield) and main parachute release
- release of TPS (front shield)
- release of the main parachute before landing

For all mechanisms heritage from Hygens is applicable.

The mass of these mechanisms has been taken into account at the various units they are attached to, and is here not specifically reported.

9 OPERATIONAL SCENARIOS OVERVIEW

Science measurements will not be executed by the *in situ* elements during interplanetary and ballistic cruise phases. Both elements have low gain patch antennas attached to their back covers for transmission of critical housekeeping information during entry and early descent.

A Mission Operations Centre (MOC) will be established at ESOC and a Science Operations Centre (SOC) will be established at ESAC. The share of responsibilities between the MOC and the SOC will be addressed during the next phase.

The tasks for the MOC may be

- Trajectory calculation and entry targeting
- Support to regular in-flight check-out
- Monitoring of the Montgolfière performance
- Ground segment support; including arrangements for DtE
- Interface with SKA (if available and if this option is retained)
- Interface with JPL mission operations

The tasks of the SOC may be

- Support to regular in-flight check-outs during cruise
- Science planning (for Montgolfière only)
- Compilation of command request (for Montgolfière only) and transmission to MOC
- Monitoring of the scientific return (for Montgolfière only)
- Science data distribution to PI-teams
- Interface with VLBI observations if implemented
- Science data archiving

9.1.1 MONTGOLFIÈRE

9.1.1.1 Autonomy and Observation Planning

The science instruments of the Montgolfière will be operated according to a pre-planned observing time-line. This time-line will be up-linked through the orbiter s/c acting as commanding relay. The Montgolfière will autonomously sample the atmosphere during descent (by pre-planned switch on of the ASI/MET instrument).

The Montgolfière will have autonomous altitude maintenance through feed-back with a pressure sensor. A vent valve at the zenith of the balloon will be used to release warm gas for buoyancy reduction.

Furthermore the detection of the orbiter beacon and the orientation of the HGA towards the orbiter will also be autonomous.

A watchdog will be installed in the Montgolfière's on-board operations system to monitor the proper operations the mission critical autonomous functions (telemetry, cooling during cruise, etc); additional monitoring of the execution of the science observing plan is desirable, given the frequent long blackout periods of about 2 weeks.

Due to the limited total power available, only limited instrument operations may be possible during telemetry transmission periods. A more detailed analysis will be performed investigating whether the transmission of data could be limited to periods where the orbiter is sufficiently close (cf. Figure 5), thereby allowing a higher data rate at the same level of power consumption and thus effectively reducing the durations used for data transmission. Initial estimates indicate that this flexibility may be possible using the large on-board memory. In any case, periods for data transmission will also be pre-planned, but will need to be regularly updated to account for the actual measured position of the Montgolfière.

During the cruise phase and during the ballistic phase, the Montgolfière Probe will autonomously maintain the surface temperature of the MMRTG by controlling the cooling pumps.

9.1.1.2 Position Determination

By acquisition of the beacon signal orbiter the Montgolfière measures the local azimuth and elevation of the direction to the orbiter. After acquisition the orbiter will be tracked during its pass above the Montgolfière. This provides direction information (azimuth and elevation) for the entire pass. In addition will the orbiter's trajectory be reconstructed using standard radio-science equipment. The position and attitude of the Montgolfière can therefore be reconstructed post facto using these measurements. The accuracy of this reconstruction requires further analysis.

The Lander and Montgolfière trajectories will also be reconstructed post-flight by the combined analysis of relevant science measurements (combined with relevant orbiter remote sensing observations), as was successfully carried out with Huygens, although the Huygens technique would need adaptations for the Montgolfière.

Additionally, when visible from Earth, the position of the Montgolfière may be measured by DtE and VLBI techniques.

There is no identified requirement for real time, or near-real time position determination. The Montgolfière has only to be able to autonomously determine the direction to the orbiter for establishing telemetry contacts, which will be performed by using a beacon signal. For all other purposes the knowledge on the position is only required post-flight.

9.1.2 LANDER PROBE

9.1.2.1 Autonomy and Observation Planning

Due to its limited lifetime the Lander will have a completely pre-programmed execution sequence. The critical descent events will be triggered by measurement devices with adequate backup (see section 8.2.2.6). The science investigations will be entirely pre-planned and will be executed autonomously.

In the current baseline it is assumed that the telemetry system would continuously transmit data in parallel with performing science instrument operations. A sufficiently large on-board memory allows for storage of data for later transmission. A trade-off needs to be made in the next phase of the study, whether the transmission of more science data could delayed until the orbiter is closer, which allows for higher data rates. This would effectively provide more power for the instrumentation at an increased risk of loosing data (e.g. due to failure).

9.1.2.2 Position Determination

The orbiter will follow the Lander during its descent and surface operations. Therefore position information will be available from the direction information from the orbiter's antenna orientation.

As was the case with Huygens, it will also be foreseen that the descent of Lander will be followed with VLBI from Earth. However, the landing site itself will be eclipsed from Earth, and it is anticipated that the signal from the Lander could be followed up to an altitude of about 100 km (about 15 – 30 min after entry).

10 MAJOR OPEN ENGINEERING ISSUES OR TRADES

In the following a brief list and description is given of important open engineering questions that need addressing during the next study phase.

10.1 Open Issues related to the Montgolfière Probe

Aerodynamic heat flux and heat load calculations

- Initial values obtained, based on Huygens derived correlations need to be further consolidated.

Aerodynamic stability during entry:

- The present configuration is the result of a large effort in trying to keep the centre of mass as close to the front shield as possible in order to guarantee the stability during all flight phases. However, a complete verification is pending, and has not been possible within the short time allocated to this study.
- Because of the large dimensions and the interface constraints of the MMRTGs an additional reduction of Probe height (to push the centre of mass further down) appears challenging. A more straightforward solution may be to increase the front shield mass artificially by thickening the ablator. However, this is a net mass increase that needs to be verified with the overall mass allocations.

Planetary protection (see section 12.5 for a discussion of planetary protection issues):

- The design of a robust cage around the MMRTG should be considered for avoiding the warm outside of the MMRTG coming into contact with Titan's surface after the Montgolfière's disposal at the end of the mission.

Deployment phase of the balloon:

- During the deployment of the balloon the following complex steps need to be taken in short time:
  - release of the lock of the MMRTG at the gondola
  - release of the balloon cover, which will be pulled off by the main parachute
  - deployment of the balloon
  - transfer of the MMRTG into the balloon; in order to relieve load on the balloon envelope material lines from the parachute will be attached to the balloon envelope at the same attachment points as the support cables of the MMRTG.
  - filling of the balloon volume by using the air stream of the descent, including the area in between the double envelope; it is important that the intermediate volume is properly filled as this is necessary for the thermal insulation of the inside volume.
  - separation of the main parachute by releasing the lines which are attached to the balloon in support of the MMRTG.

- More work on the definition of these interfaces and on the sequence of events is needed. Obviously demonstration of these mechanisms is planned, including the filling of the intermediate gas volume.
- These issues will be addressed during a Phase A study by CNES.
- Accommodation and deployment of support cables for parachute to balloon and balloon to gondola

Issues related to the late integration of MMRTG:

- Design considerations that take the accessibility of the area around the MMRTG for late integration into account could not be addressed at an adequate level of detail. Initial thoughts were collected and a high level strategy is discussed, but more details need to be defined.
- Tests with a demo model are foreseen.

Thermal considerations of the MMRTG:

- In the Titan environment, the MMRTG will likely be too cold for optimum performance. An additional insulation layer should be wrapped around the MMRTG to keep the inside at higher temperature and thereby closer to its optimum operation point. Note that this additional layer will not have an effect on the heating of the gas, as the same amount of energy will be radiated.
- This additional layer will also be beneficial for keeping the balloon material better insulated from the MMRTG.
- The periods where no cooling can be provided to the MMRTG while in stowed configuration need to be addressed in more detail and a detailed thermal model is needed to evaluate the effects on the rise of temperature in the inside of the Montgolfière Probe. The following phases were identified:
    - Immediately prior to launch, launch, and early orbit
    - After separation of the POIS (which includes the radiator), during entry, and during descent before opening of the balloon.
- The design and accommodation of the heat pipe in the context of the gondola configuration, the MMRTG and the balloon envelope in stowed configuration and its safe separation during the balloon deployment needs additional assessment.
- Detailed design of cooling pipes for MMRTG being robust against freeze-out needs addressing
- The separation of fluid lines prior to separation of the POIS by ensuring no contamination of the entry probe by the cooling fluid (water).

Definition of interfaces: the Montgolfière Probe has the following critical interfaces, which need to be defined early, while at the same time maintaining flexibility to accommodate changes due to ongoing developments:

- Balloon to: gondola, MMRTG, TPS, ELDI system, zenith valve
- MMRTG to: balloon, gondola POIS; electric interface to gondola

Determination of attitude and position

- The strategy and the achievable accuracy of the position determination need to be evaluated in more detail. It appears that all basic means are available, but a more detailed study is required.

10.2 Open Issues related to the Lander Probe

Landing:

- Landing stability at splashdown (landing into a Titan lake) has been only verified at first order and will require dedicated dynamical and structural analyses. Finally, floatation of the Lander (after splashdown) has been found possible but marginal. Therefore, further investigation is recommended.
- The strategy of avoiding the parachute falling on the lander needs revisiting with respect to more detailed simulations on parachute separation and free-fall, or by investigating alternative options.

Trade off of parachute staging:

- Science trade-off between descent time and floating time needs to be performed.
- In the current design it was decided to use only one parachute, which effectively slows down the descent. For this reason Huygens used two parachutes, where the second one was smaller.
- The chosen design has the advantage that more time can be spent for atmospheric sampling, at the cost of more total energy required.
- Alternatively a second parachute could be used, which would save energy during the descent, but the total amount of available energy needs to be reduced to account for the additional mass for an additional mechanism and for the second parachute.

TPS sizing:

- With the updated delivery profile the Lander will be delivered on a later Titan fly-by, which reduces the entry velocity by about a factor of 2. This allows for some mass savings of the TPS. Detailed aerothermodynamic calculations are required to update the heat flux and the total heat load for this entry velocity.
- With the updated numbers of the TPS also the aerodynamic calculations need to be performed for verification of stability.

Optimization of telemetry use and energy consumption profile

- The profile of the available telemetry rate as a function of time has a steep increase towards the end of the operational lifetime. Therefore less energy would be required in case of a delayed transmission of the same amount of data, as opposed to simultaneous transmission.

- The instrument data shall be critically reviewed and it shall be decided which data shall be transmitted before landing and which may be transmitted later, increasing the risk that in case of failure data may be lost.
- This trade-off may lead to a detailed instrument operations plan and a finally to a telemetry plan, which, if optimized, may provide additional power for use by the payload.

11 TECHNOLOGY DEVELOPMENT

In case of selection for further study, a detailed Technical Development Plan (TDP) will be established. A preliminary list of items includes:

- Test and verification of balloon and MMRTG deployment sequence in conjunction with the gondola
- Test and demonstration flights for balloon
- Development of sun sensor/star tracker with sensitivity in IR for operations in cryogenic environment (80 – 90 °K).
- Adaptation of a baro-altimeter for Titan environment
- Qualification of FLASH memory technology for space
- Development of a miniaturized short range (up to 100 m) low resource altimeter for lander
- Demonstration of communications scenario between the orbiter and the Montgolfière, which uses two HGA antennas pointed towards each other, including determination of the achievable pointing accuracy and telemetry rate.

In case of selection of the TSSM mission for further study, CNES has committed in carrying out a Phase A study, which among others will investigate the following issues:

- Assessment of Material (<55 g/m^2) w.r.t.
  - Sufficient rigidity for deployment and filling
  - Compatibility with packaging for about 10 years
  - Compatibility with cold Titan atmosphere (80 – 90 °K)
  - Support of the vent valve
- Balloon design issues requiring further analysis & verification
  - Deployment/insertion of the MMRTG into the balloon and its support within the lower half of the balloon
  - Filling of double wall structure (double wall is needed for insulation)
  - Thermal performance of the double walled balloon by numerical simulations and sub-scale experiments
  - Validation of assumptions on the heating of the gas by the MMRTG during the filling process
  - Packaging of the balloon
- Design of zenith vent valve and verification of its compatibility with operations in Titan's environment
- Assumptions will be validated through demonstration by prototypes

The technology readiness level of instrumentation needs to be brought to level 5 – 6 at the time of AO. It is foreseen that instrument assessment teams will be formed, which shall take the responsibility for adequately preparing possible instruments for being able to respond to an AO for instrumentation with designs at sufficient TRL.

With respect to the payload, the sampling of the liquid (Lander) and of the atmosphere (Montgolfière) may need additional technology developments. This critically depends on the detailed instrument implementation. This, for instance, is one of the items that needs development by the instrument assessment teams.

12 PROGRAMMATICS

12.1 General Issues & Assumptions

It is assumed that the development with heavily rely on the heritage from Huygens, where ever possible, and will additionally benefit from developments from Beagle-2 and those for ExoMars. It has to be noted that several critical elements will not be provided under ESA responsibility, specifically the balloon (provided by CNES) and the MMRTG and RHU's (provided by NASA). The interface, including separation mechanisms, to the NASA-provided orbiter will be managed by ESA.

The accommodation of an RTG (MMRTG) for the Montgolfière Probe, with its conjectured requirements of late integration, poses a specific complexity on the design. Early design considerations and verifications of accessibility during integrations need to be verified with a mock-up. A special launch-pad cooling unit may be required.

The suggested model philosophy followed a hybrid approach between a single PFM and an EM/FM approach. Given the mission complexity the hybrid approach was considered most adequate. The following models would be foreseen:

- Integration model (IM): required for verification of integration of parachutes, balloon, MMRTG, back cover and heat shield
- Structural and Thermal Model (STM): to be used for structural and thermal model verification
- Avionics Text Bench (ATB): test and verification of control functions for entry and descent.
- Drop Test Qualification Model: considered for tests of aerodynamic verification; for the Montgolfière Probe several tests for demonstration of balloon deployment are foreseen.
- Engineering Qualification Model (EQM): this model may be constructed from the drop test QM and from the ATB. In addition to its use for qualification, it may be kept at ESOC for serving as test bench.
- Proto Flight Model (PFM): will include both FM equipment having passed acceptance testing, and PFM equipment having passed qualification testing.

12.2 Contributions and Responsibilities

ESA will provide and contribute the following items to the TSSM mission:

- provision of the overall system
- overall management of the *in situ* elements
- all remaining items and integration that are not contributed from other sources (see below)
- the interface structure and separation mechanism to the NASA orbiter s/c
- joint management of the interface between the ISE's and the NASA orbiter s/c

The contribution from NASA will include

- MMRTG: NASA will provide and integrate the MMRTG; in order to facilitate the necessary preparations and verifications NASA will provide a full scale mechanical and electrical simulation model of the MMRTG in support of the ESA development.
- mechanical support structure for integration of the ISE's including their separation mechanisms
- communications support to and from the ISE's; during the interplanetary cruise phase and during the science phase when telemetry and telecommands will use the NASA orbiter as relay link.
- joint management of the interface between the ISE's and the NASA orbiter s/c

The balloon and material, its container, the vent valve, and internal structural support for keeping the MMRTG inside the balloon will be provided by CNES.

Instrumentation and possibly related technology developments will be conducted under responsibility of national funding agencies. This also includes a possible exchange of instrumentation between the NASA and ESA member states, when instruments being contributed by one partner may be integrated on a mission element of the other.

12.3 Management Approach

The planned organization of the ESA study team is shown in Figure 56. Interfaces to the science community and to the NASA science and engineering teams are also indicated.

The following functions and responsibilities will be assigned by ESA for the following study:

- ESA Study Scientist (SS):
  - Responsible for all science aspects related to the study needs
  - Interface with the Joint Study Science Team
  - Contributes to the mission definition during iteration phases
  - Acts as co-chair of the Joint Study Science Team
  - Specification of the science requirements and science management aspects
  - Definition of the science operations

- ESA Study Manager (SM):
  - Overall study management, including schedule and resources management

- Acts as satellite system engineer, with the support of the payload manager, the study scientist and experts
- Responsible for all programmatic aspects
- Ensures consistency between technology developments and mission needs
- Acts as the technical officer for the industrial assessment studies; in this function the industrial teams report to the SM and will be guided by the SM.
- Acts as the prime contact point for the interface with the NASA/JPL technical teams on technical matters

- ESA Study Payload Manager (SPM):
  - Acts as payload system engineer, with the support of experts
  - Responsible for payload interfaces, support the study manager for payload related technology developments
  - Follows payload assessment activities, including technology developments
  - Collection of payload specifications from the payload teams

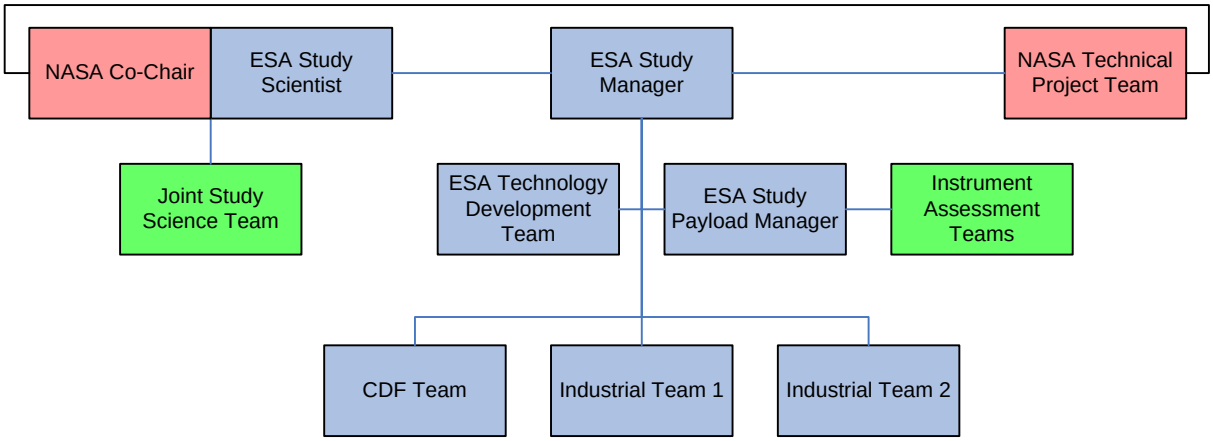

Figure 56 Planned organization of the ESA study team for the future studies.

Additionally technical support will be arranged as needed from ESA Technical and from the Operations Directorates.

The Study Manager will invite members of the Science Team and of NASA technical teams related to the TSSM study to participate during critical milestones and review meetings with the purpose of ensuring transparency for the benefit of interface related issues and for the common science goals of the mission.

12.4 Interface Management

The following interfaces were identified:

- ESA-NASA: the ESA *in situ* elements will be attached to the NASA provided orbiter. The orbiter will act as a telemetry relay during the inter-planetary cruise phase as well as during the science observation phase. While being attached the Lander Probe will additionally be provided with power.

- Payload instruments: Instruments will be provided by the science community following an AO and selection procedure.
- Gondola to balloon: the balloon structure, containers including other peripheral hardware and the support of the MMRTG will be provided by CNES.

These three interfaces will be controlled with ICD's. A draft of the ESA-NASA ICD is available already. This needs to be continuously maintained as more details are becoming available during the next study phases. In addition to the documentation of the interfaces, interface simulators will be defined and exchanged for verification of critical items during the development. One such item where the exchange of hardware simulation will be required is the verification of the telemetry and telecommand interface. This will be achieved by exchange of simulators.

The interface to the payload instruments will be developed starting with the AO for the payload instrument assessment. The assessment will be followed by the ESA Study Payload Manager, which allows for feed-back to the ongoing system study.

The definition of the interface to the balloon will be addressed in the next phase of the study. Deployment considerations as well as considerations of stability/rigidity between gondola and balloon shall be considered, which may need some detailed simulation. Demonstration of the deployment is foreseen.

12.5 Planetary Protection

Titan is currently classified as category II target, which implies no specific requirements or limitations on the implementation of the mission. Relatively simple documentation of the mission and possible impact site is required. Based on the results of the Cassini/Huygens mission, however there is ongoing discussion about a possible re-classification as category III for orbiter and category IV for *in situ* elements. Category IV includes avoidance of contamination with a probability of less than 10^{-4}.

During the current assessment, due to the limited amount of time, the emphasis was put on the study of a possible technical implementation, and its feasibility. Therefore the implications arising from planetary protection requirements on the technical design could not be addressed in detail. Nevertheless, mitigation options were discussed by the Jovian and Saturninan Planetary Protection Working Group ([RD6]). It is argued that a Mars "Special Regions" approach may be adopted, which involves demonstrating that there is no possibility of replication of a viable cell on Titan, and that therefore the planetary protection requirement can be met. The basis of the Mars "Special Regions" approach [Beaty, D.W. et al.: "Findings of the Special Regions Science Analysis Group", Astrobiology (2006)] is to rely on physical parameters that preclude replication of terrestrial life that persist for protracted periods (>1000 years). Key for Titan is its low temperature, being ~96°K on average with only a few degrees geographic and seasonal variation, which is well below 248°K being required for replication of terrestrial life.

From first principles (low surface temperature), it was argued that the probability of contamination of a potentially sensitive area (e.g. heated by a cryovolcanism of meteorite impact) is well below 10^{-4}, due to their low density on the surface.

The MMRTG of the Montgolfière and RHU's of both the Montgolfière and the Lander are the only sources of heat of the ISE's. Long duration heating of the surface by the MMRTG (<2 kW at EOM; half-life 88 yr) can be avoided by ensuring that no contact is made with the surface, after disposal at end of mission. This could relatively trivially be implemented by a non-thermal conductive cage around the MMRTG. The warm surface of the MMRTG would then be cooled by ambient air, and no significant rise in temperature around the site of disposal could occur.

Considerations with respect to the RHU's are similar as for Huygens: it is assumed that after the switch-off of the vehicles, they would quickly cool down to ambient, and would therefore not pose a risk of contamination.

Furthermore a preliminary analysis on risk of local heating due to an unforeseen event (e.g. a failure causing a crash onto the surface) was performed [RD6]. With conservative assumptions, it was demonstrated that no contamination of a liquid water body could occur above the anticipated 10^{-4} probability requirement.

In conclusion, planetary protection measures appear relatively straightforward, and may not involve complex prevention measures. A further refinement of the model on contamination of a liquid area by impact (as described in [RD6]) and generations of datasets from Cassini in support of this analysis is required, but will unlikely yield a more stringent requirement on the system. Sterilization or other measures of similar complexity will in all likelihood not be required.

Planetary protection issues will be included in the following industrial study phase. As a conservative estimate, in case of re-classification of Titan as a target, a preliminary schedule impact for the procurement of FM units and system integration time of +20%, and of additional system test time of +10% was estimated. This was also included as a potential cost increase.

12.6 Schedule

A preliminary implementation schedule is provided in Figure 57, which includes the decision making process as outlined by the ESA Cosmic Vision 2015-25 program, but which may need revision. The preliminary schedule shows compatibility with a launch in 2020.

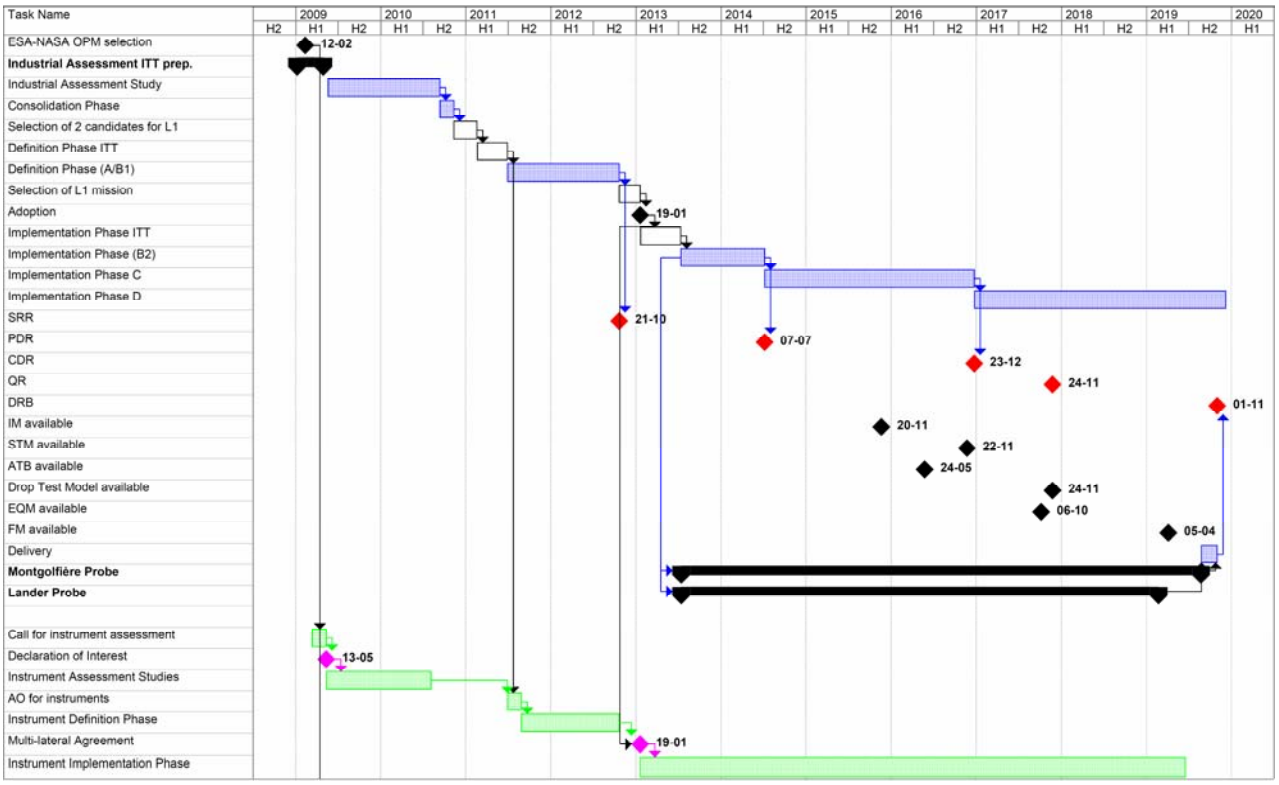

Figure 57 Preliminary high level implementation schedule

12.7 Estimated Mission Cost

The *Cosmic Vision 2015–25* call for mission ideas allocated 650 M€ for the cost to ESA for an L-class mission proposal. Preliminary cost estimates confirmed that this limit will not be exceeded provided the following assumptions are correct:

- The balloon technology development and balloon material for flight will be provided by CNES without additional ESA contribution.
- The NASA provided orbiter will carry and release the ESA *in situ* elements.
- The MMRTG and all RHU's will be provided by NASA at no cost to ESA.

Additional margin was taken into account to provide for an expected cost increase, if more stringent planetary protection requirements arise, in case Titan is elevated to category IV.

13 REFERENCE DOCUMENTATION

[RD1] TandEM CDF Study Report, Study of Saturn Moon Titan With Montgolfière Balloon and Lander, CDF-78(A), October 2008
[RD2] TandEM Cosmic Vision proposal, "TandEM Titan and Enceladus Mission", 29 June 2007
[RD3] "Titan Explorer Mission Concept Study" final report, NASA, October 2008
[RD4] TSSM Titan Atmospheric Environment Working Group report, (draft), September 2008
[RD5] TSSM Titan Surface Working Group report, SRE-PA/2008.0047/CE/RJ, 7 July 2008
[RD6] Report of the Jovian and Saturnian Planetary Protection Working Group, (draft), November 2008
[RD7] "Titan Explorer Mission Concept Study" final report, NASA, January 2008
[RD8] "Titan Saturn System Mission (TSSM) Science Requirement Document (Sci-RD)"
[RD9] "Reference Payload Definition Document for the TandEM Assessment Study," SCI-PA/2008.028/CE
[RD10] Huygens separation mechanisms, Dr.Udo, R. Herlach, P.Tatlias, B. Schmid, D. Musset, Oerlikon Contraves AG Space, Zuerich Switzerland
[RD11] COSPAR Planetary Protection Policy, 20 October 2002; Amended 24 March 2005
[RD12] Huygens aerodynamics Databases HUY.ASPI.HIT.TN.0006
[RD13] Nelson, H. F., Park, C., and Whiting, E. E., "Titan Atmospheric Composition by Hypervelocity Shock-Layer Analysis," Journal of Thermophysics and Heat Transfer, Vol. 5, No. 2, April–June 1991, pp. 157–165
[RD14] Cassini Titan Probe Phase A2. Aerodynamic and Aerothermodynamic Assessment CR 57/88
[RD15] Engineering Models for Titan's Atmosphere R. V. Yelle, D. F. Strobell, E. Lellouch and D Gautier, 1994.

14 ACRONYMS

ADPMS	Advanced Data and Power Management System
ASIC	Application-Specific Integrated Circuit
BOL	Beginning of Life
CDMU	Command & Data Management Unit
CoG	Centre of Gravity
CoM	Centre of Mass
DHS	Data Handling System
DtE	Direct to Earth
EDIS	Entry Descent and Inflation Subsystem
EDL	Entry Descent and Landing
EDLS	Entry Descent and Landing Subsystem
EOL	End of Life
ESA	European Space Agency
ESAC	European Space Astronomy Centre
ESOC	European Space Operations Centre
ESTEC	European Space Research and Technology Centre (ESTEC)

FPA	Flight Path Angle
FPGA	Field-Programmable Gate Array
GA	Gravity Assist
GNC	Guidance and Navigation Control
HGA	High Gain Antenna
HICDS	Highly Integrated Control and Data System
I/F	InterFace
IR	Infra-Red
ISE	*In Situ* Element
JSDT	Joint Titan-Saturn Science Definition Team
LCL	Latching Current Limiter
LGA	Low Gain Antenna
LOS	Line Of Sight
MMRTG	Multi-Mission Radioisotope Thermoelectric Generator
PCDU	Power Conditioning and Distribution Unit
POIS	Probe to Orbiter Interface Subsystem
RHU	Radioisotope Heater Unit
SCOC3	Spacecraft Controller On-a Chip with LEON3
SDRAM	Synchronous Dynamic Random Access Memory
S^3R	Sequential Switching Shunt Regulator
SEP	Solar Electric Propulsion
SOC	Science Operations Centre
SOI	Saturn Orbit Injection
TOI	Titan Orbit Injection
TPS	Thermal Protection System
TRL	Technology Readiness Level
TWTA	Travelling Wave Tube Amplifiers
VLBI	Very Large Baseline Interferometry

APPENDIX A SCIENCE TRACEABILITY MATRICES

Table A-1 Science traceability matrix: montgolfière

MISSION GOALS	SCIENCE OBJECTIVES	SCIENCE INVESTIGATIONS	REQUIRED MEASUREMENTS/ DETERMINATION	PLANNING MEASUREMENT APPROACH	PLAN. INSTR.	DATA PRODUCTS	MISSION REQUIREMENTS
Goal A: How does Titan function as a system; to what extent are there similarities and differences with Earth and other solar system bodies?	O2: Characterize the relative importance of exogenic and endogenic oxygen sources.	I1: Quantify the flux of exospheric oxygen into the atmosphere.	M3: O content of the aerosols	A1: *In situ* analysis of the aerosols collected at the level of the montgolfière	TMCA	Mass spectra over the mass range 10–600 Daltons	Collect aerosols that are falling from higher altitudes; 1 km and 5° attitude knowledge of montgolfière.
			M4: Amount of O bearing molecules in the troposphere	A1: Infrared spectra of the atmosphere, including CO and CO_2	BIS	Near-IR atmosphere vertical profiles between 1 and 5.6 µm with a spectral sampling of 10.5 nm	Adapt the observation strategy to the motion of the montgolfière. Coordination with VISTA-B for context is required.
		I2: Quantify the flux of endogenic oxygen from the surface and interior.	M1: Inventory of surface constituents containing oxygen, including major isotopologues at 250 m or better resolution	A2: Infrared spectral maps of the surface at wavelengths absorbed by the O bearing molecules (4.92 µm for CO_2) at 10% level within a pixel	BIS	Near-IR atmosphere vertical profiles between 1 and 5.6 µm with a spectral sampling of 10.5 nm	Adapt the observation strategy to the motion of the montgolfière. Coordination with VISTA-B for context is required.
	O3: Characterize the major processes controlling the global distribution of atmospheric chemical constituents.	I1: Characterize the major chemical cycles.	M1: Vertical, latitudinal, and temporal dependence of condensed and gaseous species in the atmosphere from 0 to 1500 km with precision better than 10%	A5: Pump the atmosphere into the chemical analyzer to analyze ethane mole fraction and other volatile species in troposphere (gas and condensed phase), with a precision of 5%	TMCA	Mass spectra over the mass range 10–600 Daltons.	Tracking of the montgolfière (lat, long, alt); 1 km and 5°attitude knowledge required.
		I2: Determine the relative importance of global transport.	M3: Ethane mole fraction in the troposphere (gas and condensed phases) at different longitudes (day/night variations); ethane/methane	A1: Pump the atmosphere into the chemical analyzer to analyze ethane mole fraction in troposphere (gas and condensed phase), with a precision of 5%	TMCA	Mass spectra over the mass range 10–100 Daltons.	Tracking of the montgolfière (lat, long, alt); 1 km and 5° attitude knowledge of montgolfière
	O4: Characterize the atmospheric circulation and flow of energy.	I1: Determine the atmospheric thermal and dynamical state.	M5: Track the drift of the montgolfière to infer strength and directions of winds.	A1: The location of the montgolfière relative to Titan by tri-axial accelerometers and gyroscopes (inertial platform) to infer wind field	ASI/ MET	Trajectory and attitude reconstruction, wind field and gusts	ASI should be placed as close as possible to the center of gravity of the gondola. 1 km and 5° attitude knowledge of montgolfière.

KEY: O1…O4 = Objective 1…Objective 4; I1…I4 = Investigation 1 …Investigation 4; A1…A4 = Approach 1…Approach 4; M1…M4 = Measurement 1…Measurement 4

Table A-1 Science traceability matrix: montgolfière (continued)

MISSION GOALS	SCIENCE OBJECTIVES	SCIENCE INVESTIGATIONS	REQUIRED MEASUREMENTS/ DETERMINATION	PLANNING MEASUREMENT APPROACH	PLAN. INSTR.	DATA PRODUCTS	MISSION REQUIREMENTS
				and gusts.			
Goal A: How does Titan function as a system; to what extent are there similarities and differences with Earth and other solar system bodies?	O4: Characterize the atmospheric circulation and flow of energy.	I1: Determine the atmospheric thermal and dynamical state.	M6: Measure deposition of sunlight as a function of altitude to infer the radiation balance in the troposphere.	A1: Solar light arriving at the altitude of the montgolfière during its journey in the tropical regions	BIS	Near-IR atmosphere vertical profiles between 1 and 5.6 µm with a spectral sampling of 10.5 nm	Adapt the observation strategy to the motion of the montgolfière. Coordination with VISTA-B for context is required. 1 km and 5° attitude knowledge of montgolfière.
			M7: Vertical profile of temperature, pressure, and density (T and P accuracy to 0.1 K and 1 mPa and resolution to 0.02 K and 0.1% respectively). Determine the trajectory of the montgolfière during entry and descent and floating phase	A1: Measure T by a Pt wire resistance thermometer and P by Kiel probe and capacitive gauges. Pressure and temperature measurements during the descent. Monitor meteorological conditions during the montgolfière journey	ASI/ MET	Direct T and P measurements as a function of time and inferred wind field along the probe track	ASI pressure inlet and thermometers should have access to the atmospheric unperturbed flow (outside the descent probe boundary layer). The trajectory of the probe (entry and descent module reconstructed from the engineering sensor data (e.g., IMU), the high sensitive scientific accelerometer (and/or IMU). Coordination with orbiter RSA data.
				A2: Three-axis *in situ* accelerometer measurements to a precision of 10^{-5} m/s^2 during entry and during the montgolfière journey	ASI/ MET	Vertical mass density profile and inferred pressure and Temperature vertical profile starting from altitude >1600 km down to 160 km Plots of the trajectory and attitude of the probe during entry, descent and floating phase	ASI-ACC should be placed as close as possible to the entry module CoG. ASI operating before nominal interface entry altitude (1270 km). Coordination with orbiter RSA data.
			M8: Pressure, temperature variations in space and time (T and P accuracy to 0.1 K and 1 mPa and resolution to 0.02 K and 0.1% respectively)	A1: Pressure, temperature, and accelerometry during the journey of the montgolfière	ASI/ MET	Direct T and P measurements as a function of time and inferred wind field along the probe track	1 km and 5° attitude knowledge of montgolfière.
			M9: Determine large surface temperature	A1: Infrared spectra of the surface between 5 and 5.6 µm will enable us to see T variations larger than 50 K.	BIS	Infrared maps of the surface between 1 and 5.6 µm with a spectral sampling of 10.5 nm.	Adapt the observation strategy to the motion of the montgolfière. Coordination with VISTA-B for context is required.

KEY: O1…O4 = Objective 1…Objective 4; I1…I4 = Investigation 1 …Investigation 4; A1…A4 = Approach 1…Approach 4; M1…M4 = Measurement 1…Measurement 4

Table A-1 Science traceability matrix: montgolfière (continued)

MISSION GOALS	SCIENCE OBJECTIVES	SCIENCE INVESTIGATIONS	REQUIRED MEASUREMENTS/ DETERMINATION	PLANNING MEASUREMENT APPROACH	PLAN. INSTR.	DATA PRODUCTS	MISSION REQUIREMENTS
Goal A: How does Titan function as a system; to what extent are there similarities and differences with Earth and other solar system bodies?	O4: Characterize the atmospheric circulation and flow of energy.	I1: Determine the atmospheric thermal and dynamical state.	M10: Timing (local time, orbital phase) of cloud occurrence, evolution, cloud base/top and appearance	A1: Continuous monitoring of cloud formation	VISTA-B	1360 x 1024 multi-spectral images 48°FOV	1 km and 5° attitude knowledge of montgolfière required.
				A2: Continuous monitoring of meteorological conditions	ASI/ MET	Direct T and P measurements and inferred wind field along the probe track	1 km and 5° attitude knowledge of montgolfière
		I2: Determine the impact of haze and clouds.	M4: Track the motion of clouds (and cryovolcanic vents, if any). Search for orographic clouds.	A1: Imaging from the gondola at 10 m resolution	VISTA-B	1360 x 1024 multi-spectral images 48°FOV	1 km and 5° attitude knowledge of montgolfière
				A2: Infrared spectral maps of the clouds and terrain	BIS	Infrared maps of the surface between 1 and 5.6 µm with a spectral sampling of 10.5 nm.	Adapt the observation strategy to the motion of the montgolfière. Coordination with VISTA-B for context is required.
			M5: Particle size distribution and optical properties of clouds and haze	A1: Infrared measurements of reflective light	BIS	Infrared maps between 1 and 5.6 µm with a spectral sampling of 10.5 nm.	Adapt the observation strategy to the motion of the montgolfière. Coordination with VISTA-B for context is required.
			M6: Profile of methane mole fraction and its variations in the equatorial regions; fraction of methane in the condensed phase compared to the total atmospheric methane abundance	A1: Infrared spectral maps to measure the width of the methane absorption bands to determine the amount of methane	BIS	Infrared spectra between 1 and 5.6 µm with a spectral sampling of 10.5 nm.	Adapt the observation strategy to the motion of the montgolfière. Coordination with VISTA-B for context is required.
				A2: Pump the atmosphere into the chemical analyzer to analyze methane mole fraction in troposphere (gas and condensed phase), with a precision of 1%	TMCA	Mass spectra over the mass range 12–20 Daltons	Tracking of the montgolfière (lat, long, alt); 1 km and 5° attitude knowledge required.
				A3: *In situ* monitoring of T and P conditions. Simultaneous measurements of pressure and T are necessary to assess the phase of the species (e.g., conden-sation) and to associate a certain pressure level in the atmosphere (or equivalent altitude level) to the mole fractions	ASI/ MET	T and P time series	1 km and 5° attitude knowledge of montgolfière

KEY: O1…O4 = Objective 1…Objective 4; I1…I4 = Investigation 1 …Investigation 4; A1…A4 = Approach 1…Approach 4; M1…M4 = Measurement 1…Measurement 4

Table A-1 Science traceability matrix: montgolfière (continued)

MISSION GOALS	SCIENCE OBJECTIVES	SCIENCE INVESTIGATIONS	REQUIRED MEASUREMENTS/ DETERMINATION	PLANNING MEASUREMENT APPROACH	PLAN. INSTR.	DATA PRODUCTS	MISSION REQUIREMENTS
				determined by TMCA.			
Goal A: How does Titan function as a system; to what extent are there similarities and differences with Earth and other solar system bodies?	O4: Characterize the atmospheric circulation and flow of energy.	I3: Determine the effects of atmospheric composition.	M3: Profile of ethane mole fraction and its variations in the equatorial regions; fraction of ethane in the condensed phase compared to the total atmospheric ethane abundance	A1: Infrared spectral maps to measure the width of the ethane absorption bands to determine the amount of ethane	BIS	Near-IR image spectra between 1 and 5.6 μm with a spectral sampling of 10.5 nm.	Adapt the observation strategy to the motion of the montgolfière. Coordination with VISTA-B for context is required.
				A2: Pump the atmosphere into the chemical analyzer to analyze ethane mole fraction in troposphere (gas and condensed phase), with a precision of 1%	TMCA	Mass spectra over the mass range 20–30 Daltons	Tracking of the montgolfière (lat, long, alt); 1 km and 5° attitude knowledge required.
				A3: *In situ* monitoring of T and P conditions Simultaneous measurements of pressure and T are necessary to assess the phase of the species (e.g., condensation) and to associate a certain pressure level in the atmosphere (or equivalent altitude level) to the mole fractions determined by TMCA.	ASI/ MET	T and P time series	1 km and 5° attitude knowledge of montgolfière.
			M4: Determine the topography and find correlation with clouds and turbulences.	A1: Topography and clouds are determined by the stereo imaging	VISTA-B	1360 x 1024 stereo images 48°FOV; 3D digital terrain and cloud models; cloud albedo time series	1 km and 5° attitude knowledge of montgolfière
				A2: Topography is determined by first echo of the radar sounder	TRS	Time series of the first return radar echoes	Precise identification of the trajectory of the montgolfière increases the quality of the measurements; 1 km and 5° attitude knowledge required.
				A3: Infrared spectrometry to monitor the clouds	BIS	Infrared spectra between 1 and 5.6 μm with a spectral sampling of 10.5 nm.	Adapt the observation strategy to the motion of the montgolfière. Coordination with VISTA-B for context

KEY: O1…O4 = Objective 1…Objective 4; I1…I4 = Investigation 1 …Investigation 4; A1…A4 = Approach 1…Approach 4; M1…M4 = Measurement 1…Measurement 4

Table A-1 Science traceability matrix: montgolfière (continued)

MISSION GOALS	SCIENCE OBJECTIVES	SCIENCE INVESTIGATIONS	REQUIRED MEASUREMENTS/ DETERMINATION	PLANNING MEASUREMENT APPROACH	PLAN. INSTR.	DATA PRODUCTS	MISSION REQUIREMENTS
Goal A: How does Titan function as a system; to what extent are there similarities and differences with Earth and other solar system bodies?	O4: Characterize the atmospheric circulation and flow of energy.	I3: Determine the effects of atmospheric composition.	M4: Determine the topography and find correlation with clouds and turbulences.	A4: *In situ* monitoring of meteorological conditions (T, P, and wind) to investigate thermal variations, turbulence and dynamics (e.g., gravity waves and tides)	ASI/ MET	T and P plots as a function of time	1 km and 5° attitude knowledge of montgolfière.
		I4: Determine the effects of surface processes on meteorology.	M4: Identify active volcanism in the equatorial region with 50 m resolution from orbit and .2.5 m resolution from 10km altitude	A1: Infrared spectral maps	BIS	Infrared maps of the surface between 1 and 5.6 µm with a spectral sampling of 10.5 nm.	Adapt the observation strategy to the motion of the montgolfière. Coordination with VISTA-B for context
				A2: Stereo and high-res imaging from the Gondola	VISTA-B	Digital images and surface albedo time series	1 km and 5° attitude knowledge requirement of montgolfière
			M6: Search for possible surface methane sources (vents, etc.) in the equatorial regions.	A1: Stereo and high-res imaging from the Gondola	VISTA-B	Digital images and surface albedo time series	1 km and 5° attitude knowledge of montgolfière
				A2: Monitor atmospheric methane concentration.	TMCA	Mass spectra Mass spectra over the mass range 12–20 Daltons, with a precision of 1%	Precise location of montgolfière to 1 km and 5° attitude knowledge.
				A3: *In situ* monitoring of meteorological conditions by direct T and P measurements (T and P accuracy to 0.1 K and 1 mPa and resolution to 0.02 K and 0.1% respectively) and gondola attitude	ASI/ MET	T and P time series plots and inferred wind field along montgolfière track	Precise location of montgolfière to 1 km and 5° attitude knowledge.
				A4: Infrared spectral maps to measure the width of the methane absorption bands to determine the amount of methane	BIS	Infrared maps of the surface between 1 and 5.6 µm with a spectral sampling of 10.5 nm.	Adapt the observation strategy to the motion of the montgolfière. Coordination with VISTA-B for context
			M7: Global distribution of surface wind directions	A1: Direction of dunes/cloud movement	VISTA-B	1360 x 1024 stereo images 48°FOV; high resl'n 1 x 1024 line scans 7° FOV	Precise location of montgolfière to 1 km and 5° attitude knowledge .

KEY: O1…O4 = Objective 1…Objective 4; I1…I4 = Investigation 1 …Investigation 4; A1…A4 = Approach 1…Approach 4; M1…M4 = Measurement 1…Measurement 4

Table A-1 Science traceability matrix: montgolfière (continued)

MISSION GOALS	SCIENCE OBJECTIVES	SCIENCE INVESTIGATIONS	REQUIRED MEASUREMENTS/ DETERMINATION	PLANNING MEASUREMENT APPROACH	PLAN. INSTR.	DATA PRODUCTS	MISSION REQUIREMENTS
Goal A: How does Titan function as a system; to what extent are there similarities and differences with Earth and other solar system bodies?	O4: Characterize the atmospheric circulation and flow of energy.	I5: Determine the exchange of momentum, energy and matter between the surface and atmosphere and characterize the planetary boundary layer.	M7: Global distribution of surface wind directions	A2: Wind field inferred from T and P measurements (T and P accuracy to 0.1 K and 1 mPa and resolution to 0.02 K and 0.1% respectively) and monitoring the gondola attitude	ASI/ MET	Wind field along the montgolfière track and eventual wind gusts	Wind field inferred from T and P measurements and monitoring the gondola attitude; 1 km and 5° attitude knowledge requirement of montgolfière
			M6: Global distribution of surface roughness and topography	A1: Radar measurements	TRS	Time series of the amplitude of return radar echoes.	Precise location of montgolfière—1 km and 5° attitude knowledge required.
				A2: Stereo imaging (10 m/pix)	VISTA-B	1360 x 1024 stereo images 48°FOV; high res 1 x 1024 line scans; 3D dune structure	Precise location of montgolfière—1 km and 5° attitude knowledge required.
				A3: Measure the shadows of reliefs within the infrared maps	BIS	Infrared maps of the surface between 1 and 5.6 μm with a spectral sampling of 10.5 nm.	Adapt the observation strategy to the motion of the montgolfière. Coordination with VISTA-B for context is required.
			M7: Diurnal temperature variations and time-series meteorology	A1: Measure the temperature by a Pt wire resistance thermometer with $\Delta T = 0.1$ K	ASI/ MET	T and P plots as a function of time	Same as ASI/MET above
			M8: Distribution of condensates at the surface	A1: Infrared identification of condensate species	BIS	Infrared maps of the surface between 1 and 5.6 μm with a spectral sampling of 10.5 nm.	Adapt the observation strategy to the motion of the montgolfière. Coordination with VISTA-B for context is required.
				A2: High spatial resolution color images of the surface at equatorial latitudes; ground truth for orbiter measurement	VISTA-B	1360 x 1024 multispectral images 48°FOV Color images and albedo time series	Precise location of montgolfière to 1 km and 5° attitude knowledge of montgolfière
			M9: Abundance of water ice at the surface	A1: Infrared mapping through the methane windows and compare windows where ice absorbs (e.g., 1.6 and 2.0 μm) and where it does not (1.05 μm).	BIS	Infrared maps of the surface between 1 and 5.6 μm with a spectral sampling of 10.5 nm.	Adapt the observation strategy to the motion of the montgolfière. Coordination with VISTA-B for context is required.

KEY: O1…O4 = Objective 1…Objective 4; I1…I4 = Investigation 1 …Investigation 4; A1…A4 = Approach 1…Approach 4; M1…M4 = Measurement 1…Measurement 4

Table A-1 Science traceability matrix: montgolfière (continued)

MISSION GOALS	SCIENCE OBJECTIVES	SCIENCE INVESTIGATIONS	REQUIRED MEASUREMENTS/ DETERMINATION	PLANNING MEASUREMENT APPROACH	PLAN. INSTR.	DATA PRODUCTS	MISSION REQUIREMENTS
Goal A: How does Titan function as a system; to what extent are there similarities and differences with Earth and other solar system bodies?	O4: Characterize the atmospheric circulation and flow of energy.	I6: Determine the connection between weather, ionosphere, and electricity.	M2: Global electric circuit and fair-weather electric field in the range from 0–10 kHz. With a height resolution of 1 km	A1: Measurement of electric field using dipole antennas; vertical and horizontal electric field in the frequency range from DC to VLF (~10 kHz)	TEEP-B	Time series spectra of electric field	1 km and 5° attitude knowledge of montgolfière
			M3: Extra low and low frequency (ELF-VLF) magnetic components of the atmospheric electricity from 0–10 kHz	A1: Measurement of magnetic field using loop antenna; vertical and horizontal electric field in the frequency range from DC to VLF (~10 kHz nas or search coils)	TEEP-B	Time series magnetic field spectra	1 km and 5° attitude knowledge of montgolfière
			M4: Search for electric discharges.	A1: Long exposure nighttime imaging	VISTA-B	1360 x 1024 images 48°FOV Flash saturated images	Precise location of montgolfière from Inertial Navigation System (INS); 1 km requirement
				A2: Electric field and optical sensors	TEEP-B	Time series electric field spectra	Coordinated with VISTA-B
			M5: Electrical conductivity and permittivity of the atmosphere (positive and negative ions + electrons) to 1 km resolution in the range 10^{-14} to 10^{-6} Sm^{-1} and electrons only, with a height resolution to 100 m in the range 10^{-11} to 10^{-6} Sm^{-1}	A1: Relaxation probe to measure the conductivity of all charged species	TEEP-B	Time series of conductivity (all charged species)	Time series of conductivity (all charged species)
				A2: Mutual impedance probe which measures the conductivity of electronics only	TEEP-B	Amplitude and phase of electric signal	Amplitude and phase of electric signal
	O5: Characterize the amount of liquid on the Titan surface today.	I3: Determine surface composition that might reveal the presence of liquids.	M1: Optical maps in the methane windows at 2.5 m resolution	A1: Use the infrared images at different incidence angles to determine the nature of the surface (liquid or solid)	BIS	Infrared maps of the surface between 1 and 5.6 µm with a spectral sampling of 10.5 nm.	Adapt the observation strategy to the motion of the montgolfière. Coordination with VISTA-B for context is required.
			M2: Precipitation rate, solid or liquid nature of precipitation	A1: *In situ* monitoring of T and P conditions with reference to the altitude level	ASI/ MET	T and P time series	1 km and 5° attitude knowledge of montgolfière
				A3: *In situ* observations at	VISTA-	1360 x1024 multispectral	Precise location of montgolfière

KEY: O1…O4 = Objective 1…Objective 4; I1…I4 = Investigation 1 …Investigation 4; A1…A4 = Approach 1…Approach 4; M1…M4 = Measurement 1…Measurement 4

Table A-1 Science traceability matrix: montgolfière (continued)

MISSION GOALS	SCIENCE OBJECTIVES	SCIENCE INVESTIGATIONS	REQUIRED MEASUREMENTS/ DETERMINATION	PLANNING MEASUREMENT APPROACH	PLAN. INSTR.	DATA PRODUCTS	MISSION REQUIREMENTS
				all wavelengths.	B	images 48°FOV	to 1 km and 5° attitude knowledge of montgolfière
Goal A: How does Titan function as a system; to what extent are there similarities and differences with Earth and other solar system bodies?	O5: Characterize the amount of liquid on the Titan surface today.	I4: Determine the nature of precipitation responsible for the formation of valley networks in the tropical regions.	M1: Lateral variations of surface compounds in the valley networks at 5 m resolution	A1: Map lateral variations of surface composition in the river networks and at their mouth	BIS	Infrared maps of the surface between 1 and 5.6 μm with a spectral sampling of 10.5 nm.	Adapt the observation strategy to the motion of the montgolfière. Coordination with VISTA-B for context is required.
				A3: High spatial resolution color images of the surface at equatorial latitudes; ground truth for orbiter measurement	VISTA-B	1360 x 1024 multispectral images 48°FOV; Color images and albedo time series	Precise location of montgolfière to 1 km and 5° attitude knowledge.
	O6: Characterize the major processes transforming the surface throughout time.	I1: Determine the origin of major crustal features; correlate regional elevation changes with geomorph-ology and compositional variations.	M5: Measure regional topography	A1: Stereo images of the surface	VISTA-B	1360 x 1024 stereo images 48°FOV; 3D digital terrain model	Precise location of montgolfière to 1 km and 5° attitude knowledge. .
				A2: Reflection of radar signal	TRS	Time series of the first return radar echoes	Precise identification of the trajectory of the montgolfière increases the quality of the measurements
		I2: Characterize the origin of major surface features, including the effects of liquid flow, tectonic, volcanic, and impact events.	M4: Geological maps at 2.5 m resolution	A1: Infrared mapping through the methane windows	BIS	Infrared maps of the surface between 1 and 5.6 μm with a spectral sampling of 10.5 nm.	Adapt the observation strategy to the motion of the montgolfière. Coordination with VISTA-B for context is required.
		I3: Determine the internal magnetic signal.	M1: Magnetic map, taken from a constant altitude	A1: Dual sensor magnetometer fixed to boom on gondola	MAG	Normal mode 16 Hz data from primary sensor and 1 Hz data from secondary sensor, with burst mode of 128 Hz data from primary sensor triggered by command or autonomously. Normal mode 900 bits per second (bps), burst mode 6500 bps.	Precise location of montgolfière to 1 km and 5° attitude knowledge 1 km continuous magnetic field data, as much coverage of the surface as possible. Consideration of magnetic cleanliness requirements vs. boom length. Complementarities with orbiter measurements during Titan flybys.

KEY: O1…O4 = Objective 1…Objective 4; I1…I4 = Investigation 1 …Investigation 4; A1…A4 = Approach 1…Approach 4; M1…M4 = Measurement 1…Measurement 4

Table A-1 Science traceability matrix: montgolfière (continued)

MISSION GOALS	SCIENCE OBJECTIVES	SCIENCE INVESTIGATIONS	REQUIRED MEASUREMENTS/ DETERMINATION	PLANNING MEASUREMENT APPROACH	PLAN. INSTR.	DATA PRODUCTS	MISSION REQUIREMENTS
Goal A: How does Titan function as a system; to what extent are there similarities and differences with Earth and other solar system bodies?	O6: Characterize the major processes transforming the surface throughout time.	I4: Detect and measure the depth of shallow subsurface reservoirs of liquid (hydrocarbons).	M2: Subsurface sounding at frequency between 150 and 200 MHz in order to detect liquid reservoirs less than 1 km deep.	A1: High resolution subsurface profiles over few hundred meters (500 m) spot size and vertical resolution <6 m	TRS	Time series of radar profiles representing the sub-surface interfaces	Precise location of the montgolfière makes it possible an integrated multiscale analysis of the TRS profiles with the radar measurements acquired by the sounder on the orbiter. Precise location of montgolfière to 1 km and 5° attitude knowledge.
		I5: Determine the subsurface structures and constrain the stratigraphic history of dunes.	M1: Subsurface sounding along the montgolfière journey at a frequency between 150 and 200 MHz (vertical resolution of less than 10 meters and spatial resolution less than 200 meters)	A1: Radar sounding	TRS	Time series of radar profiles representing the sub-surface stratification	Comparison between optical remote sensing images and radar profiles. Precise location of the montgolfière makes it possible an integrated multiscale analysis of the TRS profiles with the radar measurements acquired by the sounder on the orbiter. Precise location of montgolfière to 1 km and 5° attitude knowledge.
	O7: Determine the existence of a subsurface liquid water ocean.	I2: Determine if the crust is decoupled from the interior and the thickness and rigidity of the icy crust.	M1: Map of geological structures at different true anomalies	A1: High-resolution mapping of surface features with their precise location	VISTA-B	Geological image maps	Precise location of montgolfière to 1 km and 5° attitude knowledge.
		I3: Determine the induced magnetic field signatures in order to confirm subsurface liquid and place constraints on the conductivity and depth of the liquid	M3: *In situ* vector magnetic field measurements	A1: Dual sensor magnetometer fixed to boom on gondola	MAG	Normal mode 16 Hz data from primary sensor and 1 Hz data from secondary sensor, with burst mode of 128 Hz data from primary sensor triggered by command or autonomously. Normal mode 900 bits per second (bps), burst mode 6500 bps.	Precise location of montgolfière to 1 km and 5° attitude knowledge. Continuous magnetic field data combined with magnetic field measurements from the orbiter and lander. Nightside data at 0600 Saturn Local Time highly desirable. Desirable (not required) to have some measurements with the lander, montgolfière, and orbiter in a line radiating from Saturn.

KEY: O1…O4 = Objective 1…Objective 4; I1…I4 = Investigation 1 …Investigation 4; A1…A4 = Approach 1…Approach 4; M1…M4 = Measurement 1…Measurement 4

Table A-1 Science traceability matrix: montgolfière (continued)

MISSION GOALS	SCIENCE OBJECTIVES	SCIENCE INVESTIGATIONS	REQUIRED MEASUREMENTS/ DETERMINATION	PLANNING MEASUREMENT APPROACH	PLAN. INSTR.	DATA PRODUCTS	MISSION REQUIREMENTS
Goal A: How does Titan function as a system; to what extent are there similarities and differences with Earth and other solar system bodies?	O8: Determine the state of internal differentiation, whether Titan has a metal core and an intrinsic magnetic field, and constrain the crustal expression of thermal evolution of Titan's interior.	I2: Determine whether Titan has a dynamo.	M2: *In situ* vector magnetic field measurements	A1: Dual sensor magnetometer fixed to boom on gondola	MAG	Normal mode 16 Hz data from primary sensor and 1 Hz data from secondary sensor, with burst mode of 128 Hz data from primary sensor triggered by command or autonomously. Normal mode 900 bits per second (bps), burst mode 6500 bps.	Precise location of montgolfière to 1 km and 5° attitude knowledge. Continuous magnetic field data combined with magnetic field measurements from the orbiter and lander. Nightside data at 0600 Saturn Local Time highly desirable. Desirable (not required) to have some measurements with the lander, montgolfière, and orbiter in a line radiating from Saturn.
		I3: Quantify exchange between interior and atmosphere.	M3: Measure noble gases and isotopes (esp., Ar, Kr, Xe) to ppb levels in gas phase and aerosols	A1: *In situ* measurement of aerosols and atmospheric gas phase, with a precision of 1%	TMCA	Mass spectra over the mass range 10–150 Daltons	Good location to 1 km and 5° attitude knowledge of montgolfière
			M4: Subsurface layering	A1: High resolution subsurface profiles over few hundred meters (500 m) spot size and vertical resolution <6 m	TRS	Time series of radar profiles representing the sub-surface stratification	Precise location of the montgolfière to integrate multiscale analysis of the TRS profiles with the radar measurements acquired by the sounder on the orbiter; 1 km and 5° attitude knowledge of montgolfière
Goal B: To what level of complexity has prebiotic chemistry evolved in the Titan system?	O1: Determine the chemical pathways leading to formation of complex organics at all altitudes in the Titan atmosphere and their deposition on the surface.	I1: Assay the speciation and abundance of atmospheric trace molecular constituents.	M4: Concentration of molecular constituents in the troposphere with S/N ratio >100	A1: IR reflectance spectra with long integration times to enable spectral summing over homogeneous regions.	BIS	Infrared spectra between 1 and 5.6 µm with a spectral sampling of 10.5 nm.	Adapt the observation strategy to the motion of the montgolfière. Coordination with VISTA-B for context is required.
			M5: Latitudinal and vertical distribution of minor species and its temporal variation	A1: *In situ* analysis of minor species	TMCA	0–600 Da Mass spectra	Same location of the montgolfière at different times; analysis of only low molecular mass species
			M6: Day-night variation of minor species to infer information about condensation	A1: *In situ* analysis of minor species gas and condensed phase	TMCA	Mass spectra	Same location of the montgolfière during at least one full Titan day

KEY: O1…O4 = Objective 1…Objective 4; I1…I4 = Investigation 1 …Investigation 4; A1…A4 = Approach 1…Approach 4; M1…M4 = Measurement 1…Measurement 4

Table A-1 Science traceability matrix: montgolfière (continued)

MISSION GOALS	SCIENCE OBJECTIVES	SCIENCE INVESTIGATIONS	REQUIRED MEASUREMENTS/ DETERMINATION	PLANNING MEASUREMENT APPROACH	PLAN. INSTR.	DATA PRODUCTS	MISSION REQUIREMENTS
Goal B: To what level of complexity has prebiotic chemistry evolved in the Titan system?	O1: Determine the chemical pathways leading to formation of complex organics at all altitudes in the Titan atmosphere and their deposition on the surface.	I1: Assay the speciation and abundance of atmospheric trace molecular constituents.	M7: Monitor T and P conditions to help determine species abundances and condensation.	A1: *In situ* measurements of T and P with reference to the altitude level. Simultaneous measurements of P and T are necessary to assess the phase of the species (e.g., condensation) and to associate a certain pressure level in the atmosphere (or equivalent altitude level) to the mole fractions determined by TMCA.	ASI/ MET	T and P time series	1 km and 5° attitude knowledge of montgolfière.
		I2: Assay the molecular complexity of the condensed phase.	M2: Chemical composition (elemental, molecular isotopic, and chiral) of aerosols	A1: Collect aerosols during their descent to the surface	TMCA	0–600 Da Mass spectra	1 km and 5° attitude knowledge of montgolfière
			M3: Chemical abundance of gases in troposphere	A1: *In situ* analysis of major and minor species	TMCA	0–600 Da Mass spectra	1 km and 5° attitude knowledge of montgolfière
			M4: Monitoring of T and P (T and P accuracy to 0.1 K and 1 mPa; and resolution to 0.02 K and 0.1% respectively) conditions to asses condensation status	A1: *In situ* measurements of T and P with reference to the altitude level	ASI/ MET	T and P time series	1 km and 5° attitude knowledge of montgolfière
		I3: Quantify the sources of chemical energy for atmospheric chemistry.	M3: Search for electric discharges	A1: Electric field and optical sensors	TEEP-B	Time series spectra	Coordinated with VISTA-B
			M4: Infrared spectra of relevant complex organics	A1: Identify organic species in the 5–5.6 µm wavelength range	BIS	Infrared maps of the surface between 1 and 5.6 µm with a spectral sampling of 10.5 nm.	Adapt the observation strategy to the motion of the montgolfière. Coordination with VISTA-B for context is required.

KEY: O1…O4 = Objective 1…Objective 4; I1…I4 = Investigation 1 …Investigation 4; A1…A4 = Approach 1…Approach 4; M1…M4 = Measurement 1…Measurement 4

Table A-1 Science traceability matrix: montgolfière (continued)

MISSION GOALS	SCIENCE OBJECTIVES	SCIENCE INVESTIGATIONS	REQUIRED MEASUREMENTS/ DETERMINATION	PLANNING MEASUREMENT APPROACH	PLAN. INSTR.	DATA PRODUCTS	MISSION REQUIREMENTS
Goal B: To what level of complexity has prebiotic chemistry evolved in the Titan system?	O1: Determine the chemical pathways leading to formation of complex organics at all altitudes in the Titan atmosphere and their deposition on the surface.	I4: Determine surface composition.	M3: High spatial resolution (2.5 meters at 10 km) infrared spectra at wavelengths larger than 4.8 µm	A1: Identify organic species in the 5–5.6 µm wavelength range	BIS	Infrared maps of the surface between 1 and 5.6 µm with a spectral sampling of 10.5 nm.	Adapt the observation strategy to the motion of the montgolfière. Coordination with VISTA-B for context is required.
			M4: *In situ* sampling of surface organic inventory	A1: MS analysis of collected surface material	TMCA	Mass spectra	Surface composition measured when landing.
	O2: Characterize the degree to which the Titan organic inventory is different from known abiotic organic material in meteorites.	I1: Assay the composition of organic deposits exposed at the surface, including dunes, lakes, and seas.	M5: High-resolution images to detect organic materials	A1: Identify organic species in the 5–5.6 µm wavelength range	BIS	Infrared maps of the surface between 1 and 5.6 µm with a spectral sampling of 10.5 nm.	Adapt the observation strategy to the motion of the montgolfière. Coordination with VISTA-B for context is required.
				A2: Stereo images	VISTA-B	1360x1024 stereo images 48°FOV; digital terrain models	Precise location of montgolfière to 1 km and 5° attitude knowledge .
		I3: Determine the location and the composition of complex organics in and around impact craters in the equatorial regions.	M1: High-spatial resolution mapping of organics in areas such as impact craters and cryovolcanoes.	A1: High spatial resolution (2.5 meters at 10 km) infrared spectra at wavelengths between 5 and 6 µm	BIS	Infrared maps of the surface between 1 and 5.6 µm with a spectral sampling of 10.5 nm.	Adapt the observation strategy to the motion of the montgolfière. Coordination with VISTA-B for context is required.
				A2: High resolution color images	VISTA-B	1360x1024 multispectral images 48°FOV color albedo maps	Precise location of montgolfière tp 1 km and 5° attitude knowledge.
	O3: Characterize what chemical modification of organics occurs on the surface.	I1: Determine the roles of cratering and cryovolcanism in modification and hydrolysis of organics.	M4: Subsurface stratification of organics.	A1: Radar sounding of the subsurface at frequency between 150 and 200 MHz allowing a spatial resolution of a few hundred meters (500 m) and vertical resolution <6 m	TRS	Time series of radar profiles representing the sub-surface stratification	Precise identification of the trajectory of the montgolfière to 1 km and 5° attitude knowledge required.

KEY: O1…O4 = Objective 1…Objective 4; I1…I4 = Investigation 1 …Investigation 4; A1…A4 = Approach 1…Approach 4; M1…M4 = Measurement 1…Measurement 4

Table A-1 Science traceability matrix: montgolfière (continued)

MISSION GOALS	SCIENCE OBJECTIVES	SCIENCE INVESTIGATIONS	REQUIRED MEASUREMENTS/ DETERMINATION	PLANNING MEASUREMENT APPROACH	PLAN. INSTR.	DATA PRODUCTS	MISSION REQUIREMENTS
Goal B: To what level of complexity has prebiotic chemistry evolved in the Titan system?	O3: Characterize what chemical modification of organics occurs on the surface.	I2: Determine the importance of surface inorganic compounds as surface catalysts or doping agents.	M2: Identify inorganic salts and compounds containing phosphorous and other potentially reactive inorganic agents in equatorial regions.	A1: Partially met with repeated near-IR mapping spectroscopy within the atmospheric transmission windows. High spatial resolution (2.5 m at 10 km) infrared mapping of the surface	BIS	Infrared maps of the surface between 1 and 5.6 μm with a spectral sampling of 10.5 nm.	Adapt the observation strategy to the motion of the montgolfière. Coordination with VISTA-B for context is required.
	O4: Characterize the complexity of species in the subsurface ocean.	I1: Determine whether evidence of sub-surface ocean species is present in cryovolcanic sites.	M2: Map compounds such as ammonia, sulfates, and more complex organics (e.g., CH_3COOH) at cryovolcanic sites	A1: Near-IR mapping spectroscopy within the atmospheric transmission windows with 2.5 m spatial resolution.	BIS	Infrared maps of the surface between 1 and 5.6 μm with a spectral sampling of 10.5 nm.	Adapt the observation strategy to the motion of the montgolfière. Coordination with VISTA-B for context is required.
	O5: Characterize bulk composition, sources of nitrogen and methane, and exchange between the surface and the interior.	I1: Determine whether carbon dioxide is primarily internally derived or photochemically produced.	M3: Profile of CO and CO2 in the troposphere	A1: Infrared spectroscopy within the methane windows.	BIS	CO and CO2 Profiles as a function of position and time.	Precise identification of the trajectory of the montgolfière to 1 km and 5° attitude knowledge required
		I2: Determine whether methane is primordial or derived from carbon dioxide.	M5: Map of surface CO_2 in the equatorial regions	A1: High spatial resolution (2.5 m at 10 km) infrared mapping of the surface.	BIS	Infrared maps of the surface between 1 and 5.6 μm with a spectral sampling of 10.5 nm.	Adapt the observation strategy to the motion of the montgolfière. Coordination with VISTA-B for context is required.
		I3: Determine whether molecular nitrogen is derived from ammonia.	M5: Detect ammonia in surface material: down to 1% in local deposits	A1: High spatial resolution (2.5 m at 10 km) infrared mapping of the surface	BIS	Infrared maps of the surface between 1 and 5.6 μm with a spectral sampling of 10.5 nm.	Adapt the observation strategy to the motion of the montgolfière. Coordination with VISTA-B for context is required.
		I4: Determine whether pockets of partial melt are present at depth.	M2: Subsurface sounding at frequency between 150 and 200 MHz in order to detect liquid reservoirs less than 1 km deep.	A1: High resolution subsurface profiles over few hundred meters (500 m) spot size and vertical resolution <6 m	TRS	Time series of radar profiles representing the sub-surface interfaces	Precise location of the montgolfière makes it possible an integrated multiscale analysis of the TRS profiles with the radar measurements acquired by the sounder on the orbiter. Precise location of montgolfière to 1 km and 5° attitude knowledge.

KEY: O1…O4 = Objective 1…Objective 4; I1…I4 = Investigation 1 …Investigation 4; A1…A4 = Approach 1…Approach 4; M1…M4 = Measurement 1…Measurement 4

Table A-2 Science traceability matrix: lake lander

MISSION GOALS	SCIENCE OBJECTIVES	SCIENCE INVESTIGATIONS	REQUIRED MEASUREMENTS/ DETERMINATIONS	PLANNING MEASUREMENT APPROACH	PLAN INSTR.	DATA PRODUCTS	MISSION REQUIREMENTS
Goal A: How does Titan function as a system; to what extent are there similarities and differences with Earth and other solar system bodies?	O1: Determine how energy is deposited in the upper atmosphere to drive the chemistry and the escape rate of major atmospheric constituents.	I1: Quantify the deposition of radiation into Titan's atmosphere.	M4: Vertical profile of the magnetic field magnitude and direction to quantify the magnetic shielding effect of the ionosphere and extent of the penetration of Saturn's magnetic field.	A1: Measure dual sensor (gradiometer) vector magnetic field along the path of the probe during the entry and descent with a good knowledge of the location of the probe to reconstruct the descent.	SPP	High time resolution (100 Hz TBC) vector, 3 axis magnetic field measure-ment from primary magnetic field sensor with a lower time resolution data from the secondary magnetic field sensor(s) (1 Hz TBC) to allow characterization of the contamination field coming from the probe. Max data rate 0.04 kBytes/sec.	Magnetometer on during descent, and some consideration of the magnetic cleanliness of the lander. A dual sensor magnetometer with the sensors mounted ideally on a boom or mast away from the probe body to allow characterization of the magnetic field coming from the probe to enable ground processing to remove this contaminating field and achieve a more accurate measurement of the ambient magnetic field (so-called gradiometer configuration). This could also be achieved (if a boom or mast is not feasible) by having an primary sensor at an extremity of the probe and several secondary sensors fitted along an axis of the probe to provide a gradiometer type measurement.
		I2: Quantify the escape flux of elemental hydrogen, carbon, nitrogen.	M3: Magnetic field of Titan during descent to correlate with orbiter data. Measure vector magnetic field perturbations of order a few nT (with a resolution of order 0.04 nT) to quantify the escape flux of elemental hydrogen, carbon and nitrogen.	A1: Vector magnetometry (part of a combined instrument, integrated with a low energy plasma and particles instrument, energetic particle spectrometer and Langmuir probe).	SPP	Magnetic field vector at 1 s resolution from both sensors Ion and electron thermal and supra-thermal velocity moments of density, temperature and magnetosphere-ionosphere winds.	
	O2: Characterize the relative importance of exogenic and endogenic oxygen sources.	I2: Quantify the flux of endogenic oxygen from the surface and interior.	M2: Amount of O in the lake	A1: GC x GC separation followed by high resolution MS and MEMS sensor analysis.	TLCA	Mass spectra as a function of GC x GC retention time over the mass range 1–500 Daltons with 10,000 mass resolution plus 1 Mb MEMS sensor image; 1% precision.	Liquid sampling from the lake.
			M3: Isotopic ratio $^{18}O/^{16}O$	A1: GC x GC separation followed by pyrolysis and isotopic mass spectrometry.	TLCA	Selected ion chromatograms for O isotopes; 1% precision.	Lake and atmosphere sampling
			M4: Nature and composition of O-bearing molecules	A1: GC x GC separation followed by high resolution MS and MEMS sensor analysis.	TLCA	Mass spectra as a function of GC x GC retention time over the mass range 1–500 Daltons with 10,000 mass resolution plus 1 Mb MEMS	Lake and atmosphere sampling

KEY: O1…O4 = Objective 1…Objective 4; I1…I4 = Investigation 1 …Investigation 4; A1…A4 = Approach 1…Approach 4; M1…M4 = Measurement 1…Measurement 4

Table A-2 Science traceability matrix: lake lander (continued)

MISSION GOALS	SCIENCE OBJECTIVES	SCIENCE INVESTIGATIONS	REQUIRED MEASUREMENTS/ DETERMINATIONS	PLANNING MEASUREMENT APPROACH	PLAN INSTR.	DATA PRODUCTS	MISSION REQUIREMENTS
						sensor image; 1% precision.	
Goal A: How does Titan function as a system; to what extent are there similarities and differences with Earth and other solar system bodies?	O3: Characterize the major processes controlling the global distribution of atmospheric chemical constituents.	I1: Characterize the major chemical cycles.	M1: Methane and ethane mole fraction in the troposphere	A4: Direct gas inlet into MS	TLCA	Mass spectra from 1–500 Daltons with resolution >1000; precision 1%.	Atmospheric sampling during the descent.
		I2: Determine the relative importance of global transport.	M2: Isotopic ratios of C and N in both the liquid phase and in the aerosols that may be present in the lake	A1: Collect the liquid phase and the compounds in suspension and analyze with isotopic mass spectrometry. Liquid separation by GC x GC / combustion furnace / isotope ratio mass spectrometer for C and N ratios. Sol analysis by pyrolysis of filtered solids.	TLCA	Selected ion chromatograms for C and N isotopes; precision 0.1‰ for C, 0.3‰ for N.	Lake sampling with solid and liquid separation.
	O4: Characterize the atmospheric circulation and flow of energy.	I1: Determine the atmospheric thermal and dynamical state.	M3: Vertical profile of temperature, pressure (T and P accuracy to 0.1 K and 1 mP and resolution to 0.02 K and 0.1% respectively) and density in the northern hemisphere above a lake.	A1: Measure T by a Pt wire resistance thermometer and P by Kiel probe and capacitive gauges during the descent, monitor meteorological conditions at the surface of the lake	ASI/ MET	Vertical mass density profile and inferred pressure and temperature vertical profile during entry (upper atmosphere) and direct T and p measurements. Wind field and gusts.	ASI-ACC should be placed as close as possible to the entry module Center of Mass. ASI pressure inlet and thermometers should has access to the atmospheric unperturbed flow (outside the descent probe boundary layer) The trajectory of the probe (entry and descent module reconstructed from the engineering sensor data (e.g., IMU), the high sensitive scientific accelerometer (and/or IMU)
			M3: Vertical profile of temperature, pressure (T and P accuracy to 0.1 K and 1 mPa and resolution to 0.02 K and 0.1% respectively) and density in the northern hemisphere above a lake.	A2: Three-axis *in situ* accelerometer measurements during entry to a precision of 10^{-5} m/s^2 in order to reconstruct the location of the lander during its descent.	ASI/ MET	Vertical density profile and inferred pressure and temperature vertical profile starting from altitude >1600 km down to 160 km.	ASI-ACC should be placed as close as possible to the entry module Center of Mass. ASI operates before nominal interface entry altitude (1270 km).

KEY: O1…O4 = Objective 1…Objective 4; I1…I4 = Investigation 1 …Investigation 4; A1…A4 = Approach 1…Approach 4; M1…M4 = Measurement 1…Measurement 4

Table A-2 Science traceability matrix: lake lander (continued)

MISSION GOALS	SCIENCE OBJECTIVES	SCIENCE INVESTIGATIONS	REQUIRED MEASUREMENTS/ DETERMINATIONS	PLANNING MEASUREMENT APPROACH	PLAN INSTR.	DATA PRODUCTS	MISSION REQUIREMENTS
			M4: Surface temperature of lakes to 0.1 K accuracy with a resolution of 0.02 K	A1: Measure the temperature at the surface of the lake with a Pt wire resistance thermometer	ASI/ MET	Temperature time series.	Continuous measurements for duration of lander lifetime.
Goal A: How does Titan function as a system; to what extent are there similarities and differences with Earth and other solar system bodies?	O4: Characterize the atmospheric circulation and flow of energy.	I2: Determine the effect of haze and clouds.	M3: Extent and lateral and vertical distribution of clouds above the lakes	A1: Acquire image in the VIS/NIR during the probe's descent from an altitude of ~50 km	TiPI	VIS/NIR images of any clouds during the descent	The amount of light is minimal and comes from Saturn shine and diffuse scattering in Titan's atmosphere.
		I3: Determine the effects of atmospheric composition.	M2: Mole fraction of methane, ethane, and other compounds in the troposphere.	A1: Direct gas inlet into MS	TLCA	Mass spectra from 1–10,000 Daltons with resolution >1000; precision 1%	Atmospheric sampling during the descent.
		I4: Determine the effects of surface processes on meteorology.	M3: Temperature gradients between liquid surface and surrounding terrains with 1 K precision. Pressure and temperature at the surface of the lake	A2: Measure T by a Pt wire resistance thermometer and P by Kiel probe and capacitive gauges	ASI/ MET	Time series of (T, P)	Continuous measurements for duration of lander lifetime.
			M5: Nature of the molecules evaporating from the lake	A1: Direct gas inlet into sorption bed followed by heated injection into GC x GC MS	TLCA	Mass spectra as a function of GC x GC retention time over the mass range 1–500 Daltons with 10,000 mass resolution; precision 1%.	Collect atmospheric sample above the lake surface.
		I5: Determine the exchange of momentum, energy and matter between the surface and atmosphere and characterize the planetary boundary layer.	M1: Wind directions at the surface of the lake	A1: Measure T by a Pt wire resistance thermometer and P by Kiel probe and capacitive gauges	ASI/ MET	Direct temperature, pressure, as a function of time, inferred density	Continuous measurements for duration of lander lifetime.
			M2: Temperature of the atmosphere at the surface of the lake to 0.1 K	A1: T measurements with fast sampling to study the boundary layer	ASI/ MET	Direct temperature time series	Continuous measurements for duration of lander lifetime.
			M3: Wave motion on lake	A1: Record motion of liquid lander through accelerometers	SPP	Time series data from accelerometers	Continuous measurements for duration of lander lifetime.
			M4: Methane humidity	A1: Atmospheric sound	SPP	Sound speed data as a	Continuous measurements for

KEY: O1…O4 = Objective 1…Objective 4; I1…I4 = Investigation 1 …Investigation 4; A1…A4 = Approach 1…Approach 4; M1…M4 = Measurement 1…Measurement 4

Table A-2 Science traceability matrix: lake lander (continued)

MISSION GOALS	SCIENCE OBJECTIVES	SCIENCE INVESTIGATIONS	REQUIRED MEASUREMENTS/ DETERMINATIONS	PLANNING MEASUREMENT APPROACH	PLAN INSTR.	DATA PRODUCTS	MISSION REQUIREMENTS
			as a function altitude and time	speed		function of time.	duration of lander lifetime.
			M5: Distribution of condensates at the surface	A1: Record images of the lake just before landing	TiPI	At least three images 1024 x 1024 pixels with 60° FOV	Huygens like measurement with LEDs turned on
Goal A: How does Titan function as a system; to what extent are there similarities and differences with Earth and other solar system bodies?	O4: Characterize the atmospheric circulation and flow of energy.	I6: Determine the connection between weather, ionosphere and electricity.	M1: Electrical conductivity and permittivity of the atmosphere (positive and negative ions + electrons) to 1 km resolution in the range 10^{-14} to 10^{-6} Sm^{-1} and electrons only, with a height resolution to 100 m in the range 10^{-11} to 10^{-6} Sm^{-1}	A1: Relaxation probe to measure the conductivity of all charged species	ASI/ MET	Time series of voltages and conductivity (all charged species) derived from the characteristic time for charging or discharging of the probe	Measurements during descent.
				A2: Mutual impedance probe which measures the conductivity of electrons only	ASI/ MET	Amplitude and phase of electric signal	Measurements during descent
			M2: Global electric circuit and fair-weather electric field in the range from 0–10 kHz. With a height resolution of 1 km	A1: Measurement of electric field using dipole antennas	ASI/ MET	Time series spectra of electric field	Vertical and horizontal electric field in the frequency range from DC to VLF (~10 kHz)
			M3: Extremely low frequency-very low frequency (ELF-VLF) magnetic components from 0–10 kHz	A1: Measurement of magnetic field using loop antennas or search coils	ASI/ MET	Time series magnetic field spectra	Measurements during descent
			M4: Search for electric discharges	A1: Electric field and optical sensors	ASI/ MET	Time series electric field spectra and eventual flash detection	Coordinated with TiPI
	O5: Characterize the amount of liquid on the Titan surface today.	I1: Quantify the total major hydrocarbon (methane/ethane) inventory present in the lakes and seas.	M3: Separate ethane, ethylene acetylene, and hydrogen cyanide in the liquid mixture	A1: GC x GC MS	TLCA	Mass spectra as a function of GC x GC retention time over the mass range 1–100 Daltons with 10,000 mass resolution; precision 1%, sensitivity 0.1 ppb.	Lake sampling
			M4: Bulk properties such as sound speed,	A1: Acoustic force transducers (1–10 MHz),	SPP	Time series 5 x 16 bit signals vs. mission time at 1	Sensors need to be exposed to liquid after landing. Acoustic

KEY: O1…O4 = Objective 1…Objective 4; I1…I4 = Investigation 1 …Investigation 4; A1…A4 = Approach 1…Approach 4; M1…M4 = Measurement 1…Measurement 4

Table A-2 Science traceability matrix: lake lander (continued)

MISSION GOALS	SCIENCE OBJECTIVES	SCIENCE INVESTIGATIONS	REQUIRED MEASUREMENTS/ DETERMINATIONS	PLANNING MEASUREMENT APPROACH	PLAN INSTR.	DATA PRODUCTS	MISSION REQUIREMENTS
			density, refractive index, thermal conductivity, permittivity	archimedes float, refractometer, line heat source, capacitor stack		Hz, in addition one full acoustic sample ~80 kB) every 10 s to 20 s desirable.	sensors need to be facing each other with clear path between them.
Goal A: How does Titan function as a system; to what extent are there similarities and differences with Earth and other solar system bodies?	O5: Characterize the amount of liquid on the Titan surface today.	I1: Quantify the total major hydrocarbon (methane/ethane) inventory present in the lakes and seas.	M5: Permittivity and electric conductivity) in the range 10^{-14} to 10^{-6} Sm^{-1} of the surface (liquid or solid substrate	A1: Mutual impedance probe which measures permittivity and the conductivity of electrons and relaxation probe which measures the conductivity of all charged species	ASI/ MET	Amplitude and phase of electric signal and time series of voltages and conductivity derived from the characteristic time for charging/discharging of the probe	Lake sampling
		I2: Determine the depth of the lake at the landing site.	M1: Acoustic sounding	A1: SONAR: 10–20 khz acoustic pulse every 1 to 10 s.	SPP	Time series: signal propagation time vs. mission time @ 1 Hz	Sonar needs to be immersed into lake, facing vertically downward.
			M2: Monitor probe motion at and after splashdown	A1: Accelerometers	SPP	Time series: 3 x 16 bit @ 1 to 100 Hz	Location at center of mass of probe
	O6: Characterize the major processes transforming the surface throughout time.	I2: Characterize the origin of major surface features, including the effects of liquid flow, tectonic, volcanic, and impact events.	M3: Map the distribution of different surface features around the landing site	A1: Record images before and after landing	TiPI	At least 2 images before landing covering 60° with 1024x1024; 3 LED wavelength BGR/NIR 20 time delayed additional images; just the difference to the last initial image will be transmitted	Use Saturn shine to map Titan's surface.
	O7: Determine the existence of a subsurface liquid water ocean.	I3: Determine the induced magnetic field signatures in order to confirm subsurface liquid and place constraints on the conductivity and depth of the liquid	M3: Vector magnetic field measurements on the Titan surface to quantify the induced magnetic field and hence constrain the presence of a sub-surface conducting layer (possibly liquid water ocean)	A1: Measure dual sensor (gradiometer) vector magnetic field on Titan's surface	SPP	Dual sensor three-axis magnetic field data at 1 Hz (14 bit/axis)	Knowledge of probe attitude and location. Continuous magnetic field data (desirable, to combine data with magnetic field measurements from the montgolfière and orbiter). Also desirable (not required) to have some measurements with the lake lander, montgolfière, and orbiter in a line radiating from Saturn. Consideration of magnetic cleanliness requirement, and use of gradiometer configuration.

KEY: O1…O4 = Objective 1…Objective 4; I1…I4 = Investigation 1 …Investigation 4; A1…A4 = Approach 1…Approach 4; M1…M4 = Measurement 1…Measurement 4

Table A-2 Science traceability matrix: lake lander (continued)

MISSION GOALS	SCIENCE OBJECTIVES	SCIENCE INVESTIGATIONS	REQUIRED MEASUREMENTS/ DETERMINATIONS	PLANNING MEASUREMENT APPROACH	PLAN INSTR.	DATA PRODUCTS	MISSION REQUIREMENTS
Goal A: How does Titan function as a system; to what extent are there similarities and differences with Earth and other solar system bodies?	O8: Determine the state of internal differentiation, whether Titan has a metal core and an intrinsic magnetic field, and constrain the crustal expression of thermal evolution of Titan's interior.	I3: Quantify exchange between interior and atmosphere.	M1: D/H in methane and ethane to 0.1 per mil in the atmosphere and the lake	A1: Isotope ratio mass spectrometry with GC separation of Hydrogen in atmosphere and pyrolytic reduction to measure D/H in methane and ethane.	TLCA	Selected ion chromatograms for D/H isotopes; precision 5‰	Lake sampling
			M2: Measure noble gases	A1: Direct inlet into noble gas concentrator / getter and then into an MS	TLCA	Mass spectra from 1 to 150 Daltons with mass resolution of 200 and sensitivities exceeding 1 ppb; precision 1%	*In situ* analysis of noble gases during the descent and at the surface of the lake
Goal B: To what level of complexity has prebiotic chemistry evolved in the Titan system?	O1: Determine the chemical pathways leading to formation of complex organics at all altitudes in the Titan atmosphere and their deposition on the surface.	I1: Assay the speciation and abundance of atmospheric trace molecular constituents.	M3: Detailed molecular analysis of the lake and atmosphere above the lake	A1: GC x GC separation followed by high resolution MS.	TLCA	Mass spectra as a function of GC x GC retention time over the mass range 1–500 Daltons with 10,000 mass resolution; sensitivity 1 ppb, precision 1%	Liquid and atmosphere sampling
		I3: Quantify the sources of chemical energy for atmospheric chemistry.	M4: Search for electric discharges during descent	A1: Electric field	ASI/ MET	Time series spectra	Altitude and attitude measured during the descent by accelerometers and gyros.
				A2: Acquire image in the VIS/NIR during the probe's descent	TiPI	VIS/NIR image of any clouds during the descent	Knowledge of position during descent.
		14: Determine surface composition.	M2: Map the distribution of different surface features	A1: Record images just after landing	TiPI	At least three images covering 60° with 1024 x 1024 pixels if the landing site; three LED wavelength BGR/NIR	LEDs turned on
		I5: Determine the composition of organics in the lake and the isotopic ratios of major elements.	M1: Isotopic ratio of C, N, and O in the organic molecules to 0.1 per mil	A1: GC x GC separation followed by conversion and isotopic mass spectrometry. Combustion for C and N analysis and pyrolysis for O analysis.	TLCA	Selected ion chromatograms for C, N, and O isotopes; precision 0.1‰ for C, 0.3‰ for N, 1% for O	Lake sampling

KEY: O1…O4 = Objective 1…Objective 4; I1…I4 = Investigation 1 …Investigation 4; A1…A4 = Approach 1…Approach 4; M1…M4 = Measurement 1…Measurement 4

Table A-2 Science traceability matrix: lake lander (continued)

MISSION GOALS	SCIENCE OBJECTIVES	SCIENCE INVESTIGATIONS	REQUIRED MEASUREMENTS/ DETERMINATIONS	PLANNING MEASUREMENT APPROACH	PLAN INSTR.	DATA PRODUCTS	MISSION REQUIREMENTS
Goal B: To what level of complexity has prebiotic chemistry evolved in the Titan system?	O2: Characterize the degree to which the Titan organic inventory is different from known abiotic material in meteorites.	I1: Assay the composition of organic deposits exposed at the surface, including dunes, lakes, and seas.	M2: Inventory organic content of the lakes, including potential solid species in suspension	A1: GC x GC-MS for liquids. Pyrolysis GC x GC – MS for solids	TLCA	Mass spectra as a function of GC x GC retention time over the mass range 1–500 Daltons with 10,000 mass resolution; sensitivity 1 ppb, precision 1%	Lake sampling with solid and liquid separation before analysis
			M3: Determine otical and electrical properties of the liquid (transparency, refraction)	A1: Measure refractive index, permittivity, and conductivity	SPP	Time series of readout of CCD array	2 kB @ 1 Hz
			M4: Determine optical properties of the lake materials to identify time dependent variations	A1: Measure surface albedo variations just before and after landing	TiPI	At least three images before and after landing covering 60° with 1024 x1024 pixels if the landing site; three LED wavelength BGR/NIR. 20 time delayed additional images; just the difference to the last initial image will be transmitted	LEDs turned on
		I2: Determine the chirality of organic molecules.	M1: Chirality of complex organics	A1: GC x GC-MS with derivatization and chiral columns.	TLCA	Mass spectra as a function of GC x GC retention time over the mass range 1–500 Daltons with 10,000 mass resolution plus 1Mb MEMS sensor image; sensitivity 0.1 ppm, precision 1%, 5% with MEMS.	Lake sampling
	O3: Characterize what chemical modification of organics occurs at the surface.	I1: Determine the roles of cratering and cryovolcanism in modification and hydrolysis of organics.	M3: Search for complex oxygenated organics dissolved or in suspension	A1: GC x GC-MS for liquids. Pyrolysis GC x GC – MS for solids	TLCA	Mass spectra as a function of GC x GC retention time over the mass range 1–500 Daltons with 10,000 mass resolution; sensitivity 1 ppb	Lake sampling with solid and liquid separation before analysis

KEY: O1…O4 = Objective 1…Objective 4; I1…I4 = Investigation 1 …Investigation 4; A1…A4 = Approach 1…Approach 4; M1…M4 = Measurement 1…Measurement 4

Table A-2 Science traceability matrix: lake lander (continued)

MISSION GOALS	SCIENCE OBJECTIVES	SCIENCE INVESTIGATIONS	REQUIRED MEASUREMENTS/ DETERMINATIONS	PLANNING MEASUREMENT APPROACH	PLAN INSTR.	DATA PRODUCTS	MISSION REQUIREMENTS
Goal B: To what level of complexity has prebiotic chemistry evolved in the Titan system?	O5: Characterize bulk composition, sources of nitrogen and methane, and exchange between the surface and the interior.	I1: Determine whether carbon dioxide is primarily internally derived or photochemically produced.	M2: Isotopic composition of atmospheric carbon and oxygen species from the surface to 1500 km.	A2: GC x GC separation of lake samples followed by conversion and isotopic mass spectrometry. Combustion for C analysis and pyrolysis for O analysis.	TLCA	Selected ion chromatograms for C, N, and O isotopes; precision 0.1‰ for C, 1% for O	Lake sampling
		I2: Determine whether methane is primordial or derived from carbon dioxide.	M3: Isotopic composition in lake of carbon in methane to 0.1 per mil and compare with isotopic composition in the atmosphere	A1: Isotope ratio mass spectrometry with GC separation of methane in atmosphere or lake liquid and combustion to measure C isotopes	TLCA	Selected ion chromatograms for C,N, and O isotopes; precision 0.1‰ for C	Lake and atmosphere sampling
			M4: Isotopic ratio of C in other lake organics	A1: GC x GC separation followed by combustion and isotopic mass spectrometry.	TLCA	Selected ion chromatograms for C, N, and O isotopes; precision 0.1‰ for C	Lake sampling
		I3: Determine whether molecular nitrogen is derived from ammonia.	M3: Isotopic composition of atmospheric nitrogen and noble gas isotopic ratios (Ar, Kr, Xe) to a precision of 0.1 per mil	A1: Direct inlet into noble gas concentrator / getter and then into a MS	TLCA	Direct inlet into noble gas concentrator / getter and then into an MS	Measurement made during descent and on the surface.
			M4: Analyze dissolved N_2 and ammonia in the lakes and determine their isotopic composition	A1: Membrane inlet with cold trapping of ammonia followed by pyrolysis and isotopic mass spectrometry.	TLCA	Selected ion chromatograms for C, N, and O isotopes; precision 0.3‰ for N, 5‰ for H	Lake sampling
		I5: Determine the isotopic ratios of noble gases	M1: Quantify noble gas isotopic ratios (Ar, Kr Xe)	A2: Direct inlet into noble gas concentrator / getter and then into a MS	TLCA	Direct inlet into noble gas concentrator / getter and then into an MS	Measurement made during descent and on the surface.

KEY: O1…O4 = Objective 1…Objective 4; I1…I4 = Investigation 1 …Investigation 4; A1…A4 = Approach 1…Approach 4; M1…M4 = Measurement 1…Measurement 4

Table A-3 Science traceability matrix: geosoucer

MISSION GOALS	SCIENCE OBJECTIVES	SCIENCE INVESTIGATIONS	REQUIRED MEASUREMENTS	PLANNING MEASUREMENT APPROACH	PLAN INSTR	DATA PRODUCTS	MISSION REQUIREMENTS
Goal A: How does Titan function as a system; to what extent are there similarities and differences with Earth and other solar system bodies?	O6: Characterize the major processes transforming the surface throughout time.	I3: Determine the internal magnetic signal	M2: Measure vector field with <0.1nT precision on the surface	A1: Three magnetic sensors record the magnetic field at the surface	GEO-PACK	Time series of magnetic field	Continuous magnetic field data combined with magnetic field measurements from the orbiter and montgolfière. Best if measurements are acquired simultaneously but not a very strong requirement. >1/2 Titan = 8 Earth days: may resolve field fluctuations on time scale of Saturn rotation >10 Titan days = 6 Earth months: may resolve field fluctuations on Titan orbit time scale
		I6: Characterize the dynamics off the crust	M1: Detection of shallow quakes	A1: Three seismic sensor which will provide the direction of the quake. (S-P) method for the distance	GEO-PACK	Times series of mass displacement	2 Titan days = 32 Earth days: low S/N
				A2: Displacement of the surface recorded by the beacon	GEO-PACK	Time series of Doppler-shift measurements	2 Titan days
			M2: Deformation of the surface due to tidal forces	A2: Displacement of the surface recorded by the beacon	GEO-PACK	Time series of Doppler-shift measurements	1–2 Titan days

KEY: O1…O4 = Objective 1…Objective 4; I1…I4 = Investigation 1 …Investigation 4; A1…A4 = Approach 1…Approach 4; M1…M4 = Measurement 1…Measurement 4

Table A-3 Science traceability matrix: geosaucer (continued)

MISSION GOALS	SCIENCE OBJECTIVES	SCIENCE INVESTIGATIONS	REQUIRED MEASUREMENTS	PLANNING MEASUREMENT APPROACH	PLAN INSTR	DATA PRODUCTS	MISSION REQUIREMENTS
Goal A: How does Titan function as a system; to what extent are there similarities and differences with Earth and other solar system bodies?	O7: Determine the existence of a subsurface liquid water ocean.	I2: Determine if the crust is decoupled from the interior and the thickness and rigidity of the icy crust.	M4: deformation of the crust during Titan eccentric orbit around Saturn	A1: Displacement of the surface recorded by the beacon. The amplitude of the deformation and its phase lag provide information on the presence of a liquid layer.	GEO-PACK	Time series of Doppler-shift measurements	1–2 Titan days
		I3: Determine the induced magnetic field signatures in order to confirm subsurface liquid and place constraints on the conductivity and depth of the liquid	M2: Measure vector field with <0.1nT precision on the surface	A2: Three magnetic sensors record the magnetic field at the surface	GEO-PACK	2 Titan days = 32 Earth days: low S/N, large thermal quakes unlikely because of almost constant surface temp on Titan	By measuring the magnetic field at the surface, in the troposphere and in orbit, the induced signal of an Europa-like ocean could be detected.
		I4: Characterize the depth of the icy crust and the nature of the underlying layer.	M1: Record the seismic waves reflected at the base of the icy crust	A1: Three seismic sensors will record the waves produced by tidal or telluric events. The time between the direct wave and the reflective waves will provide the information on the depth of the icy crust and the nature of the underlying layer	GEO-PACK	Times series of mass displacement	2 Titan days

KEY: O1…O4 = Objective 1…Objective 4; I1…I4 = Investigation 1 …Investigation 4; A1…A4 = Approach 1…Approach 4; M1…M4 = Measurement 1…Measurement 4

Table A-3 Science traceability matrix: geosaucer (continued)

MISSION GOALS	SCIENCE OBJECTIVES	SCIENCE INVESTIGATIONS	REQUIRED MEASUREMENTS	PLANNING MEASUREMENT APPROACH	PLAN INSTR	DATA PRODUCTS	MISSION REQUIREMENTS
Goal A: How does Titan function as a system; to what extent are there similarities and differences with Earth and other solar system bodies?	O8: Determine the state of internal differentiation, whether Titan has a metal core and an intrinsic magnetic field, and constrain the crustal expression of thermal evolution of Titan's interior.	I2: Determine whether Titan has a dynamo	M2: Measure vector field with <0.1nT precision on the surface	A1: Three magnetic sensors record the magnetic field at the surface	GEO-PACK	Time series of magnetic field	Continuous magnetic field data combined with magnetic field measurements from the orbiter and montgolfière.
		I3: Characterize Titan's internal structure	M1: Detect the waves that travel through Titan's interior	A1: Three seismic sensor, which will record the waves that travel through Titan-s interior. Quakes generated by tides or telluric activity will provide the signal	GEO-PACK	Times series of mass displacement	2 Titan days
			M2: Motion of the surface— the presence of a liquid iron core partially controls the amplitude and phase lag of the surface displacement.	A2: Displacement of the surface recorded by the beacon	GEO-PACK	Time series of Doppler-shift measurements	2 Titan days

KEY: O1…O4 = Objective 1…Objective 4; I1…I4 = Investigation 1 …Investigation 4; A1…A4 = Approach 1…Approach 4; M1…M4 = Measurement 1…Measurement 4

Table A-4 Complementarity of TSSM mission elements

Mission Goals	Science Objectives	Science Investigations	Orbiter	Montgol-fière	Lake Lander
Goal A: How does Titan function as a system; to what extent are there similarities and differences with Earth and other solar system bodies?	O1: Determine how energy is deposited in the upper atmosphere to drive the chemistry and the escape rate of major atmospheric constituents.	I1: Quantify the deposition of radiation into Titan's atmosphere.	**X**		x
		I2: Quantify the escape flux of elemental hydrogen, carbon, nitrogen.	X		x
	O2: Characterize the relative importance of exogenic and endogenic oxygen sources.	I1: Quantify the flux of exospheric oxygen into the atmosphere.	**X**	x	x
		I2: Quantify the flux of endogenic oxygen from the surface and interior.	**X**		**X**
	O3: Characterize the major processes controlling the global distribution of atmospheric chemical constituents.	I1: Characterize the major chemical cycles.	**X**		x
		I2: Determine the relative importance of global transport.	**X**		
	O4: Characterize the atmospheric circulation and flow of energy and its variability on short-timescales.	I1: Determine the atmospheric thermal and dynamical state.	**X**	**X**	x
		I2: Determine the impact of haze and clouds.	x	**X**	
		I3: Determine the effects of atmospheric composition.	**X**	**X**	
		I4: Determine the effects of surface processes on meteorology.	**X**	**X**	
		I5: Determine the exchange of momentum, energy and matter between the surface and atmosphere and characterize the planetary boundary layer.		**X**	x
		I6: Determine the connection between weather, ionosphere, and electricity.		**X**	x
	O5: Characterize the amount of liquid on the Titan surface today.	I1: Quantify the total major-hydrocarbon (methane/ethane) inventory present in the lakes and seas.	x		**X**
		I2: Determine the depth of lake	x		**X**
		I3: Determine surface composition that might reveal the presence of liquids		**X**	
		I4: Determine the nature of precipitation responsible for the formation of valley networks in the equatorial regions.		**X**	
	O6: Characterize the major processes transforming the surface throughout time.	I1: Determine the origin of major crustal features; correlate regional elevation changes with geomorphology and compositional variations.	**X**	x	
		I2: Characterize the origin of major surface features, including the effects of liquid flow, tectonic, volcanic, and impact events.	**X**		
		I3: Determine the internal magnetic signal of Titan	x	**X**	x
		I4: Detect and measure the depth of shallow subsurface reservoirs of liquid (hydrocarbons).	x	**X**	
		I5: Determine the subsurface structures and constrain the stratigraphic history of dunes.		**X**	

KEY: O1…O4 = Objective 1…Objective 4; I1…I4 = Investigation 1 …Investigation 4,
X = Primary, **x** = Secondary

Table A-4 Complementarity of TSSM mission elements (continued)

Mission Goals	Science Objectives	Science Investigations	Orbiter	Montgol-fière	Lake Lander
Goal A: How does Titan function as a system; to what extent are there similarities and differences with Earth and other solar system bodies?	O7: Determine the existence of a subsurface liquid water ocean.	I1: Determine crustal/subcrustal structure; reflectance of subsurface stratification.	**X**		
		I2: Determine if the crust is decoupled from the interior and the thickness and rigidity of the icy crust.	**X**	x	
		I3: Determine the induced magnetic field signatures in order to confirm subsurface liquid and place constraints on the conductivity and depth of the liquid	x	**X**	x
	O8: Determine the state of internal differentiation, whether Titan has a metal core and an intrinsic magnetic field, and constrain the crustal expression of thermal evolution of Titan's interior.	I1: Map interior structure of Titan.	**X**		
		I2: Determine whether Titan has a dynamo.	x	**X**	
		I3: Quantify exchange between interior and atmosphere.		x	**X**
Goal B: To what level of complexity has prebiotic chemistry evolved in the Titan system?	O1: Determine the processes leading to formation of complex organics in the Titan atmosphere and their deposition on the surface.	I1: Assay the speciation and abundances of atmospheric trace molecular constituents.	**X**	**X**	x
		I2: Assay the molecular complexity of the condensed phase.	x	**X**	
		I3: Quantify the sources of chemical energy for atmospheric chemistry.	**X**	x	x
		I4: Determine surface composition.	x	**X**	
		I5: Determine the composition of organics in the lake and the isotopic ratios of major elements.			**X**
	O2: Characterize the degree to which the Titan organic inventory is different from known abiotic organic material in meteorites.	I1: Assay the composition of organic deposits exposed at the surface, including dunes, lakes, seas.	**X**	x	**X**
		I2: Determine the chirality of organic molecules.			**X**
		I3: Determine the location and the composition of complex organics in and around impact craters in equatorial regions.		**X**	
	O3: Characterize what chemical modification of organics occurs on the surface.	I1: Determine the roles of cratering and cryovolcanism in modification and hydrolysis of organics.	**X**	x	x
		I2: Determine the importance of surface inorganic compounds as surface catalysts or doping agents.	x	**X**	
		I3: Quantify the sources of energy for surface chemistry and identify the sites where it may have been present.	**X**		
		I4: Quantify the amount of aerosols deposited on Titan's surface and their modification as they get buried.	**X**		
	O4: Characterize the complexity of species in the subsurface ocean.	I1: Determine whether evidence of sub-surface ocean species is present in cryovolcanic sites.	**X**	x	

KEY: O1…O4 = Objective 1…Objective 4; I1…I4 = Investigation 1 …Investigation 4,
X = Primary, **x** = Secondary

Table A-4 Complementarity of TSSM mission elements (continued)

Mission Goals		Science Objectives	Science Investigations	Orbiter	Montgol-fière	Lake Lander
Goal B: To what level of complexity has prebiotic chemistry evolved in the Titan system?		O5: Characterize bulk composition, sources of nitrogen and methane, and exchange between the surface and the interior.	I1: Determine whether carbon dioxide is primarily internally derived or photochemically produced.	X		X
			I2: Determine whether methane is primordial or derived from carbon dioxide.	x	x	X
			I3: Determine whether molecular nitrogen is derived from ammonia.	x	x	X
			I4: Determine whether pockets of partial melt are present at depth.	X	x	
			I5: Determine the isotopic ratios of noble gases'.	x		X
Goal C: What can be learned from Enceladus and Saturn's magnetosphere about the origin and evolution of Titan?	Saturn Magnetosphere	O1: Determine how Titan's atmosphere evolves by virtue of its coupling to the Saturn magnetosphere and Titan's low gravity.	I1: Determine how energy is deposited in the upper atmosphere of Titan to drive the chemistry and the escape rate of major atmospheric constituents.	X		
			I2: Determine the escape rates and mechanisms of major atmospheric species on Titan.	X		
	Enceladus	O2: Infer the crustal and deep internal structure of Enceladus, including the presence of gravity anomalies, and the moon's tidal history.	I1: Test for the presence of crustal or deeper structures associated with Enceladus' internal activity, including an interface between a solid crust and a liquid layer, as well as partial melt pockets	X		
			I2: Test for true polar wander on Enceladus.	X		
		O3: Characterize the chemistry of the Enceladus plumes.	I1: Determine the composition of the plume, including isotopic abundances.	X		
		O4: Understand the formation of the active region near the south pole, and whether liquid water exists beneath the area.	I1: Characterize the global and regional geomorphology of Enceladus' surface.	X		
			I2: Determine whether thermal anomalies exist underneath the surface.	X		
			I3: Determine the origin of the surface organic materials and its connection with interior reservoirs.	X		
		O5: Identify and characterize candidate sites on Enceladus for future *in situ* exploration.	I1: Determine whether extrusion of water ice or liquid water has occurred recently.	X		
			I2: Determine whether areas of extremely thin crust or exposed liquid within cracks exist.	X		

KEY: O1…O4 = Objective 1…Objective 4; I1…I4 = Investigation 1 …Investigation 4,
X = Primary, **x** = Secondary

APPENDIX B LETTER OF COMMITMENT (CNES)

cnes
CENTRE NATIONAL D'ETUDES SPATIALES

Direction de la Prospective, de la Stratégie, des Programmes, de la Valorisation et des Relations Internationales
Head, Space Science and Exploration Office

Affaire suivie par : francis.rocard@cnes.fr

Pr. David SOUTHWOOD
Directeur du Programme Scientifique
European Space Agency
8-10 rue Mario Nikis
75738 PARIS cedex 15

Paris, July 16, 2008
DSP/EU - 2008.001.7168

Subject: **CNES support to study for the Titan Montgolfiere (TSSM mission)**

Dear Pr Southwood,

Following the selection of the TANDEM proposal, led by Dr. Athena Coustenis from LESIA (CNRS and Observatoire de Paris), as a Cosmic Vision mission candidate, ESA and NASA have carried on the study of a joint mission to the Saturn and Titan system (TSSM).

One element of the mission is a balloon to fly in the Titan atmosphere. In our letter dated June 23, 2007, and signed by my predecessor Richard Bonneville, CNES has announced its intention to provide the balloon envelope and the inflation subsystem. This message is to confirm that should the TSSM proposal be selected jointly by ESA and NASA, CNES would provide these two elements.

To this aim, CNES intends to support the feasibility study of the montgolfiere balloon, including the critical points identified since April 2008 in the frame of the CNES-JPL working group on the montgolfiere design. This group has indeed identified a common design based on a double wall Montgolfiere balloon without an additional He balloon. The feasibility phase covers the development of the balloon fabrication technique, the fabrication of prototypes of balloon systems, the fabrication and demonstration of the packing technique for the cruise phase, the engineering work for the flight physics analysis and the demonstration of the deployment feasibility.

Best regards,

F. Casoli

Fabienne CASOLI

Strategy and Programmes Directorate
Head, Space Science and Exploration Office

APPENDIX C INSTRUMENTED MONTGOLFIÈRE HEAT SHIELD FOR TITAN GEOPHYSICS – THE ‚GEOSAUCER'

This section was provided by a study team that was assigned by the JSDT to derive a concept for using the heat shield as carrier as a possibility for additional instrumentation. The implementation described below did not undergo the same assessment process, as the ESA in situ *elements described before. Therefore this optional instrumentation package is included here as an appendix for information and to complete the picture.*

This instrumentation was investigated with the understanding that this option is at elevated risk. The available volume is to be considered as 'spare' volume between the (nadir) outside of the gondola and the inner surface of the heat shield. It was agreed that, being a elevated risk, the implementation of this option must not become a system driver to the design of the gondola and/or of the heat shield, but rather be use 'spare' resources, when available.

C.1 Background

Emerging from the rationale of having as the two TSSM *in situ* elements (ISE's) the Lander and Montgolfière, a way was sought to implement in the mission some of the Titan solid surface science that cannot be addressed by the two baseline ISEs alone. Given the availability of up to ~20 kg of unallocated mass margin in the conceptual design of the Montgolfière system, it was suggested to consider a small package of instruments along with their own dedicated power supply, thermal control, and communications subsystems that would be affixed on the inside of the Montgolfière ISE's front shield to reach Titan's surface hitching a ride with the heatshield as it is jettisoned following atmospheric entry. Given the low gravity of Titan, its dense atmosphere, and the aerodynamic properties of the shield, impact conditions on the icy regolith of Titan are expected to be sufficiently benign to permit on-surface operations of this instrument package while remaining attached to the shield. The perceived measurements of highest importance attributed to the package are related to the physics of the interior of Titan, addressing i) the non-synchronous rotation state of the crust as a result of a subsurface ocean as suggested by Cassini observations [1], ii) tidal deformations of the satellite's outer ice shell in the presence of a subsurface ocean, iii) the magnetic field induced in a subsurface ocean during Titan's passage within Saturn's magnetosphere, iv) Titan's internal structure. It is recognized that this concept of an 'instrumented heat shield' or the so-called 'Geosaucer' represents a high-risk approach to include geophysics science within the TSSM ISE's but with a potentially large science pay-off. This package is considered by making clever use of available resources in the Montgolfière system offering high-value science as an investigation of opportunity on the TSSM mission.

C.2 Science Case

The proposed instrument package shall determine key geophysical parameters to help understanding Titan's formation and evolution. To this effect, investigations have to be conducted on the following aspects of Titan:

- Tidal distortion and rotational state
- Subsurface properties
- Time-variable magnetic field
- Seismic activity
- Environmental conditions

Recent Cassini radar observations of Titan show that its rotational period is changing and is different from its orbital period indicating Titan's crust being decoupled from the core by an internal water ocean [2]. Therefore, tidally-induced surface displacements and forced librations of the outer shell should be observable. This could be investigated with a radio science transponder included in a package on the surface. In addition, information on the atmosphere-ice-ocean system can be gained due to the link between atmospheric changes and the rate of change of Titan's rotation. For these observations, a single station on the surface is sufficient, which provides a two-way link from/to an Earth ground station. Since the instrument is coupled to the surface, exposed to seismic, tectonics and wind chill, a drift connected to the 16-day tidal cycle is expected. Thus, a minimum lifetime for the instrument is required to be ~1 Titan day (16 Earth days) given by a max/min tidal distortion.

Titan seems to lack a strong intrinsic magnetic field; however it is embedded in Saturn's magnetosphere and thus is subjected to an inducing field which has two principal frequencies due to Saturn's rotation and Titan's revolution at expected amplitudes of 2 – 4 nT. Therefore, a magnetometer on a surface package would further define both the inducing and induced field and thus provide clues on the magnetic environment of Titan. Furthermore, the location and thickness of the internal ocean could be determined by detailed analysis of the electromagnetic induction signal.

With a recording signal as weak as a few nT, S/N is a critical issue. To resolve the above mentioned frequencies, a minimum lifetime a magnetic surface experiment should be ~9 Earth months with a time resolution of 1 vector/min.

Titan's seismic activity should be probed by an ultra broad band seismometer experiment. This would determine the level of seismic activity on the surface by observing body-waves of mainly tidally-induced deep quakes which may be located close to the ice-ocean interface. Thermally-induced shallow quakes are less likely on Titan. It is anticipated that the physical extent of individual sources will be smaller than on Earth, and that the seismic attenuation is likely to be lower. It has been estimated that tectonics on Titan are ~50 times weaker than on Earth [3]. Together, these suggest that the optimum bandwidth for body-wave observations is likely to be in the range 0.03 to 3 Hz. For crustal observations, higher frequencies are desirable, and for observations using local sources, they are essential. For the former, frequencies up to 20 Hz may be adequate; for the latter, frequencies up to 80 Hz are essential.

A seismometer would also allow characterizing the structure of the outer ice shell and thus would provide clues on the internal ocean. Since the noise level is high due to Titan's dense atmosphere, the S/N is critical. A minimum lifetime of ~2 Titan days (32 Earth days) is aimed for.

Further information on the environmental conditions on Titan can be provided with an acoustic experiment similar to the one flown on the Huygens probe. This instrument will determine the wind speed and direction close to the surface and thus will be able to identify any atmospheric turbulence. Furthermore, it can trace Methane drizzle and rain precipitating on the ground [4]. These measurements will contribute to a good overview of the atmospheric conditions and will add relevant information to the understanding of the atmosphere-surface-interior coupling on Titan.

To carry out useful geophysics science, these four instruments are proposed as the payload of an instrumented Montgolfière heat shield – the 'Geosaucer' – to provide the required measurements to analyze and understand the conditions and processes on, above, and below the moon's solid surface.

C.3 Package Design Constraints

As the Geosaucer concept assumes that science instruments as well as subsystems of the package are incorporated into the Montgolfière entry system without having to strongly modify the design of that ISE, the package needs to accept the severe limitations imposed with respect to available volume as indicated in Figure 58 below. Moreover, at this stage uncertainties still exist in the envelopes of the Montgolfière gondola equipment, shown by various colours in Figure 58. Therefore, the package layout should be modular to some extent so as to allow rearrangement in view of changes of the gondola configuration.

Mass is less of a constraint for the package as currently about 20 kg could be available to the package.

Overall, design constraints on the package are harsh, driven by Titan's cold environment, the desired substantial lifetime of the package on the surface of several months, and the obvious need to transmit the science data, which represents a driver for the power subsystem sizing and presents challenges in the choice of a suitable antenna configuration.

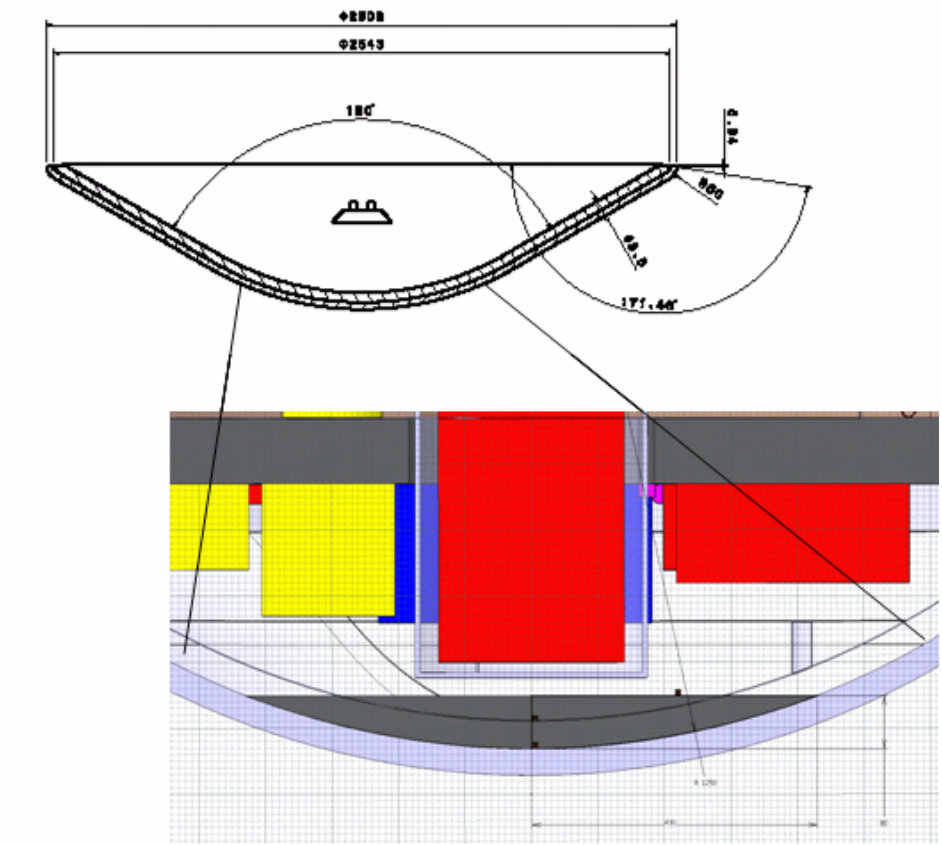

Figure 58 Montgolfière front shield with (bottom) preliminary volume allocation for Geosaucer equipments shaded gray at the inside of the heat shield ('bottom' fraction of a circle).The colourred boxes above indicate equipment of the gondola.

C.4 Descent, Impact, and Operations Scenario

C.4.1 DESCENT AND IMPACT

The heat shield separation from the Montgolfière is expected to take place at an altitude of 131 km at a speed of approximately 110 m/s, after which the heat shield continues an uncontrolled descent to the surface. Considering force balances on the shield, an impact velocity of 1.88 m/s has been derived, using the following parameters:

- Geometry: diameter of 2.1 m; nose cone angle of 60°, radius of curvature of 1.5 m
- Drag Coefficient: C_d ~2,1
- Density profile at Titan: Yelle model for Titan's atmosphere [1,5], see Figure 59 (left).

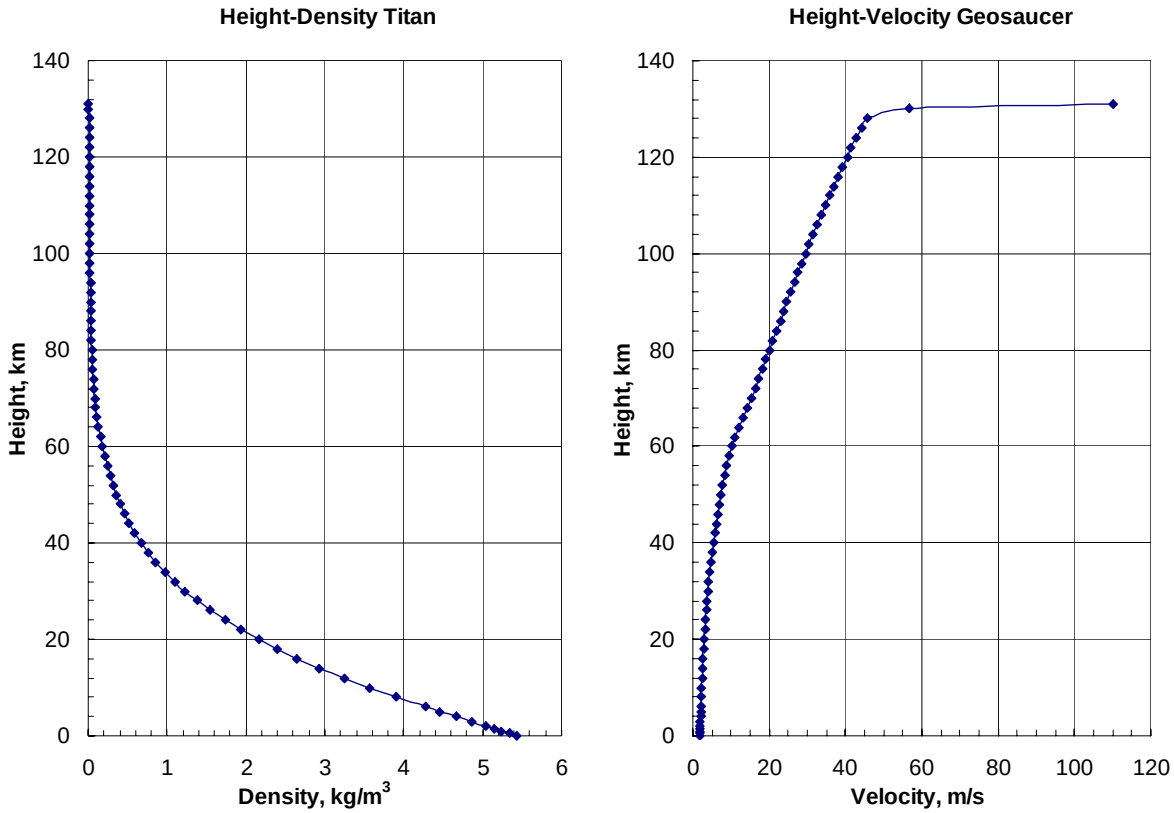

Figure 59 Left: Density profile at Titan; right: Velocity profile for Geosaucer.

Since the descent is uncontrolled, a desired final attitude on the surface cannot be guaranteed. This is mainly due to perturbations, induced by winds on Titan, which can reach as much as 1 m/s in the lowest 5 km of descent [6,7], as well as aerodynamic forces which may cause instabilities. Further analyses using CFD or similar means have to be performed for a satisfying estimate of the flight stability, also with respect to the moments of inertia, i.e. the centre of gravity of the system. Furthermore, the introduction of additional stabilizing mechanisms, such as a dedicated parachute, may be evaluated.

However, the baseline design of the package does not consider any additional deceleration devices or stabilizers, and the overall system is designed to cope with the impact conditions of the front shield as they result from Montgolfière entry system design.

C.4.2 ATTITUDE ON THE SURFACE AND OPERATIONS

The desired final attitude of the front shield is mainly restricted by communication needs. An evaluation of possible cases, i.e. an open-side-up or down position or a partially stuck position at an odd angle can be seen in Figure 60. Since the ablative thermal protection system on the outer side of the heat shield prohibits the installation of antennas, the open-side-up attitude is the desired one.

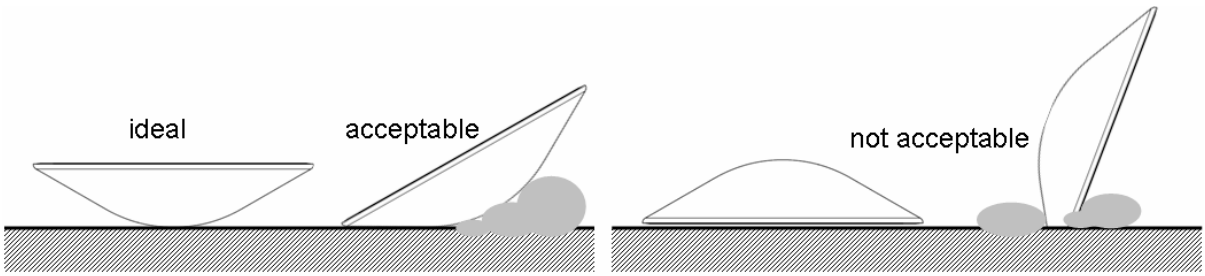

Figure 60 Front shield on-surface attitudes

C.5 Design Space

In Figure 61, a block diagram of the design aspects considered in the present, initial Geosaucer study is shown. In several ways, volumes of items have been a driver in choosing design solutions, given the tight envelope that was specified for the package. Other aspects having entered the preliminary design exercise have been a suitable placement of instruments to enable the desired science return, as well as the choice of a possible antenna arrangement and antenna placement.

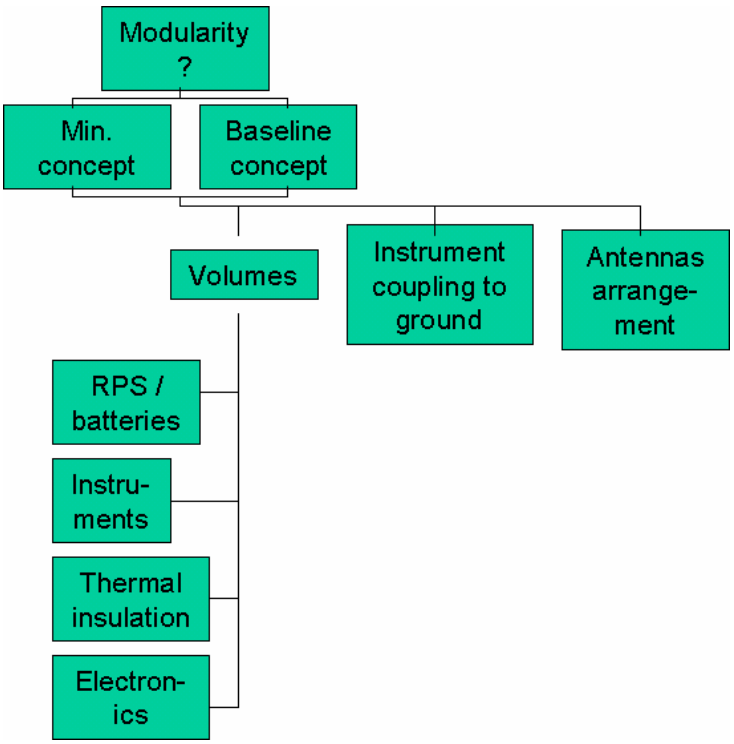

Figure 61 Block diagram of aspects considered in Geosaucer design study

C.6 Preliminary Design

C.6.1 INSTRUMENT ACCOMMODATION

The Geosaucer includes several science instruments such as a magnetometer, RS beacon, Micro-seismometer (μ-SEIS) and additional environmental sensors (planetary acoustic experiment) dedicated to various aspects of Titan's geophysical science as outlined above. All instruments, along with the required subsystems, are accommodated in the Montgolfière heat shield.

a) A magnetometer will measure the magnetic field in the vicinity of the Geosaucer's landing site in the bandwidth DC to 20 Hz, depending on science requirements and available telemetry. The instrument is a tri-axial magnetometer array based on small magnetoresistive (MR) sensors. MR sensors offer considerable mass reductions (~30 g/sensor) but have lower TRL. However due to the large mass of fluxgates and the accommodation of a boom, MR sensors are a preferred option for the Geosaucer. This option will require further development effort but this is considered feasible in the time frame of TSSM.
The sensor electronics would either be of a digital FPGA based design which is currently being developed, or of an ASIC based design which would require further specific development but offers considerable reduction of instrument power.

b) A radio science (RS) beacon consists of an X-band transponder that has been designed to obtain two-way Doppler measurements from the radio link between the Geosaucer and the Earth. The instrument consists of electronics for the transponder, patch antenna(s) on the front shield internal structure, and links to the Command and Data Management Subsystem (CDMS) and the Power Control and Distribution Unit (PCDU). The selected transponder is a derivate of the 'Lander Radioscience experiment (LaRa)' currently in development for the ESA ExoMars mission.

c) A Micro-seismometer (μ-SEIS) will measure body-waves from earthquakes at regional and teleseismic distances. The experiment contains a tri-axial seismometer array (each axis weights 100 g and needs 50 mW) which enables the identification of the original direction of the respective seismic source and a quantitative analysis of the signal. The μ-SEIS is a short-period instrument which operates at frequencies above 1 Hz with a noise level of <10 $nms^{-2}/\sqrt{(Hz)}$ based on a compact set-up. A broadband seismometer would have been the preferred choice for the geosaucer science objectives, see above. However, corresponding available instrument concepts are too excessive in mass and volume for the tight constraints applicable to the instrumented front shield. Therefore, a concession had to be made in favour of a short period device.

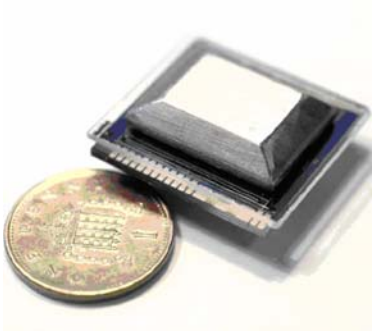

Figure 62 Packaged µ-SEIS single axis sensor head (Imperial College London)

The unit for each µ-SEIS axis has a dimension of 50 × 50 × 50 mm. The µ-SEIS electronics based on an ASIC design exists as a breadboard at Imperial College London. A micro-machined silicon suspension is used as the sensing element. This acts as a spring/proof-mass system, converting any external vibration to a displacement of the proof mass. This displacement is measured using a position transducer which consists of a series of electrodes on the proof mass and fixed frame forming a capacitive transducer together with sensitive readout electronics. The signal passes through a feedback controller and transconductance amplifiers to produce currents in a series of coils which form parallel electromagnetic actuators to maintain the position of the proof mass. There are two feedback loops, one producing the signal, and the second producing low-frequency integral control. One further coil is used to produce actuation from an external calibration signal.

d) An environmental package consists of the Planetary Acoustics Experiment (ACU). The ACU comprises 3 acoustic sensors ('microphone'), an acoustic drizzle detector ('microphone plus membrane') and a dedicated data acquisition and processing unit. The 4 sensors would be distributed symmetrically near the outer edge of the front shield's inner surface with 90° angular spacing.

C.6.2 DATA BUDGET AND COMMUNICATIONS SUBSYSTEM

The data rates of the magnetometer and the µ-Seismometer are shown in Table 28. If operated for satisfaction of the science objectives, both instruments produce a total accumulated data volume of about 500 Mbit per earth day.

A relay communication strategy via the TSSM Saturn orbiter has been analyzed and dimensioned taking into account the approximate distance between the Geosaucer on Titan's surface and the orbiter. The average distance during the first 150 days is mostly very large. Figure 5 shows the distance for the uplink scenario of the Montgolfière, which is somewhat similar for the Geosaucer. Consequently this prohibits a periodic communication between Geosaucer and orbiter, and therefore a communications link will only made with the orbiter during Titan fly-by's. This directly influences the required lifetime of the Geosaucer, which is set to be 135 days, as a first estimation, yielding a total of 5 communication sessions between orbiter and surface module with 10 – 12 hours communication time each (see Figure 5). In the intermediate periods data is to be

processed, i.e. compressed and/or filtered, and stored onboard the package, although a detailed data-processing routine has not been defined yet during the present, initial study.

Table 28 Instruments Data Rate

No.	Name	Operation Duration per Earth day [h]	Data Rate package-internal and for transmission, respectively (Bits/s)
1	µ-Seismometer	continuously	4800
2	Magnetometer	continuously	900
3	Radioscience	1.00	TBD
		Total Accumulated Data Volume per Earth Day [Bits]	492483600
		Total Accumulated Data Volume per Earth Day [MBits]	492
		Accumulated Data Volume per Science Mode Phase [Mbits]	29549
			29549
3	Communication Far-1 (see below)	7.44	900
4	Communication Close (see below)	2.88	10000
		Design downlink capability per Titan fly-by of TSSM orbiter [Bits]	127785600
		Design downlink capability per Titan fly-by of TSSM orbiter [MBits]	128

The radio science X-band transponder is also used for the communications subsystem of the Geosaucer, with an input power of 20 W. An array of combined patch/slit antennas for X-band communications is considered as the antenna system. A possible solution is displayed in Figure 63. Special aspect of this mission which influence the antenna design have to be taken into account: i) the influence of the heat-shield on the antenna characteristics, ii) the influence of the energy output on the electronics, iii) the material properties under Titan atmospheric conditions iv) the properties of the radiation characteristics. In follow-on studies, a trade-off study considering the placement of the patches either at the inside of the heat shield or on a separate flat structure has to be carried out.

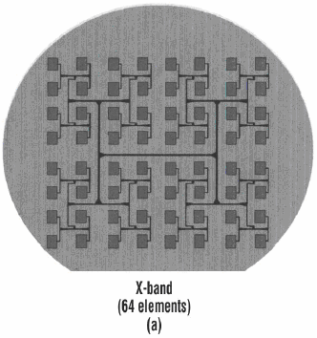

Figure 63 Sample X-band patch antenna module with 64 elements and electronics

Table 29 provides the results of the link budget calculation for the given communications scenario, using X-Band and the suggested patch antenna design. During each communication window a total duration of 0.43 days with distances smaller than 50000 km has been evaluated, where a S/N of

16 dB can be established for data rates of 0.9 up to 10 kbit/s. This configuration leads to a first estimation of a total of 128 Mbits that can be transmitted during each communication period.

Table 29 Link Budget Results

No.	Case Name	Distance [km]	Data Rate [kbit/s]	S/N [dB]	Duration per Comm. Window[d]
1	Far-1	50,000	0.9	16	0.31
2	Far-2	50,000	10	5.6	s.a.
3	Close	15,000	10	16	0.12

C.6.3 ENERGY BUDGET AND POWER SUBSYSTEM

C.6.3.1 Power subsystem dimensioning

For the estimation of the power system, the following operation modes of the Geosaucer (Table 30) have been identified: the general or normal mode is the Science Mode (SCM), when communication is off, payload instruments are in use and batteries could be charged. A short time before the estimated communication period the transponder is turned on, waiting for a signal from the orbiter which initiates the Communication Mode. This mode is used only during the rare occasions of communication (see above), where high peak power consumption has to be sustained. Estimated power requirements during these modes are displayed in Table 30 and an example power concept budget for one communication phase is shown in Figure 64.

Table 30 Modes of Operation

No.	Name	Definition/Description	Acronym	Peak Power Consumption (W)	Duration	Total Energy Used During Mode (Whr)
1	Science Mode	Instruments in use; batteries charged	SCM	0.25	60d, 30d	> 800
2	Pre-Comm Mode	Receiver in use, waiting for Signal to start data transmission	PCM	0.45	1d	10.8
3	Communications Mode	Instruments + Comms in use	CM	20.25	10 hrs about 5 times during LT	240

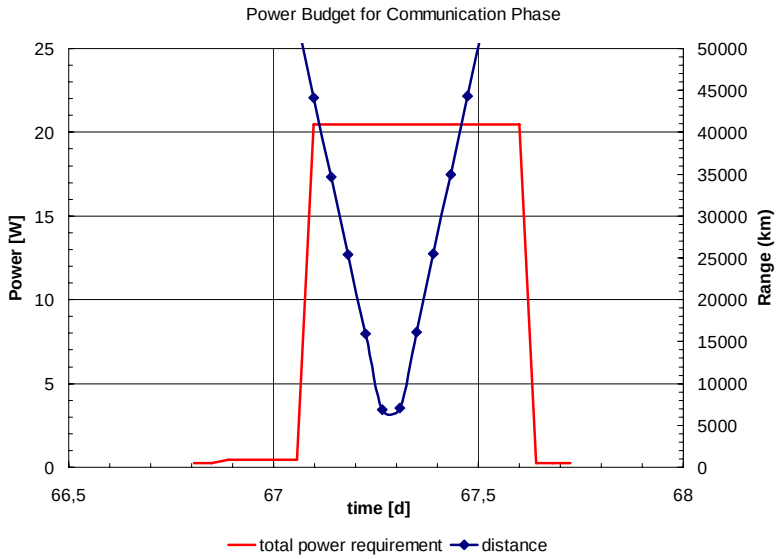

Figure 64 Power Concept (example) for day 67, Comm. Phase 2

C.6.3.2 Radioisotope Thermal Generator

During the Science Mode power demands are sustained by a small nuclear power source (RTG), adopted from the Russian MetNet RTG, which provides a continuous electrical power of 0.5 W with a thermal power output of 8.5 W and a system mass of 0.3 kg.

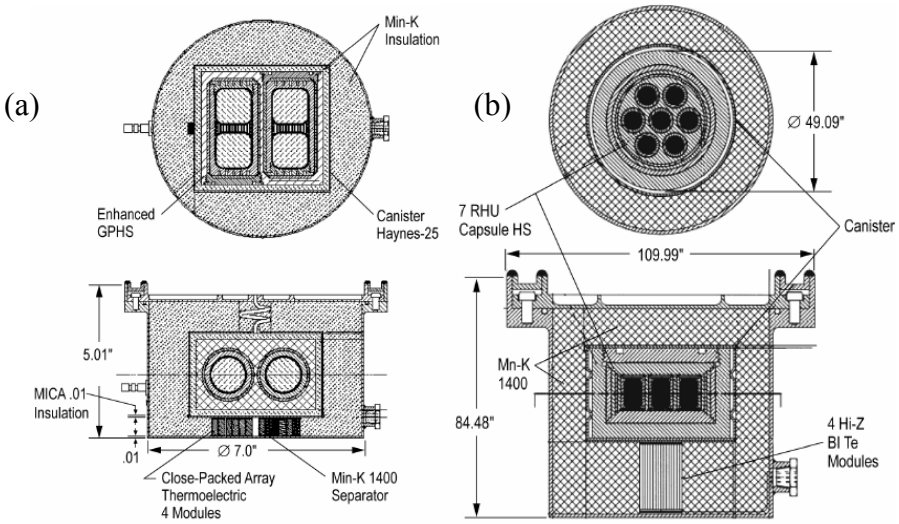

Figure 65 US-developments: (a) GPHS-based RTG (b) RHU-based RTG [8]

Alternative US developments are either using General Purpose Heat Sources (GPHS) with Close-Packed Array (CPA) thermoelectric modules for energy conversion or RHU-based systems, which provide 18 W (GPHS) and (max) 0.160 W (RHU) electrical power (see Figure 65) with a mass of 3-5 kg [8]. For further studies, a trade-off between the mentioned Russian RPS and a US-based

concept will be performed, taking into account safety and testing aspects as well as available space and mechanical configuration aspects.

C.6.3.3 Secondary Batteries

To provide the peak loads as needed for the communication passes, a secondary battery is part of the Geosaucer power subsystem. A cell-block design of 48 Single Cell Li-Ion Batteries ABSL 18650HC, connected in series and parallel provides a total energy of 252 Wh, which may be sufficient for a 10 h communication period using 20 W power at a nominal bus voltage of 28 V. Battery parameters can be found in Table 31. To guarantee the required lifetime, the power system design requires consideration of charge/discharge cycles of the batteries during the 30 – 60 days in between communication periods, which has to be addressed in further studies.

Table 31 Battery Parameters

Parameter	Single Cell	8s6p Configuration
Cell	ABSL 18650HC	
Dimensions [mm x mm]	18 x 65	variable footprint
mass [kg]	0.042	2.016
Vmax [V]	4.2	33.6
Vmin [V]	2.5	20
C [Ah]	1.5	9

An equipment summary of the power subsystem is displayed in Table 32.

Table 32 Elements of the Power Subsystem

No.	Name	Quantity	Total Peak Power Output (W)	Total Mass (kg)	Dimensions
1	Secondary Batteries	TBD	25 W	2.016	Variable
2	RTG (baseline: Russian)	TBD	0.5 W	0.3	

C.6.4 THERMAL CONTROL

The design of the thermal control system is mainly driven by the equipment temperature limits, the RTGs's heat and the harsh environmental conditions on Titan (temperature of 94 °K and a pressure of 1.6 bar, with possible near-surface winds) which are especially critical during descent of the heat shield, when the Geosaucer instruments and subsystems are directly exposed to the cold environment while possibly being in airflow with strong convective cooling. Thus, the following requirements for the thermal system have been identified:

- Ensure temperature limits of the secondary batteries (0 °C – 40 °C) with special consideration of the operational lifetime
- Ensure temperature limits of electronics

- Ensure removal of the RTGs's heat (for Russian RTG = 8.5 W) during hot phases, such as during cruise when the Geosaucer equipments are in proximity to the Montgolfière's MMRTG, as well as adequate use of the heat during on-surface operation
- Minimize heat leaks through the insulation, which also has to survive the impact as well as take over structural support
- For risk and complexity minimization use only passive control.

For the insulation, a variety of possible materials, such as fumed silica powder or open cell melamine foam (Basotect), have been identified. However, testing under Titan environment, with respect to the long lifetime has to be performed. Also, a mathematical modelling of the system has not been established during these initial considerations.

C.6.5 MECHANICAL CONFIGURATION

To cope with an as yet uncertain volume allocation along the inside of the Montgolfière front heat shield, the Geosaucer equipment will be designed for integration in a distributed arrangement on the heat shield structure. Fig. 11 a) and b) shows the assembly of the instruments on the heat shield viewed from the top and side, respectively. The three magnetometer arrays should be allocated along a measurement axis which is free from magnetic disturbance. However, since a final low field axis needs to be studied in detail, they are initially in an equilateral triangle arrangement on the outer surface of the Geosaucer for this report. The μ-Seis sensors follow the same arrangements. The RS beacon instrument and the energy systems are placed in the central part of the heat shield.

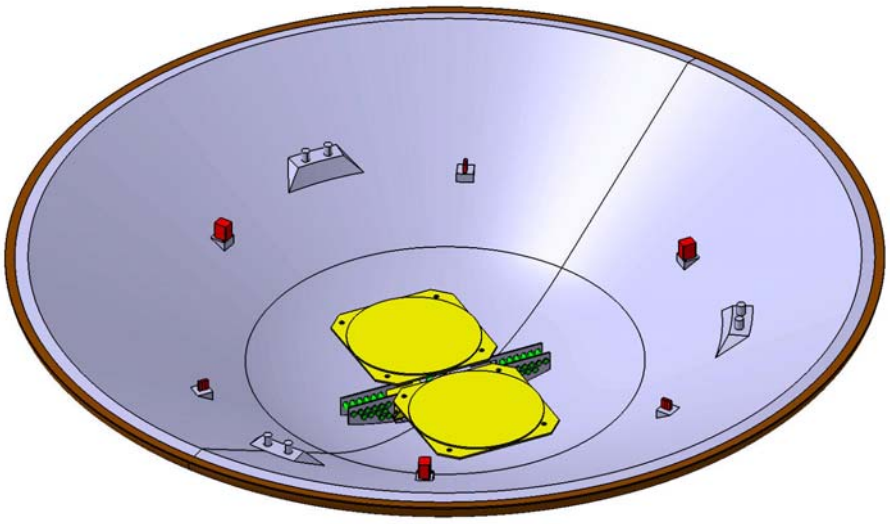

Figure 66 Top view of the Geosaucer instrument configuration with the magnetometer sensor arrays (red big boxes), the μ-Seis (small red boxes), the two antennae (yellow) and the RPS and battery (green).

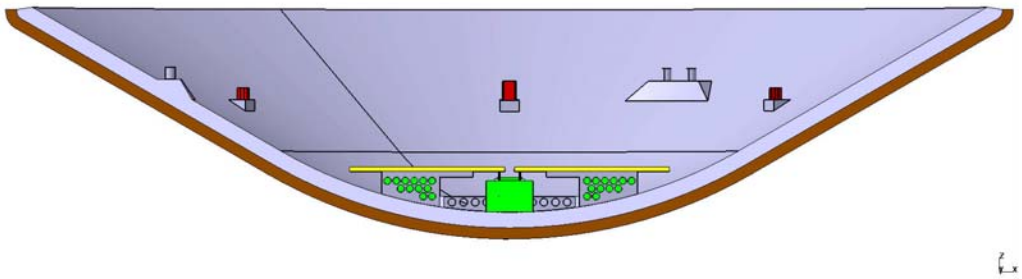

Figure 67 Side view of the Geosaucer configuration.

C.6.6 MASS BUDGET

The derived system mass budget is displayed in Table 33. For all instruments, components and subsystems a standard mass margin of 20% is applied. Including the mass of the heat shield, a total system mass of the Geosaucer of about 24.6 kg has been estimated, where 12.6 kg are accounted for components integrated within the heat shield, whereas the heat shield is a residue of the mission itself. The scientific instrumentation including the three magnetometers, the seismometer and the environmental sensors with all associated electronics, account for about 16% of the total mass. The communication system, which will also partially be used to do radio science, contributes about 11% of the system mass, although the mass budget for the RS beacon antennas has to be considered as preliminary, since a detailed study of the antenna design has to be performed during further investigation. This applies also to the thermal subsystem, which has been included in the mass budget with 1 kg, as well as to an eventually necessary decent stabilisation system, also accounted for with 1 kg here. The descent stabilisation system (mechanisms), together with the mounting and protective structures represents about 19% of the total system mass. The power system accounts for 22% of the total system mass. Figure 68 illustrates the system mass budget breakdown (without heat shield mass).

Table 33 Geasaucer mass budget.

Instrument	Mass (kg)	Dimensions (l/w/h)	Quantity (no)	Margin (%)	Total (kg)
Instrumented Heat Shield	12				12
Magnetoresistive sensor	0.1	10 x 10 x 30	9	20	1.08
Magnetometer electronics	0.15	50 x 70 x 30	1	20	0.18
RS beacon transponder	0.82	120 x 120 x 30	1	20	0.984
RS beacon antennas	0.14	400 dia x 5	2	20	0.336
Seismometer	0.4	50 x 50 x 50	3	20	1.44
Environmental sensors (ACU)	0.062	TBD	4	20	0.3
Batteries	0.042	18 dia x 65	48	20	2.4192
RTG	0.3	80 dia x 120	1	20	0.36
Descent stabilisation system	1	TBD	1	20	1.2
Thermal Insulation	1	TBD		20	1.2
Harness and connectors	2.4			20	2.88
Mounting & protective structures	1			20	1.2
Total	19.41		70	20	24.61

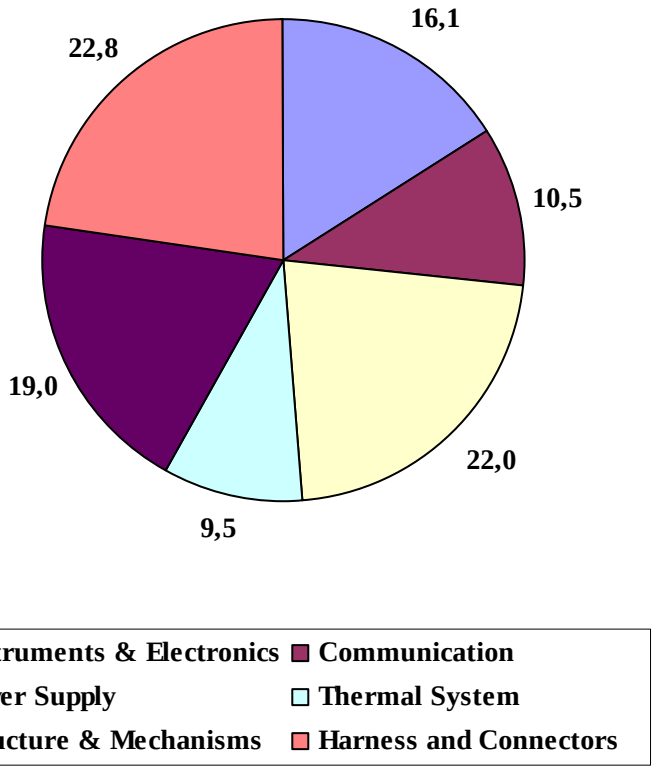

Figure 68 Geosaucer system mass breakdown (percentages).

C.7 Issues for Further Study

C.7.1 INSTRUMENTATION

Further investigation of the influence of the landed heat shield attitude (see section C.4.2) on the measurements of each instrument needs to be conducted (considering limited contact surface).

The number of antennas required for the radio science experiment can vary aiming to obtain the best S/N for a 2-Ways Doppler Tracking between Titan and Earth. This still needs to be looked into. In general, further investigations on the optimal placement of each experiment on the heat shield structure considering available space and interactions with the environment have to be carried out.

C.7.2 SUBSYSTEMS

A variety of issues for further studies considering the different subsystems have been identified so far. Intensive and detailed investigations have to be carried out taking the special environment on Titan and its influence on the different subsystems into account, e.g. with respect to antennas and thermal control. For the communication subsystem an early prototype test program for the design of the antenna array is highly recommended. Further analyses have to be performed considering the thermal insulation under Titan environment and considering the overall system design, as well as trades on the choice of the nuclear power source and heat source.

To ensure the operation in general, a detailed analysis of the descent with respect to the desired on-surface attitude has to be performed.

C.8 Summary

The Geosaucer instrument package is a maximum utilisation of the available heat shield of one of the TSSM *in situ* elements. It will be able to do high value science and thus will contribute in combination with instruments on the Lander and the Montgolfière to a comprehensive understanding of the overall condition and processes on Titan. The Geosaucer is dedicated to solid surface science and should contain a magnetometer, a radio science beacon, a micro-seismometer and a planetary acoustics experiment. These instruments will investigate several aspects such as the magnetic field, seismic activities and near surface atmospheric conditions which will not only add further knowledge to our common understanding of Titan but will address one of its key questions: its subsurface ocean.

Preliminary studies on the feasibility of an ‘instrumented heat shield’ has been undertaken considering design constraints, descent, impact and operation scenarios, communication and power subsystems, mechanical configuration etc.

For the whole instrument package a data volume of ~500 Mbit per day is expected which will be transferred via the TSSM Saturn orbiter to Earth. In the current mission concept, the orbiter will perform in the first year after arrival a Saturn system tour including several Titan and Enceladus fly-bys. This gives constrains on the communication of the *in situ* elements. Considering the

minimum required lifetime of the Geosaucer (135 days) 5 communication windows of ~10 – 12 h are determined (orbiter-to-*in situ* element range <50000 km) within that a total data volume of 128 Mbits will be transmitted via the antenna of the radio science instrument.

To ensure the operation of the Geosaucer, the power subsystem should contain either a Russan RPS or an alternative US-based concept. For the case of integrating the Russian RTG, 48 secondary batteries are needed to guarantee the required lifetime.

A total system mass of ~24.6 kg has been estimated for the Geosaucer of which 12.6 kg is dedicated to the integrated components within the heat shield. However, detailed studies on the mass of the communication system, thermal subsystems or descent stabilisation system are needed. This requires also further studies of the flight stability estimation to ensure optimal on-surface attitude of the heat shield, trade off of the radioisotope thermal generators, etc.

The concept of an 'instrumented heat shield' is a high-risk but feasible approach to cover Titan's geophysics with a potential high scientific impact in the TSSM mission.

C.9 Bibliography

[1] B.W. Stiles, R.L. Kirk, R.D. Lorenz, S. Hensley, E. Lee, S.J. Ostro, M.D. Allison, P.S. Callahan, Y. Gim, L. Iess, P. Perci del Marmo, G. Hamilton, W.T.L. Johnson, R.D. West, The Cassini RADAR Team (2008). Determining Titan's Spin State from Cassini Radar Images. Astron. J., 135, 1669-1680.

[2] R.D. Lorenz, Stiles, W. Bryan, R.L. Kirk, M.D. Allison, P. Persi del Marmo, L. Iess, J.I. Lunine, S.J. Ostro, S. Hensley (2008). Titan's Rotation Reveals an Internal Ocean and Changing Zonal Winds. Science, 319, 1649.

[3] R.D. Lorenz (2002). DPS Meeting #34, #22.01. Energetics of Titan's Bizarre Landscape. Bulletin of the American Astronomical Society, 34, 878

[4] S.D.B. Graves, C.P. McKay, C.A. Griffith, F. Ferri, M. Fulchignoni (2008). Rain and hail can reach the surface of Titan. Planet. Space Sci., 56, 346-357.

[5] R.V. Yelle, D.F. Strobell, E. Lellouch, D. Gautier (1997).The Yelle Titan Atmosphere Engineering Models, Proceedings of ESA Conference on Huygens: Science, Payload and Mission, 243

[6] M. K. Bird, M. Allison, S. W. Asmar, D. H. Atkinson, I. M. Avruch, R. Dutta-Roy, Y. Dzierma, P. Edenhofer,W. M. Folkner, L. I. Gurvits, D. V. Johnston, D. Plettemeier, S. V. Pogrebenko, R. A. Preston, G. L. Tyler (2005). The vertical profile of winds on Titan. Nature, 438, 800.

[7] M. G. Tomasko, B. Archinal, T. Becker, B. Bézard, M. Bushroe, M. Combes, D. Cook, A. Coustenis, C. de Bergh, L. E. Dafoe, L. Doose, S. Douté, A. Eibl, S. Engel, F. Gliem, B. Grieger, K. Holso, E. Howington-Kraus, E. Karkoschka, H. U. Keller, R. Kirk, R. Kramm, M. Küppers, P. Lanagan, E. Lellouch, M. Lemmon, J. Lunine, E. McFarlane, J. Moores, G. M. Prout, B. Rizk, M. Rosiek, P. Rueffer, S. E. Schröder, B. Schmitt, C. See, P. Smith, L. Soderblom, N. Thomas and R. West (2005). Rain, winds and haze during the Huygens probe's descent to Titan's surface. Nature, 438, 756-778.

[8] R.D. Abelson, T.S. Balin, K.E. Marshall, H. Noravian, J.E. Randolph, C. M. Satter, G. R. Schmidt, J. H. Shirley (2004). Enabling Exploration with Small Radioisotope Power Systems, JPL Pub 04-10, Pasadena, CA: Jet Propulsion Laboratory, National Aeronautics and Space Administration